Synthesis of

Dualsteric Muscarinic M_1 Acetylcholine Receptor Ligands and Neuroprotective Esters of Silibinin

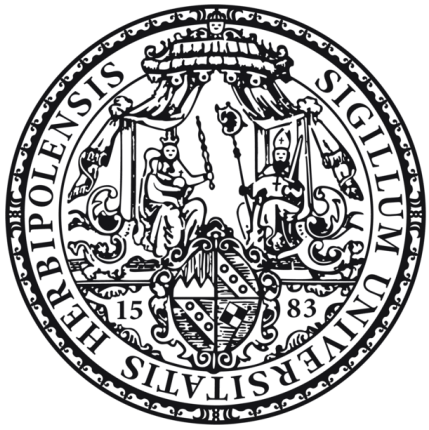

Dissertation zur Erlangung des naturwissenschaftlichen Doktorgrades

an der Fakultät für Chemie und Pharmazie

der Julius-Maximilians-Universität Würzburg

vorgelegt von

Simon Schramm

aus Münchberg

Würzburg, im September 2018

Eingereicht bei der Fakultät für Chemie und Pharmazie am

_____

Gutachter der Dissertation

1. Gutachter: _____

2. Gutachter: _____

Prüfer des öffentlichen Promotionskolloquiums

1. Prüfer: _____

2. Prüfer: _____

3. Prüfer: _____

Tag des öffentlichen Promotionskolloquiums

_____

Doktorurkunde ausgehändigt am

_____

Table of Contents

Publications

[I] Huang, G.; **Schramm**, **S**.; Heilmann, J.; Biedermann, D.; Křen, V.; Decker, M. Unconventional application of the Mitsunobu reaction: Selective flavonolignan dehydration yielding hydnocarpins. *Beilstein J. Org. Chem.* **2016**, *12*, 662-669.

[II] Gunesch, S.; **Schramm**, **S**.; Decker, M. Natural antioxidants in hybrids for the treatment of neurodegenerative diseases: a successful strategy? *Future Med. Chem.* **2017**, *9*, 711-713.

[III] Schramm, **S**.; Huang, G.; Gunesch, S.; Lang, F.; Roa, J.; Högger, P.; Sabaté, R.; Maher, P.; Decker, M. Regioselective synthesis of 7-*O*-esters of the flavonolignan silibinin and SARs lead to compounds with overadditive neuroprotective effects. *Eur. J. Med. Chem.* **2018**, *146*, 93-107.

[IV] Schramm, **S**.; Gunesch, S.; Lang, F.; Saedtler, M.; Meinel, L.; Högger, P.; Decker, M. Investigations into Neuroprotectivity, Stability and Water Solubility of 7-*O*-Cinnamoyl-silibinin, its Hemisuccinate and Dehydro Derivatives. *Arch. Pharm. Chem. Life Sci., accepted*.

Abbreviations

Aβ	β-Amyloid
AC	Adenylyl cyclase
ACh	Acetylcholine
AChE	Acetylcholinesterase
AChR	Acetylcholine receptor
ADAM17	A disintegrin and metalloproteinase domain 17
APP	Amyloid precursor protein
ATP	Adenosine triphosphate
BACE-1	β-Secretase, β-site APP cleaving enzyme 1
Boc	*tert*-Butoxycarbonyl
BQCA	Benzyl quinolone carboxylic acid
cAMP	Cyclic adenosine monophosphate
cat	Catalytic amount
CDI	1,1'-Carbonyldiimidazole
CDK-5	Cyclin dependent kinase 5
ChAT	Choline acetyl transferase
CHT1	Choline transporter 1
CNS	Central nervous system
CoA	Coenzyme A
DAG	Diacylglycerol
DIAD	Diisopropyl azodicarboxylate
DMAP	4-(Dimethylamino)pyridine
DMF	*N*,*N*-Dimethylformamide
DMSO	Dimethyl sulfoxide
EC_{50}	Half maximum effective concentration
eq	Equivalents
GIRK	G-protein-activated inwardly rectifying potassium channel
GPCR	G-protein coupled receptor
GSK-3β	Glycogen synthase kinase 3β

HPLC	High performance liquid chromatography
IP1	Inositol monophosphate
IP3	Inositol trisphosphate
LCMS	Liquid chromatography – mass spectrometry
nAChR	Nicotinic acetylcholine receptor
NMR	Nuclear magnetic resonance spectroscopy
mAChR	Muscarinic acetylcholine receptor
MAPK	Mitogen-activated protein kinase
mRNA	Messenger ribonucleic acid
MT	Microtubule
MTT	3-(4,5-Dimethylthiazol-2-yl)-2,5-diphenyltetrazolium bromide
m/z	Mass-to-charge ratio
NFT	Neurofibrillary tangle
NMDA	*N*-Methyl-*D*-aspartic acid
PAINS	Pan assay interference compounds
PIP2	Phosphatidyl 4,5-bisphosphate
PLCβ	Phospholipase Cβ
PKC	Protein kinase C
PPA2	Protein phosphatase 2A
PrP^C	Cellular prion protein
SAMP8	Senescence Accelerated Mouse - Prone 8
SAR	Structure – activity relationship
TBPB	1-(1‘-(2-Tolyl)-1,4‘-bipiperidin-4-yl)-1H benzo[d]imidazol-2(3H)-one
TFA	Trifluoro acetic acid
THF	Tetrahydrofuran
TLC	Thin layer chromatography
TPTZ	Tripyridyltriazine
Ts	Tosyl
VAChT	Vesicular acetylcholine transporter

1. Introduction

Alzheimer's disease (AD) is the most common form of dementia in today's ageing society. The illness manifests in memory impairment and loss as well as loss of orientation and causes aggression, depression and distrust. It is among the top five causes of death according to the World Health Organization [1] and 47 million people are reportedly suffering from the illness in 2018 [2]. This even exceeds the predicted number of 32 to 42 million by the year 2020 [3, 4]. The cost of caregiving in 2015 was estimated to be US$818 million [2, 5] showing that dementia is also an important economic factor. More importantly, the disease is a heavy burden not only for the patients themselves but also for the people around them: family, friends and caregivers. Therefore, a cure for AD or at least modest symptomatic treatment slowing progression of the disease or even delaying death would improve the situation of everyone involved. To date, only a handful of drugs have been approved for treatment of AD. Memantine is an *N*-methyl-*D*-aspartic acid (NMDA) receptor antagonist. The other four compounds are acetylcholinesterase (AChE) inhibitors, namely rivastigmine, galantamine, donepezil and tacrine (Figure **1**). While all these compounds have positive effects on memory and behaviour, they show either no sufficient activity or are accompanied by unwanted side effects. Tacrine, for example, was withdrawn from the market due to its dose-dependent hepatotoxicity. This situation makes new therapeutic approaches desirable, yet the complex pathological network of AD complicates research for new and more effective drugs.

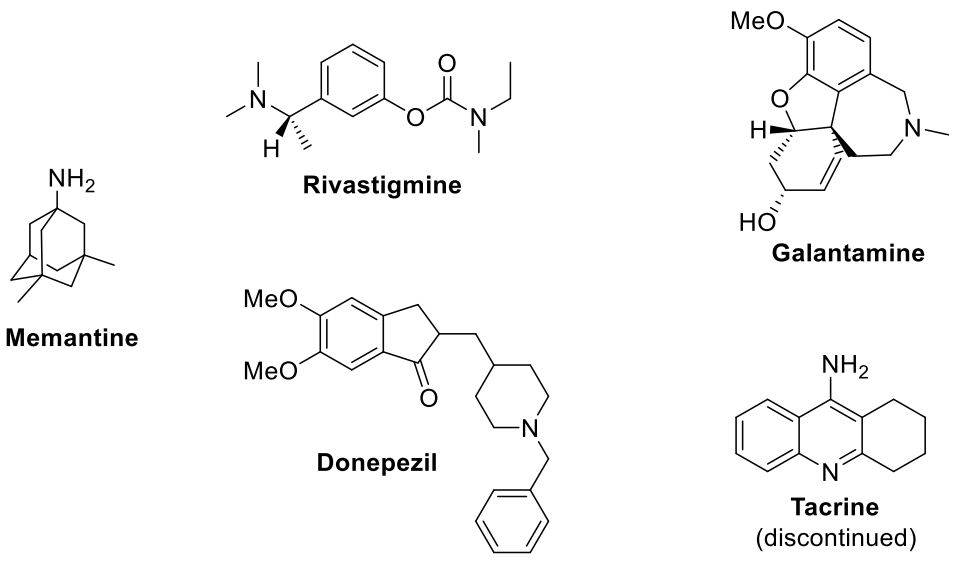

Figure 1. Structures of approved AD therapeutics.

2. Pathologies of Alzheimer's Disease

The causes of AD and biological pathways of its pathogenesis remain to be fully understood. There are several hypotheses that try to explain disease progression, namely the amyloid hypothesis, the τ hypothesis and the cholinergic hypothesis. There are, however, further factors playing a role in AD's pathogenesis like mitochondrial dysfunction, inflammatory processes, oxidative stress and genetic prerequisites. All these processes are intertwined with each other resulting in a complex pathological network complicating elucidation of a definitive cause as well as the development of treatments.

2.1. Amyloid Cascade Hypothesis

The most prominent hypothesis is the amyloid hypothesis [6, 7]. Formation of senile plaques with β-amyloid (Aβ) as their main constituent can be directly observed in AD brains (Figure **2**) [8]. The formation of Aβ is caused by mutations to amyloid precursor protein (APP) creating an imbalance, resulting in insoluble and neurotoxic Aβ proteins, which in turn lead to neuronal cell death and ultimately to dementia [6, 7].

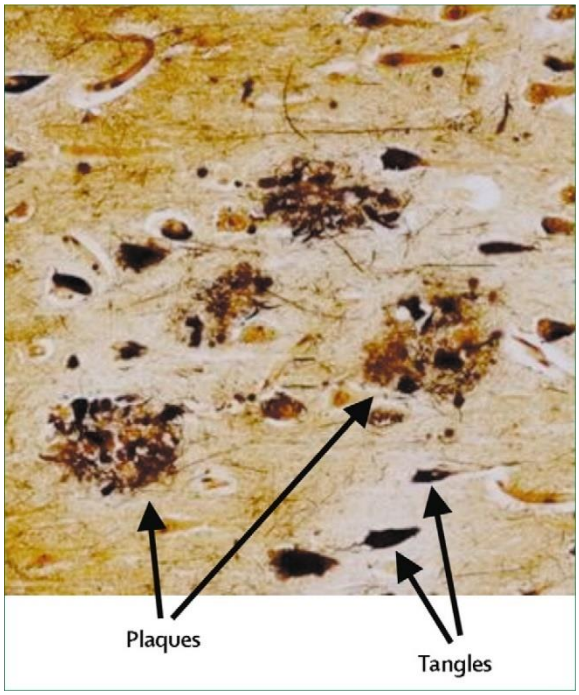

Figure 2. Aβ plaques and neurofibrillary tangles (NFTs) in the cerebral cortex in Alzheimer's disease. Plaques are extracellular deposits of Aβ surrounded by dystrophic neurites, reactive astrocytes, and microglia, whereas tangles are intracellular aggregates composed of a hyperphosphorylated form of the microtubule-associated protein τ [8].

APP is a member of the APP-family of single-pass transmembrane proteins and is considered to contribute positively to cell proliferation and cell health [9, 10]. APP possesses a large extracellular *N*-terminal domain and a small intracellular *C*-terminus and is the only family member with an Aβ domain. APP's processing follows two major pathways, depending on the secretase cleaving APP (Figure **3**).

In the non-amyloidogenic pathway, APP is cleaved by α-secretase in the Aβ domain, releasing soluble APPα (APPsα) into the extracellular space, where it can execute its intended biological functions like regulation of neuronal stem cell proliferation and early central nervous system (CNS) development [11, 12].

Cleavage of APP by β-secretase, also called BACE-1, leads to the amyloidogenic pathway. In this case, APP is cleaved just after the Aβ domain releasing APPsβ. The remaining *C*-terminal domain is further cleaved by the γ-secretase complex resulting in the production of Aβ peptides. These peptides – depending on their length – are prone to accumulation and oligomerization forming neurotoxic Aβ plaques [13, 14].

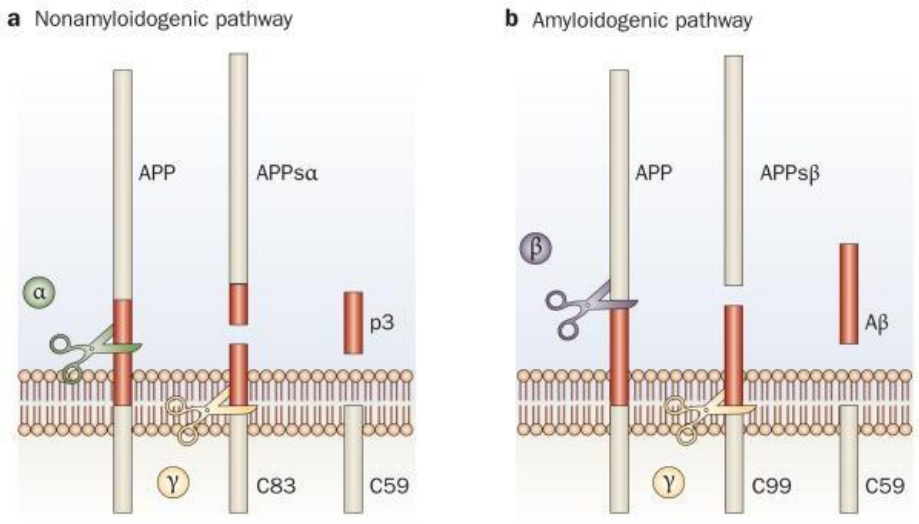

Figure 3. Processing of APP by the secretases. **a)** In the nonamyloidogenic pathway, APP is first cleaved by α-secretase within the Aβ sequence, which releases the APPsα ectodomain. Further processing of the resulting carboxyl terminal by γ-secretase results in the release of the p3 fragment. **b)** The amyloidogenic pathway is initiated when β-secretase cleaves APP at the amino terminus of the Aβ peptide and releases the APPsβ ectodomain. Further processing of the resulting carboxy-terminal fragment by γ-secretase results in the release of Aβ. Abbreviations: Aβ, amyloid-β; APP, amyloid precursor protein; APPsα, soluble amyloid precursor protein-α; APPsβ, soluble amyloid precursor protein-β; C83, carboxy-terminal fragment 83; C59, carboxy-terminal fragment 59; C99, carboxy-terminal fragment 99 [15].

Based on the amyloid hypothesis, there are several possibilities to interact with the cascade to alter disease progression. Firstly, promoting the cleavage by α-secretase or inhibiting β-secretase and/or γ-secretase and therefore favouring the non-amyloidogenic pathway. Secondly, reduction of Aβ plaques, either through compounds with anti-aggregating properties or by promoting removal of the deposits [15]. However, until now all therapeutic approaches based on the amyloid cascade hypothesis have failed in clinical trials as their translation from preclinical to clinical phases did not meet the desired efficacy [16].

2.2. τ Hypothesis

The second hypothesis that needs to be discussed revolves around neurofibrillary tangles (NFTs), which are formed by hyperphosphorylated τ proteins. The τ protein is a protein associated with microtubules, promoting tubulin assembly and stabilizing the aggregates within cells, and is mainly found in axons (Figure **4**). Furthermore, τ proteins play a crucial role in the axonal transport by modulation of anterograde and retrograde transports. Phosphorylated τ proteins can even prevent neuronal cell death by stabilizing β-catenin [17].

Six isoforms of τ are expressed in human brains by alternative mRNA splicing of exons 2, 3 or 10. Depending on the presence or absence of exon 10, τ proteins possess either three or four microtubule-binding domains, resulting in differing binding strengths [18, 19]. In a healthy brain, both isoforms occur in a 1:1 ratio. Any off-balance affects the interactions with microtubules. Phosphorylation is one of the mechanisms of τ protein regulation. In an unaffected brain, τ is phosphorylated on two to three residues. In a tauopathic brain, the protein is hyperphosphorylated with up to nine residues affected, caused by an imbalance between the activities of τ kinases (GSK-3β, CDK-5, MAPK) and τ phosphatases (PPA2). In the hyperphosphorylated state, interaction with microtubules is reduced and τ protein degradation is lowered by resistances towards proteases and the ubiquitin-proteasome pathway [20-22]. This leads to accumulation of hyperphosphorylated τ proteins and their fibrillization to NFTs, present in AD brains.

Therapeutic approaches to the τ hypothesis are 1) inhibition of abnormal hyperphosphorylation of τ by modulation of kinase activities on the one hand, and activation of τ phosphatases on the other hand [23]; 2) activation of disassembling mechanisms (i. e. the ubiquitin-proteasome pathway) and 3) use of anti-aggregating small molecules [17]. Similar to the

amyloid hypothesis, these approaches did not yield any compounds passing clinical trials. In fact, attempts to modulate kinases did not show the necessary positive results and often lead to off-target effects *in vivo* [24].

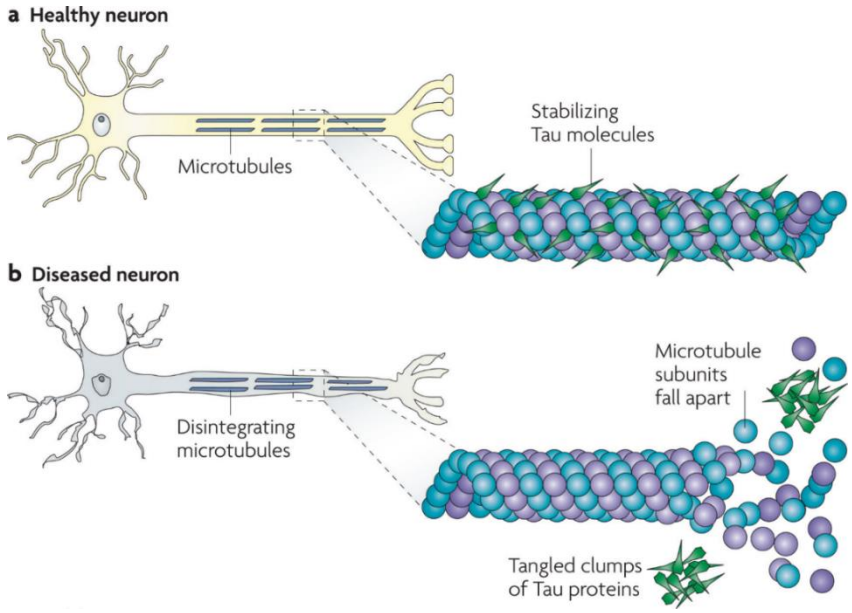

Figure 4. τ in healthy neurons and in tauopathies. τ facilitates microtubule (MT) stabilization within cells and it is particularly enriched in neurons. MTs serve as "tracks" that are essential for normal trafficking of cellular cargo along the lengthy axonal projections of neurons, and it is thought that τ function is compromised in Alzheimer's disease and other tauopathies. This probably results both from τ hyperphosphorylation, which reduces the binding of τ to MTs and through the sequestration of hyperphosphorylated τ into neurofibrillary tangles (NFTs) so that there is less τ to bind MTs. The loss of τ function leads to MT instability and reduced axonal transport, which could contribute to neuropathology [24].

2.3. Cholinergic Hypothesis

Cholinergic dysfunction and a loss of neurons is the base of the third hypothesis. In AD the cognitive decline is associated with a general loss of cholinergic function in the CNS. Cholinergic neurons, which are found all throughout the brain and take part in all brain functions, use the endogenous neurotransmitter acetylcholine (ACh). Proteins that produce, store, transport and degenerate the neurotransmitters are crucial for healthy neurotransmission [25].

ACh is produced by choline acetyltransferase (ChAT) which reacts acetyl-CoA with choline in the cytoplasm of neurons (Figure **5**) [26]. ACh is transported into synaptic vesicles by the vesicular acetylcholine transporter (VAChT) and is then released into the synaptic cleft to

activate postsynaptic nicotinic and/or muscarinic acetylcholine receptors (AChR), causing downstream effects. Unlike most neurotransmitters, which must be re-uptaken by neurons for their inactivation, ACh is rapidly cleaved in the synaptic cleft by acetylcholinesterase (AChE) producing choline and acetate [27]. Choline re-uptake after hydrolysis of ACh from the synaptic cleft is rate limiting to the production of new ACh within neurons [28]. It was shown that knockout mice, missing the necessary choline transporter 1 (CHT1), are nonviable, proving the importance of the transporter to the reproduction of ACh [29].

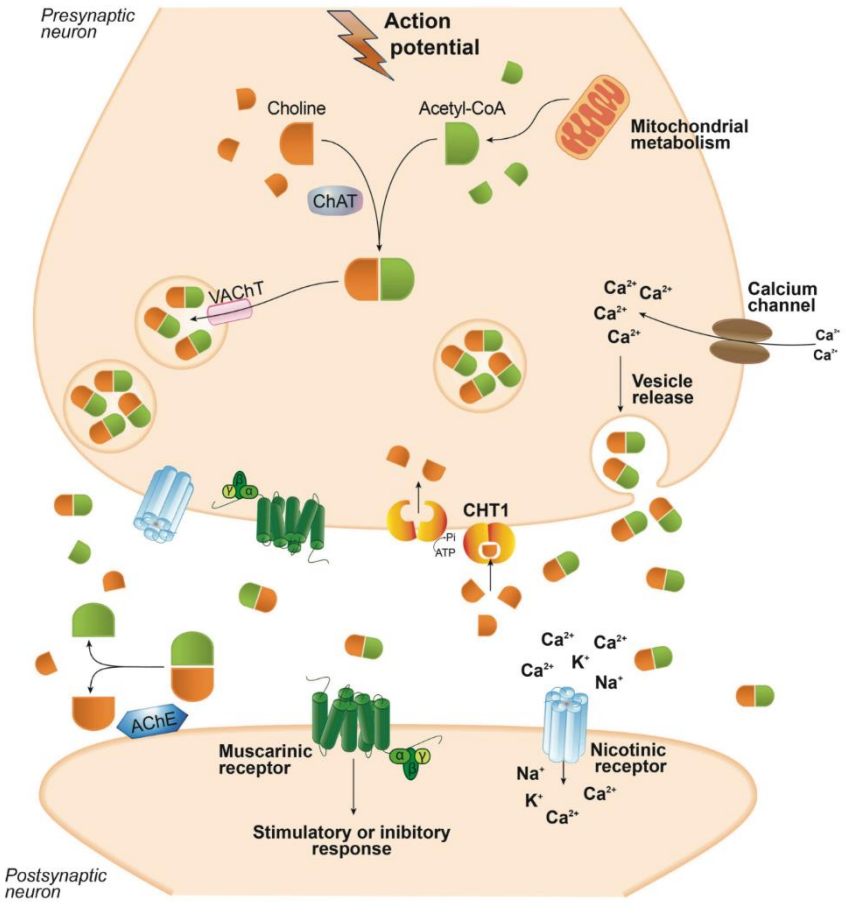

Figure 5. Schematic representation of biological aspects involving acetylcholine neurotransmission [25].

A disrupted cholinergic system can influence cognition, memory and behaviour. In AD reduced activities of ChAT and acetyl-CoA lead to decreased production of ACh, which results in a loss of cognitive functions. Furthermore, reports showed that impairments of AChRs in animal models lead to deficits similar to those in AD. These impairments can at least be partially reversed using cholinergic drugs [30-32]. Therefore, a therapeutic approach based on the

cholinergic hypothesis is the enhancement of ACh production and transport either by increasing concentrations of precursor substances or by reducing the activity of proteins degrading ACh, like AChE. The latter is used in practice with AChE inhibitors as stated above (*cf*. Part **1.**). A second approach is targeting the synaptic cleft or the postsynapse by addressing nicotinic and muscarinic AChRs directly with small molecules.

3. Design and Synthesis of Dualsteric M_1-Receptor Agonists

3.1. Acetylcholine Receptors

Activation of AChRs was shown to restore cognitive functions and memory, making them an interesting therapeutic target. These receptors are divided into two subclasses, nicotinic acetylcholine receptors (nAChRs) and muscarinic acetylcholine receptors (mAChRs). This differentiation is made depending on the drug the receptor type responds to – nicotine or muscarine [33].

Nicotinic AChRs are, in general, ionotropic receptors and therefore belong to the superfamily of ligand-gated ion channels. Activation, by an agonist like ACh or other nicotinergic substances, stabilizes the receptor in an open state, enabling the gating of cations, like Na^+, K^+ and Ca^{2+}, through the cell membrane. In the cholinergic system, nAChRs can regulate the release of neurotransmitters. However, there is a wide variety of subtypes of nAChRs, which take on different roles in the cholinergic system as well as in non-neuronal tissues and the peripheral nervous system [34].

Muscarinic AChRs are G-protein coupled receptors (GPCRs) and are expressed in both the central and peripheral nervous system. Muscarinic AChRs are activated by ACh or muscarinic substances and their responses are dependent on subtype and localization of the receptor [35]. These receptors play a central role in human physiology. Regulation of muscle contraction, heart rate, glandular secretion and functions of the CNS like motor, sensory, cognitive, behavioural and autonomic processes are among their functions [36]. Changes in mAChR activities and levels have been shown to be part of the pathophysiology of Parkinson's disease, schizophrenia, depression and AD.

Muscarinic AChRs are divided into five subtypes M_1 to M_5. Each subtype is distinctly distributed in the CNS and peripheral tissues. Receptors M_1, M_4 and M_5 are mainly expressed in the CNS. M_2 and M_3 are additionally expressed in peripheral tissues. Most types of tissues show a characteristic expression of two or more of mAChR subtypes [37, 38].

Subtypes M_1, M_3 and M_5 couple to the family of $G_{q/11}$-proteins, activating phospholipase C (PLC), thus initiating the phosphatidylinositol triphosphate cascade. Phosphatidyl 4,5-bisphosphate (PIP2) is cleaved into diacylglycerol (DAG) and inositol 1,4,5-trisphosphate (IP3). DAG activates protein kinase C (PKC) and IP3 controls the intracellular Ca^{2+} release. PIP2 is further responsible for activation of other membrane proteins, such as ion exchangers and the M-current channel. Receptors M_2 and M_4 couple to $G_{i/0}$-proteins. These receptors inhibit adenylyl cyclase (AC) activity on the one hand and activation of G-protein-gated K^+-channels on the other hand. Inhibition of AC reduces production of cAMP from ATP (Figure **6**).

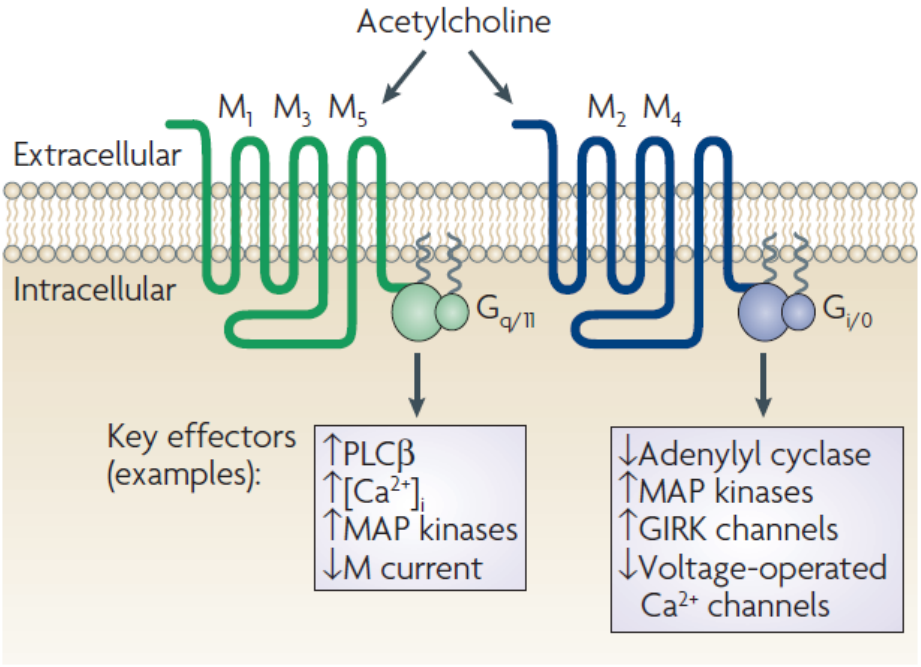

Figure 6. Subclassification of mAChRs based on differential G-protein-coupling properties. In this simplified scheme, only some of the key downstream effector proteins (enzymes or ion channels) are indicated. It is well documented that distinct mAChRs can modulate the activity of a wide array of phospholipases, ion channels, protein kinases and other signalling molecules. Moreover, the cellular effects caused by mAChR stimulation are mediated by both activated G-protein α-subunits as well as free βγ complexes generated following receptor-mediated G-protein activation [37].

Due to the complexity of downstream events, functions and physiological roles of mAChRs are only partially understood. Elucidation of specific receptor functions is complicated by insufficient subtype selectivity of small molecule ligands. However, *in vivo* models of knockout mice missing one of the subtype receptors were able to shed some light on the physiological roles of each individual mAChR subtype [39, 40]. Using M_2 knockout mice it was shown that the M_2-subtype influences muscarinic-agonist induced analgesia [41], reduces the inhibition of muscarinic receptor-mediated Ca^{2+}-channels [42] and controls the cholinergic deceleration of the heart rate [43]. The M_3-subtype was shown to mainly play a part in smooth muscle contractions (urinary bladder, ileum, stomach fundus, trachea and gallbladder), as M_3 knockout mice did not show a contraction in these tissues [44]. Cognitive and behavioural deficits, however, were not observed [45]. M_4 knockout mice showed increased locomotor activity and mice missing the M_5 receptor showed reduced dilation of cerebral arteries [46, 47].

3.2. The Muscarinic M_1 Acetylcholine Receptor

The M_1-subtype makes up for 50-60% of mAChRs in the forebrain and is expressed in the cerebral cortex, hippocampus and striatum. These brain regions are responsible for functions impaired in AD, like memory, cognition and learning, making the muscarinic M_1 acetylcholine receptor a target for AD treatment. Furthermore, activation of the M_1-receptor was shown to positively influence both the formation of Aβ and NFTs [48-51]. Stimulation of the receptor increases the production of α-secretase through PKC activation, favouring the non-amyloidogenic pathway and therefore suppressing the aggregation of toxic Aβ and the formation of plaques. Activation of PKC also modulates the GSK-3β cascade stabilizing microtubules and ameliorating τ pathology.

It was further shown that receptor activation can reverse decreased cerebral blood flow and protect against oxidative stress, caspase activation, DNA damage and mitochondrial impairment in cells (Figure **7**) [52, 53]. The positive effects M_1 activation can exert, were recently shown in transgenic mice [54]. As postsynaptic AChRs remain mostly intact during presynaptic cholinergic hypofunction, targeting the mAChRs directly may circumvent the depletion of the endogenous neurotransmitter ACh both in early and later stages of the disease. There have been promising attempts targeting the M_1-receptor, but these were overruled by side effects. The unwanted effects can be explained by off-target actions by

activation of other mAChR subtypes. Specific and selective targeting of the subtypes is essential for further investigations of AD pathology and the development of treatments.

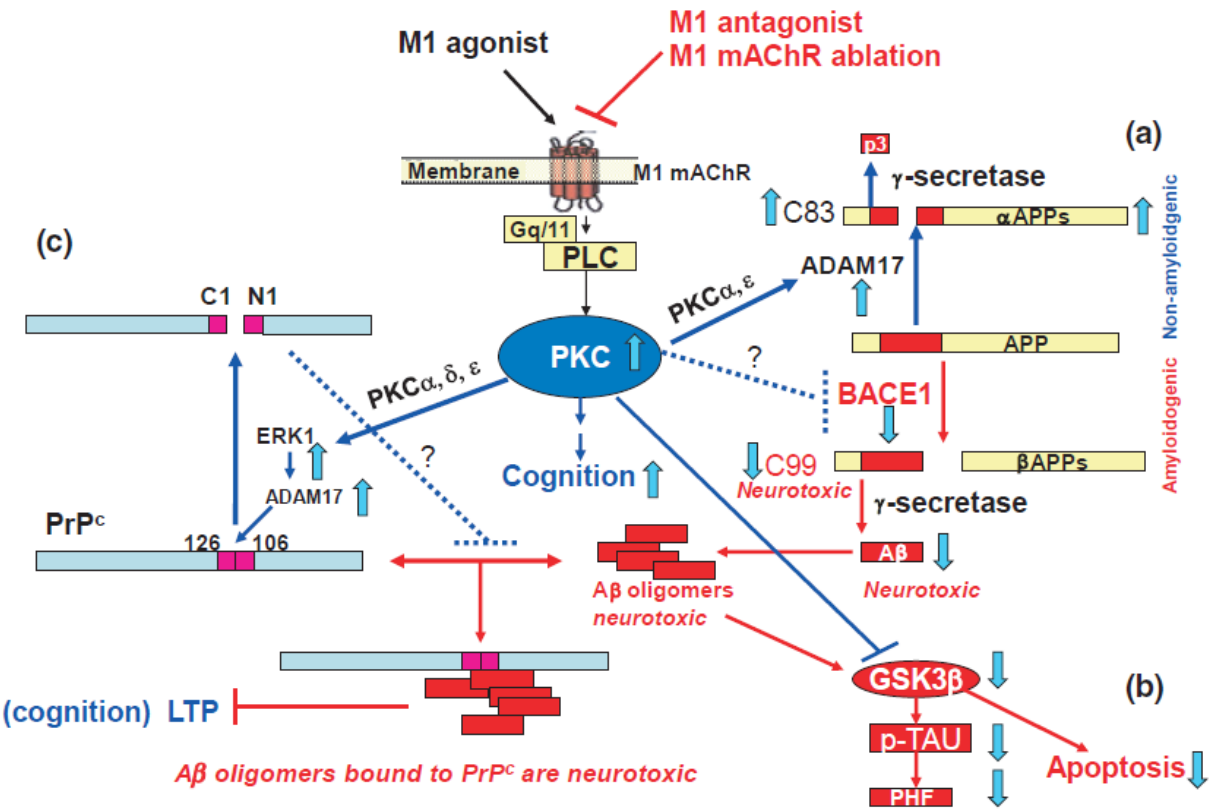

Figure 7. The linkage of M_1AChR with cognition and Aβ, hyperphosphorylated τ (tau-p), and PrP^C. M_1AChR-induced activation of PKC by an M_1 agonist – (i) restores cognitive deficits; (ii) activates ADAM17 and inhibits BACE leading to decrease of Aβ and C99 and increase of αAPPs and C88 **(a)**; (iii) inhibits GSK-3β, decreasing Aβ-induced apoptosis and tau-p, respectively **(b)**; and (iv) cleaves PrP^C to C1 and N1 fragments and may prevent binding of Aβ oligomers to PrP^C, preventing LTP inhibition and cognitive deficits **(c)**. M_1 antagonists or ablation of M_1AChR prevents the effects of an M_1 agonist and can elevate Aβ levels, GSK-3β, tau-p. Abbreviations: ADAM17, A disintegrin and metalloproteinase domain 17; $G_{q/11}$, a G-protein; PrP^C, cellular prion protein; PLC, phospholipase C; LTP, long-term potentiation; symbol: arrow – activation; block arrow – upwards (increase), downwards (decrease); 'T-shaped' line – inhibition [51].

3.3. Design of Dualsteric Target Compounds

Selectively targeting one mAChR subtype is a very challenging task. The five subtypes share the same endogenous ligand and main binding pocket – the orthosteric binding site – which makes the development of a selective orthosteric ligand extremely difficult. Besides the orthosteric site, secondary binding sites – allosteric binding pockets – have been identified. Allosteric binding sites are less conserved than orthosteric ones and show greater divergence in their amino acid sequence. Therefore, the allosteric sites can be used to develop selective

ligands among the receptor subtypes. Allosteric ligands, however, have been shown to cause diverse receptor responses and are categorized into allosteric agonists and allosteric (positive or negative) modulators [55]. Allosteric agonists are able to activate the receptor by themselves, whereas modulators only modify affinity and/or efficacy of an orthosteric ligand [56, 57]. Binding of both allosteric and orthosteric ligands to a receptor may exert cooperative features, influencing each other in positive, negative or neutral ways [56]. A combination of orthosteric and allosteric ligands connected by a linker is called a dualsteric ligand. These ligands are designed to bind to a specific receptor (or subtype) via the allosteric part as well as causing a receptor response through binding of the orthosteric moiety (Figure **8**). This message - address concept has the advantage that it is not reliant on the endogenous ligand on the one hand and that these dualsteric ligands may be able to cause biased signalling, activating a specific downstream signal, on the other hand [56, 57].

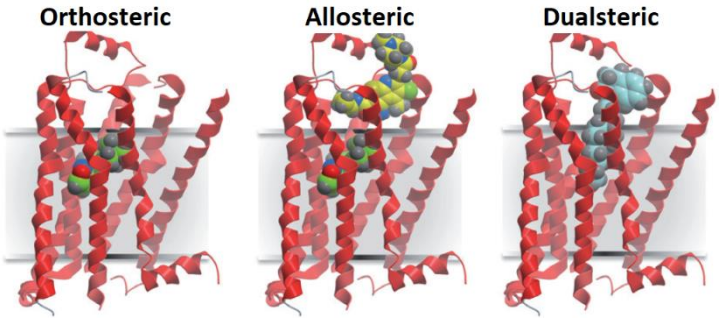

Well-defined SAR	✓	✗	✗
High affinity	✓	✗	✓
Subtype selectivity	✗	✓	✓
Spatial and temporal selectivity of endogenous signalling	✗	✓	✗

Figure 8. Modes of targeting mAChRs by different classes of ligands. Orthosteric ligands (green) bind to the site recognized by the endogenous agonist (acetylcholine) for the receptor. Allosteric ligands (yellow) bind to a topographically distinct site. Dualsteric ligands (blue) concomitantly interact with both orthosteric and allosteric sites. The key properties generally associated with each mode of receptor targeting are also indicated [35].

Designing such a ligand one needs to be aware of the possible changes of altering the pharmacophores. Upon binding of the allosteric part, the receptor might change its conformation and the affinity of the orthosteric part and vice versa. Furthermore, the connection of the linker moiety plays a crucial role, as this may prevent pharmacophores to

bind or at least alter binding to the receptor. Length and rigidity of the linker also need to fit the requirements of the receptor that both pharmacophores can reach their binding sites. This is especially true for receptors of which the structure has not been elucidated yet, as it was the case with the M_1AChR at the beginning of this work. A crystal structure of the M_1AChR with binding of the inverse agonist tiotropium was published only recently [58].

The aim of this work was the synthesis of two sets of compounds, each connecting the cholinergic agent carbachol via an alkyl linker to two M_1-selective allosteric ligands.

The orthosteric part carbachol was chosen because it is a derivative of the endogenous neurotransmitter acetylcholine and therefore acts as an AChR agonist. A significant advantage compared to acetylcholine is that carbachol is less prone to hydrolysis and inhibits AChE, which would further counteract the cholinergic hypofunction in AD [59].

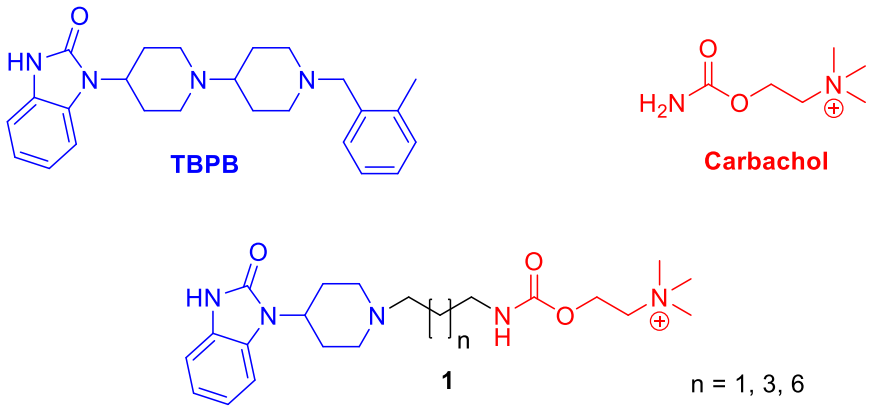

Figure 9. Design of target structures **1**. Combination of TBPB and carbachol by alkylene linkers of variable length.

The allosteric moieties were chosen to be TBPB and BQCA. TBPB was developed at the Vanderbilt University as an M_1AChR selective allosteric agonist [60]. It was shown that its selectivity is indeed a consequence of the compound's binding to an allosteric site rather than the orthosteric site. Activation by TBPB led to a shift towards the non-amyloidogenic pathway and reduced Aβ production *in vitro*. The binding domain of TBPB is the same as the one of AC-42. For AC-42 and its analogues, it was shown that the allosteric site is adjacent to the orthosteric site and both sites can be linked [61, 62]. Due to the structural similarities, the same should be possible for TBPB. In a previously published paper by our working group, a similar approach was taken. TBPB was connected to AF292, described as a selective M_1-

agonist [63], but these dualsteric compounds did not show the intended agonism [64]. AF292 was therefore replaced by carbachol. Figure **9** shows the design of target structures **1** combining TBPB with carbachol to form dualsteric ligands.

The second allosteric moiety is BQCA. It is described as a positive allosteric modulator [65], capable of reducing the concentration of acetylcholine required to activate the receptor by 129-fold, without activity at other mAChR subtypes [66, 67]. The structure of BQCA was intensively studied to develop structure - activity relationships [reviewed in 68, 69]. Fine tuning of these compounds is rather difficult as each change in structure shows its advantages and disadvantages. We, therefore, decided to incorporate a fluorine at position 8 of the A-ring and substitute the benzyl moiety (B-ring) with a naphthalene moiety to increase potency at the receptor [70], similar to the compounds described before by our group [64]. Figure **10** shows the target structures **2** combining carbachol with the BQCA-derived moiety.

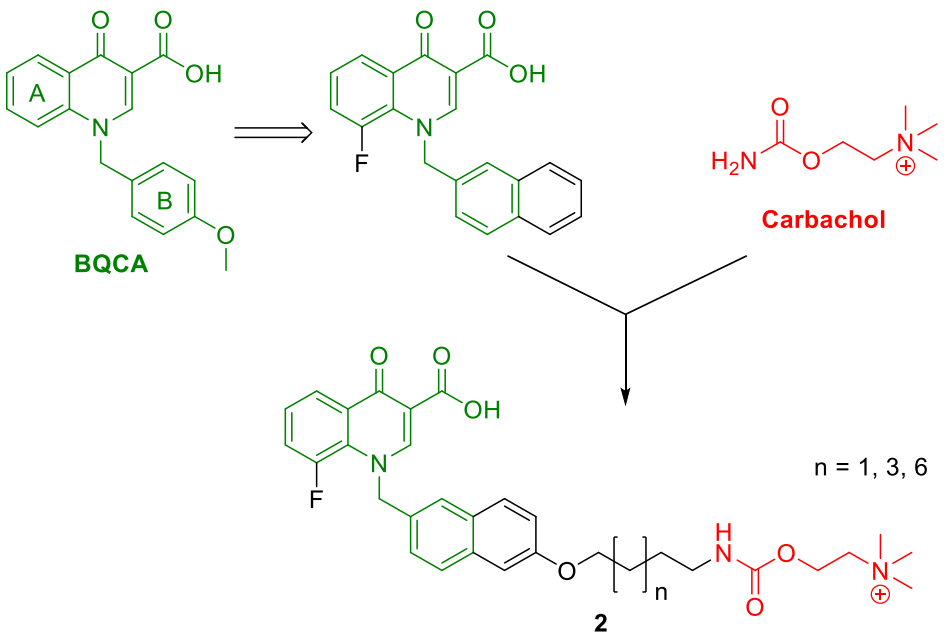

Figure 10. Design of target structures **2**. Combination of BQCA and carbachol by alkylene linkers of variable length.

It is also important to mention, that the designed compounds are quaternary salts, which are not able to penetrate the blood-brain barrier. Thus, they are not designed to be used as drug molecules but rather as tools for investigation of dualsteric ligands and the pharmacology of the M_1-receptor.

3.4. Synthesis of Dualsteric Ligands

3.4.1. Synthesis of Dualsteric TBPB-derived Compounds

The overall strategy for the synthesis of the TBPB-compounds **1** was a straightforward approach. TBPB-building block **3** was connected to the Boc-protected linkers **4** before the carbachol moiety was introduced in the last steps (Scheme **1**).

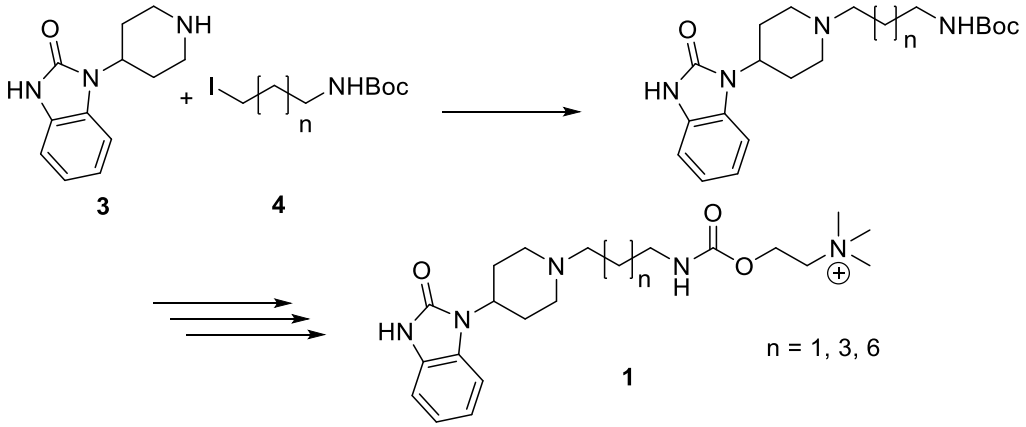

Scheme 1. Short depiction of the synthetic strategy.

Synthesis of the TBPB-building block **3** is well described in literature [71, 72] and could be achieved in excellent yields (Scheme **2**). A nucleophilic substitution reaction of commercially available 1-fluoro-2-nitrobenzene with a carboxyl protected 4-aminopiperidine in dimethylformamide yielded nitroaniline **5**. Reduction of the nitro group was achieved using hydrogen atmosphere and palladium on activated charcoal in quantitative yields within five hours. The benzimidazolone moiety was synthesised in a ring closing reaction with carbonyldiimidazole in tetrahydrofuran at room temperature, which was adopted from Xu *et al.* [73]. Deprotection of the piperidine was achieved by basic hydrolysis. Due to the high polarity of building block **3**, its subsequent extraction proved to be the most difficult part of these first few steps. Repeated extraction steps were required to reach satisfying yields.

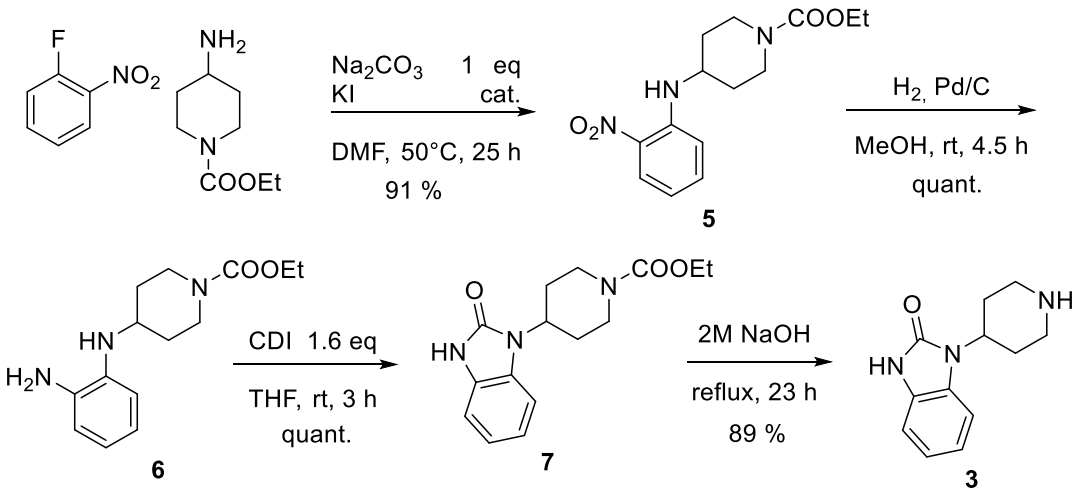

Scheme 2. Synthesis of TBPB-building block **3**.

The C_8-linker **4c** was synthesised from 1,8-octandiol. Mono-tosylation of the diol gave compound **8**, which was subjected to a substitution reaction with sodium azide in dimethylformamide. The azide was reduced with lithium aluminium hydride yielding 8-aminooctanol **9**. For the synthesis of the linkers **4**, 3-aminopropanol, 5-aminopentanol and 8-aminooctanol **9** were Boc-protected under basic aqueous conditions. The Boc-protected compounds **10** were subsequently used in an Appel reaction to introduce iodine as a leaving group (Scheme **3**).

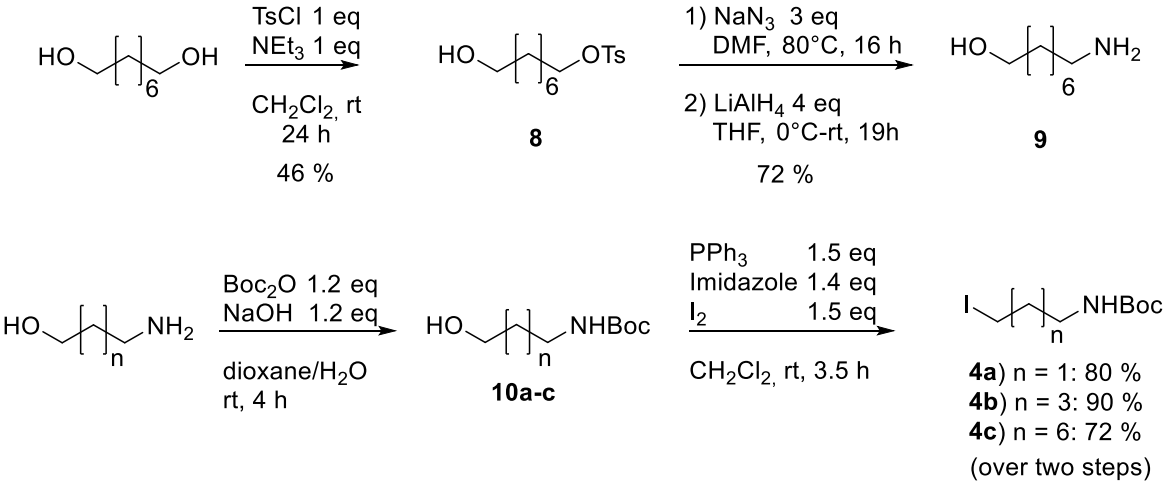

Scheme 3. Synthesis of linkers **4**.

The two building blocks **3** and **4** were connected in another substitution reaction to give compounds **11**. Crucial for successful purification by column chromatography was the use of deactivated silica gel because the basic compounds would otherwise react with the slightly acidic stationary phase and decompose. Deactivation was achieved by packing of the column with an additional 1.5% triethylamine in the solvent system. After packing the triethylamine was omitted. The next synthesis step was the removal of the protection group. Deprotection was achieved using 4 M HCl in dioxane as solvent. Extraction of the free amines **12** proved to be as difficult as described above (for compound **3**). The carbamates **13** were synthesised using 2-chloroethyl chloroformate under basic conditions. At first, reactions were run in dimethylformamide with potassium carbonate as a base. Compounds **13a** and **13b** were synthesised this way, but only in low yields. For compound **13c** the procedure was therefore changed to using pyridine as a base in dry dichloromethane. This reaction was finished within 30 min and showed a highly improved yield (Scheme **4**).

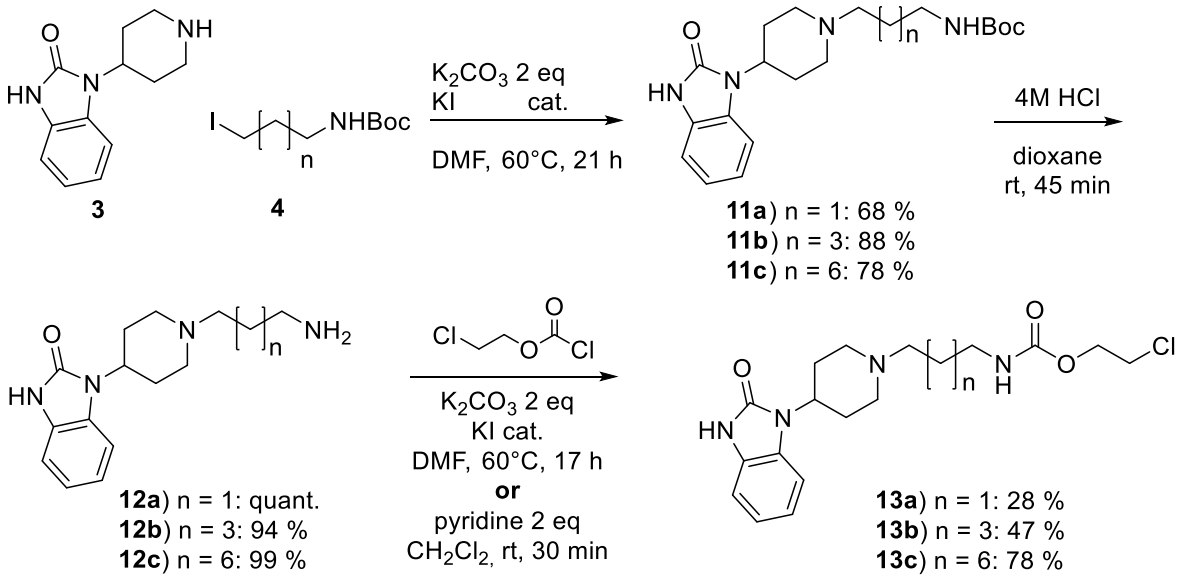

Scheme 4. Synthesis of precursor **13**.

The previously described deprotection using HCl in dioxane was also attempted using trifluoroacetic acid in dichloromethane. While this reaction was also successful, the subsequent carbamate formation proved to be more difficult. Traces of the trifluoroacetic acid salt would react with the chloroformate to form an asymmetric anhydride. The trifluoro-

moiety of the anhydride reacted more easily with the amine, resulting in a significant impurity **14**, which was hardly removable by column chromatography (Scheme **5**).

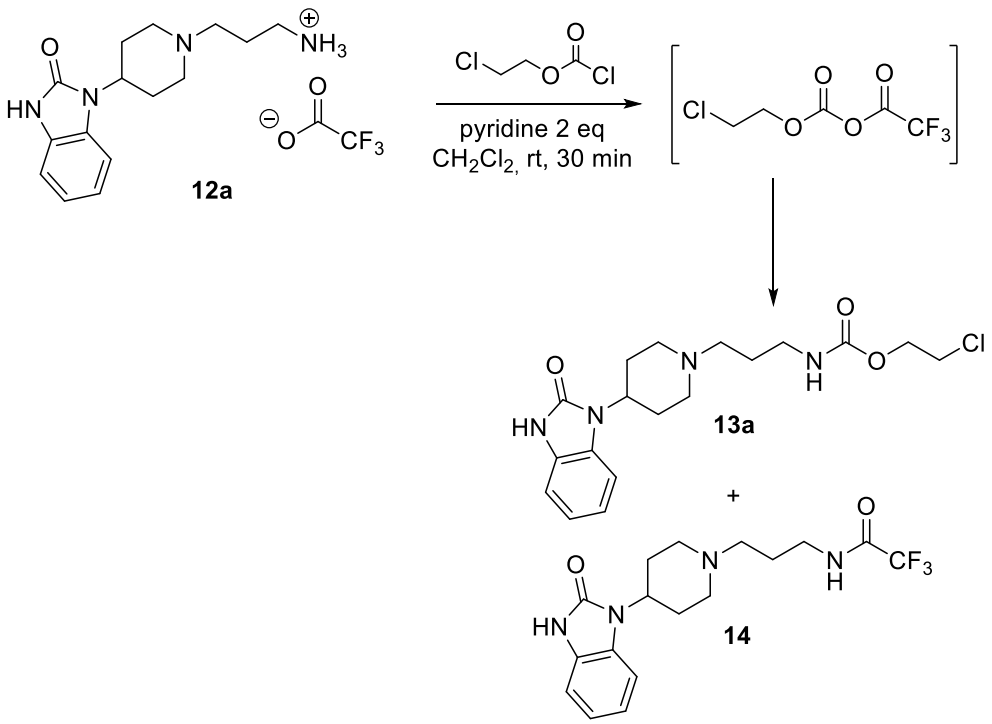

Scheme 5. TFA-salts cause impurities in the carbamate formation.

The last reaction in the sequence was the substitution reaction of the chloro-compounds **13** with trimethylamine for the formation of the carbachol moiety and target compounds **1** (Scheme **6**).

These reactions required a large excess of trimethylamine. The respective starting material **13** was dissolved acetonitrile and trimethylamine in water was added. The reaction was heated to 70°C - 80°C in a sealed vessel for at least one night to show full conversion of the starting material **13**. After the reaction finished, volatiles were removed *in vacuo* to leave the crude product, which contained not only compound **1** but several decomposition products, due to hydrolysis, and trimethylamine salts. Purification of the compounds proved to be very difficult. Normal phase column chromatography was not possible as the compounds did not move over the stationary phase. Attempts at crystallisation also failed. On the one hand because of the compounds' hygroscopic nature and on the other hand, because these compounds behave like detergents, with one end being a salt and the other being quite unpolar. Acidification to

form di-salts did not improve the crystallisation behaviour. The only possible way to purify the compounds was the use of HPLC and additional observation by MS. Due to the high number of byproducts and difficult purification, compounds **1** were obtained in yields of only 13% to 20%.

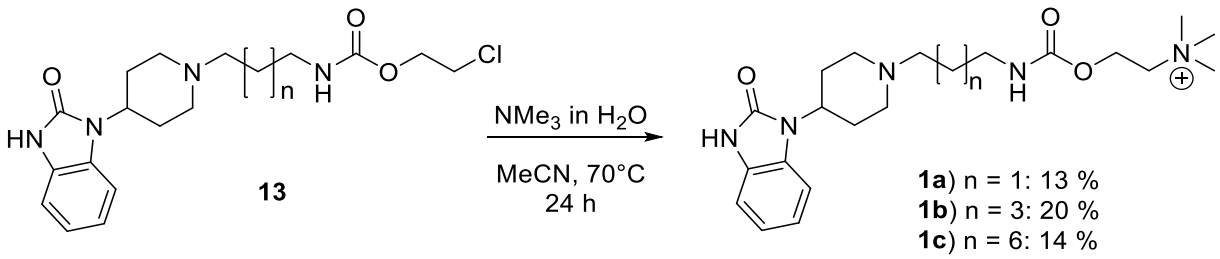

Scheme 6. Last step of the synthesis of dualsteric compounds **1**.

3.4.2. Synthesis of Dualsteric BQCA-derived Compounds

For the synthesis of the dualsteric BQCA-compounds, two strategies were tested. The initial strategy for the synthesis of compounds **2** is shown in Scheme **7**. The route involved the syntheses of the BQCA building block **15** and the naphthyl moiety **16**. The nitrile **17** then needed to be reduced to an amine **18** to reach the last steps of the synthesis.

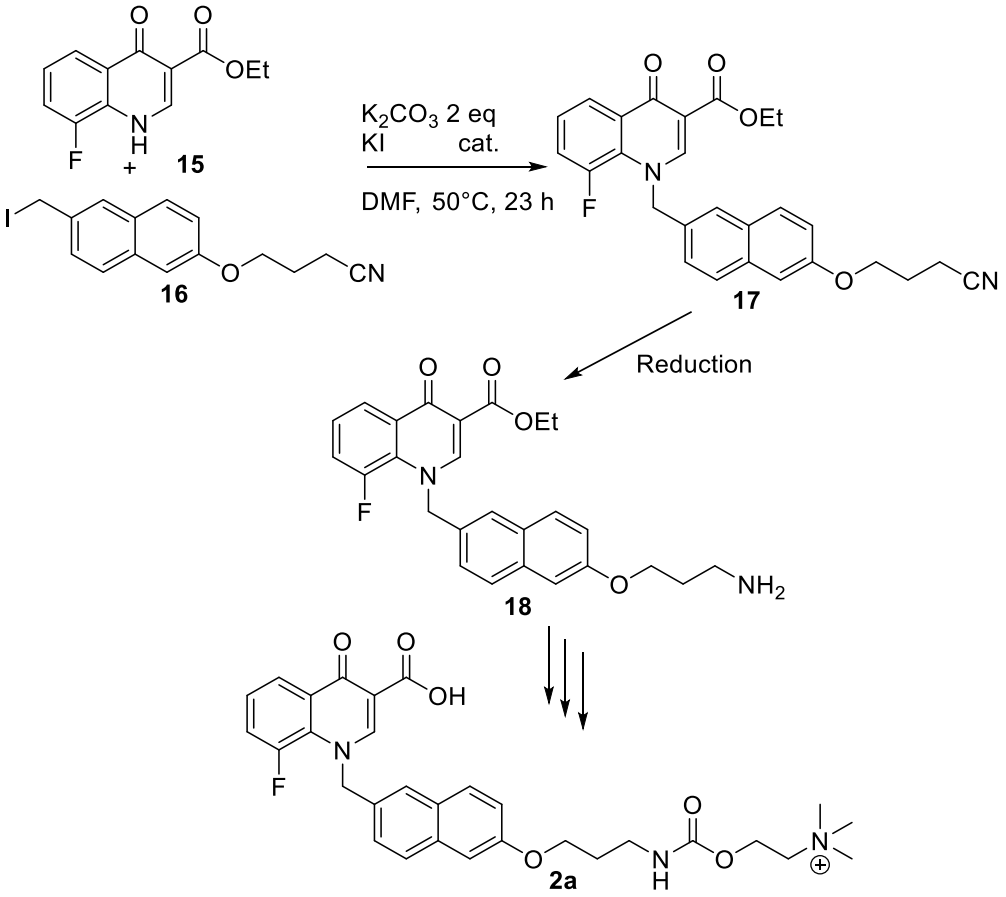

Scheme 7. Initial synthesis strategy for dualsteric compounds **2**.

Building block **15** was obtained by a one-pot Gould-Jacobs-synthesis [74, 75], reacting 2-fluoroaniline with diethyl ethoxymethylenemalonate solventless, followed by refluxing in diphenyl ether in a microwave reactor (Scheme **8**). For building block **16**, 6-hydroxy-2-naphthoic acid was esterified and reduced to 6-(hydroxymethyl)naphthalen-2-ol **19**. The diol **19** was reacted with 1-chloro-3-iodopropane. The resulting chloro-compound **20** was converted into the respective nitrile **21** through reaction with sodium cyanide. An Appel reaction yielded the second building block **16** (Scheme **8**).

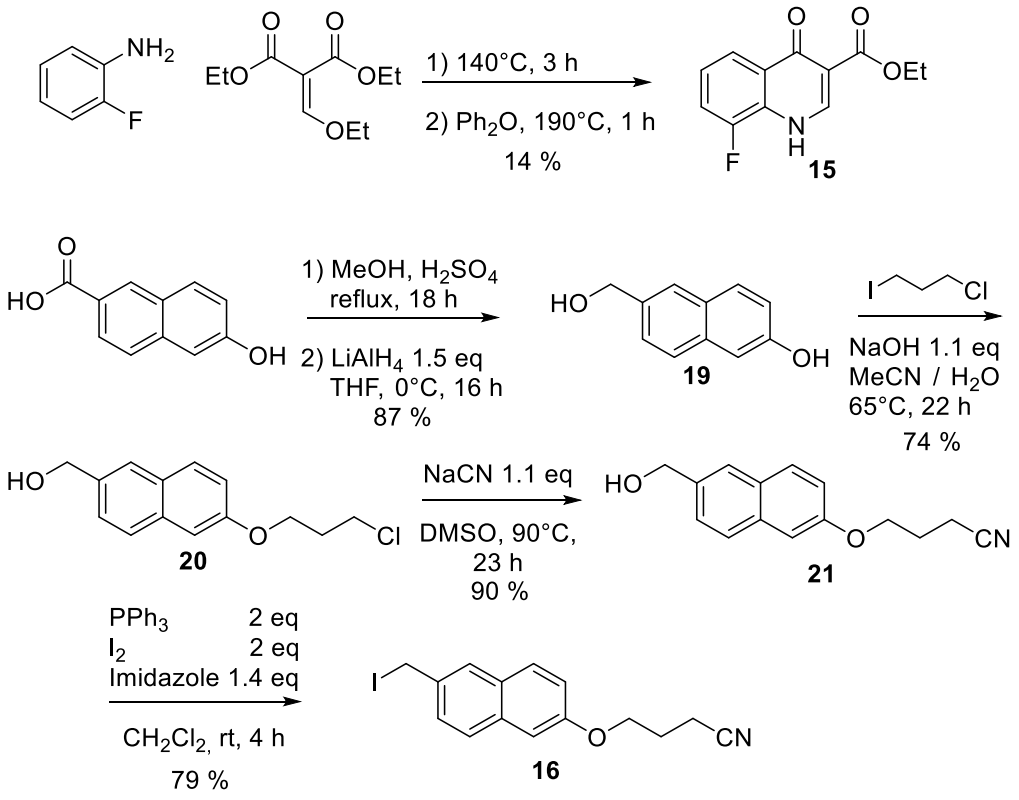

Scheme 8. Synthesis of building blocks **15** and **16**.

The quinolone **15** and the naphthyl moiety **16** were connected in a substitution reaction. The next step in the synthesis was the reduction of the nitrile **17** to yield the amine **18** (Scheme **9**). Several reduction methods were tested, but none of them led to the desired product. Reactions with borane [76] showed slow conversion and a variety of unidentified byproducts upon harshening the conditions. The reduction under hydrogen atmosphere with platinum oxide [77], and palladium on activated charcoal showed no conversion and hydrogenation of the alkene, respectively. In the reaction with Raney nickel [78] several byproducts, like reduced alkene and ester cleavage were identified by LCMS. Because a selective reduction of the nitrile seemed unlikely, this strategy was discarded and a similar route to the above described TBPB-compounds **1** was pursued.

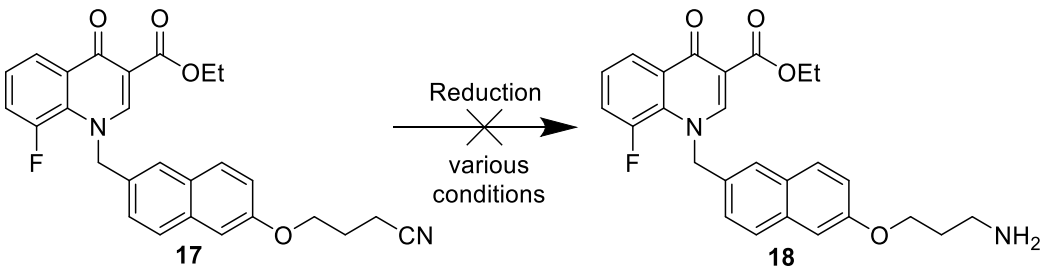

Scheme 9. Attempted reduction to the amine **18**.

The second route used the same strategy of Boc-protection and deprotection as described above (*cf*. **3.4.1.**). The quinolone building block **15**, the naphthyl compound **19** and the linkers **4** were prepared as shown above (first route). The linkers **4** were connected to the naphthyl alcohol **19** in a substitution reaction to yield alcohols **22**. Introduction of the iodine leaving group by an Appel reaction gave compounds **23** (Scheme **10**). The iodine compounds **23** were used in the next reaction as fast as possible. During the second and third synthesis, they proved to be quite unstable. The reaction, extraction and column chromatography were working as expected, but upon evaporation of the solvent, the pure compounds **23** changed colour from yellow to orange/brown and TLC showed partial decomposition. Usage of bromine instead of iodine should circumvent these issues (*cf*. **3.4.3.**).

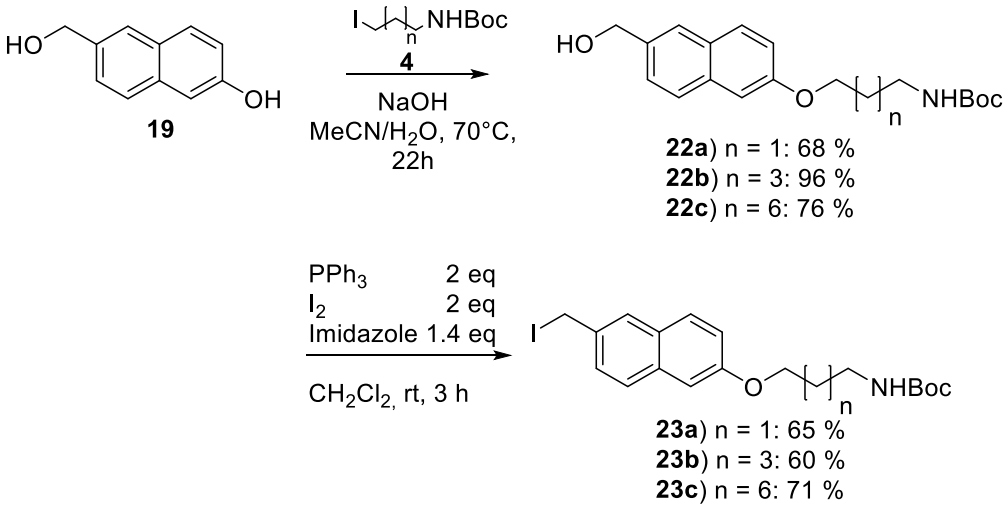

Scheme 10. Synthesis of naphthyl linkers **23**.

In the next step, the prepared iodine compounds **23** were connected to the quinolone core **15** in dimethylformamide under basic conditions (Scheme **11**). Boc-deprotection of **24** gave the free amines **25**. Subsequent formation of the carbamate with 2-chloroethyl chloroformate in dichloromethane with pyridine as base yielded the precursors **26**. Substitution with trimethylamine, in the second to last reaction, was conducted as described above (*cf*. **3.4.1.**). For saponification of the ester in the last step, the crude quaternary salts were dissolved in ethanol and lithium hydroxide was added in a very small amount of water. Due to the unpolar nature of the quinolones, a larger amount of water would cause precipitation, slowing the deprotection significantly. This reaction is only progressing in a reasonable timeframe without

producing major byproducts if it is a clear solution. Reaction progression was monitored by LCMS measurements, as the starting materials and products **2** showed the same retention on TLC and on HPLC. The disappearance of the ester's *m/z* ratio indicated full conversion. Target dualsteric compounds **2** were obtained in yields of 14% to 19% (Scheme **11**).

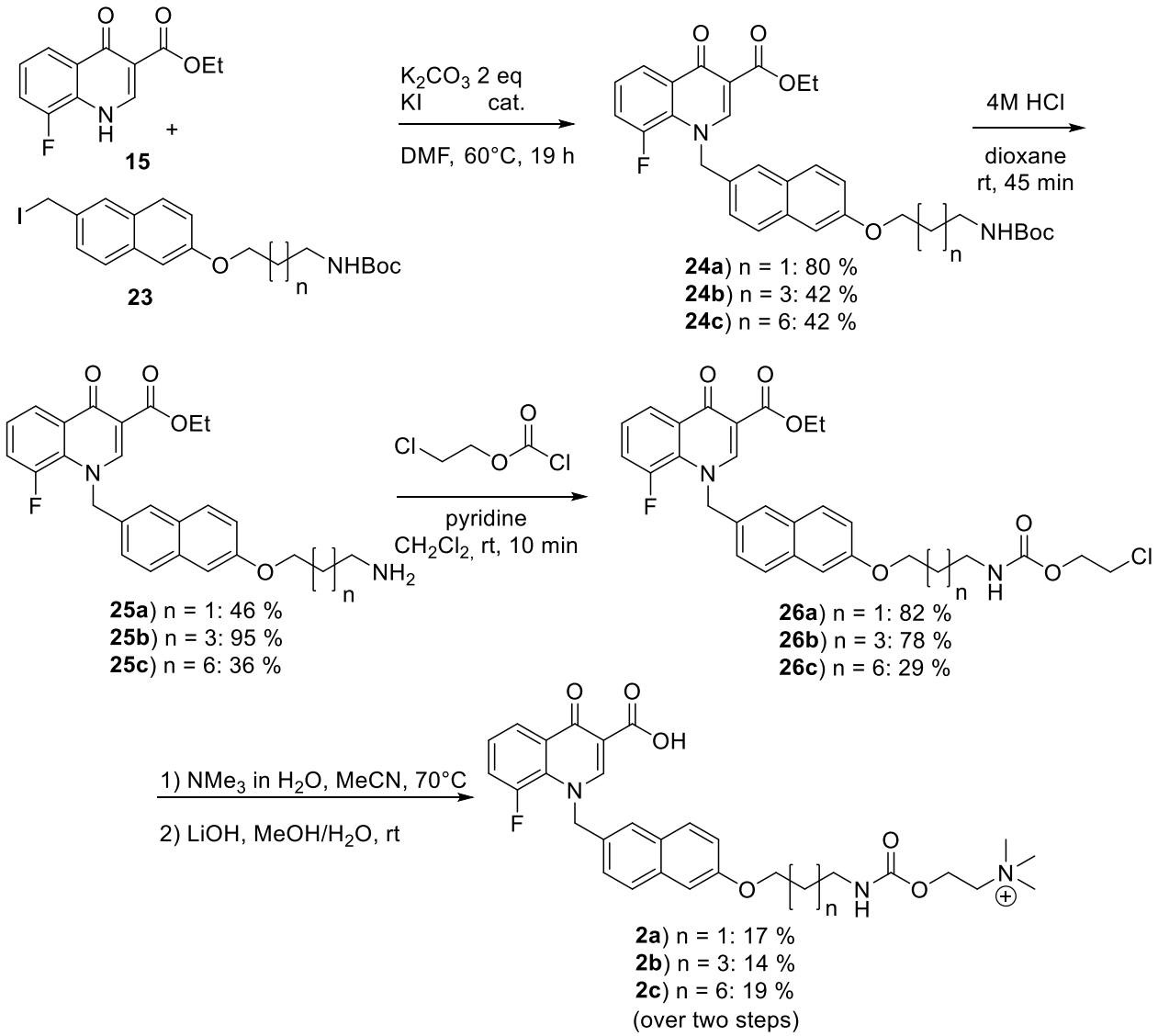

Scheme 11. Synthesis of dualsteric compounds **2**.

3.4.3. Synthesis of Reference Compounds

To be able to prove dualsteric binding modes of the designed compounds, reference compounds were required. Thus, the individual allosteric moieties connected to the linkers missing the orthosteric part were synthesised. Some of these compounds were already

published in previous work by Chen *et al.* [64]. The TBPB reference compounds **27** were synthesised by simple reaction of the piperidine **3** with the respective haloalkane (Scheme **12**).

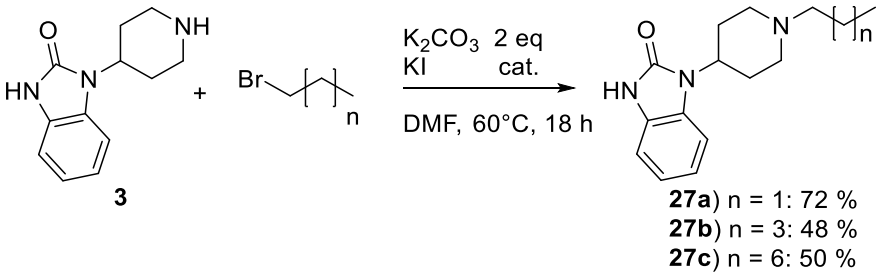

Scheme 12. Synthesis of TBPB reference compounds **27**.

The BQCA reference compounds were synthesised analogously to the quinolone compounds described above (Schemes **10** and **11**). The alcohol **19** was reacted with the respective haloalkane. The alcohols **28** were converted into the respective bromines **29** via an Appel reaction. The bromo-compounds **29** proved much more stable than the respective iodo-compounds **23** (*cf*. **3.4.2.**). Substitution of the bromine by quinolone **15** led to the esters **30**, which were hydrolysed in the last step to yield BQCA reference compounds **31** (Scheme **13**).

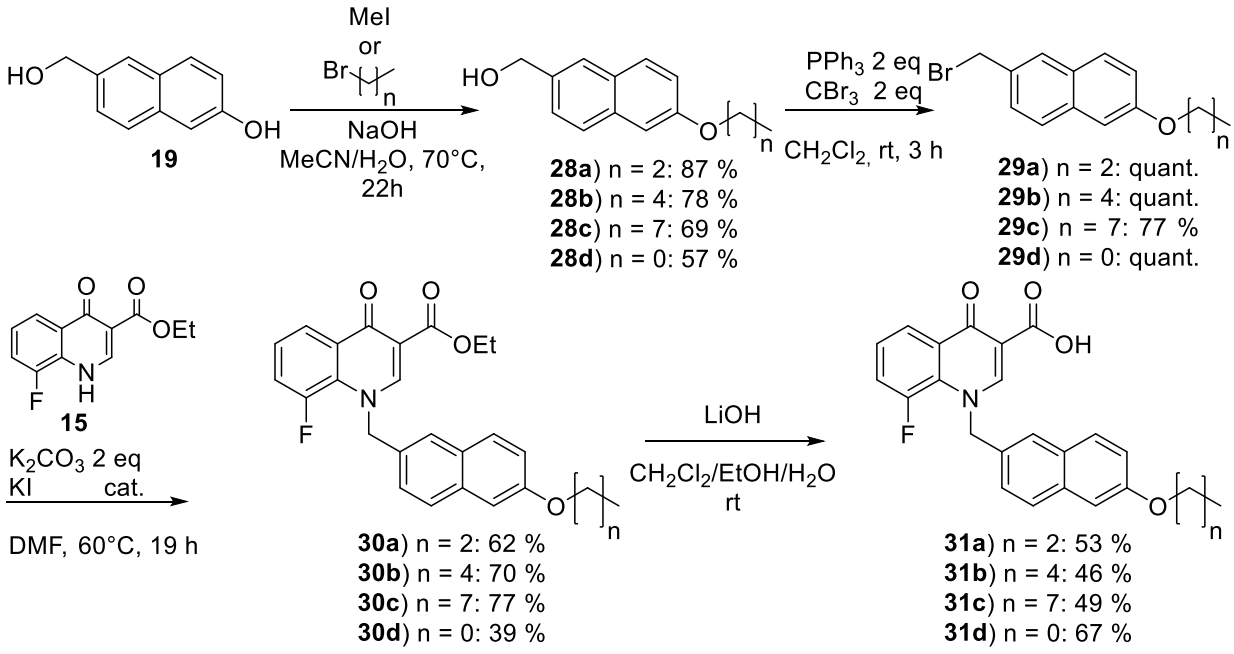

Scheme 13. Synthesis of BQCA reference compounds **31**.

3.5. Biological Activities of Dualsteric Ligands

The dualsteric compounds **1** and **2**, as well as reference compounds **27** and **31**, were evaluated in a modified version of the IP1 accumulation assay developed by CisBio Bioassays [79, 80]. The assays were conducted by Luca Agnetta (AK Decker, Universität Würzburg) to evaluate receptor responses through the phospholipase C pathway.

As described above (*cf*. **3.1.**), binding of an agonist to $G_{q/11}$-proteins causes activation of phospholipase C. Subsequently PIP2 is hydrolysed, releasing DAG and IP3. By measuring the IP3 concentration, a ligand-mediated G_q-coupled receptor response can be quantified. Measurement of the IP3 concentration is difficult due to its instability. However, IP3 hydrolyses rapidly to inositol biphosphate (IP2) and inositol monophosphate (IP1), which accumulates in the cell. The addition of LiCl stabilizes IP1. The concentration of IP1 and therefore indirectly the concentration of IP3 can be determined.

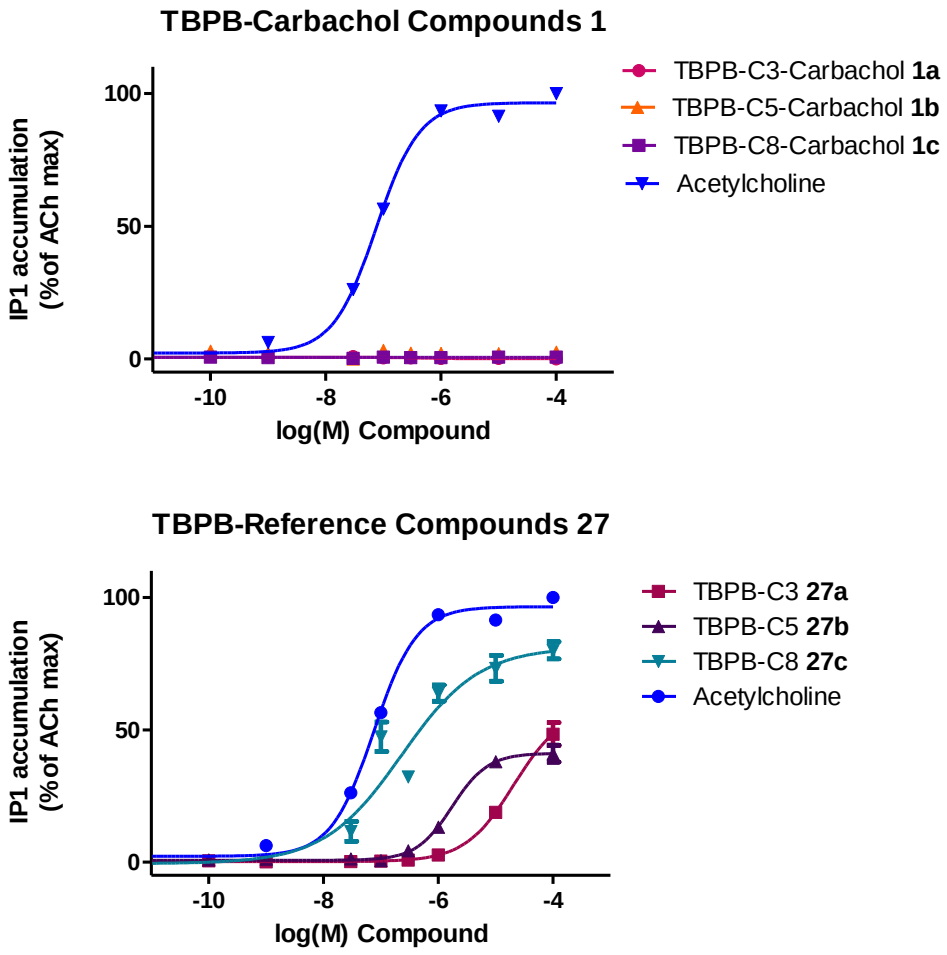

Figure 11. Dose-response curves of dualsteric compounds **1** (top) and reference compounds **27** (bottom) measured in the IP1 accumulation assay.

Figure **11** shows the dose-response curves of the putative dualsteric TBPB-carbachol compounds **1** and the alkyl reference compounds **27** in comparison to ACh as the positive control, with its maximum response set to 100%. The carbachol compounds **1** did not show any receptor response, suggesting that they did not cause a downstream signal either because they did not bind to the receptor or they were antagonists. The reference compounds **27**, however, showed partial agonism depending on their chain lengths. This finding is in line with the previously published results for compound **27c**, suggesting some form of allosteric agonism, as seen in radioligand binding studies [64].

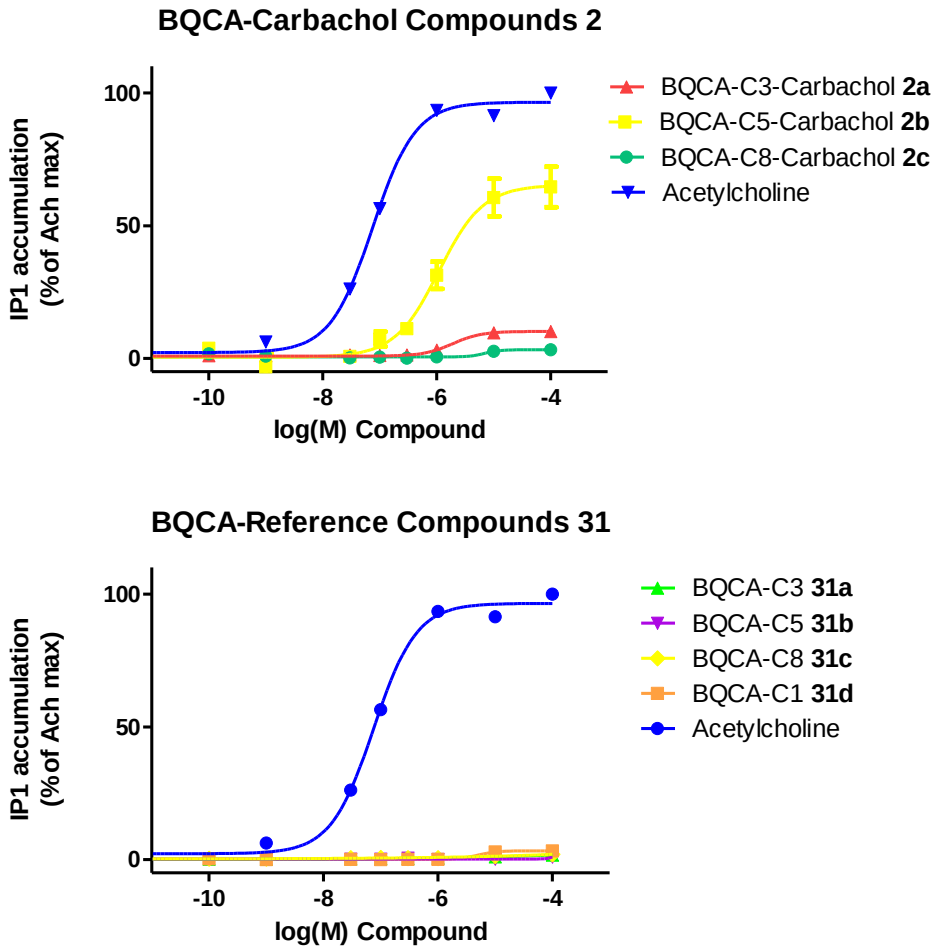

Figure 12. Dose-response curves of dualsteric compounds **2** (top) and reference compounds **31** (bottom) measured in the IP1 accumulation assay.

Figure **12** shows the dose-response curves of the putative dualsteric BQCA-carbachol compounds **2** and the alkyl reference compounds **31** in comparison to ACh as the positive control, with its maximum response set to 100%. In case of the alkyl reference compounds **31**, no receptor response and therefore no agonism was observed. This is the expected result, as

the BQCA compounds are described as allosteric modulators and should not activate the receptor without binding of an orthosteric ligand [64]. In contrast, all the dualsteric compounds **2** showed partial agonism, with the C_5-linker exhibiting the highest response. This finding proves binding to the orthosteric site and a dualsteric binding mode is certainly possible, but this has to be elucidated in additional studies.

Further investigations of the synthesised dualsteric compounds and their alkyl reference compounds will be conducted at the University of Bonn in the working group of PD Dr. Christian Tränkle to determine subtype selectivity and binding modes, as well as affinities and possible biased signalling.

4. Oxidative Stress and Natural Antioxidant Hybrids in Alzheimer's Disease

Another hallmark of the pathophysiology of AD is neurotoxic oxidative stress [81, 82]. Increased levels of oxidation products from proteins, DNA and lipids are found in tissues of AD patients post-mortem [82]. Abnormal formation of reactive oxygen species (ROS) and reactive nitrogen species (RNS) contributes to and enhances neuronal cell death. In healthy tissues, ROS and RNS are formed during metabolic reactions. These metabolites, however, are rather unstable and their levels are kept low by endogenous antioxidant mechanisms. An imbalance of the levels of oxidants to the endogenous antioxidants leads to oxidative stress and subsequent cell death [83]. Exogenous antioxidant small molecules [84] may, therefore, decelerate disease progression in early stages of AD.

Besides incorporation of antioxidants into hybrid molecules [85], natural antioxidants like flavonoids, alkaloids, terpenes, carotenoids, vitamins, stilbene derivatives, curcuminoids, phenolic acids, and polyphenols have been investigated regarding neurodegenerative diseases [86, 87]. Some of the compounds have shown some remarkable results *in vitro* but their specific modes of action are difficult to evaluate due to their structural diversity [88]. Additionally, some of the compounds are considered to be pan assay interference compounds (PAINS) [89]. Curcumin, for example, is suspected to generate false positive results *in vitro*, because of its structural features, like instability, low solubility and especially due to its fluorescent properties [89]. Research of natural antioxidants as therapeutics, therefore, challenges scientists to carefully evaluate the applicable assays and readouts to fit the compound's chemical properties and verify the molecule's stability (and possible metabolites or degradation products) to be able to move from an *in vitro* setting to successful *in vivo* tests [II].

4.1. Silibinin and Design of Neuroprotective Antioxidants

The flavonolignan silibinin **32** is a potent natural antioxidant [90]. Silibinin **32** and derivatives thereof (including silymarin) have been shown to exert hepatoprotective, anticancer, hypocholesterolemic, cardioprotective, neuroactive and neuroprotective activities [91-96].

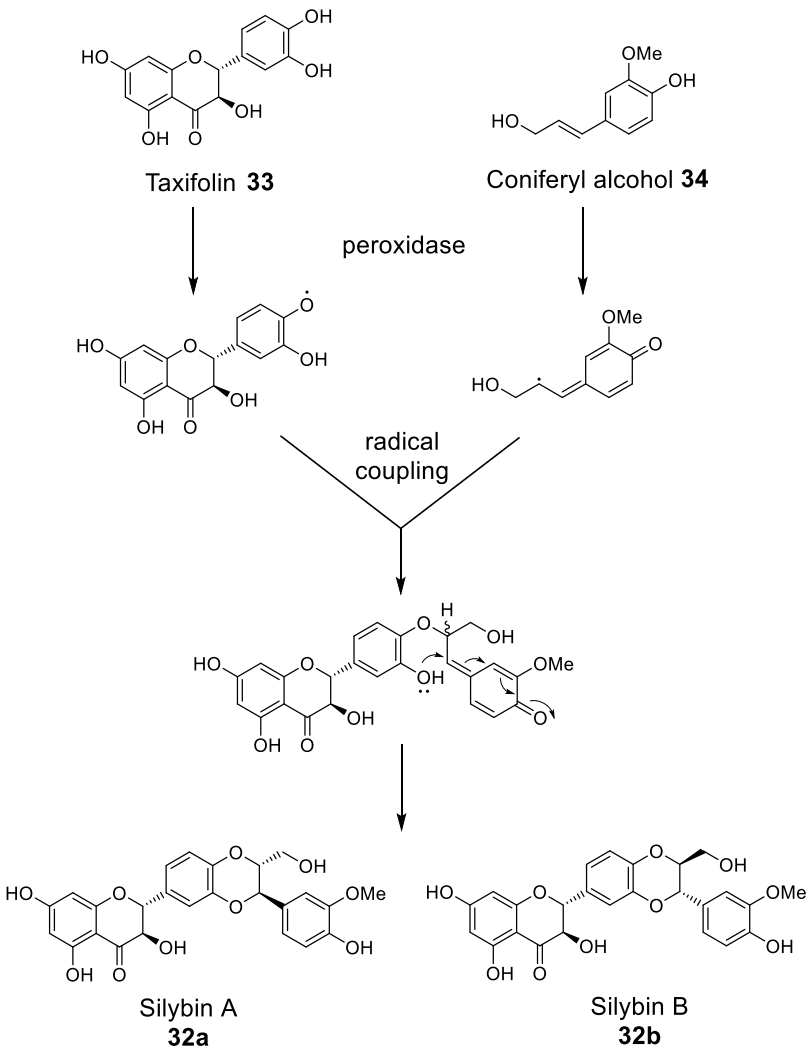

Scheme 14. Biosynthesis of silibinin **32**.

Silibinin **32** is extracted from milk thistle (*Silybum marianum* (L.) GAERTN.) as a diastereomeric mixture of silybin A **32a** and silybin B **32b**. This mixture is the result of the final step of the biosynthetic pathway, a radical reaction between taxifolin **33** and coniferyl alcohol **34** (Scheme **14**) [97]. These diastereomers were shown to exhibit distinct metabolic profiles [98] and biological effects. Antiaggregating effects on Aβ formation [99], antiproliferative effects

in human carcinoma cells [100], antiangiogenic and anti-aging effects [101, 102] and modulation of endocrine functions [103] are expressed by both diastereomers **32a** and **32b** as well as their derivatives in varying degrees, making examinations of the pure diastereomers a necessity. Silibinin **32** contains five hydroxy groups. Their influences on antioxidant and radical scavenging properties have been thoroughly investigated [104-106]. Conclusively, the phenolic 20-OH-group, as well as the secondary alcohol at position 3, are essential for the compound's antioxidative properties. Both the 5-OH-moiety and the primary alcohol at position 23 have no influence. The 7-OH-group, however, appears to possess a pro-oxidative character (Scheme **15**) [105]. Blockage of this pro-oxidative moiety by introduction of other radical scavengers might improve the compound's overall antioxidative properties.

Other potent antioxidants are naturally occurring phenolic acids like ferulic acid **35** (Scheme **15**), which also has positive effects on AD pathology. Among them are memory improving effects in mice and antiaggregating effects against Aβ [107-109].

Combining the antioxidant properties of both silibinin **32** and ferulic acid **35** by esterification at position 7 of silibinin may, therefore, produce a compound with superior neuroprotective effects and improved bioavailability due to higher lipophilicity (Scheme **15**). Ester bonds may be hydrolysed in solution or by esterases in tissues [110]. The stability of silibinin esters is, however, suggested to be enhanced by the inhibition of esterases [90,111-113]. Some of the silibinin esters described in literature show unexpected high stability, most likely due to steric hindrance of enzyme accessibility. This was also confirmed previously by our group [114] and Gažák *et al.* [101]. Nonetheless, determination of compound stability is necessary to distinguish the compound's effects from the effects of decomposition products [II].

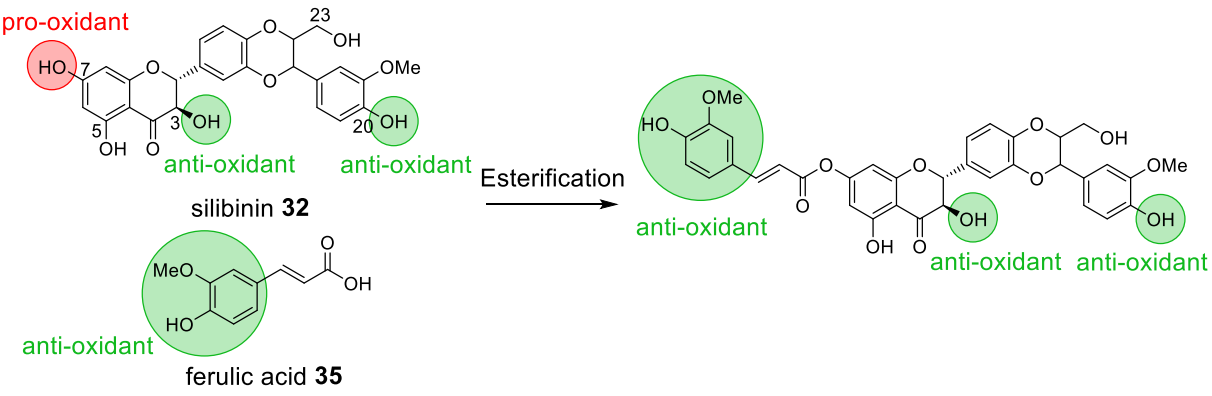

Scheme 15. Design of target structures – 7-esterification of silibinin **32** with ferulic acid **35**.

To explore structure - activity relationships (SARs), a library of 7-*O*-esters of silibinin **32**, with substituted and non-substituted cinnamic, dihydro cinnamic and benzoic acids, was synthesised. This should give insight how hydroxy and methoxy substituents at the aromatic system of the acid and the Michael system influence both antioxidative behaviour and neuroprotection.

4.2. Synthesis of 7-*O*-Silibinin Esters

A variety of silibinin esters have been synthesised before [90]. Reported regioselective methods include Mitsunobu esterification at the 23-position [95, 114], the use of acyl chlorides for both 7-*O*- and 23-*O*-esters [115] and 3-*O*-, 7-*O*-, 20-*O*- and 23-*O*- galloyl esters of silibinin **32** using protection/deprotection strategies [101]. For the synthesis of the 7-*O*- ester library, we were looking for methods, that do not require time-consuming protection group strategies in order to yield the desired compounds, as well as consistent regioselectivity.

The first tested method was the Mitsunobu esterification using silibinin **32** and ferulic acid **35**, which indeed yielded the 7-*O*- ester in contrast to literature reports [95, 114]. This method, however, proved to be inconsistent and very much dependent on the acid used (previous work by Guozheng Huang [116]). Furthermore, the Mitsunobu reaction produces dehydration-byproducts that are difficult to separate from the main product. The formation of one of the byproducts – hydnocarpin D **36** from silibinin **32** – was optimized by our group and represents the first one-pot semi-synthetic method for the preparation of hydnocarpin-type flavonolignans (Scheme **16**) [I].

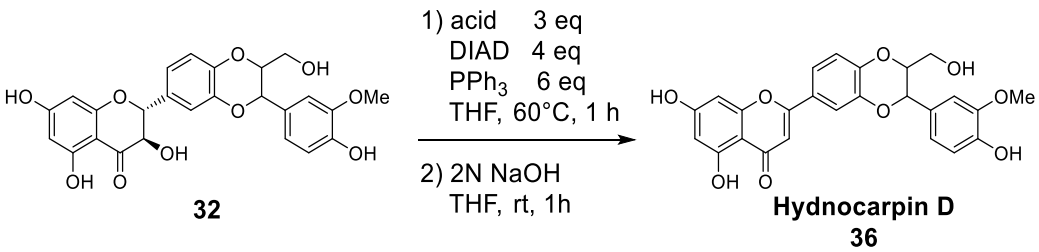

Scheme 16. Synthesis of hydnocarpin D **36** by optimized Mitsunobu dehydration [I].

Because of the inconsistencies in regioselectivity of the Mitsunobu reaction, we started testing 7-esterification using acyl chlorides under basic conditions similar to literature reports

[101, 115]. *In situ* preparation of the acyl chlorides using oxalyl chloride and dimethylformamide as catalyst in dichloromethane as solvent and adding this solution to a solution of silibinin **32** and triethylamine in tetrahydrofuran, yielded the desired 7-*O*- esters consistently. This method does not require protection groups and produces only minor byproducts, which are separable by column chromatography. With the use of this method, sixteen esters of silibinin **37** - **43** were prepared, consisting of cinnamic acid, ferulic acid, sinapinic acid, and protected caffeic acid derivatives as well as their dihydro and simple benzoic acid derivatives (Table **1**) [III]. Furthermore, both individual pure diastereomers 7-*O*-feruloylsilybin A **43a** and 7-*O*-feruloyl-silybin B **43b** were prepared from pure silybin A and B, respectively, to investigate their putative differing antioxidant and neuroprotective effects.

Byproducts like di- or tri-esters connected to OH-groups of silibinin **32** were not detected, as these would show significant shifts of adjacent protons in NMRs of the crude products. The only byproducts observed were di-esters like compound **42**, which was obtained by preparative HPLC. It is no surprise that acyl chlorides of acids, bearing unprotected phenolic hydroxy groups – like ferulic acid and sinapinic acid – would react with each other forming such multi-esters. The application of this esterification method is therefore limited by the number of hydroxy substituents of the acid. This fact was confirmed by the attempt of synthesising 7-*O*-caffeoylsilibinin **44**, as caffeic acid is another potent radical scavenger [117]. Synthesis of this compound without protection groups failed most likely due to the above described formation of byproducts (Scheme **17**). Protection groups for the catechol moiety were tested subsequently. Benzyl protection, silyl ethers, and an acetonide protection group (compounds **40**) were investigated, but none of the deprotection conditions led to the target compound as either no deprotection was observed or decomposition of the respective silibinin ester took place upon harshening reaction conditions. Benzyl deprotection by simple hydrogenation, like it was used in the preparation of galloyl esters by Gažák *et al.* [101], was not an option due to the hydrogenation of the double bond (dihydro derivatives of the acids used were prepared this way [118]).

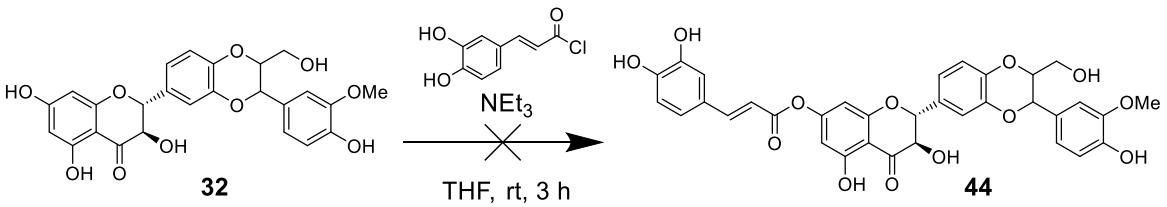

Scheme 17. Attempted synthesis of 7-*O*-caffeoylsilibinin **44** via acyl chlorides.

Table **1**. Reaction conditions and structures of synthesised esters (**37** - **43**) [III].

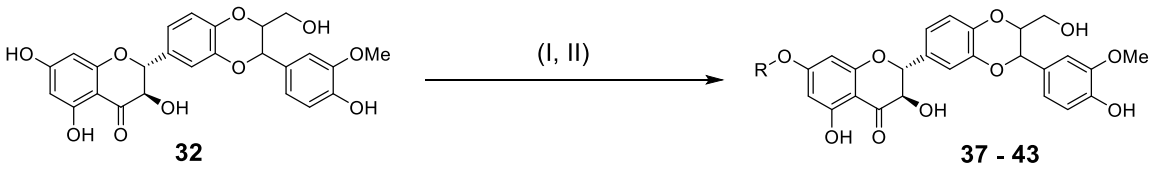

Reagents and conditions: (I) acid, oxalyl chloride, CH_2Cl_2, rt; (II) silibinin (**32**), NEt_3, THF, rt, 3 h

No.	Name	Structure	Yield [%]
37a	7-*O*-Cinnamoylsilibinin	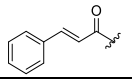	72
37b	7-*O*-Dihydrocinnamoylsilibinin	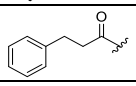	40
37c	7-*O*-Benzoylsilibinin		55
38a	7-*O*-Feruloylsilibinin[a]	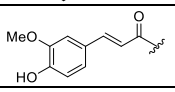	55
38b	7-*O*-Dihydroferuloylsilibinin	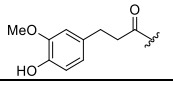	18
38c	7-*O*-Vanillylsilibinin	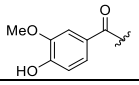	20
39a	7-*O*-Sinapoylsilibinin	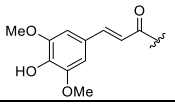	11
39b	7-*O*-Dihydrosinapoylsilibinin	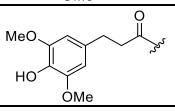	50
39c	7-*O*-Syringoylsilibinin	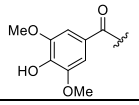	25
40a	7-*O*-[3,4-*O*-(1-Methylethylidene)caffeoyl]silibinin	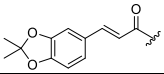	63
40b	7-*O*-[3,4-*O*-(1-Methylethylidene)dihydrocaffeoyl]silibinin	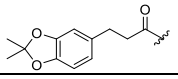	40
40c	7-*O*-[3,4-*O*-(1-Methylethylidene) 3,4-dihydroxybenzyl]silibinin	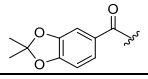	37
41	23-*O*-Cinnamoylsilibinin[b]	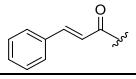	37
42	7-*O*-[4-((4-Hydroxy-3,5-dimethoxybenzoyl)-oxy)-3,5-dimethoxybenzoyl]silibinin[c]	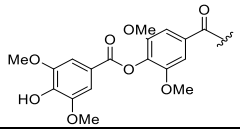	7
43a	7-*O*-Feruloylsilybin A[d]	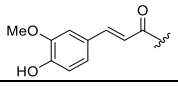	23
43b	7-*O*-Feruloylsilybin B[e]	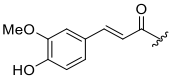	27

a: pyridine was used as base and solvent. b: 1 equivalent of NEt_3 was used in the reaction. In this case the general structure does not apply as the 23-*O*- ester of silibinin was yielded. c: byproduct in the synthesis of compound **39c**. d: silybin A **32a** was used as starting material. e: silybin B **32b** was used as starting material.

Lastly, the 2,3-dehydrosilibinin derivative of 7-*O*-cinnamoylsilibinin **37a** was prepared as a reference compound. Literature reports suggest that dehydrosilibinin **45** is a superior antioxidant and radical scavenger compared to silibinin **32** [119, 120] and stability measurements revealed formation of such compounds during testing in assay medium (*cf*. **4.5.**). Therefore, the influence on neuroprotection of the dehydro-derivatives needed to be assessed. For the synthesis of 2,3-dehydrosilibinin **45**, silibinin **32** was oxidised in the presence of sodium hydrogen carbonate under strong reflux in methanol as described by Gažák *et al.* [121]. Subsequent reaction with the *in situ* prepared cinnamoyl chloride yielded the target compound **46** (Scheme **18**) [IV]. This reaction was, however, not as easy as described. Preparation of **45** needed strong reflux (>100 °C), because lower temperatures would lead to incomplete conversions (10% - 20% silibinin **32** remaining) and decomposition after longer reaction times. Usage of impure dehydrosilibinin **45** (less than 90% purity) would lead to many (by-)products in the reaction to **46**, as leftover silibinin **32** was more reactive than the oxidised form **45**. Pure **45** is therefore essential for a successful reaction to 7-*O*-cinnamoyl-2,3-dehydrosilibinin **46**.

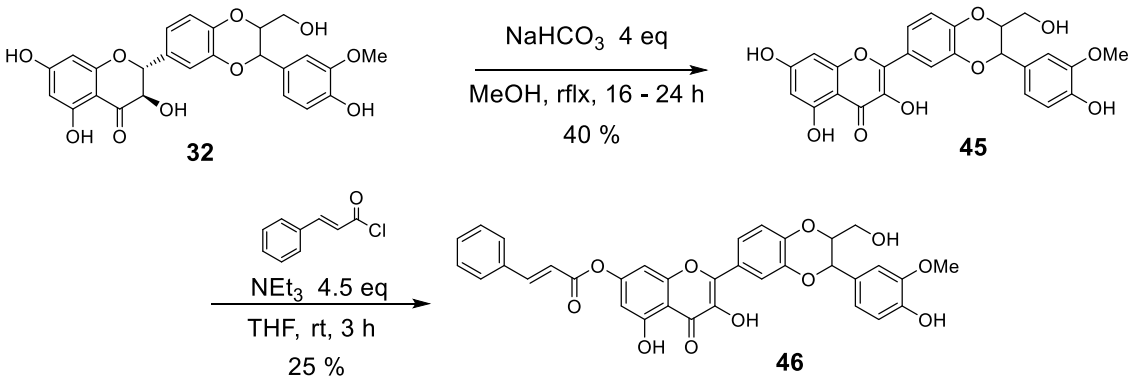

Scheme 18. Synthesis of 7-*O*-cinnamoyl-2,3-dehydrosilibinin **46** [IV].

4.3. Antioxidant Properties

The physicochemical antioxidant properties of the synthesised compounds were evaluated in the ferric reducing antioxidant power (FRAP) assay in cooperation with Florian Lang (AK Högger, Klinische Pharmazie, Universität Würzburg) [122, 123]. An unspecific redox-reaction between the putative antioxidant compound and an iron complex takes place in this assay. Ferric-tripyridyltriazine (Fe^{III}-TPTZ) is used in an excess and reduced by the antioxidant to its ferrous form (Fe^{II}-TPTZ). The ferrous complex shows a blue colour whereas the ferric compound is colourless. The colour change from colourless to blue is determined and quantified through a change in absorption. To enable the reaction, the antioxidant needs to be able to reduce the complex. Iron(II)sulfate is used for calibration and as a reference. Silibinin **32**, ascorbic acid (AA) and trolox (T) were tested for comparison with the synthesised esters **37** - **42**. Because of the required concentrations (up to 1 mM), methanol had to be used as a solvent, as most of the synthesised compounds were not soluble in aqueous media.

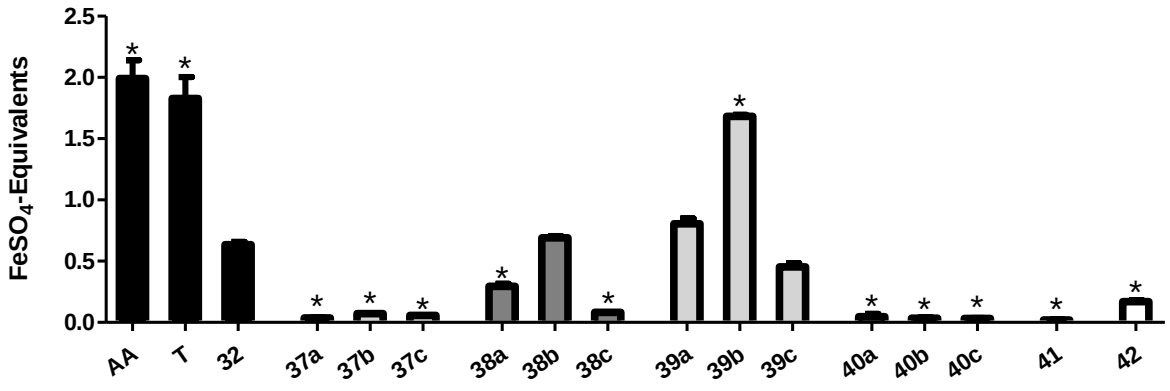

Figure 13. Compounds **32** and **37** - **42** were studied in the FRAP-assay. $FeSO_4$ was used for calibration. Results are presented as equivalents of 1 mM $FeSO_4$ (n = 3-5; mean ± SD). Significance was defined as *p < 0.05 [III].

Figure **13** shows the results of the FRAP assay. Silibinin **32** shows 0.6 $FeSO_4$ equivalents and ascorbic acid (AA) and trolox (T) 2.0 and 2.8 equivalents, respectively. The esterification of silibinin generally had a negative effect on antioxidant activity measured in this assay. Compounds **37** and **40**, which lack additional OH-groups, almost completely lost the reducing ability of silibinin **32**. Esters **38** and **39** more or less stayed on the same level as the parent compound, as they contain a fifth hydroxyl group. Furthermore, dihydro-compounds (**b**) showed the highest antioxidant activities compared to their unsaturated (**a**) and benzoic acid

derivative (**c**) counterparts. Only 7-*O*-dihydrosinapoylsilibinin **39b** showed a significant improvement over silibinin **32**, reaching effects comparable to trolox (T).

7-*O*-Cinnamoylsilibinin **37a** and 7-*O*-feruolylsilibinin **38a**, including its diastereomers **43a** and **43b**, were further compared to their individual components, silibinin **32** and cinnamic acid (CA) or ferulic acid **35**, respectively, and to equimolar mixtures (Figure **14**).

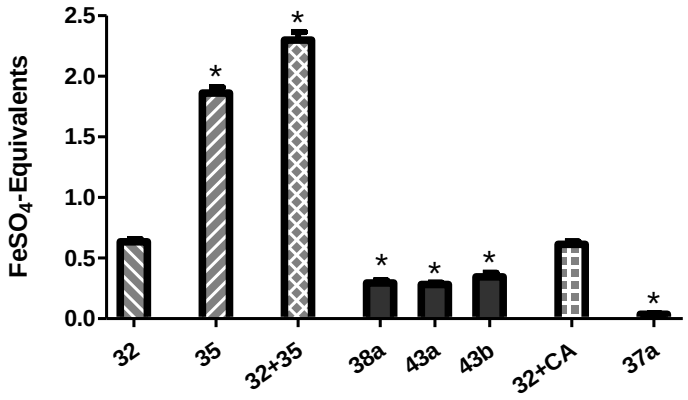

Figure 14. Compounds **38a**, **43a**, **43b,** and **37a** were studied in comparison to silibinin **32**, ferulic acid **35**, cinnamic acid (CA) and the respective 1:1 mixtures. $FeSO_4$ was used for calibration. Results are presented as equivalents of 1 mM $FeSO_4$ (n = 3-5; mean ± SD). Significance was defined as $^{*}p < 0.05$ [III].

The equimolar mixture of silibinin **32** and ferulic acid **35** showed the highest activity, even exceeding the effect of ferulic acid **35**. The ester **38a** and its diastereomers, however, showed lower activity than silibinin **35**, with no difference between isomers **43a** and **43b**. The cinnamic acid ester **37a** showed almost no activity. The equimolar mixture of silibinin **32** and CA showed the same effect as pure silibinin **32**, as CA alone had no measurable effect in this assay (data not shown). It can be concluded, that esterification of silibinin **32** had a generally negative effect on its *in vitro* antioxidative properties in the FRAP assay and no additive effects were observed. Only one compound, namely 7-*O*-dihydosinapoylsilibinin **39a**, showed increased activity, which can be compared to trolox. SARs of these compounds are straightforward. Unsaturated esters (**b**) were the most potent antioxidants and the benzoic acid derivatives (**c**) showed the lowest activities. The weak results from the physicochemical FRAP assay, however, are no clear indication of the antioxidant and neuroprotective effects, and more elaborated cell-based assays might show different results. The outcomes may even contradict each other [124-126].

4.4. Neuroprotective Properties

4.4.1. Neuroprotection in HT-22 Cells

Neuroprotective properties were first evaluated in a cell-based model system (also called oxytosis) [114, 127, 128]. The HT-22 neuronal cells are derived from murine hippocampal tissue and are sensitive to glutamate as they miss ionotropic glutamate receptors [129]. Herein, cystine transport by the cystine/glutamate antiporter is inhibited by addition of extracellular glutamate. In consequence, levels of intracellular cysteine increase, leading to glutathione depletion and accumulation of intracellular ROS. Those will cause damage to the cell and ultimately lead to cell death [130-132]. It was shown that antioxidants like flavonoids can prevent cell death caused by oxidative stress in this cell line [127, 128]. Experiments were conducted by Sandra Gunesch (AK Decker, Universität Würzburg) to evaluate neuroprotective as well as neurotoxic effects of the synthesised esters.

Figure **15** shows the screening of the potential of esters **37** - **42** to rescue cells from neurotoxic cell death at concentrations of 10 µM and 25 µM. Quercetin (25 µM) was used as positive control and showed cell survival of about 80% after glutamate-induced oxidative stress. Esters bearing the Michael system (**a**) were generally the most active neuroprotectants, followed by the benzoic acid derivatives (**c**), whereby their neuroprotective properties depended on the aromatic substituents. In contrast to the findings of the FRAP-assay (*cf*. **4.3.**), the dehydro-derivatives (**b**) showed the weakest activities in this assay. The most potent neuroprotectants at 10 µM were 7-*O*-cinnamoylsilibinin **37a**, 7-*O*-feruloylsilibinin **38a** as well as the protected caffeic acid ester **40a** and dihydroxybenzoic acid ester **40c**. The decline in activity at 25 µM can be explained by the compounds innate cytotoxic effects at higher concentrations. This was previously observed for other antioxidants and heterocycles [114]. Comparing 7-*O*-cinnamoylsilibinin **37a** to 23-*O*-cinnamoylsilibinin **41**, it is evident that blocking of 7-OH group of silibinin had the desired effect on neuroprotection. The 23-*O*- ester **41** showed only moderate neuroprotection at 25 µM, whereby the 7-*O*- ester **38a** showed the highest activity of the library at only 10 µM, further supporting the intended aim of this study.

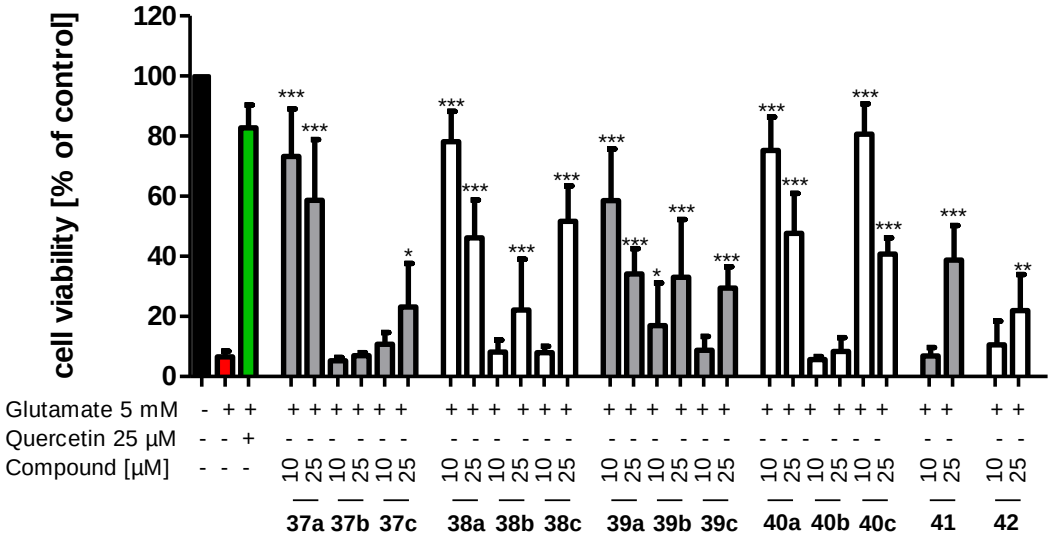

Figure 15. Compounds **37** - **42** were studied on neuronal HT-22 cells for neuroprotection against glutamate-induced oxidative stress at 10 µM and 25 µM. Results of the modified MTT test are presented as means ± SD and refer to untreated control cells which were set as 100% values. Levels of significance: * $p < 0.05$; ** $p < 0.01$; *** $p < 0.001$ [III].

The most potent compounds **37a** and **38a** were further investigated in a broader range of concentrations (1 µM, 5 µM, 10 µM, and 25 µM) and compared to their respective individual components as well as equimolar mixtures thereof. Moreover, their cytotoxicity was determined in an additional MTT-assay.

Figure **16** shows the results of the MTT-assay and the expanded neuroprotection assay of 7-*O*-cinnamoylsilibinin **37a**, its 2,3-dehydrosilibinin derivative **46**, cinnamic acid (CA), silibinin **32** and a 1:1 mixture of the two. At the highest concentration of 25 µM both the 1:1 mixture and compound **37a** showed increased neurotoxicity (Figure **16A**), which explains the decreased neuroprotection at the higher concentration observed in the screening (*cf*. above). The highest neurotoxicity was expressed by the dehydrosilibinin ester **46**. This compound started exhibiting a neurotoxic effect at 5 µM and reduced cell viability by 50% at 25 µM. Regarding neuroprotection, only the esters **37a** and **46** showed activity, demonstrating an overadditive effect compared to the individual components and the equimolar mixture. The dehydrosilibinin ester **46**, however, only showed good neuroprotection at 5 µM, before its innate cytotoxicity lowered its potential at 10 µM and 25 µM.

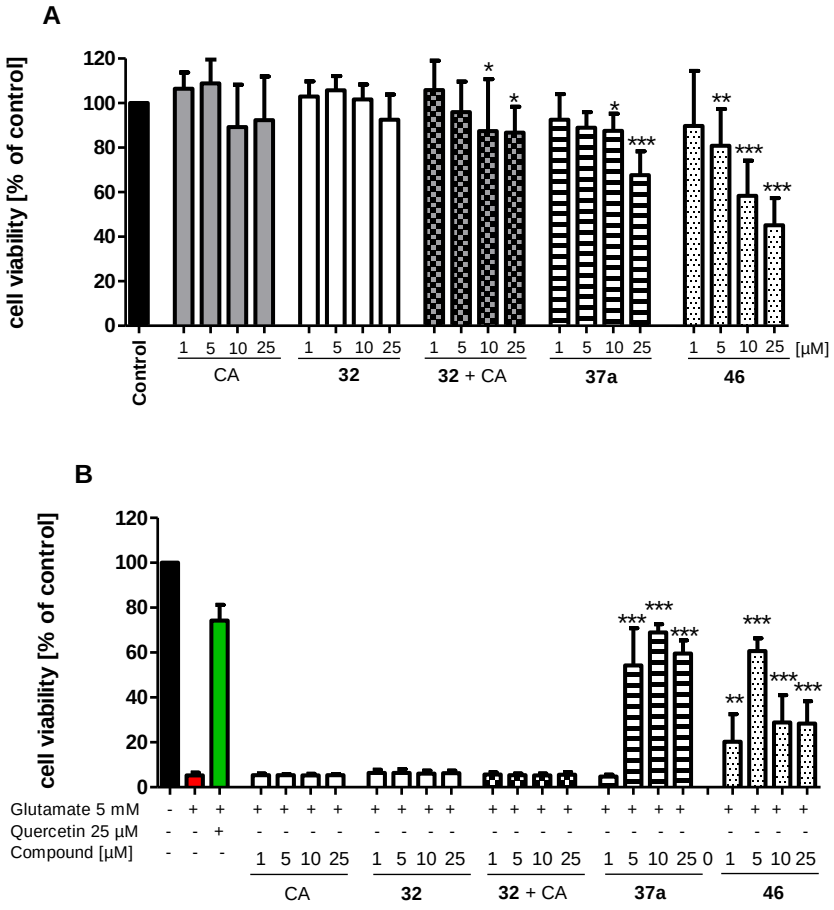

Figure 16. Compounds **32**, **37a** and **46**, as well as cinnamic acid (CA) and the 1:1 mixture of **32** and CA, were studied on neuronal HT 22 cells for A) neurotoxic effects and B) neuroprotection against glutamate-induced oxidative stress at 1-25 µM. Results of the modified MTT test are presented as means ± SD of three different independent experiments and refer to untreated control cells which were set as 100% values. Levels of significance: * $p < 0.05$; ** $p < 0.01$; *** $p < 0.001$ [III, IV].

Similar tendencies were observed with 7-*O*-feruloylsilibinin **38a**, its diastereomers **43a** and **43b**, and its components silibinin **32** and ferulic acid **35** (Figure **17**). No neurotoxic effects were shown by **32** and **35**. The equimolar mixture and the ester **38a** did, however, show neurotoxicity increasing with their concentrations (Figure **17A**). Their neuroprotective effects are depicted in Figure **17B**. Again, the individual components and the 1:1 mixture expressed no effect, whereby 7-*O*-feruloylsilibinin **38a** showed neuroprotection at 10 µM and 25 µM, further proving the overadditive properties of the esters.

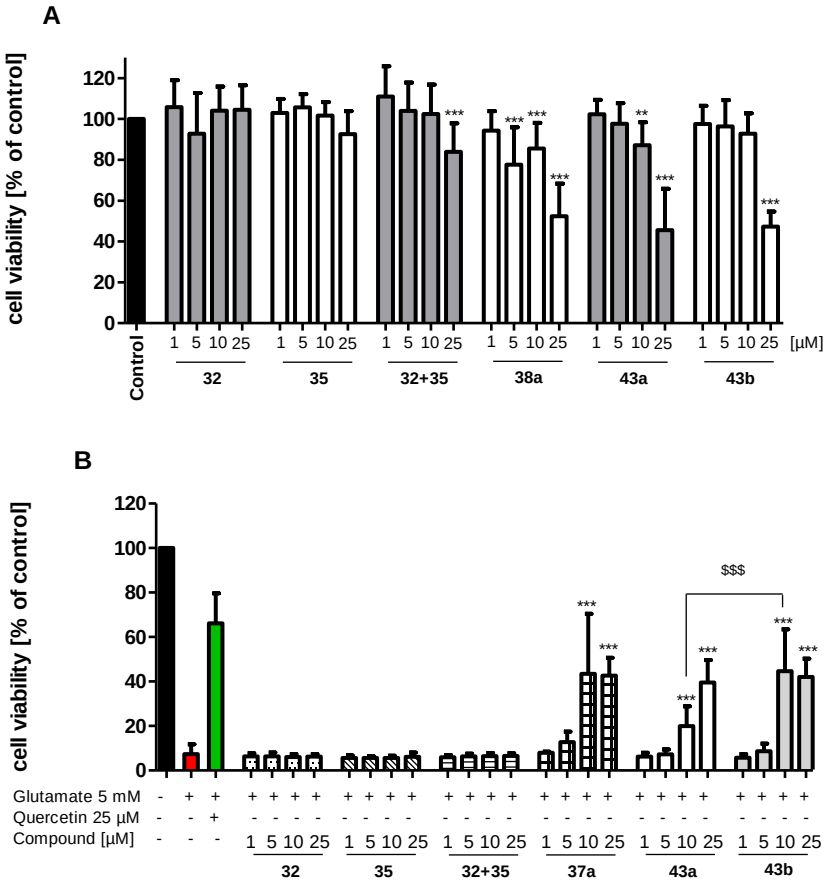

Figure 17. Compounds **32**, **35**, **38a**, **43a**, and **43b**, as well as the 1:1 mixture of **32** and **35**, were studied on neuronal HT 22 cells for A) neurotoxic effects and B) neuroprotection against glutamate-induced oxidative stress at 1-25 µM. Results of the modified MTT test are presented as means ± SD of three different independent experiments and refer to untreated control cells which were set as 100% values. Levels of significance: * $p < 0.05$; ** $p < 0.01$; *** $p < 0.001$. Levels of significance for Bonferroni's posttest are indicated as $ [III].

The individual diastereomers **43a** and **43b** were also tested (Figure **17**). Diastereomer A **43a** showed a slightly higher neurotoxic effect at 10 µM (Figure **17A**), which corresponds to the results of the neuroprotection assay (Figure **17B**), as Diastereomer B **43b** exhibits significantly higher neuroprotective activity than its counterpart at the same concentration. This result is in accordance with reports from literature [99-103].

4.4.2. Age-associated Neurotoxic Pathways

Esters 7-*O*-cinnamoylsilibinin **37a** and 7-*O*-feruloylsilibinin **38a**, including the pair of diastereomeric esters (**43a** and **43b**), were further evaluated by Pamela Maher (The Salk Institute for Biological Studies, La Jolla, California, USA) in biological studies regarding neuroprotective properties (Table **2**). The assays focus on pathologies seen in AD and age-associated neurotoxicity and include *in vitro* ischemia, inhibition of microglial activation and a PC12 cell differentiation assay [133].

The *in vitro* ischemia assay also uses HT-22 cells. Neuronal cell damage and subsequent cell death are associated with a loss of ATP [134]. The ATP loss in the assay is induced by adding iodoacetic acid to the cells. Determination of cell viability is achieved by an MTT test.

Activation of pro-inflammatory microglia is another process of AD pathology. The microglia release several pro-inflammatory and cytotoxic factors promoting neuronal cell death. Inhibition of microglial activation may, therefore, counteract disease progression [135]. Bacterial lipopolysaccharide is added to mouse BV2 microglial cells in the presence of the test compound. The resulting changes in extracellular levels of nitric oxide (NO), released by microglia activation, are indirectly measured by determination of the nitrite (NO^{2-}) concentration in cell medium.

The PC12 cell differentiation assay is motivated by impaired nerve connections in AD. Increased neurite outgrowth counteracts the impairment and leads to neuroregeneration [136]. In the assay, nerve outgrowth factor (NGF) stimulation in rat PC12 cells, by treatment with the compound, is studied by counting newly developed neurites.

Table **2** shows the results of the described assays. Compounds **32**, **35** and cinnamic acid (CA) showed no activity in the assays within the tested molar ranges and only silibinin **32** improved neurite outgrowth in PC12 cells. In contrast 7-*O*-cinnamoylsilibinin **37a** and the diastereomers of the ferulic acid ester **43a** and **43b** exhibited effects in the *in vitro* ischemia model in the low micromolar range. All tested esters showed increased activity on both microglial activation and PC12 cell differentiation, with the cinnamic acid ester **37a** being the most active, inhibiting the microglial activation with an EC_{50} value of 4.2 µM. Furthermore, the diastereomers **43a** and **43b** appeared to express distinct effects in the ischemia model and PC12 cell differentiation, but a significant difference was not reached.

Table 2. Biological activities of the most potent compounds in the following assays: *in vitro* ischemia, inhibition of microglial activation and ability to promote differentiation of PC12 cells [III].

No.	*in vitro* ischemia EC_{50} (μM ± SD)	Inhibition of microglial activation EC_{50} (μM ± SD)	PC12 cell differentiation (at 10 μM ± SD)
32	>10	>10	38 ± 3%
35	>10	>10	no
CA	>10	>10	no
37a	1.5 ± 0.2	4.2 ± 0.9	40 ± 20%
38a	>10	6.5 ± 0.8	47 ± 12%
43a	1.4 ± 0.5	9.8 ± 0.9	50 ± 10%
43b	2.2 ± 0.05	10.1 ± 3.3	67 ± 12%

4.4.3. Aβ42 and τ Protein Aggregation Inhibition

The recently described screening methods for inhibition of both Aβ42 and τ protein aggregation are other good indicators for neuroprotective properties of potential drugs [137, 138]. These assays target the more prominent hallmarks of AD, the amyloid cascade hypothesis and the τ hypothesis (*cf*. part **2.**). Compounds capable of inhibiting the formation of neurotoxic plaques may be viable in the treatment of AD. Bacterial cells overexpressing either Aβ42 or τ protein are used in this model. Inclusion bodies (IBs), possessing amyloid-like properties, are formed by Aβ in bacteria. The IBs can be stained by a specific amyloid dye, thioflavin-S. By colouring of the aggregates, the amount of aggregation or inhibition thereof can be quantified in cells treated with a test compound in comparison to untreated control cells.

The synthesised esters **37a**, **38a**, **40a**, **40c** and the pure diastereomers **43a** and **43b** were evaluated in the anti-aggregation assays by Judith Roa (Department of Pharmacy and Pharmaceutical Technology and Physical-Chemistry, University of Barcelona, Barcelona, Spain) in comparison to silibinin **32**. Figure **18A** shows the inhibition of Aβ42 aggregation of tested compounds at 10 μM and 100 μM. Silibinin **32** exhibited inhibition of 4.8% and 16% at the tested concentrations. All esters expressed inhibitions about four times as high at both concentrations. 7-*O*-Cinnamoylsilibinin **37a** and 7-*O*-feruloylsilybin B **43b** proved to be the most potent compounds, with 61% and 73%, respectively; the latter showing 20% higher inhibition than its counterpart **43a**. A similar picture is painted regarding τ aggregation inhibition (Figure **18B**). Silibinin **32** only expressed 2% inhibition at 10 μM and 10% inhibition

at 100 µM. The esters, however, showed 30% - 45% inhibition at 10 µM and 60% - 84% at 100 µM. Again, **37a** and **43b** were the most potent compounds. These results further underline the overadditive effects of the esters observed in the other neuroprotection assays. Moreover, IC_{50} values of the individual diastereomers suggest a specific mode of action. 7-*O*-Feruloylsilybin A **43a** showed IC_{50} values of 85.8 ± 5.8 µM (Aβ42) and 27.2 ± 2.3 µM (τ protein), whereby the IC_{50} values of 7-*O*-feruloylsilybin B **43b** were significantly lower with 43.6 ± 4.8 µM regarding Aβ42 and 12.9 ± 1.2 µM for τ protein aggregation.

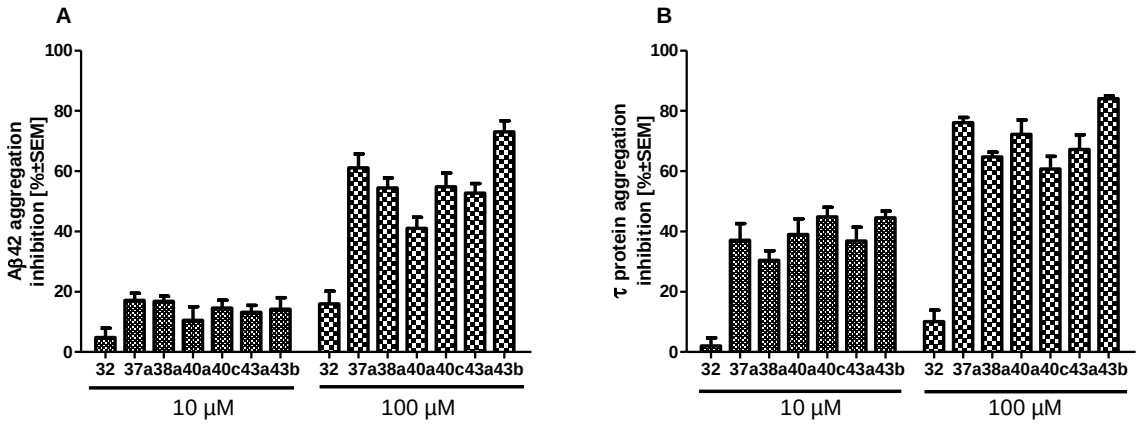

Figure 18. Results of inhibition of A) Aβ42 aggregation and B) τ protein aggregation assays. Untreated cells served as positive control, which was set as 0% (not shown) [III].

4.5. Stability of Silibinin Esters

The stability of the esters is of concern, because they may be rapidly hydrolysed by esterases or in solution (*cf*. **4.1.**) [110] and their effects need to be distinguished from the mixture of the hydrolysis products. Even though the results from the neuroprotection assay already proved overadditive effects, the stability of the esters was determined. 7-*O*-Feruloylsilibinin **38a** served as a model compound and its time-dependent stability was determined in both cell culture medium and human blood plasma by LCMS measurements in cooperation with Florian Lang (AK Högger, Klinische Pharmazie, Universität Würzburg). Solutions of **38a** (50 µM) in the respective medium were prepared and incubated at 37 °C for 24 h. After certain times, samples were taken and the area under curves (AUCs) were determined by HPLC. AUC at 0 min was set as 100%.

Figure **19** shows the time-dependent stability of 7-*O*-feruloylsilibinin **38a** in cell culture medium (blue) and human blood plasma (red). In assay medium, the ester **38a** was quickly

converted in the first hours before a plateau was reached. 25% of the initial amount remained even after 24h. The main conversion products, however, were not the hydrolysis products silibinin **32** and ferulic acid **35**. In fact, the main product was identified to be the oxidised (or disproportionated [121]) ester 7-*O*-feruloyl-2,3-dehydrosilibinin **47** (Figure **19**), with the maximum amount observed after 2 h. This was confirmed by LCMS, showing an *m/z* ratio of 657 $[M+H]^+$, which corresponds to compound **47**, and a significantly increased retention time. The same observation was made for 7-*O*-cinnamoylsilibinin **37a** forming the respective dehydro-compound **46**. These results provide further evidence for the exceptional stability of silibinin esters [101, 114].

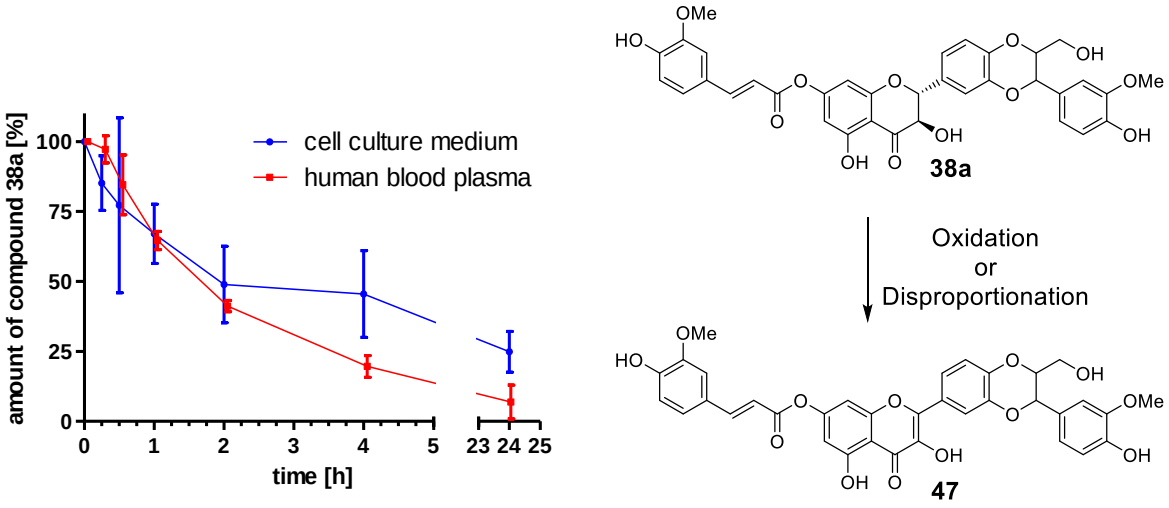

Figure 19. Time-dependent analysis of the stability of compound **38a** in assay medium (blue) and human pooled plasma (n = 6; red)). AUC was determined by HPLC. AUC at 0 min was set as 100%. The experiments were performed in triplicate (mean ± SD). Observed oxidation of silibinin ester **38a** to the 2,3-dehydrosilibinin ester **47** [III].

Stability in human blood plasma (Figure **19**, red) shows a more rapid decline of the compound, with none remaining after 8 h of incubation. The half-life of **38a** in plasma was approximately 1.5 h. In this case, ester cleavage was detected instead of formation of the oxidation product **47**.

4.6. Improvement of Solubility

While the synthesised silibinin esters show potent neuroprotective effects, their low solubility in aqueous media may complicate further biological investigations and pharmacological applications. Some of the esters were difficult to dissolve even in low concentrations and the use of dimethyl sulfoxide was inevitable. Especially at higher concentrations, as seen in the FRAP assay (*cf*. **4.3.**), dissolution in dimethyl sulfoxide and water was not possible. Functionalization of the 7-*O*- esters is possible at the 23-position of silibinin, as this primary hydroxy group plays reportedly no role in the compound's antioxidative properties [105]. The improvement of the solubility of silibinin **32** and its derivatives, by introduction of functional groups like glycosides, phosphodiesters, ethylene glycols, and acid derivatives as well as formulations using nanoemulsions have been reported before [92, 119, 139-145]. Another silibinin derivative, that is used in the clinical treatment of death cap (Amanita phalloides) poisoning [90], is silibinin 3,23-bishemisuccinate. The free acid groups of the hemisuccinates significantly improve the solubility of silibinin **32** [146]. The combination of the improved solubility of hemisuccinates with the neuroprotective properties of the 7-*O*- esters might, therefore, produce compounds with more useful physicochemical properties, that may even serve as prodrugs like the silibinin-tacrine compound reported by our group [114]. Since 7-*O*-cinnamoylsilibinin **37a** proved to be the most potent compound, it was chosen as a model. The target compound 7-*O*-cinnamoyl-23-*O*-succinyl-silibinin **48** was prepared and its neuroprotective effects in HT-22 cells, its solubility and stability were determined and compared to **37a**.

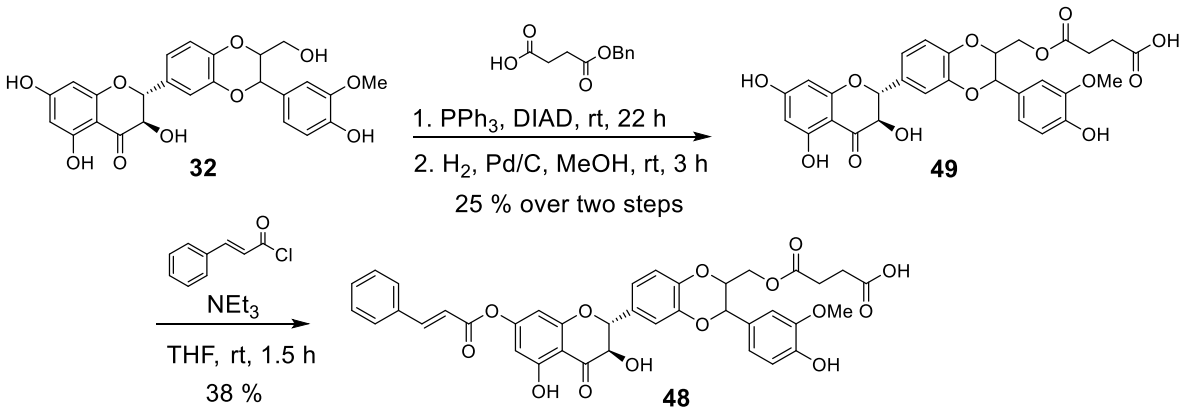

Scheme 19. Synthesis of 7-*O*-cinnamoyl-23-*O*-succinylsilibinin **48** [IV].

The hemisuccinate **48** was synthesised using a route that was previously used for the synthesis of a silibinin-tacrine codrug [114]. Silibinin **32** was reacted in a Mitsunobu esterification with mono-benzyl protected succinic acid (Scheme **19**). The protected succinylsilibinin was hydrogenated using palladium on charcoal, yielding 23-*O*-succinylsilibinin **49**. Subsequent esterification using the above described acyl chloride method gave the target compound **48** in moderate yields.

Furthermore, the respective dehydrosilibinin compounds, **50** and **51**, were synthesised as references for the stability measurements (Scheme **20**). Dehydrosilibinin **45** was prepared as described above (*cf*. **4.2.**) and served as the starting material. The same strategy using Mitsunobu esterification and subsequent hydrogenation gave 23-*O*-succinyl-2,3-dehydro-silibinin **50**, which was further esterified to yield 7-*O*-cinnamoyl-23-*O*-succinyl-2,3-dehydro-silibinin **51**.

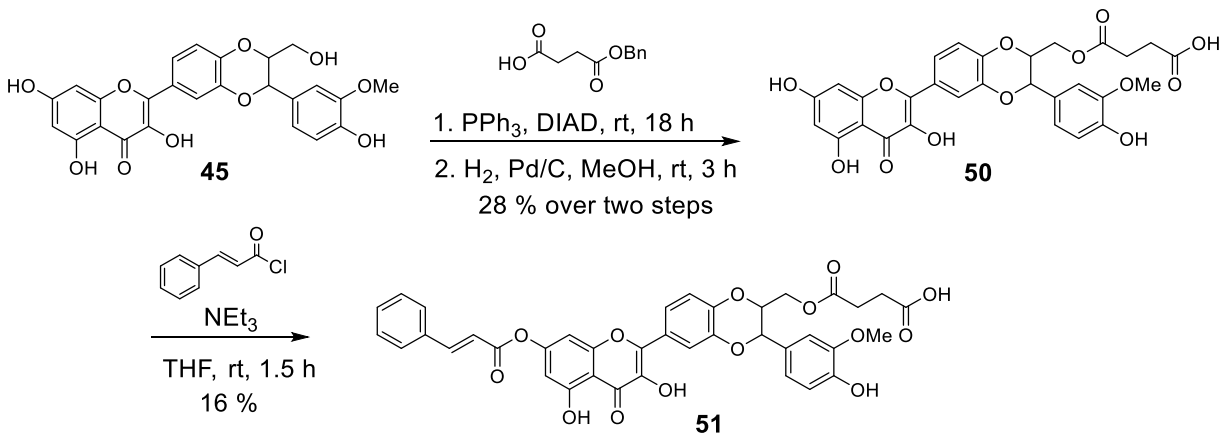

Scheme 20. Synthesis of 7-*O*-cinnamoyl-23-*O*-succinyl-2,3-dehydrosilibinin **51** [IV].

The solubility of hemisuccinate **48** was investigated in shake-flask experiments by Marco Saedtler (AK Meinel, Pharmazeutische Technologie und Biopharmazie, Universität Würzburg). Both silibinin **32** and the parent compound 7-*O*-cinnamoylsilibinin **37a** were also examined. The respective compounds were placed in Eppendorf tubes and 1 mL of PBS buffer at pH = 6.8 and pH = 7.4 was added. After shaking the samples for 24 h at 37 °C, samples were withdrawn, and the amount of dissolved compound was identified by UV-absorption and the identity of the compounds was verified by LCMS. Figure **20** shows the determined solubilities of silibinin **32**, 7-*O*-cinnamoylsilibinin **37a** and 7-*O*-cinnamoyl-23-*O*-succinylsilibinin **48**. At

pH = 6.8 the solubility of silibinin **32** was determined to be 20 µM and 48 µM at pH = 7.4. With 5 µM and 10 µM, the cinnamic acid ester **37a** showed the expected significantly reduced solubilities. This finding, however, is not accurate. LCMS measurements revealed complete hydrolysis of the ester **37a**, leaving only silibinin **32** and cinnamic acid in solution. The succinic acid ester **48**, in contrast, showed highly improved solubilities at both pH-values. With 119 µM at pH = 6.8 and even 1.5 mM at pH = 7.4, a significant improvement over the parent compound was reached, which was the intended aim of preparing the hemisuccinate **48**.

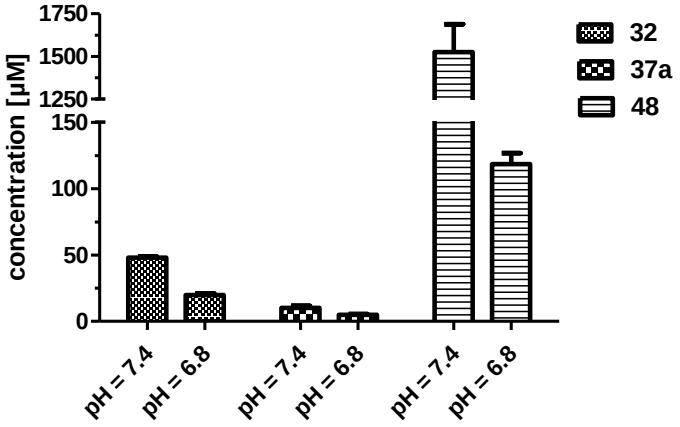

Figure 20. Determined concentrations of compounds **32**, **37a** and **48** in PBS buffer at pH = 6.8 and pH = 7.4 after 24 h at 37 °C. Amounts were determined via UV-absorption calibration curves (R^2 = 0.9998). The experiments were performed in triplicate (mean ± SD) [IV].

Next, the stability of 7-*O*-cinnamoyl-23-*O*-succinylsilibinin **48** in cell culture medium was determined (method described in part **4.5.**). Figure **21** shows the time-dependent stability of **48** including the formation of degeneration products. Newly formed compounds were analyzed by LCMS measurements and quantified via calibration curves. Within 4 h, the starting compound **48** was hydrolysed at the 7-position producing 23-*O*-succinylsilibinin **49** and cinnamic acid (CA) as the main products. Oxidation to the dehydrosilibinin ester **51** also took place in the first hours, before hydrolysis of the dehydrosilibinin ester in 7-position started. Production of silibinin **32** and dehydrosilibinin **45** has not been observed. Scheme **21** shows the main decomposition pathways of 7-*O*-cinnamoyl-23-*O*-succinylsilibinin **48** in cell culture medium.

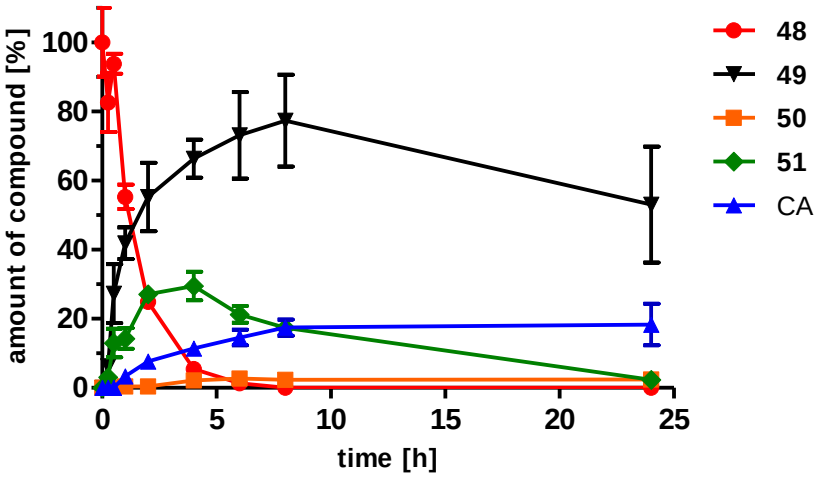

Figure 21. Time-dependent analysis of the stability of compound **48** in assay medium. HPLC-retention times were compared to the corresponding reference compounds. AUCs were determined and the amounts were determined through calibration curves (R^2 > 0.990). The amount of compound **48** at t = 0 min was set as 100 %. The experiments were performed in triplicate (mean) [IV].

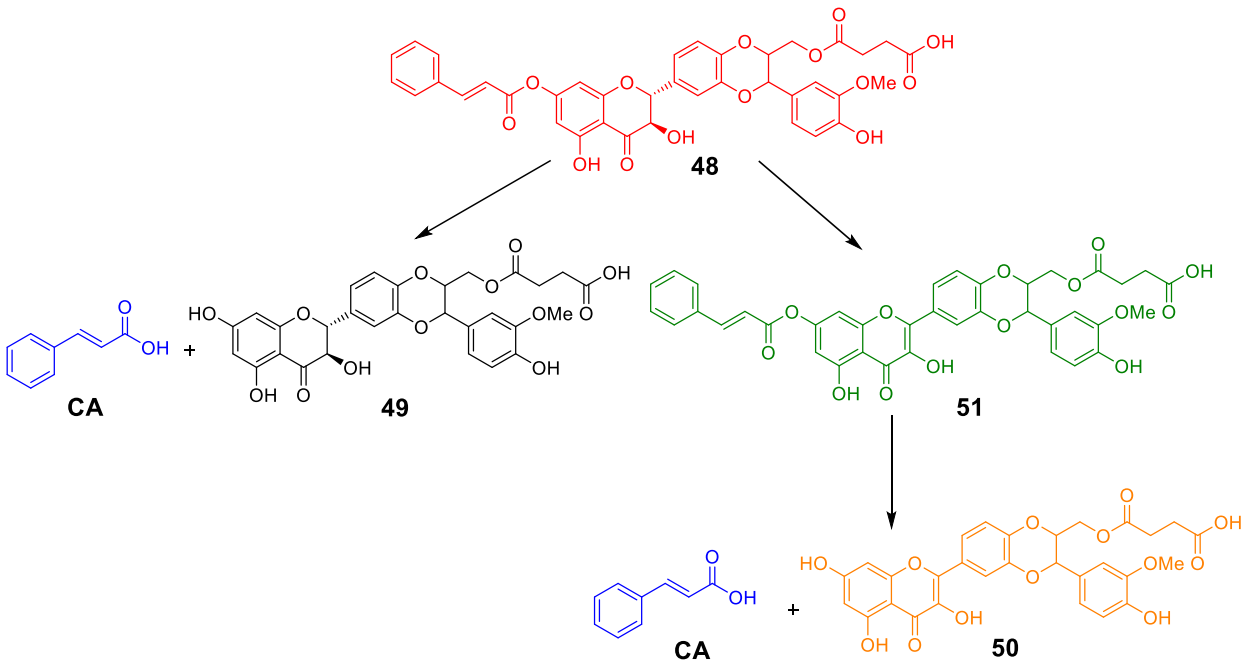

Scheme 21. Main decomposition pathways of hemisuccinate **48** in cell culture medium [IV].

The neuroprotective properties of hemisuccinate **48** were evaluated in the HT-22 hippocampal neuronal cell-model as described above (*cf*. **4.4.1.**). Figure **22** shows the neurotoxicity (**A**) and the neuroprotection (**B**) studies of compound **48** at 1 µM, 5 µM, 10 µM, and 25 µM. No neurotoxicity was observed even at 25 µM. The neuroprotection, however, is much weaker compared to 7-*O*-cinnamoylsilibinin **37a**, which started exhibiting neuroprotection at 5 µM (Figure **16B**; part **4.4.1.**). The hemisuccinate **48** only shows significant neuroprotection at 25 µM albeit weaker than **37a** at this concentration.

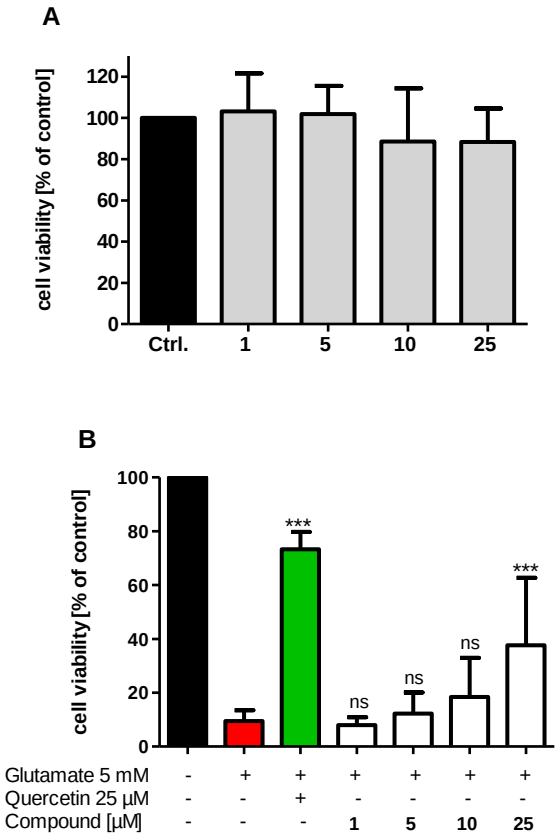

Figure 22. Compound **48** was studied on neuronal HT 22 cells for A) neurotoxic effects and B) neuroprotection against glutamate-induced oxidative stress at 1-25 µM. Results of the modified MTT test are presented as means ± SD of three different independent experiments and refer to untreated control cells which were set as 100% values. Levels of significance: * $p < 0.05$; ** $p < 0.01$; *** $p < 0.001$ [IV].

Taken together, 7-*O*-cinnamoyl-23-*O*-succinylsilibinin **48** shows the intended greatly improved solubility over the reference compound **37a**. It is, however, not a prodrug of the parent compound. As it was shown by our group before [114], it was expected that the ester bond at position 23 would be cleaved more easily, releasing the neuroprotective ester **37a**. While the soluble compound **48** also shows neuroprotection, it is not as pronounced as intended [IV].

4.7. Preliminary *In vivo* Data of 7-*O*-Cinnamoylsilibinin

Silibinin **32** has been studied in several *in vivo* models and positive effects on AD pathology and other brain impairments have been revealed. Lu *et al.* have shown that silibinin **32** is able to reduce the $A\beta_{25-35}$ induced depletion of glutathione and, therefore, prevent memory impairment in mice through antioxidative mechanisms [147]. One of the mechanisms examined was the brain energy metabolism and cholinergic function after intracerebral streptozotocin administration in mice [148]. The study showed attenuation of memory impairment by reduction of oxidative stress and recovery of ATP levels and AChE activity [148]. Silibinin **32** was further shown to attenuate lipopolysaccharide-induced long-term and spatial memory loss and cholinergic dysfunction in rats [149]. Moreover, silibinin **32** was able to reduce dopaminergic neuronal loss and motor deficits in a Parkinson's disease model in mice [150]. Another study revealed inhibition of microglial activation in SAMP8 mice, protecting against learning and memory deficits [151]. Very recently, both antioxidative and anti-apoptotic effects in APP/PS1 transgenic mice [152] and attenuation of anxiety/depression-like behaviours induced by $A\beta_{1-42}$ were described [153]. These findings show that silibinin **32** might be a viable approach for the treatment of AD and other neurodegenerative diseases. However, the compound is hampered by its suboptimal physicochemical properties in terms of solubility and bioavailability, which becomes evident in the amounts (100 mg/kg - 200 mg/kg) orally administered to the animals [147, 151, 152]. A more potent compound that shows similar or better neuroprotective and memory-improving effects at lower doses may, therefore, be desirable. With the much more pronounced neuroprotective effects of 7-*O*-cinnamoyl-silibinin **37a**, we might have such a compound at hand.

7-*O*-Cinnamoylsilibinin **37a** and silibinin **32**, as a reference compound, were tested in an AD *in vivo* model by Matthias Scheiner and Matthias Hoffmann (AK Decker, Universität Würzburg) at the lab for "Molecular Mechanisms in Neurodegenerative Diseases" at the University of Montpellier under the supervision of Dr. Tangui Maurice. The compounds were tested on mice with learning impairment induced by $A\beta_{25-35}$ [154]. Intracerebroventricular (ICV) injection of $A\beta_{25-35}$ causes histological and biochemical changes leading to learning deficits and cholinergic dysfunction, which makes treated animals useful models of AD pathology for the investigation of therapeutic agents [154]. The animals received distilled water (V) or $A\beta_{25-35}$ (9 nmol ICV) on the first day. Starting on the same day, they received compounds **32** or **37a** (1 mg/kg, 3 mg/kg

or 10 mg/kg) or 66% DMSO in an aqueous 0.9% sodium chloride solution (V2) per intraperitoneal injection (IP) once per day for seven days. The animals were tested in a Y-maze experiment on day eight. On day nine they were trained in the passive avoidance test and their performance in passive avoidance was examined on day ten. Twelve subjects were tested for each concentration.

The Y-maze test is an indicator of short-term memory impairment. Alternation behaviour and the number of arm entries are recorded. The alternation behaviour shows the ability of the animal to remember what part of the maze it has already explored, and the number of arm entries gives information about the animal's locomotor activity. The results of the Y-maze test are shown in Figure **23**.

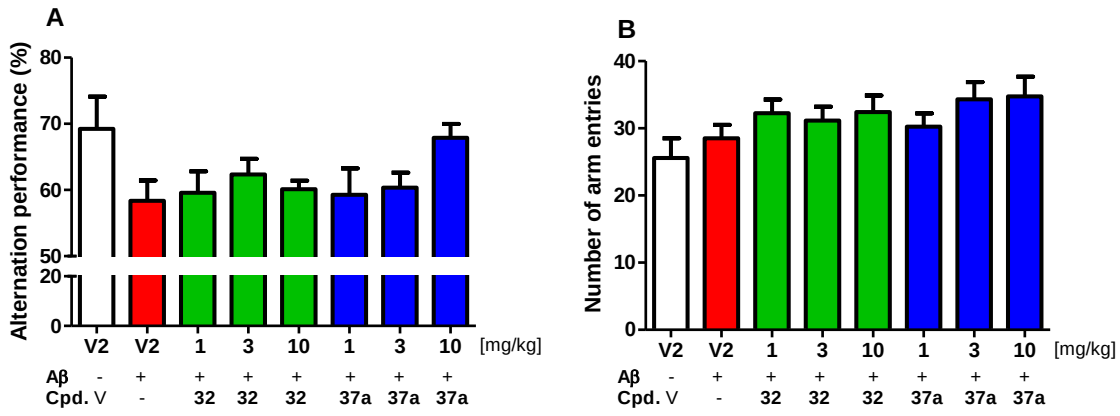

Figure 23. Effects of **32** and **37a**, administered IP, on Aß$_{25-35}$-induced learning impairments in mice: A) spontaneous alternation performance and B) number of arm entries in the Y-maze. The data are presented as mean ± SEM.

In Figure **23A** the alternation performance is depicted. Mice treated with vehicle show an alternation performance of about 70%, whereas the ones that only received Aβ$_{25-35}$ exhibited performance of less than 60%. Both silibinin **32** and the cinnamic acid ester **37a**, at 1 mg/kg and 3 mg/kg, showed no significant changes in alternation behaviour. Only at 10 mg/kg 7-*O*-cinnamoylsilibinin **37a** expressed an apparent improvement. This, however, is also not statistically significant yet and can therefore only be seen as a tendency. The number of arm entries (Figure **23B**) also showed no significant deviation.

The passive avoidance test refers to the long-term memory, described by the step-through latency. The animals are trained with light electroshocks to avoid their natural urge to move to a dark space instead of staying in a bright room. One day after the training, the mice should

be able to remember to avoid the dark area and the time spent in the illuminated room is recorded. Furthermore, if a subject enters the dark compartment, the time it needs to remember the electroshocks and escape the room is recorded (escape latency). The results of the passive avoidance test are shown in Figure **24**.

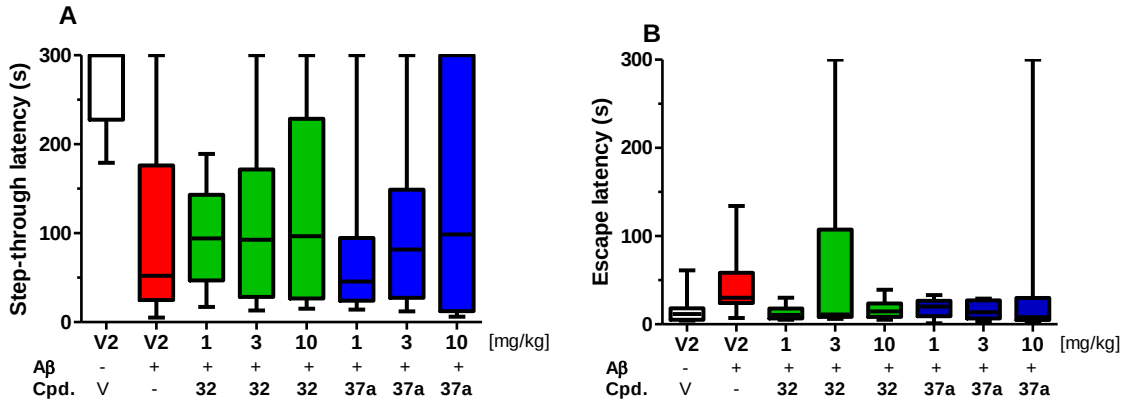

Figure 24. Effects of **32** and **37a**, administered IP, on Aß$_{25-35}$-induced learning impairments in mice: A) step-through latency and B) escape latency in the passive avoidance test. The data are presented as median and interquartile range and whiskers showing the minimum and maximum measured values.

Figure **24A** shows the results of the step-through latency test. On average, the untreated control subjects were able to avoid the dark compartment for the full duration of the experiment. The animals treated with Aβ_{25-35} showed a significant impairment in their long-term memory. Again, the subjects treated with silibinin **32** and 7-*O*-cinnamoylsilibinin **37a** showed no statistically significant improvement over the impaired mice thus far. However, a slight trend to improved memory with increased concentration of **37a** can be observed. The results of the escape latency measurements show the same tendencies (Figure **24B**).

So far, the gathered *in vivo* data from the Y-maze and the passive avoidance tests only show marginal improvements of the memory impairment induced by Aβ_{25-35} after administration of both silibinin **32** and 7-*O*-cinnamoylsilibinin **37a**. However, these results are from a small number of animals and, of course, low concentrations compared to the studies described above. More test subjects and higher concentrations may be required to reveal statistically significant effects and make sure that the presented results are accurate. Yet, in contrast to the IP administration used in this work, oral administration was performed in literature [147, 151, 152]. A comparison regarding dose and effect is therefore rather difficult.

5. Summary

Alzheimer's disease is a complex network of several pathological hallmarks. These characteristics always occur concomitantly and cannot be taken as distinct features of the disease. While there are hypotheses trying to explain the origin and progression of the illness, none of them is able to pinpoint a definitive cause. This fact challenges researchers not to focus on one individual hallmark but, bearing in mind the big picture, target two or more indications at once. This work, therefore, addresses two of the major characteristics of AD: the cholinergic hypothesis and neurotoxic oxidative stress. The former was achieved by targeting the postsynaptic muscarinic M_1 acetylcholine receptor to further investigate its pharmacology, and the latter with the synthesis of neuroprotective natural antioxidant hybrids.

The first aim was the design and synthesis of dualsteric agonists of the muscarinic M_1 acetylcholine receptor. Activation of this receptor was previously shown to improve AD pathologies like the formation of Aβ and NFTs and protect against oxidative stress and caspase activation. Selectively targeting the M_1 receptor is difficult as subtypes M_1 – M_5 of the muscarinic AChRs largely share the same orthosteric binding pocket. Orthosteric ligands are thus unsuitable for selective activation of one specific subtype. Secondary, allosteric binding sites are more diverse between subtypes. Allosteric ligands are, however, in most cases dependent on an orthosteric ligand to cause downstream signals. Dualsteric ligands thus utilize the characteristics of both orthosteric and allosteric ligands in form of a message-address concept. Bridged by an alkylene-linker, the allosteric part ensures selectivity, whereas the orthosteric moiety initiates receptor activation. Two sets of compounds were synthesised in this sense. In both cases, the orthosteric ligand carbachol is connected to an allosteric ligand via linkers of different chain length. The first set utilizes the selective allosteric M_1 agonist TBPB, the second set employs the selective M_1 positive allosteric modulator BQCA. Six compounds were obtained in twelve-step syntheses each. For each one, a reference compound lacking the carbachol moiety was synthesised. The dualsteric ligands **1a-c** and **2a-c** were tested in the IP1 assay. The assay revealed that the TBPB-dualsterics **1** are not able to activate the receptor, whereas the respective TBPB-alkyl reference compounds **27** gave signals depending on the length of the alkylene-linker, suggesting allosteric partial agonism of alkyl compounds **27** and no dualsteric binding of the putatively dualsteric compounds **1**. The

dualsteric BQCA molecules **2**, however, activated the receptor as expected. Efficacy of the C_5-linked compound **2b** was the highest, yet C_3 and C_8 compounds (**2a** and **2c**) also showed partial agonism. In this case, the reference compounds **31** showed no receptor activation, implying the intended dualsteric binding mode of the BQCA-carbachol compounds **2**. Further investigations will be conducted by the working group of Dr. Christian Tränkle at the Department of Pharmacology at the University of Bonn to confirm binding modes and determine affinities as well as selectivity of the synthesised dualsteric compounds.

The second project dealt with the design, synthesis and biological evaluation of neuroprotective esters of the flavonolignan silibinin. While silibinin is already a potent antioxidant, it has been observed that the 7-OH group has a pro-oxidative character, making this position attractive for functionalisation. In order to obtain more potent antioxidants, the pro-oxidative position was esterified with other antioxidant moieties like ferulic acid **35** and derivatives thereof. Seventeen esters of silibinin **32**, including pure diastereomers of 7-*O*-feruloylsilibinin (**43a** and **43b**) and a cinnamic acid ester of 2,3-dehydrosilibinin **46**, were synthesised by regioselective esterification using acyl chlorides under basic conditions. The physicochemical antioxidant properties were assessed in the FRAP assay. This assay revealed no improvement of the antioxidant properties except for 7-*O*-dihydrosinapinoylsilibinin **39b**. These results, however, do not correlate with the neuroprotective properties determined in the HT-22 hippocampal neuronal cell model. The assay showed overadditive neuroprotective effects of the esters exceeding those of its components and equimolar mixtures with the most potent compounds being 7-*O*-cinnamoylsilibinin **37a**, 7-*O*-feruloylsilibinin **38a** and the acetonide-protected caffeic acid ester **40a**. These potent Michael system bearing compounds may be considered as “PAINS”, but the assays used to assess antioxidant and neuroprotective activities were carefully chosen to avoid false positive readouts. The most potent compounds **37a** and **38a**, as well as the diastereomers **43a** and **43b**, were further studied in assays related to AD. *In vitro* ischemia, inhibition of microglial activation, PC12 cell differentiation and inhibition of Aβ42 and τ protein aggregation assays showed similar results in terms of overadditive effects of the synthesised esters. Moreover, the diastereomers **43a** and **43b** showed differences in their activities against oxytosis (glutamate-induced apoptosis), inhibition of Aβ42 and τ protein aggregation, and PC12 cell differentiation. The stereospecific effect or mode of action against Aβ42 and τ protein aggregation is more pronounced than that of silybin A (**32a**) and silybin B (**32b**) reported in literature and needs to be elucidated in future

work. Stability measurements in cell culture medium revealed that the esters do not only get hydrolysed but are partially oxidised to their respective 2,3-dehydrosilibinin esters. Because dehydrosilibinin **45** itself is described as a more potent antioxidant than silibinin **32**, 7-*O*-cinnamoyl-2,3-dehydrosilibinin **46** was expected to be even more potent than its un-oxidised counterpart **37a** in terms of neuroprotection. The oxytosis assay, however, showed that the neurotoxicity of **46** is much more pronounced, especially at higher concentrations, reducing its neuroprotective potential. Dehydrosilibinin esters are therefore inferior to the silibinin esters for application as neuroprotectants, because of the difficulty of their synthesis and their increased neurotoxicity. A synergistic effect of both species (silibinin and the oxidised form) might, however, be possible or even necessary for the pronounced neuroprotective effects of silibinin esters. As the dehydro-species show distinct neuroprotective properties at low concentrations, their continuous formation over time might make an essential contribution to the overall neuroprotection of the synthesised esters. Due to solubility issues for some of the ester compounds, 7-*O*-cinnamoylsilibinin **37a** was converted into a highly soluble hemisuccinate. The vastly improved solubility of 7-*O*-cinnamoyl-23-*O*-succinylsilibinin **48** was confirmed in shake-flask experiments. Contrary to expectation, stability examinations showed that the succinyl compound **48** is not cleaved to form 7-*O*-cinnamoylsilibinin **37a**. Neuroprotection assays confirmed that **48** is not a prodrug of the corresponding ester. It was determined that the main site of hydrolysis is the 7-position, cleaving **37** to silibinin **32** and cinnamic acid thus reducing the compound's neuroprotective effects. Nevertheless, the compound still showed neuroprotection at a concentration of 25 µM. The improved solubility might be more beneficial than the higher neuroprotection of the poorly soluble parent compound **37a** *in vivo*. 7-*O*-Cinnamoylsilibinin **37a** was further investigated to reduce $A\beta_{25-35}$ induced learning impairment in mice. While tendencies of improved short-term and long-term memory in the animals were observed, the effects are not yet statistically significant in both Y-maze and passive avoidance tests. A greater number of test subjects is necessary to ensure correctness of the preliminary results presented in this work. However, an effect of ester **37a** is observable *in vivo*, showing blood-brain barrier penetration. The esters synthesised are a novel approach for the treatment of AD as they show strong neuroprotective effects and their hydrolysis products or metabolites are only non-toxic natural products.

6. Zusammenfassung

Mehrere Hypothesen versuchen die Ursprünge und den Fortschritt der Alzheimer'schen Krankheit zu erklären. Eine definitive Ursache konnte allerdings bisher nicht festgestellt werden, da die Merkmale der Krankheit grundsätzlich nebeneinander auftreten. Wissenschaftler müssen also auf der Suche nach Therapien die verschiedenen pathologischen Vorgänge gleichzeitig behandeln. In dieser Arbeit wurden daher zwei der prominenteren Anzeichen der Alzheimer'schen Krankheit bearbeitet. Zum einen wurde die cholinerge Hypothese, mit Adressierung des postsynaptischen muskarinischen M_1 Acetylcholinrezeptors, thematisiert. Und zum anderen wurde neurotoxischer oxidativer Stress, mit der Entwicklung von neuroprotektiven natürlichen Antioxidantien, behandelt.

Das erste Projekt beschäftigte sich mit dem Design und der Synthese von dualsterischen Agonisten des muskarinischen M_1 Acetylcholinrezeptors. In der Literatur wurde gezeigt, dass die Aktivierung dieses Rezeptors eine Verbesserung des Krankheitsverlaufs nach sich ziehen kann. Es wurde unter anderem demonstriert, dass Verminderungen der Aggregation von Aβ und τ Proteinen, wie auch von oxidativem Stress, eintreten. Die selektive Aktivierung des M_1-Rezeptors gestaltet sich jedoch als sehr schwierig, da sich die fünf Subtypen M_1 – M_5 der muskarinischen Acetylcholinrezeptoren nur geringfügig in ihrer Substratbindestelle unterscheiden. Die Anwendung von rein orthosterischen Liganden ist daher ungenügend. Sekundäre bzw. allosterische Bindestellen, unterscheiden sich zwischen den Subtypen stärker. Allosterische Liganden sind allerdings oft von der Anwesenheit eines orthosterischen Agonisten abhängig, um den Rezeptor zu aktivieren. Die Einbeziehung beider Bindestellen gleichzeitig erlaubt jedoch die Anwendung eines Signal-Adresse-Konzepts, bei welchem ein orthosterischer Ligand (Signal) mit einem allosterischen Liganden (Adresse) über einen Linker verknüpft wird. Auf diese Weise wurden zwei Sätze dualsterischer Verbindungen hergestellt. Der orthosterische Ligand Carbachol wurde jeweils über unterschiedlich lange Alkyllinker mit einem allosterischen Liganden verbunden. Als allosterische Liganden, selektiv für den M_1-Rezeptor, wurden zum einen TBPB, ein allosterischer Agonist, und zum anderen BQCA, ein positiver allosterischer Modulator, gewählt. Sechs Verbindungen wurden in Synthesen mit jeweils zwölf Schritten hergestellt. Außerdem wurden für jede der dualsterischen Verbindungen Referenzsubstanzen, ohne die Carbachol-Einheit, synthetisiert. Die dualsterischen Liganden **1a**-**c** und **2a**-**c** wurden im IP1 Assay getestet und es zeigte sich, dass

die TBPB-Verbindungen **1** nicht in der Lage waren den Rezeptor zu aktivieren. Im Gegensatz dazu, konnten die entsprechenden Referenzverbindungen **27**, abhängig von der Kettenlänge, Rezeptorantworten auslösen. Dieser Befund zeigt allosteren Agonismus der Referenzen **27** und lässt Grund zur Annahme, dass die Verbindungen **1** keinen dualsterischen Bindemodus eingehen. Die BQCA-Substanzen **2**, auf der anderen Seite, aktivierten den Rezeptor wie erwartet. Die Verbindung mit dem C_5-Linker **2b** löste das stärkste Signal aus, aber auch die C_3- und C_8-Verbindungen (**2a** und **2c**) zeigten Partialagonismus. In diesem Fall aktivierten die Referenzsubstanzen **31** den Rezeptor nicht, was auf einen dualsterischen Bindemodus der Zielstrukturen **2** schließen lässt. Weitere Untersuchungen dieser Verbindungen werden in der Arbeitsgruppe von Dr. Christian Tränkle am Institut für Pharmakologie und Toxikologie der Universität Bonn durchgeführt und sollen näheren Aufschluss über Bindemodi, Affinitäten und Selektivität geben.

Das zweite Projekt beschäftigte sich mit dem Design, der Synthese und biologischen Evaluierung von neuroprotektiven Estern des Flavonolignans Silibinin **32**. Obwohl Silibinin **32** selbst ein starkes Antioxidans ist, wurde festgestellt, dass seine 7-OH Gruppe pro-oxidativen Charakter besitzt. Diese Position ist somit ein attraktives Ziel für Funktionalisierungen zur Verstärkung der antioxidativen Eigenschaften. Um Substanzen mit verbesserten antioxidativen Effekten herzustellen, wurde diese Gruppe mit anderen Antioxidantien, wie etwa Ferulasäure **35** und strukturell ähnlichen Derivaten, verestert. Dabei konnten siebzehn Ester, inklusive den reinen Diastereomeren von 7-*O*-Feruloylsilibinin (**43a** und **43b**) und einem Zimtsäureester von 2,3-Dehydrosilibinin **46**, durch regioselektive Veresterung mit den entsprechenden Säurechloriden im basischen Milieu hergestellt werden. Die physikochemischen antioxidativen Eigenschaften wurden mit Hilfe des FRAP-Assays bestimmt. Hier trat im Allgemeinen keine Verbesserung der Eigenschaften auf. Nur 7-*O*-Dihydrosinapinoylsilibinin **39b** zeigte gesteigertes antioxidatives Verhalten. Diese Ergebnisse stimmten jedoch nicht mit den neuroprotektiven Eigenschaften, die in einem Zellmodel mit HT-22 hippocampalen neuronalen Zellen (Oxytose Assay) getestet wurden, überein. Dieser Assay konnte beweisen, dass die dargestellten Ester ihre einzelnen Komponenten, und eine Mischung dieser, hinsichtlich ihrer Eigenschaften übertreffen und überadditive neuroprotekive Effekte besitzen. Die wirksamsten Verbindungen waren 7-*O*-Cinnamoylsilibinin **37a**, 7-*O*-Feruloylsilibinin **38a** und der Acetonid-geschützte Kaffesäureester **40a**. Diese Substanzen besitzen alle ein Michael-System und könnten deshalb

als sogenannte „PAINS“ angesehen werden. Allerdings wurden die verwendeten Assays sorgfältig ausgewählt, um falsch-positive Ergebnisse zu vermeiden. Die wirksamsten Substanzen, inklusive der beiden Diastereomeren **43a** und **43b**, wurden in weiteren, für die Alzheimer'sche Krankheit relevanten, Experimenten untersucht. Ein *in vitro* Ischämie Modell, die Inhibition von Mikroglia Aktivierung, die Aktivierung von PC12 Zell-Differenzierung und die Inhibition von Aβ und τ Protein Aggregation bestätigen die überadditiven Effekte der Ester. Die einzelnen Diastereomere **43a** und **43b** zeigten unterschiedlich stark ausgeprägte Effekte gegenüber Oxytose, Inhibition von Aβ und τ Protein Aggregation und PC12 Zell-Differenzierung. Dieser stereospezifische Effekt oder Wirkmechanismus war auffallender als die in der Literatur beschriebenen Effekte der Diastereomere Silybin A (**32a**) und Silybin B (**32b**) und muss in Zukunft näher untersucht werden. Stabilitätsuntersuchungen in Zellkulturmedium zeigten, dass die Ester nicht einfach nur hydrolysiert, sondern teilweise zu den entsprechenden Dehydrosilibininestern oxidiert werden. Da Dehydrosilibinin **45** selbst als stärkeres Antioxidans als Silibinin **32** beschrieben wird, wurde erwartet, dass der Zimtsäure-Dehydrosilibininester **46** höhere Wirksamkeit als der Silibininester **37a** zeigt. Der Neuroprotektions-Assay bewies jedoch, dass **46** ausgeprägtere Neurotoxizität besitzt und seine potentielle Neuroprotektion dadurch verschlechtert wird. Dehydrosilibininester sind den Silibininestern daher bei dieser Anwendung unterlegen, auch weil ihre Synthese deutlich aufwendiger ist. Ein synergistischer Effekt beider Spezies (Silibinin und Dehydrosilibinin) könnte allerdings möglich und vielleicht sogar nötig sein. Die kontinuierliche Generierung der Dehydrosilibininester mit der Zeit könnte ein wichtiger Faktor für die neuroprotektiven Eigenschaften der Silibininester sein, da die neuroprotektiven Effekte der Dehydro-silibininester bei niedrigen Konzentrationen sehr ausgeprägt sind. Aufgrund der problematischen Löslichkeit der hergestellten Substanzen, wurde die Löslichkeit der Ester verbessert, indem 7-*O*-Cinnamoylsilibinin **37a**, als Modell, mit gut löslichen Hemisuccinaten verbunden wurde. Die stark verbesserte Löslichkeit von 7-*O*-Cinnamoyl-23-*O*-succinylsilibinin **48** wurde in *shake-flask* Experimenten bewiesen. Stabilitätsuntersuchungen und der Neuroprotektions-Assay zeigten allerdings, dass die Succinylverbindung **48** hauptsächlich an Position 7, und damit in Zimtsäure und 23-*O*-Succinylsilibinin **50**, gespalten wurde. Hemisuccinat **48** zeigte Neuroprotektion nur bei einer Konzentration von 25 µM und ist somit kein Pro-Drug von 7-*O*-Cinnamoylsilibinin **37a**. Die erhöhte Löslichkeit könnte jedoch *in vivo* nutzbringender sein als die gesteigerte Neuroprotektion des schlechter löslichen

Derivats **37a**. 7-*O*-Cinnamoylsilibinin **37a** wurde außerdem darauf getestet $A\beta_{25-35}$ induzierte Gedächtnisbeeinträchtigungen in Mäusen zu verbessern. Obwohl Tendenzen zu verbessertem Kurzzeit- und Langzeitgedächtnis erkenntlich wurden, konnten noch keine statistisch signifikanten Verbesserungen sowohl im *Y-maze* Test als auch im *passive avoidance* Test gezeigt werden. Mehr Testsubjekte sind nötig, um die Ergebnisse zu überprüfen. Dennoch sind Effekte *in vivo* zu beobachten, die Blut-Hirn-Schranken Penetration zeigen. Die dargestellten Ester sind somit ein neuer Ansatz für die Behandlung der Alzheimer'schen Krankheit, da sie ausgeprägte neuroprotektive Effekte zeigen und ihre Spaltprodukte und Metaboliten ausschließlich nicht-toxische Naturstoffe sind.

7. Experimental Part

7.1. General

Tetrahydrofuran (THF) was freshly distilled from sodium/benzophenone. Dichloromethane was dried over calcium hydride, distilled and stored over mol sieves. All other common reagents and solvents were purchased from commercial suppliers and used as such. Microwave-assisted reactions were carried out in an MLS-rotaPREP instrument (Milestone, Leutkirch, Germany) using 10 weflon disks. Reaction progress was monitored using analytical thin layer chromatography (TLC) on precoated silica gel GF254 plates (Macherey-Nagel GmbH & Co. KG, Düren, Germany), the spots were detected under UV light (254 nm). Column chromatography was conducted using silica gel (high-purity grade, 0.035-0.070 mm, Merck KGaA, Darmstadt, Germany). Nuclear magnetic resonance spectra were performed with a Bruker AV-400 NMR instrument (Bruker, Karlsruhe, Germany). ESI mass spectral data was acquired on a Shimadzu LCMS 2020. Analytic HPLC was performed on a system from Shimadzu Products equipped with a DGU-20A3R controller, LC20AB liquid chromatograph, and an SPD-20A UV/Vis detector. Stationary phase was a Synergi 4U fusion-RP (150 × 4.6 mm) column. Mobile phase: gradient MeOH (0.1% TFA)/water (0.1% TFA) (phase A/ phase B) were used. For analytical HPLC a flow rate of 1 mL/min and for preparative HPLC a flow rate of 3 mL/min was used.

7.2. Synthesis of Dualsteric TBPB-derived Compounds **1**

Synthesis of TBPB-Building Block **3**:

Ethyl 4-((2-nitrophenyl)amino)piperidine-1-carboxylate 5

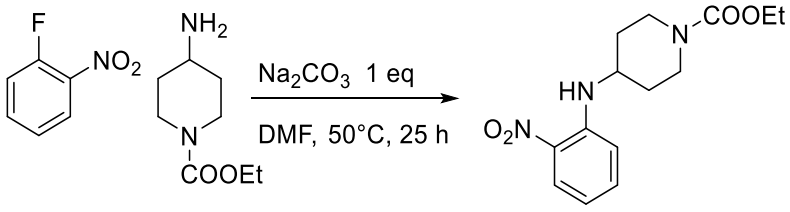

M = 293.32 g/mol

To a stirred suspension of 5.27 mL 2-fluoronitrobenzene (50 mmol, 1 eq), 83 mg potassium iodide (0.5 mmol, 0.01 eq) and 5.3 g sodium carbonate (50 mmol, 1 eq) in 75 mL dimethylformamide, 8.65 mL ethyl 4-amino-1-piperidinecarboxylate (50 mmol, 1 eq) was

added. The reaction mixture was heated at 50 °C for 25 h. After cooling to room temperature, the mixture was diluted with water and extracted with ethyl acetate. The combined organic phases were washed with 10% citric acid solution, dried over sodium sulfate and the solvent was removed. The crude product was purified by column chromatography (30 % EtOAc in petroleum ether → 50 %; elute with CH_2Cl_2), which gave 13.4 g (45.7 mmol, 91 %) of the desired product as an orange solid. **^{1}H-NMR (400 MHz, $CDCl_3$)** δ(ppm) = 1.27 (t, *J* = 7.1 Hz, 3 H, CH_3), 1.51 – 1.64 (m, 2 H, *CH_2*-CH), 2.03 – 2.12 (m, 2 H, *CH_2*-CH), 3.06 – 3.17 (m, 2 H, CH_2-N), 3.64 – 3.75 (m, 1 H, CH), 4.01 – 4.12 (m, 2 H, CH_2-N), 4.15 (q, *J* = 7.1 Hz, 2 H, *CH_2*-CH_3), 6.62 – 6.68 (m, 1 H, Ar), 6.87 (d, *J* = 8.3 Hz, 1 H, Ar), 7.40 – 7.46 (m, 1 H, Ar), 8.04 – 8.12 (m, 1 H, NH), 8.16 – 8.21 (m, 1 H, Ar)

Ethyl 4-((2-aminophenyl)amino)piperidine-1-carboxylate 6

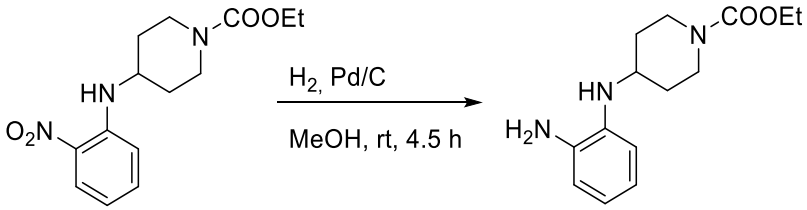

M = 263.34 g/mol

A suspension of 13.4 g of the nitro-compound **5** (45.7 mmol, 1 eq) and 1.3 g Pd/C (10 %) in 250 mL methanol was stirred at room temperature under H_2-atmosphere for 4.5 h. The reaction mixture was filtered through a pad of celite and the solvent was removed, which gave 11.4 g (43.2 mmol, 95 %) of a dark red oil as the crude product.**^{1}H-NMR (400 MHz, MeOD)** δ(ppm) = 1.25 (t, *J* = 7.0 Hz, 3 H, CH_3), 1.32 – 1.46 (m, 2 H, *CH_2*-CH), 1.95 – 2.08 (m, 2 H, *CH_2*-CH), 2.91 – 3.10 (m, 2 H, CH_2-N), 3.42 – 3.54 (m, 1 H, CH), 4.04 – 4.10 (m, 2 H, CH_2-N), 4.11 (q, *J* = 7.1 Hz, 2 H, *CH_2*-CH_3), 6.58 – 6.82 (m, 4 H, Ar)

Ethyl 4-(2-oxo-2,3-dihydro-1*H*-benzo[*d*]imidazol-1-yl)piperidine-1-carboxylate 7

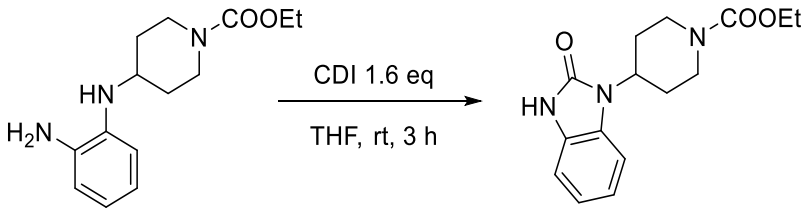

M = 289.34 g/mol

A solution of 9.38 g of the diamine **6** (35.6 mmol, 1 eq) and 9.24 g carbonyldiimidazole (57 mmol, 1.6 eq) in 250 mL tetrahydrofuran was stirred for 3 h at room temperature. The solvent was removed, and the residue was taken up in 250 mL ethyl acetate and 75 mL water. The phases were separated, and the inorganic phase was extracted with ethyl acetate. The combined organic phases were washed with brine, dried over sodium sulfate and the solvent was removed. The crude product was crystallized from diethyl ether to give 11.4 g (quant.) of the desired product as a light brown solid. **^{1}H-NMR (400 MHz, MeOD)** δ(ppm) = 1.29 (t, *J* = 7.2 Hz, 3 H, CH_3), 1.76 – 1.85 (m, 2 H, *CH_2*-CH), 2.32 – 2.46 (m, 2 H, *CH_2*-CH), 2.90 – 3.06 (m, 2 H, CH_2-N), 4.17 (q, *J* = 7.3 Hz, 2 H, *CH_2*-CH_3), 4.28 – 4.36 (m, 2 H, CH_2-N), 4.38 – 4.49 (m, 1 H, CH), 7.02 – 7.11 (m, 3 H, Ar), 7.20 – 7.25 (m, 1 H, Ar)

1-(Piperidin-4-yl)-1,3-dihydro-2*H*-benzo[*d*]imidazol-2-one 3

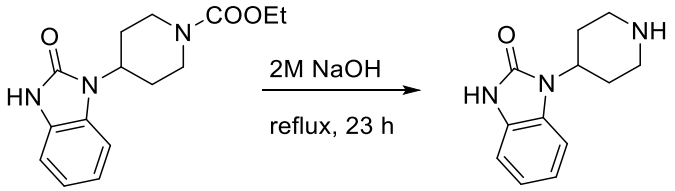

M = 217.27 g/mol

A solution of 11.4 g of the ester **7** (35.6 mmol, 1 eq) in 250 mL 2M NaOH was heated to 100°C for 23 h. After cooling to 0°C, the mixture was adjusted to pH = 1-2 with concentrated HCl and then basified with 2M NaOH solution to pH = 13. The basic solution was extracted with ethyl acetate several times. Drying of the organic phases over sodium sulfate and removal of the solvent gave 6.9 g (31.8 mmol, 89 %) of the desired product as a light brown solid. **^{1}H-NMR (400 MHz, MeOD)** δ(ppm) = 1.73 – 1.81 (m, 2 H, *CH_2*-CH), 2.39 (qd, *J* = 12.7, 4.3 Hz, 2 H, *CH_2*-CH), 2.76 (td, *J* = 12.7, 2.6 Hz, 2 H, CH_2-N), 3.17 – 3.24 (m, 2 H, CH_2-N), 4.40 (tt, *J* = 12.4, 4.3 Hz, 1 H, CH), 7.01 – 7.10 (m, 3 H, Ar), 7.32 – 7.40 (m, 1 H, Ar)

Synthesis of Linkers **4**:

tert-Butyl-(3-hydroxypropyl)carbamate 10a

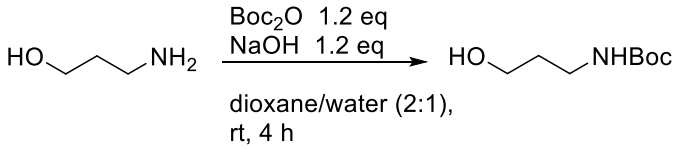

M = 175.23 g/mol

0.76 mL 3-Aminopropanol (10 mmol, 1 eq) were dissolved in 11 mL dioxane/H_2O (2:1). 6 mL 2M NaOH (1.2 eq) and 2.619 g Boc_2O (12 mmol, 1.2 eq) were added successively. The reaction mixture was stirred for 4 h at room temperature. Dioxane was removed and the residue was taken up in 40 mL of citric acid solution (10% *w/w*). The mixture was extracted with EtOAc. The combined organic phases were dried over sodium sulfate and the solvents were removed, which gave 2.17 g (quant.) of a colourless oil as the crude product and was used in the next reaction without further purification.

tert-Butyl-(3-iodopropyl)carbamate 4a

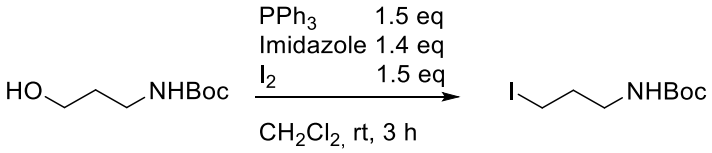

M = 285.85 g/mol

A solution of 953 g imidazole (14 mmol, 1.4 eq) and 3.934 g triphenylphosphine (15 mmol, 1.5 eq) in 45 mL dichloromethane was cooled to 0°C in an ice bath. 3.807 g iodine (15 mmol, 1.5 eq) were added slowly and the mixture was stirred for 45 min at room temperature. A solution of 2.17 g of the alcohol **10a** (10 mmol, 1 eq) in 15 mL dichloromethane was added to the reaction mixture. The reaction was stirred for 3 h at room temperature. The reaction mixture was poured into 50 mL water. The phases were separated, and the organic phase was washed with HCl (10% *w/w*). The inorganic phases were extracted with dichloromethane. The combined organic phases were dried over sodium sulfate and the solvent was removed. The crude product was purified by column chromatography (petroleum ether 5:1 EtOAc → 3:1; elute with CH_2Cl_2), which gave 2.266 g (7.95 mmol, 80 %) of the desired product as a yellow oil. **^{1}H-NMR (400 MHz, $CDCl_3$)** δ(ppm) = 1.43 (s, 9 H, Boc), 1.99 (quin, J = 6.7 Hz, 2 H, CH_2), 3.15 – 3.23 (m, 4 H, 2xCH_2), 4.65 (br. s., 1 H, NH)

***tert*-Butyl-(5-hydroxypentyl)carbamate 10b**

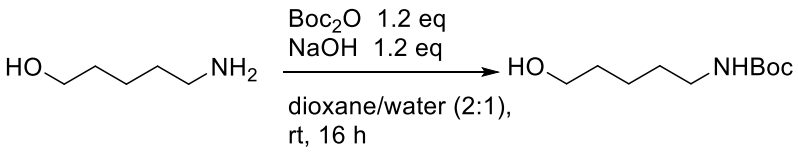

M = 203.28 g/mol

2.1 mL 5-Aminopentanol (10 mmol, 1 eq, 50% in water) were dissolved in 14 mL dioxane/H_2O (2:1). 6 mL 2M NaOH (1.2 eq) and 2.62 g Boc_2O (12 mmol, 1.2 eq) were added successively. The reaction mixture was stirred for 16 h at room temperature. Dioxane was removed and the residue was taken up in citric acid solution (10% *w/w*). The mixture was extracted with EtOAc. The combined organic phases were dried over sodium sulfate and the solvents were removed, which gave 2.42 g (quant.) of a colourless oil as the crude product and was used in the next reaction without further purification.

***tert*-Butyl-(5-iodopentyl)carbamate 4b**

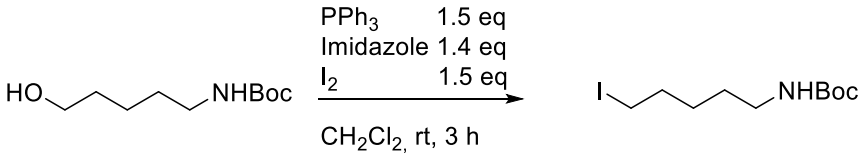

M = 313.18 g/mol

A solution of 953 g imidazole (14 mmol, 1.4 eq) and 3.934 g triphenylphosphine (15 mmol, 1.5 eq) in 30 mL dichloromethane was cooled to 0°C in an ice bath. 3.81 g Iodine (15 mmol, 1.5 eq) were added slowly and the mixture was stirred for 1 h at room temperature. A solution of 2.42 g of the alcohol **10b** (10 mmol, 1 eq) in 15 mL dichloromethane was added to the reaction mixture. The reaction was stirred for 3 h at room temperature. The reaction mixture was poured into 50 mL water. The phases were separated, and the organic phase was washed with HCl (10% *w/w*). The inorganic phases were extracted with dichloromethane. The combined organic phases were dried over sodium sulfate and the solvent was removed. The crude product was purified by column chromatography (petroleum ether 5:1 EtOAc → 3:1; elute with CH_2Cl_2), which gave 2.82 g (8.99 mmol, 90 %) of the desired product as a pale yellow oil. **^{1}H-NMR (400 MHz, $CDCl_3$)** δ(ppm) = 1.35 – 1.52 (m, 4 H, 2xCH_2), 1.41 (s, 9 H, Boc), 1.81 (quin, *J* = 7.2 Hz, 2 H, CH_2), 3.09 (q, *J* = 6.4 Hz, 2 H, BocN-*CH_2*), 3.16 (t, *J* = 7.0 Hz, 2 H, CH_2-I), 4.56 (br. s, 1 H, NH). **ESI-MS:** 336.15 *m/z* $[M+Na]^+$

8-Tosyloctan-1-ol 8

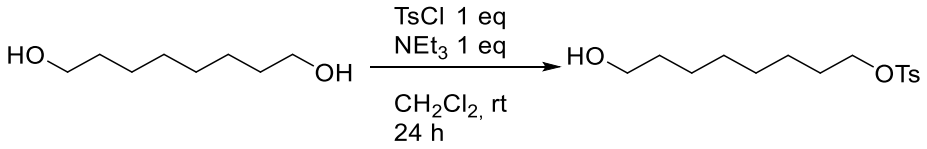

M = 300.41 g/mol

3.66 g 1,8-Octandiol (25 mmol, 1 eq) were suspended in 100 mL dichloromethane. 3.47 mL triethylamine (25 mmol, 1 eq), 4.77 g tosylchloride (25 mmol, 1 eq) and a catalytic amount of DMAP were added. The mixture was stirred at room temperature for 24 h. The mixture was washed twice with water and the organic phase was dried over sodium sulfate and the solvent was removed. Column chromatography (petroleum ether 3:1 EtOAc → 1:1) gave 3.74 g (11.55 mmol, 46 %) of the desired product as a colorless oil. **^{1}H-NMR (400 MHz, $CDCl_3$)** δ(ppm) = 1.18 – 1.32 (m, 8 H, 4xCH_2), 1.50 (dt, *J* = 15.1, 6.5 Hz, 2 H, *CH_2*-CH_2-OH), 1.60 (dt, *J* = 14.3, 6.5 Hz, 2 H, *CH_2*-CH_2-OTs), 1.78 (br. s., 1 H, OH), 2.41 (s, 3 H, CH_3), 3.57 (t, *J* = 6.7 Hz, 2 H, *CH_2*-OH), 3.98 (t, *J* = 6.5 Hz, 2 H, *CH_2*-OTs), 7.29 – 7.34 (m, 2 H, 2xAr-H), 7.73 – 7.77 (m, 2 H, 2xAr-H). **^{13}C-NMR (100 MHz, $CDCl_3$)** δ(ppm) = 21.6 (CH_3), 25.2 (CH_2), 25.6 (CH_2), 28.8 (2xCH_2), 29.1 (CH_2), 32.6 (CH_2), 62.8 (CH_2-OH), 70.7 (CH_2-OTs), 127.8 (2xAr-H), 129.8 (2xAr-H), 133.2 (Ar-C_q), 144.7 (Ar-C_q). **ESI-MS:** 301.15 *m/z* $[M+H]^+$, 323.15 *m/z* $[M+Na]^+$

8-Azidooctan-1-ol

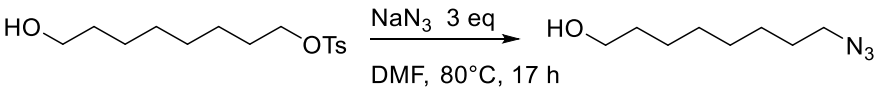

M = 171.24 g/mol

3.47 g Tosylate **8** (11.55 mmol, 1 eq) was dissolved 20 mL dimethylformamide and 2.25 g sodium azide (36.65 mmol, 3 eq) were added. The mixture was heated to 80°C for 17 h. After cooling to room temperature, water and ethyl acetate were added and the phases separated. The organic phase was washed with water several times and dried over sodium sulfate. Removal of the solvent gave 1.89 g (11.0 mmol, 95 %) of the desired product as a gold oil. **^{1}H-NMR (400 MHz, $CDCl_3$)** δ(ppm) = 1.26 – 1.39 (m, 8 H, 4xCH_2), 1.48 – 1.60 (m, 4 H, 2xCH_2), 1.91 (s, 1 H, OH), 3.22 (t, *J* = 6.9 Hz, 2 H, CH_2-N_3), 3.58 (t, *J* = 6.7 Hz, 2 H, *CH_2*-OH). **^{13}C-NMR (100 MHz, $CDCl_3$)** δ(ppm) = 25.6 (CH_2), 26.6 (CH_2), 28.8 (CH_2), 29.1 (CH_2), 29.2 (CH_2), 32.7 (CH_2), 51.4 (CH_2-N_3), 62.8 (CH_2-OH)

8-Aminooctan-1-ol 9

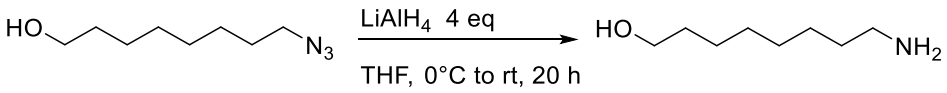

M = 145.25 g/mol

1.633 g of the crude 8-azidooctan-1-ol (9.54 mmol, 1 eq) was dissolved in tetrahydrofuran and the mixture was cooled to 0°C. 1.45 g lithium aluminium hydride (38.16 mmol, 4 eq) were added in small portions. The mixture was stirred for 20 min at 0°C and 19 h at room temperature. The reaction was quenched with water at 0°C and extracted with ethyl acetate. The combined organic phases were washed with brine and dried over sodium sulfate. Removal of the solvent gave 1.0 g (6.88 mmol, 72 %) of the desired product as a white solid. **^{1}H-NMR (400 MHz, $CDCl_3$)** δ(ppm) = 1.20 – 1.34 (m, 8 H, 4xCH_2), 1.40 (quin, *J* = 6.8 Hz, 2 H, CH_2), 1.51 (quin, *J* = 7.0 Hz, 2 H, CH_2), 1.82 (br. s., 3 H, NH_2, OH), 2.63 (t, *J* = 7.0 Hz, 2 H, *CH_2*-NH_2), 3.56 (t, *J* = 6.7 Hz, 2 H, *CH_2*-OH). **^{13}C-NMR (100 MHz, $CDCl_3$)** δ(ppm) = 25.8 (CH_2), 26.8 (CH_2), 29.4 (2xCH_2), 32.8 (CH_2), 33.6 (CH_2), 42.1 (*CH_2*-NH_2) , 62.5 (*CH_2*-OH). **ESI-MS:** *m/z* 146.25 $[M+H]^+$

***tert*-Butyl(8-hydroxyoctyl)carbamate 10c**

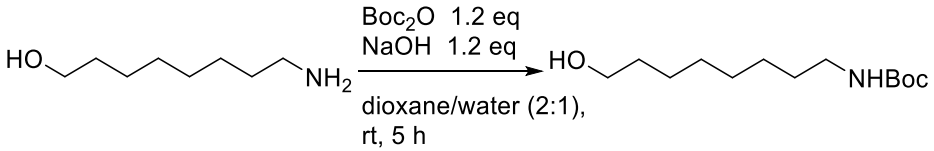

M = 245.36 g/mol

1.09 g 8-Aminooctanol **9** (7.5 mmol, 1 eq) were dissolved in 30 mL dioxane/water (2:1) and 1.96 g Boc_2O (9.0 mmol, 1.2 eq) and 360 mg sodium hydroxide (9.0 mmol, 1.2 eq) were added. The mixture was stirred for 5 h at room temperature. Volatiles were removed, and the residue was dissolved in ethyl acetate and citric acid solution (10% *w/w*). The phases were separated, and the inorganic phase was extracted with ethyl acetate. The combined organic phases were washed with brine and dried over sodium sulfate. Removal of the solvent gave 1.99 g (8.11 mmol, quant.) of the crude product as a yellow solid and was used in the next reaction without further purification.

***tert*-Butyl(8-iodooctyl)carbamate 4c**

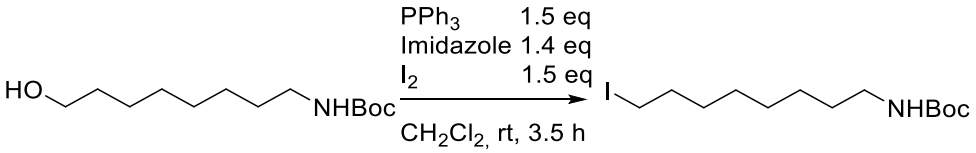

M = 355.25 g/mol

3.72 g Triphenylphosphine (14.19 mmol, 1.5 eq) and 900 mg imidazole (13.25 mmol, 1.4 eq) were dissolved in 50 mL dichloromethane. 3.60 g iodine (14.19 mmol, 1.5 eq) were added. The mixture was stirred for 1 h at room temperature. To this mixture, a solution of 2.32 g Boc-aminooctanol **10c** (9.46 mmol, 1 eq) in 10 mL dichloromethane was added. The resulting mixture was stirred for 4 h at room temperature. The reaction was quenched with water and the phases were separated. The organic phase was washed with HCl (10% *w/w*) and the combined inorganic phases were extracted with dichloromethane. The combined organic phases were dried over sodium sulfate and the solvent was removed. Column chromatography (petroleum ether 20:1 EtOAc) gave 2.4 g (6.8 mmol, 72 %) of the desired product as a colourless oil. **^{1}H-NMR (400 MHz, $CDCl_3$)** δ(ppm) = 1.26 – 1.32 (m, 6 H, 3xCH_2), 1.33 – 1.40 (m, 2 H, CH_2), 1.41 – 1.49 (m, 2 H, CH_2), 1.43 (s, 9 H, Boc-CH_3), 1.80 (quin, *J* = 7.2 Hz, 2 H, CH_2), 3.09 (q, *J* = 6.4 Hz, 2 H, BocN-CH_2), 3.17 (t, *J* = 7.0 Hz, 2 H, CH_2-I), 4.51 (br. s, 1 H, NH). **^{13}C-NMR (100 MHz, $CDCl_3$)** δ(ppm) = 7.2 (CH_2-I), 26.7 (CH_2), 28.4 (Boc-CH_3), 28.4 (CH_2), 29.1 (CH_2), 30.0 (CH_2), 30.4 (CH_2), 33.5 (CH_2), 40.6 (BocN-*CH_2*), 79.0 (Boc-C_q), 156.0 (Boc-*C*OO)

Synthesis of Target Compound **1a**:

tert-Butyl (3-(4-(2-oxo-2,3-dihydro-1_H_-benzo[_d_]imidazol-1-yl)piperidin-1-yl)propyl) carbamate 11a

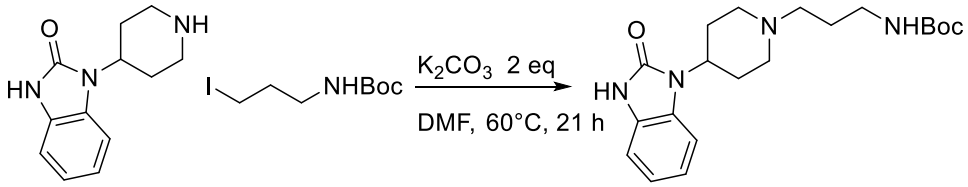

M = 374.49 g/mol

652 mg of the amine **3** (3 mmol, 1 eq) and 941 mg of the iodo-compound **4a** (3.3 mmol, 1.1 eq) were dissolved in 25 mL dimethylformamide and 829 mg potassium carbonate (6 mmol, 2 eq) and a catalytic amount of potassium iodide were added. The reaction mixture was heated at 60°C for 21 h. The mixture was partitioned between 100 mL of ethyl acetate and 100 mL water. The phases were separated, and the inorganic phase was extracted with ethyl acetate. The combined organic phases were washed with water several times, dried over sodium sulfate and the solvent was removed. Column chromatography (10% MeOH in CH_2Cl_2 on deactivated silica) gave 768 mg (2.05 mmol, 68 %) of the desired product as a white foam. **^{1}H-NMR (400 MHz, $CDCl_3$)** δ(ppm) = 1.43 (s, 9 H, Boc), 1.69 – 1.81 (m, 4 H, *CH_2*-CH, CH_2), 2.29 (t, *J* = 11.8 Hz, 2 H, CH_2-N), 2.47 – 2.61 (m, 4 H, *CH_2*-CH, CH_2-N), 3.11 (t, *J* = 6.7 Hz, 2 H, BocN-*CH_2*), 3.18 (d, *J* = 11.8 Hz, 2 H, CH_2-N), 4.34 (tt, *J* = 12.4, 4.3 Hz, 1 H, CH), 5.67 (br. s, 1 H, NH), 6.67 – 6.75 (m, 1 H), 6.99 – 7.08 (m, 3 H, Ar), 7.30 – 7.37 (m, 1 H, Ar), 10.50 (br. s, 1 H, NH). **^{13}C-NMR (100 MHz, $CDCl_3$)** δ(ppm) = 26.5 (CH_2), 27.5 (Boc), 27.9 (2xCH-*CH_2*), 38.3 (*CH_2*-N-COO), 50.1 (CH), 52.7 (2xN-CH_2), 55.4 (N-CH_2), 78.6 (Boc-C_q), 109.3 (2xAr-H), 120.9 (Ar-H), 121.2 (Ar-H), 128.3 (Ar-C_q), 128.9 (Ar-C_q), 154.8 (CO), 157.1 (Boc-*C*OO). **ESI-MS:** 375.15 *m/z* $[M+H]^+$, 398.10 $[M+Na]^+$

1-(1-(3-Aminopropyl)piperidin-4-yl)-1,3-dihydro-2*H*-benzo[*d*]imidazol-2-one 12a

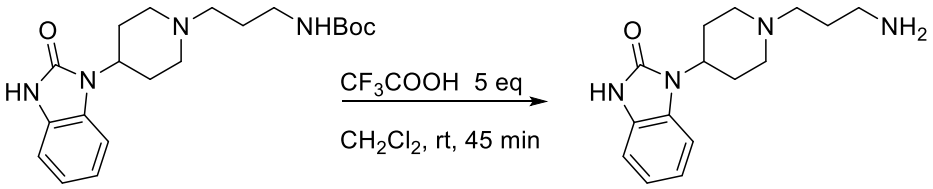

M = 274.37 g/mol

1 g of the Boc-protected amine **11a** (2.67 mmol, 1 eq) was dissolved in 25 mL dichloromethane and 1 mL trifluoro acetic acid (13 mmol, 5 eq) were added. The mixture was stirred at room temperature for 45 min. Water was added and the phases were separated. The inorganic phase was basified to pH ≥ 13 and extracted with ethyl acetate several times. The combined organic phases were washed with brine and dried over sodium sulfate. Removal of the solvent gave 800mg (2.67 mmol, quant.) of the desired product as a white foam. **^{1}H-NMR (400 MHz, $CDCl_3$)** δ(ppm) = 1.71 (quin, *J* = 6.9 Hz, 2 H, CH_2), 1.78 (dd, *J* = 12.3, 2.3 Hz, 2 H, CH_2), 2.09 (td, *J* = 12.0, 2.1 Hz, 2 H, CH_2-N), 2.38 – 2.52 (m, 4 H, , *CH_2*-CH, CH_2-N), 2.86 (t, *J* = 6.8 Hz, 2 H, *CH_2*-NH_2), 3.09 (d, *J* = 11.5 Hz, 2 H, CH_2-N), 4.31 (tt, *J* = 12.5, 4.2 Hz, 1 H, CH), 6.97 – 7.03 (m, 2 H, 2xAr), 7.07 – 7.12 (m, 1 H, Ar), 7.19 – 7.23 (m, 1 H, Ar). **^{13}C-NMR (100 MHz, $CDCl_3$)** δ(ppm) = 29.3 (CH_2), 30.3 (2xCH-*CH_2*), 40.8 (NH_2-CH_2), 50.9 (CH), 53.4 (2xN-CH_2), 56.4 (N-CH_2), 109.7 (2xAr-H), 120.9 (Ar-H), 121.1 (Ar-H), 128.3 (Ar-C_q), 129.1 (Ar-C_q), 155.3 (CO). **ESI-MS:** 275.00 *m/z* $[M+H]^+$

2-Chloroethyl (3-(4-(2-oxo-2,3-dihydro-1*H*-benzo[*d*]imidazol-1-yl)piperidin-1-yl)-propyl)carbamate 13a

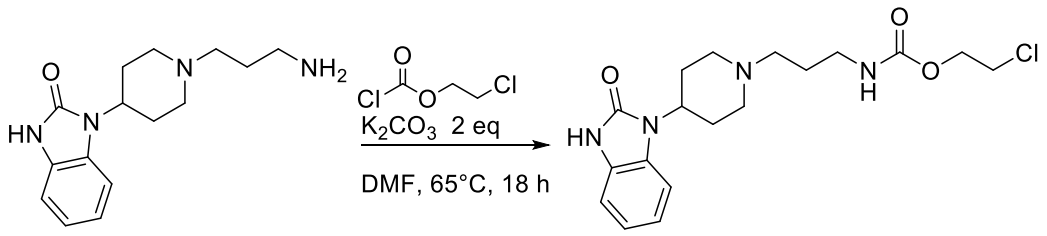

M = 380.87 g/mol

888 mg of the amine **12a** (2.67 mmol, 1 eq) were dissolved in 25 mL dimethylformamide. 738 mg potassium carbonate (5.34 mmol, 2 eq) and 276 µL 2-choroethyl chloroformiate (2.67 mmol, 1 eq) were added. The mixture was heated to 65°C for 18 h. Water was added, and the mixture extracted with ethyl acetate. The organic phases were washed with water and brine,

dried over sodium sulfate and the solvent was removed. Column chromatography (1% MeOH in CH_2Cl_2 → 3 % → 5 %; on deactivated silica) gave 288 mg (0.76 mmol, 28 %) of the desired product as a colorless oil. **^{1}H-NMR (400 MHz, $CDCl_3$)** δ(ppm) = 1.72 (quin, *J* = 6.2 Hz, 2 H, CH_2), 1.78 – 1.87 (m, 2 H, *CH_2*-CH), 2.07 – 2.19 (m, 2 H, CH_2-N), 2.38 – 2.56 (m, 4 H, *CH_2*-CH, CH_2-N), 3.10 (d, *J* = 11.8 Hz, 2 H, CH_2-N), 3.27 – 3.35 (m, 2 H, CH_2-N), 3.67 (t, *J* = 5.6 Hz, 2 H, CH_2-Cl), 4.32 (t, *J* = 5.6 Hz, 2 H, O-CH_2), 4.35 – 4.45 (m, 1 H, CH), 6.44 (br. s, 1 H, NH), 6.99 – 7.06 (m, 2 H, 2xAr), 7.08 – 7.15 (m, 1 H, Ar), 7.22 – 7.30 (m, 1 H, Ar), 10.58 (br. s., 1 H, NH). **^{13}C-NMR (100 MHz, $CDCl_3$)** δ(ppm) = 26.0 (CH_2), 29.3 (2x*CH_2*-CH), 41.0 (CH_2-N), 42.5 (CH_2-N), 57.0 (CH_2-Cl), 50.5 (CH), 53.2 (2xCH_2-N), 64.4 (O-CH_2), 109.8 (2xAr-H), 121.0 (Ar-H), 121.2 (Ar-H), 128.3 (Ar-C_q), 129.0 (Ar-C_q), 155.3 (C=O), 156.1 (C=O). **ESI-MS:** 381.05 *m/z* $[M+H]^+$

4-(2-Oxo-2,3-dihydro-1*H*-benzo[*d*]imidazol-1-yl)-1-(3-(((2-(trimethylammonio)-ethoxy)carbonyl)amino)propyl)piperidin-1-ium formate 1a

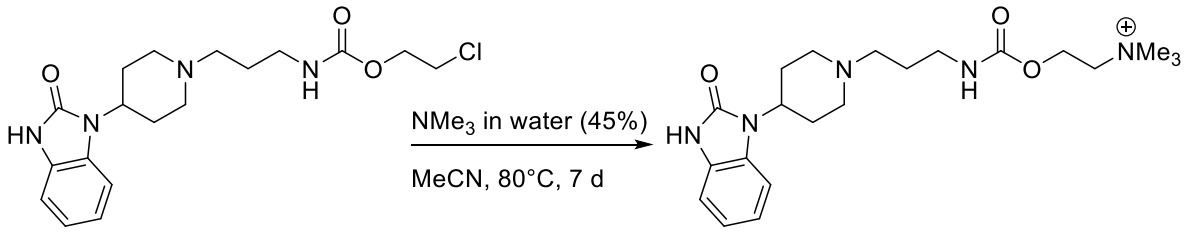

M = 404.53 g/mol

100 mg of the chloro-compound **13a** (0.26 mmol, 1 eq) were dissolved in 20 mL acetonitrile and 5 mL trimethylamine in water (45 %) were added. The mixture was heated to 80°C for 7d in a sealed vessel. The solvents were removed. Purification by preparative HPLC gave 17 mg (0.034 mmol, 13%) of the di-formiate salt of the desired product as a colorless oil. **^{1}H-NMR (400 MHz, $CDCl_3$)** δ(ppm) = 1.91 – 2.02 (m, 4 H, CH_2, *CH_2*-CH), 2.78 (q, *J* = 12.1 Hz, 2 H, *CH_2*-CH), 2.93 (t, *J* = 12.0 Hz, 2 H, CH_2-N), 2.98 – 3.06 (m, 2 H, CH_2-N), 3.26 (q, *J* = 7.5 Hz, 2 H, CH_2-NCOO), 3.23 (s, 9 H, NMe_3), 3.57 (br. d, *J* = 10.8 Hz, 2 H, CH_2-N), 3.66 – 3.78 (m, 2 H, *CH_2*-NMe_3), 4.47 – 4.57 (m, 3 H, CH, O-CH_2), 7.05 – 7.10 (m, 3 H, 3xAr), 7.29 – 7.38 (m, 1 H, Ar), 8.50 (s, 2 H, 2x$HCOO^-$). **^{13}C-NMR (100 MHz, $CDCl_3$)** δ(ppm) = 25.1 (CH_2), 26.4 (2x*CH_2*-CH), 38.0 (CH_2-NCOO), 48.5 (CH), 52.0 (2x CH_2-N), 53.07/53.11/53.15 (NMe_3), 54.3 (CH_2-N), 57.9 (O-CH_2), 65.11/65.13/65.17 (*CH_2*-NMe_3), 108.8 (Ar-H), 109.3 (Ar-H), 121.0 (Ar-H), 121.4 (Ar-H), 128.3 (Ar-C_q), 128.8 (Ar-C_q), 154.8 (C=O), 156.2 (HN*C*OO), 167.9 (2x$HCOO^-$). **ESI-MS:** 202.70 *m/z* $[M+H]^{2+}$, 404.30 *m/z* $[M]^+$

Synthesis of Target Compound **1b**:

tert-Butyl (5-(4-(2-oxo-2,3-dihydro-1_H_-benzo[_d_]imidazol-1-yl)piperidin-1-yl)pentyl) carbamate 11b

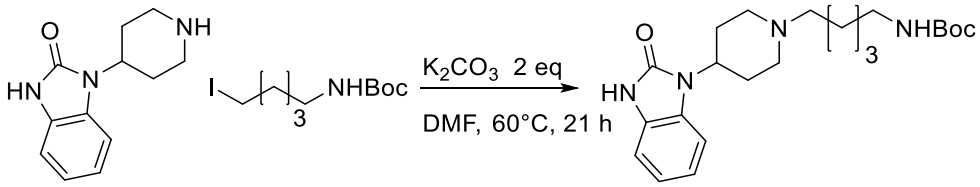

M = 402.54 g/mol

1.955 g of the amine **3** (9 mmol, 1 eq) and 2.82 g of the iodo-compound **4b** (9 mmol, 1 eq) were dissolved in 60 mL dimethylformamide and 2.49 g potassium carbonate (18 mmol, 2 eq) and a catalytic amount of potassium iodide were added. The mixture was heated to 60°C for 21 h. The solvent was evaporated to about 20 mL and 50 mL of water and 50 mL of ethyl acetate were added. The phases were separated, and the inorganic phase was extracted with ethyl acetate. The combined organic phases were washed with water several times, dried over sodium sulfate and the solvent was removed. This procedure gave 3.19 g (7.93 mmol, 88 %) of the desired product as a brown solid. **^{1}H-NMR (400 MHz, $CDCl_3$)** δ(ppm) = 1.30 – 1.58 (m, 6 H, 3xCH_2), 1.44 (s, 9 H, Boc) 1.74 – 1.86 (m, 2 H, *CH_2*-CH), 2.07 – 2.17 (m, 2 H, CH_2-N), 2.33 – 2.53 (m, 4 H, CH_2-N, *CH_2*-CH), 3.03 – 3.17 (m, 4 H, CH_2-N, BocN-*CH_2*), 4.37 (tt, *J* = 12.5, 4.2 Hz, 1 H, CH), 4.60 (br. s., 1 H, NHBoc), 7.01 – 7.06 (m, 2 H, Ar), 7.08 – 7.12 (m, 1 H, Ar), 7.26 – 7.29 (m, 1 H, Ar), 10.05 (br. s., 1 H, NH). **^{13}C-NMR (100 MHz, $CDCl_3$)** δ(ppm) = 24.8 (CH_2), 26.9 (CH_2), 28.4 (CH_2), 28.5 (Boc-CH_3), 29.3 (2xCH-*CH_2*), 30.0 (CH_2), 40.6 (BocN-*CH_2*), 50.9 (CH), 53.4 (2xN-CH_2), 58.5 (N-CH_2), 79.1 (Boc-C_q), 109.7 (Ar-H), 109.9 (Ar-H), 121.0 (Ar-H), 121.1 (Ar-H), 128.1 (Ar-C_q), 129.2 (Ar-C_q), 155.2 (CO), 156.0 (Boc-*C*OO). **ESI-MS:** 403.35 *m/z* $[M+H]^+$, 425.35 *m/z* $[M+Na]^+$

1-(1-(5-Aminopentyl)piperidin-4-yl)-1,3-dihydro-2*H*-benzo[*d*]imidazol-2-one 12b

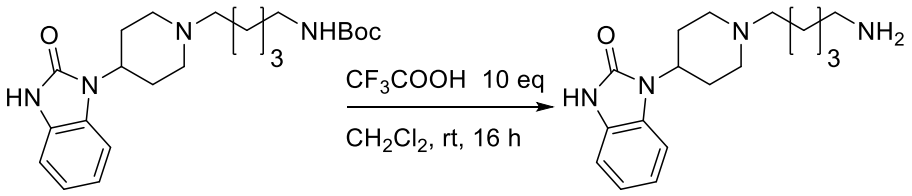

M = 302.42 g/mol

985 mg of the Boc-protected amine **11b** (2.45 mmol, 1 eq) was dissolved in 15 mL dichloromethane and 1.5 mL trifluoro acetic acid (20 mmol, 10 eq) were added. The mixture was stirred at room temperature for 16 h. Water was added, and the phases were separated. The inorganic phase was basified to pH ≥ 13 and extracted with ethyl acetate several times. The combined organic phases were washed with brine and dried over sodium sulfate. Removal of the solvent gave 695 mg (2.30 mmol, 94%) of the desired product as an orange oil. **^{1}H-NMR (400 MHz, $CDCl_3$)** δ(ppm) = 1.29 – 1.40 (m, 2 H, CH_2), 1.45 – 1.58 (m, 4 H, 2xCH_2), 1.79 (br. dd, *J* = 11.9, 2.4 Hz, 2 H, CH-*CH_2*), 2.09 (t, *J* = 11.0 Hz, 2 H, NH_2-CH_2), 2.33 – 2.40 (m, 2 H, N-CH_2), 2.46 (qd, *J* = 12.5, 3.6 Hz, 2 H, CH-*CH_2*), 2.72 (t, *J* = 7.0 Hz, 2 H, N-CH_2), 3.02 – 3.10 (m, 2 H, N-CH_2), 4.34 (tt, *J* = 12.5, 4.0 Hz, 1 H, CH), 6.95 – 7.04 (m, 2 H, 2xAr), 7.06 – 7.11 (m, 1 H, Ar), 7.24 (s, 1 H, Ar). **^{13}C-NMR (100 MHz, $CDCl_3$)** δ(ppm) = 24.8 (CH_2), 26.9 (CH_2), 29.2 (2xCH-*CH_2*), 33.1 (CH_2), 41.8 (NH_2-CH_2), 50.8 (CH), 53.3 (2xN-*CH_2*), 58.4 (N-CH_2), 109.6 (2xAr-CH), 120.7 (Ar-CH), 121.0 (Ar-CH), 128.3 (Ar-C_q), 129.1 (Ar-C_q), 170.1 (CO). **ESI-MS:** 303.25 *m/z* $[M+H]^+$

2-Chloroethyl (5-(4-(2-oxo-2,3-dihydro-1*H*-benzo[*d*]imidazol-1-yl)piperidin-1-yl)pentyl)carbamate 13b

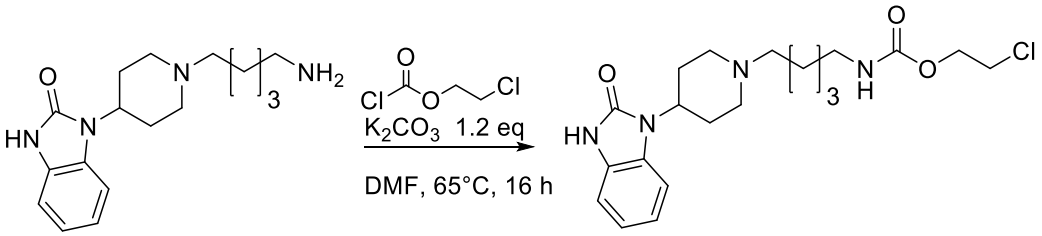

M = 408.93 g/mol

695 mg of the amine **12b** (2.3 mmol, 1 eq) were dissolved in 10 mL dimethylformamide. 413 mg potassium carbonate (2.99 mmol, 1.3 eq) and 285 µL 2-chloroethyl chloroformate (2.76 mmol, 1.2 eq) were added. The mixture was heated to 65°C for 16 h. Water was added, and the mixture extracted with ethyl acetate. The organic phases were washed with water and brine, dried over sodium sulfate and the solvent was removed. Column chromatography (1% → 7% MeOH in CH_2Cl_2; on deactivated silica) gave 435 mg (1.06 mmol, 47 %) of the desired product as a colourless oil. The product was used in the next reaction immediately. **ESI-MS:** 409.15 *m/z* $[M+H]^+$

***N*,*N*,*N*-Trimethyl-2-(((5-(4-(2-oxo-2,3-dihydro-1*H*-benzo[*d*]imidazol-1-yl)piperidin-1-yl)pentyl)carbamoyl)oxy)ethan-1-aminium formate 1b**

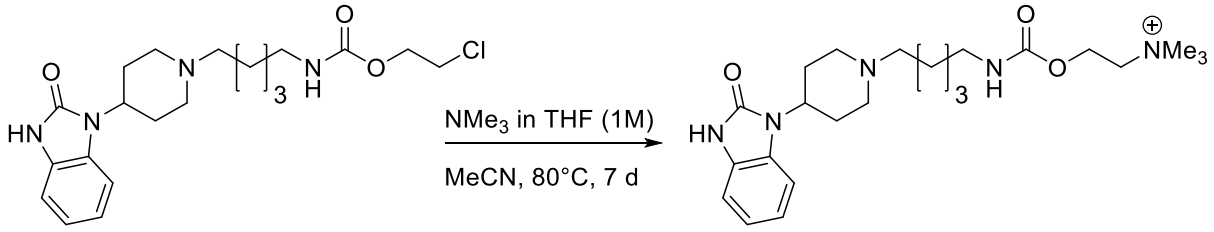

M = 432.59 g/mol

435 mg of the chloro-compound **13b** (1.06 mmol, 1 eq) were dissolved in 20 mL acetonitrile and 10 mL Trimethylamine in tetrahydrofuran (1M, 10 mmol, 10 eq) were added. The mixture was heated to 80°C for 7d in a sealed vessel. Volatiles were removed. Purification by preparative HPLC gave 84 mg (0.18 mmol, 20 %) of the formiate salt of the desired product as a white solid. **^{1}H-NMR (400 MHz, $CDCl_3$)** δ(ppm) = 1.39 – 1.48 (m, 2 H, CH_2), 1.59 (quin, *J* = 7.2 Hz, 2 H, CH_2), 1.77 – 1.87 (m, 2 H, CH_2), 2.02 (dd, *J* = 12.5, 1.5 Hz, 2 H, 2xN-*CH*$_2$), 2.88 (ddd, *J* = 26.6, 13.3, 3.5 Hz, 2 H, 2xN-*CH*$_2$), 3.08 – 3.19 (m, 4 H, 2xN-*CH*$_2$), 3.24 (s, 9 H, (NMe_3), 3.71 (dt,

J = 4.5, 2.5 Hz, 2 H, *CH*$_2$-NMe$_3$), 3.69 (br. d, *J* = 13.3 Hz, 2 H, 2xCH-*CH*$_2$), 4.52 (dquin, *J* = 4.5, 2.5 Hz, 2 H, COO-*CH*$_2$), 4.60 (tt, *J* = 12.4, 4.2 Hz, 1 H, CH), 7.05 – 7.11 (m, 3 H, 3xAr), 7.38 – 7.44 (m, 1 H, Ar), 8.55 (s, 1H, HCOO$^-$). **^{13}C-NMR (100 MHz, CDCl$_3$)** δ(ppm) = 23.5 (CH$_2$), 23.7 (CH$_2$), 26.0 (2xCH-*CH*$_2$), 28.9 (CH$_2$), 40.0 (*CH*$_2$-N-COO), 48.0 (CH), 51.8 (2xN-*CH*$_2$), 53.15/53.19/53.23 (NMe$_3$), 56.4 (N-*CH*$_2$), 57.8 (COO-*CH*$_2$), 65.14/65.18/65.21 (*CH*$_2$-NMe$_3$), 108.9 (Ar-CH), 109.3 (Ar-CH), 121.0 (Ar-CH), 121.4 (Ar-CH), 128.3 (Ar-C$_q$), 128.8 (Ar-C$_q$), 154.7 (CO), 156.1 (CO), 168.3 (HCOO$^-$). **ESI-MS:** 216.75 $[M+H]^{2+}$, 432.30 *m/z* $[M]^+$

Synthesis of Target Compound **1c**:

tert-Butyl (8-(4-(2-oxo-2,3-dihydro-1*H*-benzo[*d*]imidazol-1-yl)piperidin-1-yl)octyl)-carbamate 11c

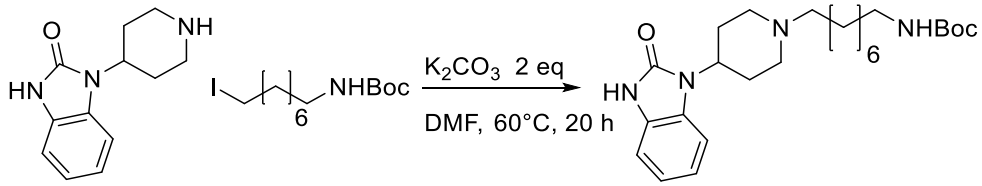

M = 374.49 g/mol

1.477 g of the amine **3** (6.8 mmol, 1 eq) and 2.4 g of the iodo-compound **4c** (6.8 mmol, 1 eq) were dissolved in 75 mL dimethylformamide and 1.880 mg potassium carbonate (13.6 mmol, 2 eq) and a catalytic amount of potassium iodide were added. The reaction mixture was heated to 60°C for 20 h. The mixture was evaporated to 20 mL and partitioned between 100 mL ethyl acetate and 100 mL water. The phases were separated, and the inorganic phase was extracted with ethyl acetate. The combined organic phases were washed with water several times, dried over sodium sulfate and the solvent was removed. Column chromatography (CH_2Cl_2 25:1 MeOH on deactivated silica) gave 2.338 g (5.26 mmol, 78 %) of the desired product as a beige solid. **^{1}H-NMR (400 MHz, CDCl$_3$)** δ(ppm) = 1.22 – 1.32 (m, 10 H, 5xCH$_2$), 1.42 (s, 9 H, Boc-CH$_3$), 1.47 – 1.57 (m, 2 H, CH$_2$), 1.80 (dd, *J* = 12.0, 2.0 Hz, 2 H, CH-*CH*$_2$), 2.15 (t, *J* = 11.3 Hz, 2 H, N-CH$_2$), 2.35 – 2.43 (m, 2 H, N-CH$_2$), 2.51 (m, 2 H, CH-*CH*$_2$), 3.03 – 3.16 (m, 4 H, N-CH$_2$, BocN-*CH*$_2$), 4.38 (tt, *J* = 12.4, 4.3 Hz, 1 H, CH), 4.64 (br. s., 1 H, NH), 6.95 – 7.03 (m, 2 H, 2xAr-H), 7.07 – 7.11 (m, 1 H, Ar-H), 7.26 – 7.30 (m, 1 H, Ar-H), 10.72 (br. s., 1 H, NH). **^{13}C-NMR (100 MHz, CDCl$_3$)** δ(ppm) = 26.7 (CH$_2$), 26.9 (CH$_2$), 27.5 (CH$_2$), 28.4 (Boc-CH$_3$), 29.1 (2x CH-*CH*$_2$), 29.2 (CH$_2$), 29.4 (CH$_2$), 30.1 (CH$_2$), 40.6 (BocN-*CH*$_2$), 50.6 (CH), 53.3 (2xN-CH$_2$), 79.0 (Boc-C$_q$),

109.7 (Ar-H), 109.9 (Ar-H), 120.1 (Ar-H), 120.9 (Ar-H), 128.3 (Ar-C_q), 129.0 (Ar-C_q), 155.4 (Boc-*C*OO), 156.0 (CO). **ESI-MS:** 445.30 *m/z* $[M+H]^+$, 443.30 *m/z* $[M-H]^-$

1-(1-(8-Aminooctyl)piperidin-4-yl)-1,3-dihydro-2*H*-benzo[*d*]imidazol-2-one 12c

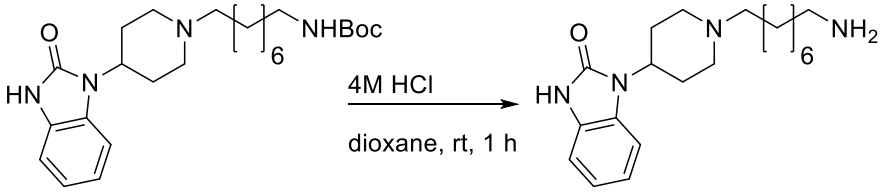

M = 344.50 g/mol

1 g of the Boc-protected amine **11c** (2.25 mmol, 1 eq) were dissolved in 40 mL dioxane and 40 mL 4M HCl (160 mmol, 70 eq) were added. The mixture was stirred at room temperature for 1 h. Volatiles were removed, and the residue dissolved in dichloromethane and water. The phases were separated. The inorganic phase was basified to pH ≥ 13 and extracted with dichloromethane several times. The combined organic phases were dried over sodium sulfate. Removal of the solvent gave 764 mg (2.22 mmol, 99%) of the desired product as a brown oil. **^{1}H-NMR (400 MHz, MeOD)** δ(ppm) = 1.30 – 1.40 (m, 8 H, 4xCH_2), 1.42 –1.51 (s, 2 H), 1.53 – 1.62 (m, 2 H), 1.77 (br. dd, *J* = 14.3, 2.3 Hz, 2 H, CH-*CH_2*), 2.17 (td, *J* = 12.2, 2.1 Hz, 2 H, N-CH_2), 2.39 – 2.45 (m, 2 H, N-CH_2), 2.53 (qd, *J* = 12.7, 3.9 Hz, 2 H, CH-*CH_2*), 2.63 (t, *J* = 7.0 Hz, 2 H, NH_2-*CH_2*), 3.13 (br. d, *J* = 12.0 Hz, 2 H, N-CH_2), 4.32 (tt, *J* = 12.5, 4.5 Hz, 1 H, CH), 7.01 – 7.09 (m, 3 H, 3xAr), 7.36 – 7.42 (m, 1 H, Ar). **^{13}C-NMR (100 MHz, MeOD)** δ(ppm) = 26.5 (CH_2), 26.6 (CH_2), 27.3 (CH_2), 28.1 (2xCH-*CH_2*), 29.2 (2xCH_2), 32.4 (CH_2), 41.2 (NH_2-CH_2), 50.5 (CH), 52.9 (2xN-CH_2), 58.3 (N-CH_2), 109.2 (Ar-CH), 109.4 (Ar-CH), 120.8 (Ar-CH), 121.1 (Ar-CH), 128.3 (Ar-C_q), 128.9 (Ar-C_q), 154.9 (CO). **ESI-MS:** 345.25 *m/z* $[M+H]^+$, 173.20 *m/z* $[M+2H]^{2+}$

2-Chloroethyl (8-(4-(2-oxo-2,3-dihydro-1*H*-benzo[*d*]imidazol-1-yl)piperidin-1-yl)octyl)carbamate 13c

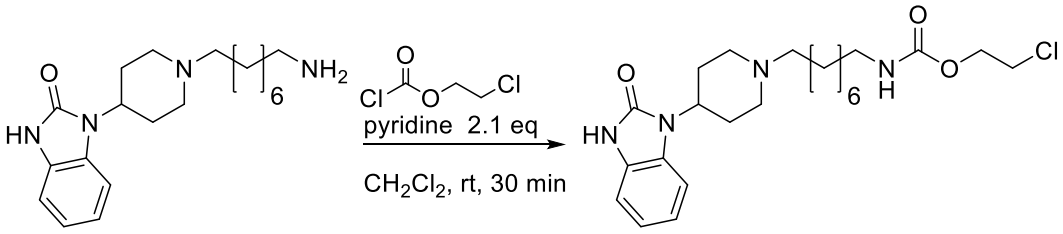

M = 451.01 g/mol

300 mg of the amine **12c** (0.87 mmol, 1 eq) were dissolved in 10 mL dichloromethane. 148 µL pyridine (1.83 mmol, 2.1 eq) and 108 µL 2-chloroethyl chloroformiate (1.05 mmol, 1.2 eq) were added. The mixture was stirred at room temperature for 30 min. Saturated ammonium chloride solution was added and the mixture extracted with dichloromethane. The organic phases were dried over sodium sulfate and the solvent was removed. Column chromatography (2% → 3 % MeOH in CH_2Cl_2; on deactivated silica) gave 306 mg (0.68 mmol, 78 %) of the desired product as a colorless oil. **^{1}H-NMR (400 MHz, $CDCl_3$)** δ(ppm) = 1.29 – 1.35 (m, 8 H, 4xCH_2), 1.45 – 1.56 (m, 4 H, 2xCH_2), 1.82 (br. dd, *J* = 12.0, 2.3 Hz, 2 H, CH-CH_2), 2.13 (td, *J* = 12.0, 1.8 Hz, 2 H, CH-CH_2), 2.35 – 2.42 (m, 2 H, N-CH_2), 2.48 (qd, *J* = 12.5, 3.8 Hz, 2 H, N-CH_2), 3.10 (br. d, *J* = 11.5 Hz, 2 H, N-CH_2), 3.18 (q, *J* = 6.8 Hz, 2 H, N-CH_2), 3.67 (t, *J* = 5.6 Hz, 2 H, CH_2-Cl), 4.31 (t, *J* = 5.6 Hz, 2 H, O-CH_2), 4.37 (tt, *J* = 12.5, 4.3 Hz, 1 H, CH), 4.83 (br. t, *J* = 4.5 Hz, 1 H, NH), 7.00 – 7.06 (m, 2 H, 2xAr), 7.07 – 7.11 (m, 1 H, Ar), 7.27 – 7.31 (m, 1 H, Ar), 9.70 (br. s., 1 H, NH). **^{13}C-NMR (100 MHz, $CDCl_3$)** δ(ppm) = 26.7 (CH_2), 27.2 (CH_2), 27.6 (CH_2), 29.2 (CH_2), 29.3 (CH_2), 29.5 (2xCH_2), 29.9 (CH_2), 41.1 (N-CH_2), 42.4 (CH_2-Cl), 50.9 (CH), 53.3 (N-CH_2), 53.4 (CH-CH_2), 58.7 (N-CH_2), 64.4 (O-CH_2), 109.6 (Ar-CH), 109.9 (Ar-CH), 121.0 (Ar-CH), 121.1 (Ar-CH), 128.0 (Ar-C_q), 129.2 (Ar-C_q), 155.0 (CO), 155.9 (COO). **ESI-MS:** 452.10 *m/z* $[M+H]^+$

4-(2-Oxo-2,3-dihydro-1*H*-benzo[*d*]imidazol-1-yl)-1-(8-(((2-(trimethylammonio)-ethoxy)carbonyl)amino)octyl)piperidin-1-ium formate 1c

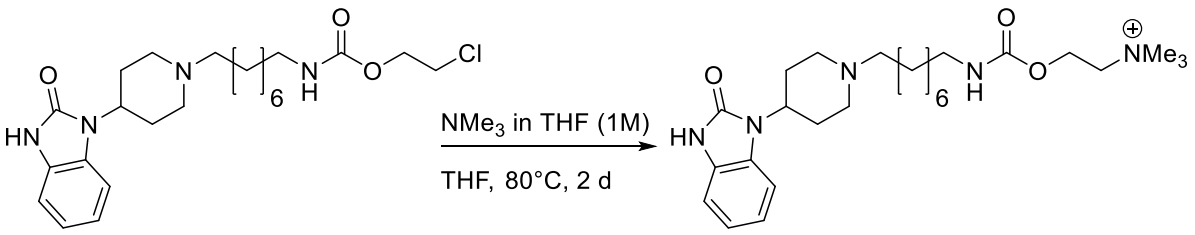

M = 474.67 g/mol

50 mg of the chloro-compound **13c** (0.22 mmol, 1 eq) were dissolved in 18 mL tetrahydrofuran and 5 mL Trimethylamine in tetrahydrofuran (1M, 5 mmol, 23 eq) were added. The mixture was heated to 80°C for 2 d in a sealed vessel. Volatiles were removed. Purification by preparative HPLC gave 14 mg (0.03 mmol, 14 %) of the di-formiate salt of the desired product as a colorless oil. **^{1}H-NMR (400 MHz, $CDCl_3$)** δ(ppm) = 1.33 – 1.44 (m, 8 H, 4xCH_2), 1.52 (quin, *J* = 6.5 Hz, 2 H, CH_2), 1.78 (br. s., 2 H, CH_2), 2.03 (br. d, *J* = 12.8 Hz, 2 H, CH-*CH_2*), 2.77 – 2.91 (m, 2 H, CH-*CH_2*), 3.07 – 3.15 (m, 6 H, 3xN-CH_2), 3.22 (s, 9 H, NMe_3), 3.66 – 3.74 (m, 4 H, N-CH_2, NMe_3-*CH_2*), 4.48 – 4.53 (m, 2 H, COO-*CH_2*), 4.53 – 4.62 (m, 1 H, CH), 7.06 – 7.10 (m, 3 H, 3xAr), 7.31 – 7.36 (m, 1 H, Ar), 8.49 (br. s., 2 H, 2x$HCOO^-$). **^{13}C-NMR (100 MHz, $CDCl_3$)** δ(ppm) = 24.0 (CH_2), 26.0 (2xCH-*CH_2*), 26.3 (2xCH_2), 28.7 (2xCH_2), 29.4 (CH_2), 40.5 (*CH_2*-N-COO), 48.0 (CH), 51.7 (2xN-*CH_2*), 53.07/53.12/53.16 (NMe_3), 56.4 (N-*CH_2*), 57.7 (COO-*CH_2*), 65.16/65.19/65.22 (*CH_2*-NMe_3), 108.7 (Ar-H), 109.3 (Ar-H), 121.0 (Ar-H), 121.4 (Ar-H), 128.3 (Ar-C_q), 128.8 (Ar-C_q), 154.7 (CO), 156.0 (CO), 167.9 ($HCOO^-$). **ESI-MS:** 237.75 $[M+H]^{2+}$, 474.25 *m/z* $[M]^+$

7.3. Synthesis of Dualsteric BQCA-derived Compounds **2**

BQCA-Building-Blocks:

Ethyl 8-fluoro-4-oxo-1,4-dihydroquinoline-3-carboxylate 15

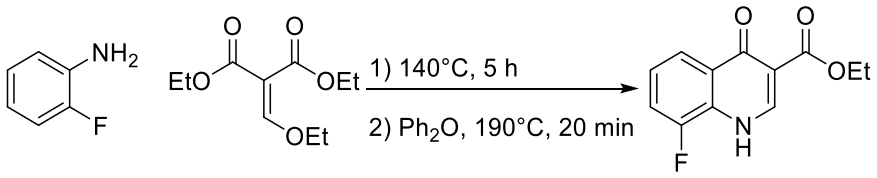

M = 235.21 g/mol

4 mL 2-fluoroaniline (41.4 mmol, 1 eq) and 8.4 mL diethyl 2-(ethoxymethylene) malonate (41.4 mmol, 1 eq) were heated to 130-150 °C for 5 h. After cooling, 20 mL diphenyl ether were added and the mixture was heated to 210 °C for 20 min in a microwave system. After cooling to room temperature diethyl ether was added and the resulting suspension was left stirring overnight. The solid was filtered and washed with diethyl ether, which gave 1.4 g (5.95 mmol, 14 %) of a beige solid. **^{1}H-NMR (400 MHz, $CDCl_3$)** δ(ppm) = 1.28 (t, *J* = 7.0 Hz, 3 H, CH_3), 4.22 (q, *J* = 7.0 Hz, 2 H, CH_2-CH_3), 7.40 (td, *J* = 8.2, 5.0 Hz, 1 H, Ar), 7.65 (ddd, *J* = 11.0, 8.0, 1.4 Hz, 1 H, Ar), 7.95 – 7.99 (m, 1 H, Ar), 8.39 (s, 1 H, CH), 12.46 (br. s, 1 H, NH). **ESI-MS:** 236.05 *m/z* $[M+H]^+$

6-(Hydroxymethyl)naphthalen-2-ol 19

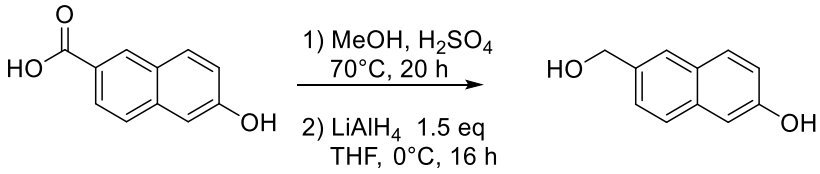

M = 174.20 g/mol

4 g 6-hydroxy-2-naphthoic acid (21.3 mmol, 1 eq) was dissolved in 30 mL methanol and 10 drops of concentrated sulfuric acid were added. The mixture was heated to 70°C for 20 h. The mixture was cooled to room temperature and the solvent was removed. 4.659 g of the crude methyl ester (21.3 mmol, 1 eq) were dissolved in dry tetrahydrofuran and the solution was cooled in an ice/salt bath to -20 °C. 1.21 g lithium aluminium hydride (31.95 mmol, 1.5 eq) were added in small portions. The mixture was stirred at 0 °C to rt for 16 h. The reaction mixture was cooled to 0 °C and 50 mL ethyl acetate and 50 mL of water were added slowly.

The phases were separated, and the inorganic phase was extracted with ethyl acetate. The combined organic phases were dried over sodium sulfate and the solvent was removed. This procedure gave 3.21 g (18.4 mmol, 87 %) of the desired product as an off-white solid. **^{1}H-NMR (400 MHz, $CDCl_3$)** δ(ppm) = 4.70 (s, 2 H, CH_2), 7.06 (dd, *J* = 8.8, 2.5 Hz, 1 H, Ar), 7.09 (d, *J* = 2.5 Hz, 1 H, Ar), 7.38 (dd, *J* = 8.5, 1.8 Hz, 1 H, Ar), 7.62 (d, *J* = 8.8 Hz, 1 H, Ar), 7.67 – 7.71 (m, 2 H, 2xAr)

Synthesis of Linkers **23:**

tert-Butyl (3-((6-(hydroxymethyl)naphthalen-2-yl)oxy)propyl)carbamate 22a

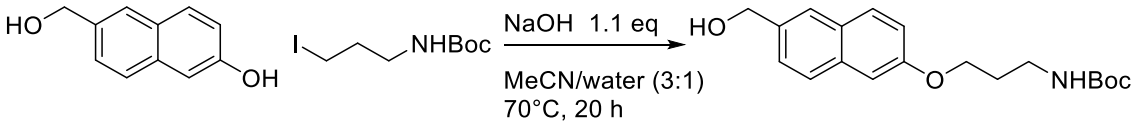

M = 331.18 g/mol

1.432 g 6-(hydroxymethyl)naphthalene-2-ol **19** (8.22 mmol, 1 eq) and 2.343 g of the iodo-compound **4a** (8.22 mmol, 1 eq) were dissolved in 100 mL acetonitrile/water (3:1). 360 mg sodium hydroxide (9 mmol, 1.1 eq) were added and the mixture was heated to 70°C for 20 h. 50 mL of water and 50 mL ethyl acetate were added. The phases were separated, and the inorganic phase was extracted with ethyl acetate. The combined organic phases were washed with brine (50 mL), dried over sodium sulfate and the solvent was removed. Column chromatography (petroleum ether 1:2 EtOAc) gave 1.86 g (5.62 mmol, 68 %) of the desired product as a pale yellow solid. **^{1}H-NMR (400 MHz, MeOD)** δ(ppm) = 1.43 (s, 9 H, Boc), 1.95 – 2.04 (m, 2 H, CH_2), 3.27 (t, *J* = 6.9 Hz, 2 H, BocNH-*CH_2*), 4.12 (t, *J* = 6.1 Hz, 2 H, CH_2-O-), 4.72 (s, 2 H, CH_2-OH), 7.12 (dd, *J* = 8.9, 2.4 Hz, 1 H, Ar), 7.21 (d, *J* = 2.5 Hz, 1 H, Ar), 7.43 (dd, *J* = 8.2, 1.6 Hz, 1 H, Ar), 7.70 – 7.74 (m, 3 H, 3xAr). **^{13}C-NMR (100 MHz, MeOD)** δ(ppm) = 27.4 (Boc-CH_3), 29.4 (CH_2), 37.2 (*CH_2*-Boc), 64.0 (CH_2-OH), 65.3 (CH_2-O-), 78.6 (Boc-C_q), 106.3 (Ar-H), 118.6 (Ar-H), 125.0 (Ar-H), 125.6 (Ar-H), 126.6 (Ar-H), 128.9 (Ar-H), 128.9 (Ar-C_q), 134.1 (Ar-C_q), 136.4 (Ar-C_q), 154.9 (Ar-C_q), 157.0 (Boc-*C*OO). **ESI-MS:** 354.20 *m/z* $[M+Na]^+$

***tert*-Butyl (3-((6-(iodomethyl)naphthalen-2-yl)oxy)propyl)carbamate 23a**

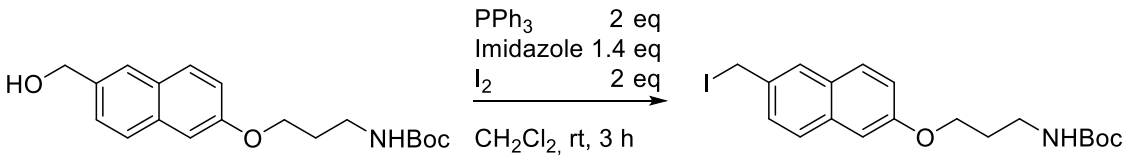

M = 441.31 g/mol

2.85 g Triphenylphosphine (10.88 mmol, 2 eq) and 519 mg imidazole (7.62 mmol, 1.4 eq) were dissolved in 40 mL dry dichloromethane and 2.76 g iodine (10.88 mmol, 2 eq) were added in portions. The mixture was stirred at room temperature for 1 h. A solution of 1.8 g of the alcohol **22a** (5.44 mmol, 1 eq) in 10 mL dry dichloromethane was added and the resulting mixture was stirred at room temperature for 3 h. 50 mL water were added, and the phases were separated. The organic phase was washed with HCl (10% *w/w*). The combined inorganic phases were extracted with ethyl acetate. The combined organic phases were dried over sodium sulfate and the solvent was removed. Column chromatography (petroleum ether 2:1 EtOAc) of the crude product gave 1.563 g (3.53 mmol, 65 %) of the desired product as a brown solid. **^{1}H-NMR (400 MHz, $CDCl_3$)** δ(ppm) = 1.44 (s, 9 H, Boc), 1.98 – 2.06 (s, 2 H, CH_2), 3.31 – 3.39 (m, 2 H, CH_2-Boc), 4.07 – 4.14 (m, 2 H, CH_2-O-), 4.61 (s, 2 H, CH_2-I), 7.07 – 7.09 (m, 1 H, Ar), 7.10 – 7.14 (m, 1 H, Ar), 7.40 – 7.44 (m, 1 H, Ar), 7.63 – 7.67 (m, 2 H, 2xAr), 7.71 – 7.74 (m, 1 H, Ar). **^{13}C-NMR (100 MHz, $CDCl_3$)** δ(ppm) = 7.1 (CH_2-I), 28.4 (Boc-CH_3), 29.6 (CH_2), 38.0 (*CH_2*-Boc), 65.8 (CH_2-O-), 79.2 (Boc-C_q), 106.8 (Ar-H), 119.4 (Ar-H), 126.9 (Ar-H), 127.5 (Ar-H), 127.6 (Ar-H), 128.8 (Ar-C_q), 129.3 (Ar-H), 134.0 (Ar-C_q), 134.3 (Ar-C_q), 156.1 (Ar-C_q), 157.3 (Boc-*C*OO). **ESI-MS:** 464.10 *m/z* $[M+Na]^+$

***tert*-Butyl (5-((6-(hydroxymethyl)naphthalen-2-yl)oxy)pentyl)carbamate 22b**

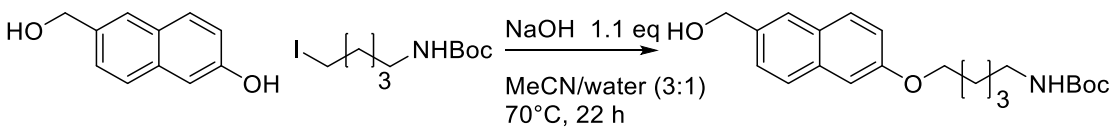

M = 359.47 g/mol

895 mg 6-(hydroxymethyl)naphthalene-2-ol **19** (5.14 mmol, 1 eq) and 2.245 g of the iodo-compound **4b** (7.16 mmol, 1.4 eq) were dissolved in 75 mL acetonitrile/water (3:1). 250 mg sodium hydroxid (9 mmol, 1.1 eq) were added and the mixture was heated to 70°C for 22 h. 50 mL of water and 50 mL ethyl acetate were added. The phases were separated, and the

inorganic phase was extracted with ethyl acetate. The combined organic phases were washed with brine, dried over sodium sulfate and the solvent was removed. Column chromatography (40% → 60% EtOAc in petroleum ether) gave 1.781 g (4.95 mmol, 96 %) of the desired product as a white solid. **^{1}H-NMR (400 MHz, $CDCl_3$)** δ(ppm) = 1.44 (s, 9 H, Boc), 1.46 – 1.57 (m, 4 H, 2xCH_2), 1.82 (quin, *J* = 6.8 Hz, 2 H, CH_2), 3.05 – 3.16 (m, 2 H, CH_2), 4.02 (t, *J* = 6.5 Hz, 2 H, CH_2), 4.78 (s, 2 H, CH_2-OH), 7.07 – 7.15 (m, 2 H, 2xAr), 7.42 (dd, *J* = 8.5, 1.8 Hz, 1 H, Ar), 7.66 – 7.71 (m, 3 H, 3xAr). **^{13}C-NMR (100 MHz, $CDCl_3$)** δ(ppm) = 23.4 (CH_2), 28.5 (Boc-CH_3), 28.9 (2xCH_2), 29.9 (CH_2), 40.5 (CH_2), 65.4 (CH_2-OH), 67.8 (O-CH_2), 79.2 (Boc-C_q), 106.6 (Ar-H), 119.2 (Ar-H), 125.5 (Ar-H), 125.9 (Ar-H), 127.1 (Ar-H), 128.8 (Ar-C_q), 129.2 (Ar-H), 134.1 (Ar-C_q), 136.2 (Ar-C_q), 157.1 (Ar-*C*O-). **ESI-MS:** 382.10 *m/z* $[M+Na]^+$

***tert*-Butyl (5-((6-(iodomethyl)naphthalen-2-yl)oxy)pentyl)carbamate 23b**

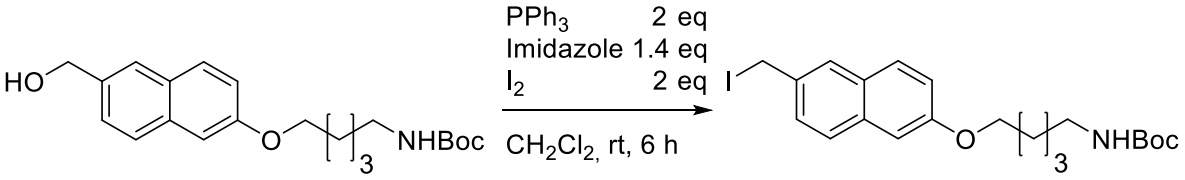

M = 469.11 g/mol

2.60 g Triphenylphosphine (9.90 mmol, 2 eq) and 472 mg imidazole (6.93 mmol, 1.4 eq) were dissolved in 50 mL dry dichloromethane and 2.51 g iodine (9.90 mmol, 2 eq) were added in portions. The mixture was stirred at room temperature for 1 h. A solution of 1.78 g of the alcohol **22b** (4.95 mmol, 1 eq) in 25 mL dry dichloromethane were added and the resulting mixture was stirred at room temperature for 6 h. 50 mL water were added, and the phases were separated. The organic phase was washed with HCl (10% *w/w*). The combined inorganic phases were extracted with ethyl acetate. The combined organic phases were dried over sodium sulfate and the solvent was removed. Column chromatography (petroleum ether 2:1 EtOAc) gave 1.37 g (2.9 mmol, 60 %) of the desired product as a yellow solid. **^{1}H-NMR (400 MHz, $CDCl_3$)** δ(ppm) = 1.45 (s, 9 H, Boc-CH_3), 1.50 – 1.61 (m, 4 H, 2xCH_2), 1.81 – 1.90 (m, 2 H, CH_2), 3.17 (m, 2 H, CH_2), 4.06 (t, *J* = 6.4 Hz, 2 H, CH_2), 4.62 (s, 2 H, I-CH_2), 7.08 (d, *J* = 2.5 Hz, 1 H, Ar-H), 7.13 (dd, *J* = 8.8, 2.5 Hz, 1 H, Ar-H), 7.43 (dd, *J* = 8.5, 2.0 Hz, 1 H, Ar-H), 7.66 (dd, *J* = 8.5, 4.5 Hz, 2 H, 2xAr-H), 7.74 (d, *J* = 1.5 Hz, 1 H, Ar-H). **^{13}C-NMR (100 MHz, $CDCl_3$)** δ(ppm) = 7.2 (CH_2-I), 23.4 (CH_2), 28.5 (Boc-CH_3), 28.9 (CH_2), 29.9 (CH_2), 40.5 (*CH_2*-Boc), 67.8 (CH_2-O-), 79.1 (Boc-C_q), 106.7 (Ar-H), 119.5 (Ar-H), 127.0 (Ar-H), 127.4 (Ar-H), 127.6 (Ar-H), 128.7 (Ar-

C_q), 129.3 (Ar-H), 134.1 (Ar-C_q), 134.2 (Ar-C_q), 157.6 (Ar-C_q), 158.8 (Boc-C=O). **ESI-MS:** 492.10 *m/z* $[M+Na]^+$

***tert*-Butyl (8-((6-(hydroxymethyl)naphthalen-2-yl)oxy)octyl)carbamate 22c**

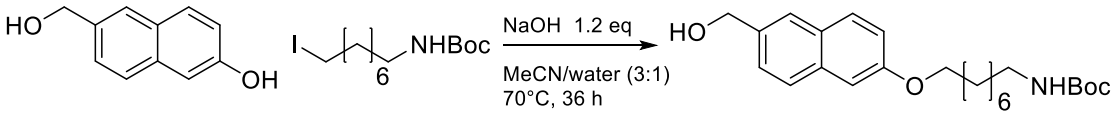

M = 401.55 g/mol

1.02 g of the alcohol **19** (5.87 mmol, 1 eq) and 282 mg sodium hydroxide (7.04 mmol, 1.2 eq) were dissolved in 75 mL acetonitrile/water (3:1) and 2.5 g of the iodo-compound **4c** (7.04 mmol, 1 eq) were added. The mixture was heated to 70 °C for 36 h. The mixture was concentrated and diluted with water. The mixture was extracted with ethyl acetate. The organic phases were washed with brine, dried over sodium sulfate and the solvent was removed. Column chromatography (40% → 45% EtOAc in petroleum ether) gave 1.79 g (4.45 mmol, 76%) of the desired product as a white solid. **^{1}H-NMR (400 MHz, $CDCl_3$)** δ(ppm) = 1.24 – 1.39 (m, 8 H, 4xCH_2), 1.43 (s, 9 H, Boc), 1.39 – 1.52 (m, 4 H, 2xCH_2), 1.76 – 1.86 (m, 2 H, CH_2), 2.50 – 2.60 (m, 1 H, OH), 3.02 – 3.11 (m, 2 H, BocNH-*CH_2*), 4.03 (t, *J* = 6.5 Hz, 2 H, -O-CH_2), 4.76 (s, 2 H, OH-CH_2), 7.09 – 7.15 (m, 2 H, 2xAr), 7.41 (dd, *J* = 8.4, 1.6 Hz, 1 H, Ar), 7.68 (dd, *J* = 7.0, 2.0 Hz, 3 H, 3xAr). **^{13}C-NMR (100 MHz, $CDCl_3$)** δ(ppm) = 26.0 (2xCH_2), 26.7 (CH_2), 28.4 (Boc-CH_3), 29.2 (CH_2), 29.3 (CH_2), 30.0 (CH_2), 40.6 (BocNH-*CH_2*), 65.3 (OH-CH_2), 68.0 (-O-CH_2), 79.1 (Boc-C_q), 106.6 (Ar-H), 119.2 (Ar-H), 125.5 (Ar-H), 125.8 (Ar-H), 127.0 (Ar-H), 128.7 (Ar-C_q), 129.3 (Ar-H), 134.1 (Ar-C_q), 136.2 (Ar-C_q), 156.1 (Boc-*C*OO), 157.2 (Ar-*C*O-). **ESI-MS:** 424.20 *m/z* $[M+Na]^+$

***tert*-Butyl (8-((6-(iodomethyl)naphthalen-2-yl)oxy)octyl)carbamate 23c**

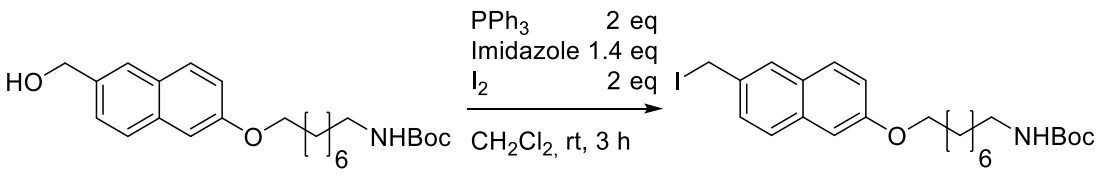

M = 511.44 g/mol

2.29 g Triphenylphosphine (8.72 mmol, 2 eq) and 415 mg imidazole (6.10 mmol, 1.4 eq) were dissolved in 50 mL dichloromethane and 2.21 g iodine (8.72 mmol, 2 eq) were added slowly. The mixture was stirred for 1 h at room temperature and 1.75 g of the alcohol **22c** (4.36 mmol,

1 eq) were added as a solution in 20 mL dichloromethane. The mixture was stirred at room temperature for 3 h and quenched with water. The phases were separated, and the organic phase was washed with HCl (10% *w/w*). The inorganic phases were extracted with dichloromethane. The organic phases were dried over sodium sulfate and the solvent was removed. Column chromatography (petroleum ether 8:1 EtOAc) gave 1.58 g (3.09 mmol, 71%) of the desired product as a yellow oil. **^{1}H-NMR (400 MHz, $CDCl_3$)** δ(ppm) = 1.27 – 1.41 (m, 8 H, 4xCH_2), 1.45 (s, 9 H, Boc), 1.42 – 1.53 (m, 4 H, 2xCH_2), 1.79 – 1.88 (m, 2 H, CH_2), 3.11 (q, *J* = 6.3 Hz, 2 H, BocNH-*CH_2*), 4.05 (t, *J* = 6.5 Hz, 2 H, -O-CH_2), 4.63 (s, 2 H, I-CH_2), 7.09 (d, *J* = 2.3 Hz, 1 H, Ar), 7.13 (dd, *J* = 9.0, 2.5 Hz, 1 H, Ar), 7.43 (dd, *J* = 8.4, 1.9 Hz, 1 H, Ar), 7.67 (dd, *J* = 8.8, 4.3 Hz, 2 H, 2xAr), 7.74 (d, *J* = 1.5 Hz, 1 H, Ar). **^{13}C-NMR (100 MHz, $CDCl_3$)** δ(ppm) = 7.2 (I-CH_2), 26.0 (CH_2), 26.8 (CH_2), 28.5 (Boc-CH_3), 29.1 (CH_2), 29.2 (2xCH_2), 29.3 (CH_2), 30.1 (CH_2), 41.4 (BocNH-*CH_2*), 68.0 (-O-CH_2), 79.1 (Boc-C_q), 106.7 (Ar-H), 119.6 (Ar-H), 127.0 (Ar-H), 127.4 (Ar-H), 127.6 (Ar-H), 128.6 (Ar-C_q), 129.2 (Ar-H), 133.0 (Ar-C_q), 134.1 (2xAr-C_q), 154.8 (Boc-*C*OO), 157.5 (Ar-*C*O-). **ESI-MS:** 534.10 *m/z* $[M+Na]^+$

Synthesis of Target Compound **2a**:

Ethyl 1-((6-(3-((*tert*-butoxycarbonyl)amino)propoxy)naphthalen-2-yl)methyl)-8-fluoro-4-oxo-1,4-dihydroquinoline-3-carboxylate 24a

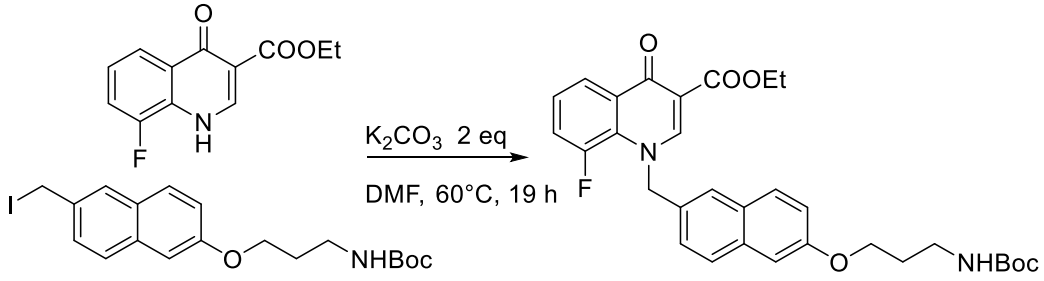

M = 548.61 g/mol

1.3 g of the iodo-compound **23a** (2.95 mmol, 1 eq) and 694 mg of the quinolone **15** (2.95 mmol, 1 eq) were dissolved in 30 mL dimethylformamide. 815 mg potassium carbonate (5.9 mmol, 2 eq) and a catalytic amount of potassium iodide were added. The mixture was heated to 60°C for 19 h. 100 mL water and 100 mL ethyl acetate were added. The phases were separated, and the inorganic phase was extracted with ethyl acetate. The combined organic phases were washed with water several times, dried over sodium sulfate and the solvent was

removed, to give 1.3 g (2.37 mmol, 80%) of the desired product as a brown solid. **^{1}H-NMR (400 MHz, $CDCl_3$)** δ(ppm) = 1.42 (t, *J* = 7.0 Hz, 3 H, CH_3), 1.43 (s, 9 H, Boc), 2.03 (quin, *J* = 6.1 Hz, 2 H, CH_2), 3.35 (q, *J* = 6.4 Hz, 2 H, BocNH-*CH_2*), 4.11 (t, *J* = 6.0 Hz, 2 H, CH_2-O-), 4.41 (q, *J* = 7.2 Hz, 2 H, *CH_2*-CH_3), 5.66 (s, 2 H, CH_2-N), 7.08 – 7.15 (m, 2 H, 2xAr), 7.21 – 7.35 (m, 4 H, 4xAr), 7.45 (s, 1 H, Ar), 7.64 (d, *J* = 8.8 Hz, 1 H, Ar), 7.70 (d, *J* = 8.5 Hz, 1 H, Ar), 8.34 – 8.38 (m, 1 H, Ar), 8.58 (s, 1 H, CH). **^{13}C-NMR (100 MHz, $CDCl_3$)** δ(ppm) = 14.4 (CH_3), 28.4 (Boc-CH_3), 29.6 (CH_2), 38.0 (BocNH-*CH_2*), 60.9 (CH_2-N), 61.1 (*CH_2*-CH_3), 65.9 (CH_2-O-), 79.3 (Boc-C_q), 106.6 (Ar-H), 111.4 (*C*=CH), 119.7 (Ar-H), 119.8 (d, *J* = 22.7 Hz, Ar-H), 123.9 (d, *J* = 2.9 Hz, Ar-H), 124.3 (Ar-H), 125.0 (Ar-H), 125.5 (d, *J* = 8.8 Hz, Ar-H), 127.9 (Ar-H), 128.54 (d, *J* = 6.6 Hz, Ar-C_q), 128.7 (Ar-C_q), 129.4 (Ar-H), 130.6 (d, *J* = 1.5 Hz, Ar-C_q), 132.0 (Ar-C_q), 134.3 (Ar-C_q), 151.6 (CH), 151.88 (d, *J* = 250.9 Hz, Ar-C_q), 156.0 (Boc-*C*OO), 157.3 (Ar-*C*O-), 165.5 (*C*OOEt), 173.2 (CO). **ESI-MS:** 571.20 *m/z* $[M+Na]^+$

Ethyl 1-((6-(3-aminopropoxy)naphthalen-2-yl)methyl)-8-fluoro-4-oxo-1,4-dihydroquinoline-3-carboxylate 25a

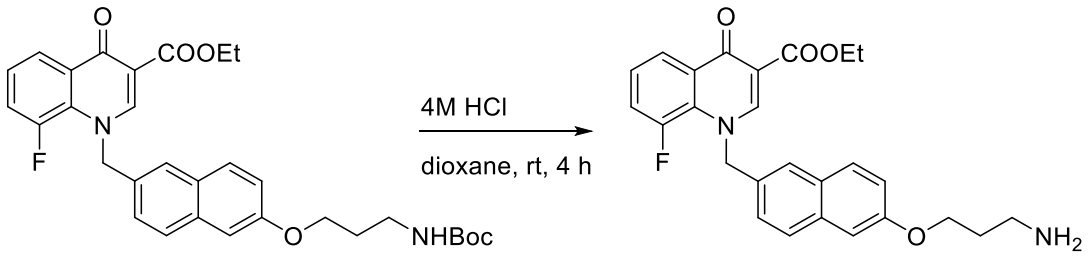

M = 448.49 g/mol

539 mg of the Boc-protected amine **24a** (0.98 mmol, 1 eq) were dissolved in 60 mL dioxane and 40 mL 4M HCl (160 mmol, 160 eq) were added. The mixture was stirred at room temperature for 4 h. Volatiles were removed, and the residue dissolved in dichloromethane and water. The phases were separated. The inorganic phase was basified to pH ≥ 13 and extracted with dichloromethane several times. The combined organic phases were dried over sodium sulfate. Removal of the solvent gave 200 mg (0.45 mmol, 46 %) of the desired product as a brown oil. **^{1}H-NMR (400 MHz, $CDCl_3$)** δ(ppm) = 1.40 (t, *J* = 7.2 Hz, 3 H, CH_3), 1.96 (quin, *J* = 6.5 Hz, 2 H, CH_2), 2.92 (t, *J* = 6.8 Hz, 2 H, NH_2-*CH_2*), 4.13 (t, *J* = 6.1 Hz, 2 H, O-CH_2), 4.39 (q, *J* = 7.2 Hz, 2 H, *CH_2*-CH_3), 5.62 (br. d, *J* = 2.0 Hz, 2 H, N-CH_2), 7.08 – 7.15 (m, 2 H, 2xAr), 7.18 – 7.32 (m, 3 H, 3xAr), 7.42 (br. s, 1 H, Ar), 7.61 (d, *J* = 9.0 Hz, 1 H, Ar), 7.67 (d, *J* = 8.8 Hz, 1 H, Ar), 8.31 – 8.36 (m, 1 H, Ar), 8.56 (s, 1 H, CH). **^{13}C-NMR (100 MHz, $CDCl_3$)** δ(ppm) = 14.4 (CH_3), 32.9

(CH_2), 39.2 (NH_2-*CH_2*), 60.89/61.05 (N-CH_2), 61.1 (*CH_2*-CH_3), 66.0 (O-CH_2), 106.5 (Ar-H), 111.3 (*C*=CH), 119.78 (Ar-H), 119.82 (d, *J* = 22.7 Hz, Ar-H), 123.83 (d, *J* = 3.7 Hz, Ar-H), 124.3 (Ar-H), 125.0 (Ar-H), 125.49 (d, J = 8.1 Hz, Ar-H), 127.9 (Ar-H), 128.51 (d, *J* = 6.6 Hz, Ar-C_q), 128.60 (Ar-C_q), 129.4 (Ar-H), 130.51 (d, *J* = 1.5 Hz, Ar-C_q), 131.9 (Ar-C_q), 134.3 (Ar-C_q), 151.61 (CH), 151.86 (d, *J* = 250.9 Hz, Ar-CF), 157.5 (Ar-*C*O-), 165.4 (*C*OOEt), 173.2 (CO). **ESI-MS:** 449.10 *m/z* $[M+H]^+$, 225.10 *m/z* $[M+2H]^{2+}$

Ethyl 1-((6-(3-(((2-chloroethoxy)carbonyl)amino)propoxy)naphthalen-2-yl)methyl)-8-fluoro-4-oxo-1,4-dihydroquinoline-3-carboxylate 26a

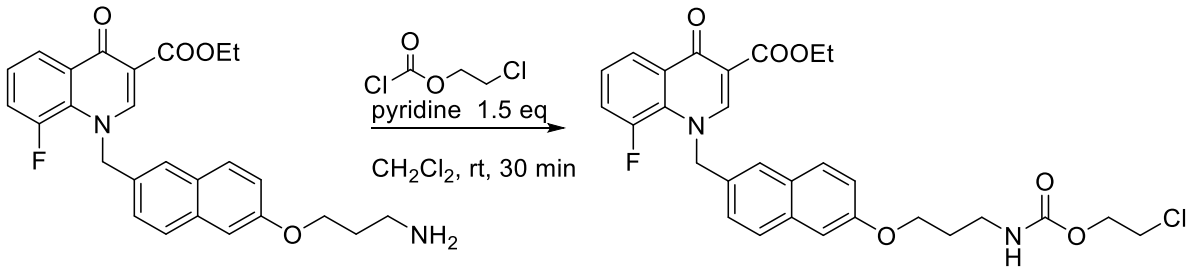

M = 555.00 g/mol

100 mg of the amine **25a** (0.22 mmol, 1 eq) were dissolved in 40 mL dichloromethane and 26.6 µL pyridine (0.33 mmol, 1.5 eq) and 27.3 µL 2-chloroethyl chloroformate (0.26 mmol, 1.2 eq) were added. The mixture was stirred for 30 min at room temperature. Saturated ammonium chloride solution was added, and the mixture extracted with dichloromethane. The organic phases were dried, and the solvent was removed. Column chromatography (1% MeOH in CH_2Cl_2; on deactivated silica) gave 100 mg (0.18 mmol, 82 %) of the desired product as a colourless oil. **^{1}H-NMR (400 MHz, $CDCl_3$)** *δ*(ppm) = 1.40 (t, *J* = 7.2 Hz, 3 H, CH_3), 2.05 (quin, *J* = 6.3 Hz, 2 H, CH_2), 3.42 (q, *J* = 6.5 Hz, 2 H, NH-*CH_2*), 3.62 – 3.66 (m, 2 H, O-CH_2), 4.11 (t, *J* = 5.9 Hz, 2 H, CH_2-Cl), 4.29 (t, *J* = 5.5 Hz, 2 H, O-CH_2), 4.40 (q, *J* = 7.1 Hz, 2 H, *CH_2*CH_3), 5.16 (br. s., 1 H, NH), 5.64 (d, *J* = 2.0 Hz, 2 H, N-CH_2), 7.08 (d, *J* = 2.3 Hz, 1 H, Ar), 7.12 (dd, *J* = 8.9, 2.4 Hz, 1 H, Ar), 7.19 – 7.33 (m, 3 H, 3xAr), 7.43 (br. s, 1 H, Ar), 7.62 (d, *J* = 9.0 Hz, 1 H, Ar), 7.68 (d, *J* = 8.5 Hz, 1 H, Ar), 8.32 – 8.36 (m, 1 H, Ar), 8.57 (s, 1 H, CH). **^{13}C-NMR (100 MHz, $CDCl_3$)** *δ*(ppm) = 14.4 (CH_3), 29.3 (CH_2), 38.6 (NH-CH_2), 42.3 (O-CH_2), 60.89/61.05 (N-CH_2), 61.12 (*CH_2*-CH_3), 64.5 (O-CH_2), 65.8 (CH_2-Cl), 106.6 (Ar-H), 111.4 (*C*=CH), 119.64 (Ar-H), 119.83 (d, *J* = 22.7 Hz, Ar-H), 123.85 (d, *J* = 2.9 Hz, Ar-H), 124.4 (Ar-H), 125.0 (Ar-H), 125.51 (d, *J* = 8.1 Hz, Ar-H), 127.9 (Ar-H), 128.52 (d, *J* = 7.3 Hz, Ar-C_q), 128.7 (Ar-C_q), 129.5 (Ar-H), 130.67 (d, *J* = 1.5 Hz, Ar-C_q),

131.9 (Ar-C_q), 134.2 (Ar-C_q), 151.62 (CH), 151.78 (d, *J* = 253.1 Hz, Ar-CF), 156.0 (NH*C*OO), 157.2 (Ar-*C*O-), 165.4 (*C*OOEt), 173.2 (CO). **ESI-MS:** 555.10 *m/z* $[M+H]^+$

3-Carboxy-8-fluoro-4-oxo-1-((6-(3-(((2-(trimethylammonio)ethoxy)carbonyl)amino)-propoxy)naphthalen-2-yl)methyl)-1,4-dihydroquinolin-1-ium formate 2a

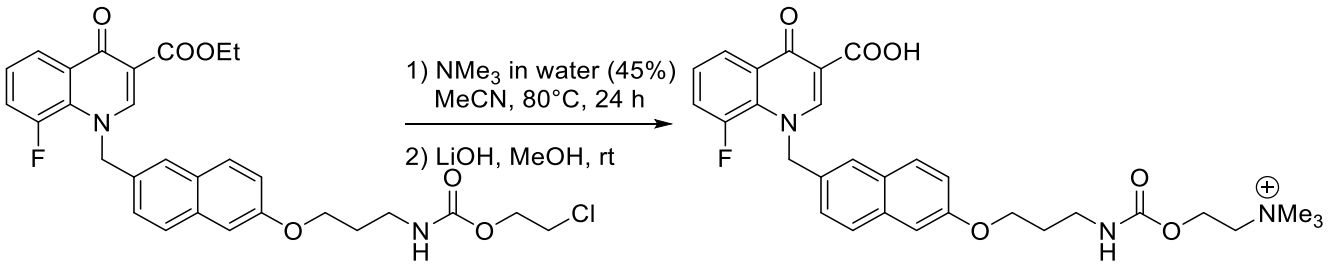

M = 550.61 g/mol

64 mg of the chloro-compound **26a** (0.115 mmol, 1 eq) were dissolved in 12 mL acetonitrile and 10 mL trimethylamine in water (45w%) were added. The mixture was heated to 75 °C for 1 d in a sealed vessel. Volatiles were removed. The residue was dissolved in methanol and 17 mg lithium hydroxide (6.9 mmol, 6 eq) in water were added. The mixture was stirred at room temperature until LCMS showed disappearance of the ester. 2M HCl was added to neutralize the mixture. Volatiles were removed, and the residue was purified by preparative HPLC to give 13 mg (0.020 mmol, 17 %) of the formiate salt of the product as a colorless oil. **^{1}H-NMR (400 MHz, $CDCl_3$)** δ(ppm) = 2.03 (br. t, *J* = 5.0 Hz, 2 H, CH_2), 3.17 (s, 9 H, NMe_3), 3.33 – 3.38 (m, 2 H, NH-CH_2), 3.64 (br. s., 2 H, *CH_2*-NMe_3), 4.11 (br. s., 2 H, O-CH_2), 4.49 (br. s., 2 H, O-CH_2), 5.92 (br. s., 2 H, N-CH_2), 7.10 (d, *J* = 7.5 Hz, 1 H, Ar), 7.19 (br. s., 1 H, Ar), 7.28 (d, *J* = 5.0 Hz, 1 H, Ar), 7.51 – 7.62 (m, 3 H, 3xAr), 7.66 (d, *J* = 7.8 Hz, 1 H, Ar), 7.75 (br. d, *J* = 5.5 Hz, 1 H, Ar), 8.33 (d, *J* = 7.0 Hz, 1 H, Ar), 8.40 (s, 2 H, $HCOO^-$), 9.04 (br. s., 1 H, CH). **^{13}C-NMR (100 MHz, $CDCl_3$)** δ(ppm) = 29.1 (CH_2), 37.6 (NH-CH_2), 53.03/53.07/53.10 (NMe_3), 57.8 (O-CH_2), 61.3 (N-CH_2), 65.0 (O-CH_2), 65.12/65.15/65.19 (*CH_2*-NMe_3), 106.2 (Ar-H), 111.3 (*C*=CH), 119.2 (Ar-H), 121.0 (d, J = 23.5 Hz, Ar-H), 122.5 (d, J = 2.9 Hz, Ar-H), 124.3 (Ar-H), 124.9 (Ar-H), 126.8 (d, J = 8.8 Hz, Ar-H), 127.5 (Ar-H), 128.8 (Ar-C_q), 128.9 (Ar-C_q), 129.1 (Ar-H), 130.7 (d, J = 1.5 Hz, Ar-C_q), 132.3 (Ar-C_q), 134.4 (Ar-C_q), 151.8 (CH), 152.1 (d, J = 254.6 Hz, Ar-CF), 156.1 (NH*C*OO), 157.5 (Ar-*C*O-), 166.9 (*C*OOH), 167.5 ($HCOO^-$), 173.5 (CO). **ESI-MS:** 275.70 *m/z* $[M+H]^{2+}$, 550.25 *m/z* $[M]^+$

Synthesis of Target Compound **2b**:

Ethyl 1-((6-(5-((*tert*-butoxycarbonyl)amino)pentoxy)naphthalen-2-yl)methyl)-8-fluoro-4-oxo-1,4-dihydroquinoline-3-carboxylate 24b

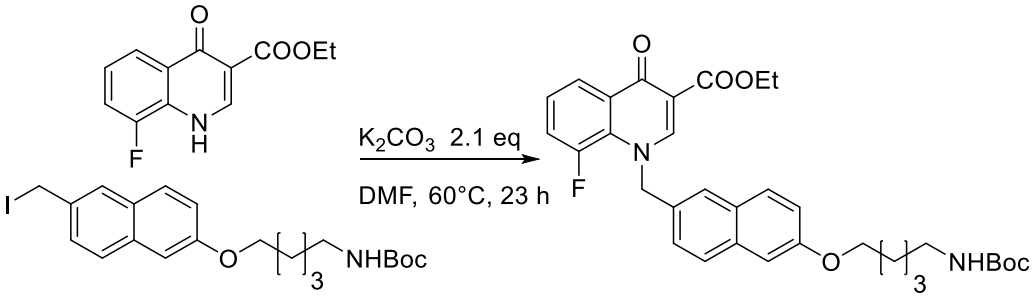

M = 576.67 g/mol

1.373 g of the iodo-compound **23b** (2.93 mmol, 1 eq) and 689 mg of the quinolone **15** (2.93 mmol, 1eq) were dissolved in 30 mL dimethylformamide. 850 mg potassium carbonate (6.15 mmol, 2.1 eq) and a catalytic amount of potassium iodide were added. The mixture was heated to 60°C for 23 h. 100 mL water and 100 mL ethyl acetate were added. The phases were separated, and the inorganic phase was extracted with ethyl acetate. The combined organic phases were washed with water several times, dried over sodium sulfate and the solvent was removed. Column chromatography (petroleum ether : EtOAc 1:1 → 1:3) gave 708 mg (1.25 mmol, 42 %) of the desired product as a white solid. **^{1}H-NMR (400 MHz, $CDCl_3$)** δ(ppm) = 1.39 (t, *J* = 7.2 Hz, 3 H, CH_3), 1.42 (s, 9 H, Boc), 1.46 – 1.60 (m, 4 H, 2xCH_2), 1.83 (quin, *J* = 6.8 Hz, 2 H, CH_2), 3.13 (q, *J* = 5.8 Hz, 2 H, BocN-CH_2), 4.02 (t, *J* = 6.5 Hz, 2 H, O-CH_2), 4.39 (q, *J* = 7.1 Hz, 2 H, *CH_2*-CH_3), 5.62 (d, *J* = 2.0 Hz, 2 H, N-CH_2), 7.06 (d, *J* = 2.5 Hz, 1 H, Ar), 7.11 (dd, *J* = 9.0, 2.5 Hz, 1 H, Ar), 7.17 – 7.37 (m, 3 H, 3xAr), 7.42 (br. s, 1 H, Ar), 7.60 (d, *J* = 9.0 Hz, 1 H, Ar), 7.67 (d, *J* = 8.8 Hz, 1 H, Ar), 8.31 – 8.36 (m, 1 H, Ar), 8.56 (s, 1 H, CH). **^{13}C-NMR (100 MHz, $CDCl_3$)** δ(ppm) = 14.4 (CH_3), 23.4 (CH_2), 28.4 (Boc-CH_3), 28.8 (CH_2), 29.9 (CH_2), 40.5 (BocN-*CH_2*), 60.90/61.05 (N-CH_2), 61.09 (O-CH_2), 67.8 (*CH_2*-CH_3), 79.1 (Boc-C_q), 106.5 (Ar-H), 111.3 (*C*=CH), 119.80 (Ar-H), 119.81 (d, *J* = 22.7 Hz, Ar-H), 123.82 (d, *J* = 3.7 Hz, Ar-H), 124.3 (Ar-H), 125.0 (Ar-H), 125.48 (d, *J* = 8.8 Hz, Ar-H), 127.8 (Ar-H), 128.48 (Ar-C_q), 128.51 (d, *J* = 11 Hz, Ar-C_q), 129.3 (Ar-H), 130.47 (d, *J* = 1.5 Hz, Ar-C_q), 131.9 (Ar-C_q), 134.3 (Ar-C_q), 151.62 (CH), 151.86 (d, *J* = 250.2 Hz, Ar-CF), 156.0 (Ar-*C*O-), 157.6 (Boc-*C*OO), 165.4 (*C*OOEt), 173.2 (CO). **ESI-MS:** 599.25 *m/z* $[M+Na]^+$

Ethyl 1-((6-((5-aminopentyl)oxy)naphthalen-2-yl)methyl)-8-fluoro-4-oxo-1,4-dihydroquinoline-3-carboxylate 25b

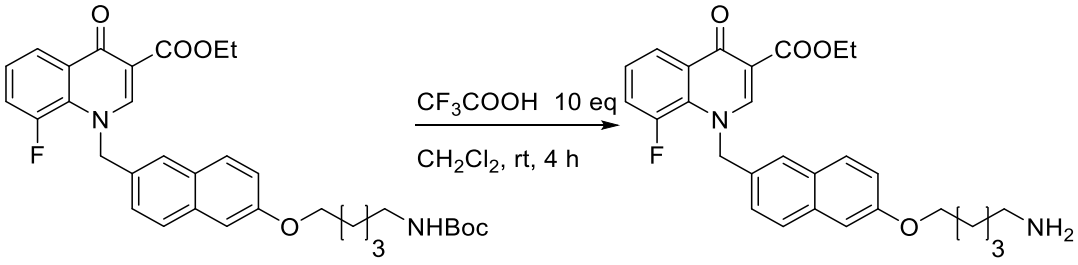

M = 476.55 g/mol

586 mg of the Boc-protected amine **24b** (1.0 mmol, 1 eq) was dissolved in 25 mL dichloromethane and 1 mL trifluoro acetic acid (10 mmol, 10 eq) were added. The mixture was stirred at room temperature for 4 h. Water was added, and the phases were separated. The inorganic phase was basified to pH ≥ 13 and extracted with ethyl acetate several times. The combined organic phases were washed with brine and dried over sodium sulfate. Removal of the solvent gave 215 mg (0.45 mmol, 45 %) of the desired product as a colorless oil. **^{1}H-NMR (400 MHz, $CDCl_3$)** δ(ppm) = 1.34 (t, *J* = 7.2 Hz, 3 H, CH_3), 1.43 – 1.52 (m, 4 H, 2xCH_2), 1.75 – 1.84 (m, 2 H, CH_2), 2.61 – 2.69 (m, 1 H, NH_2-*CH_2*), 3.95 – 4.01 (m, 2 H, O-CH_2), 4.33 (q, *J* = 7.0 Hz, 2 H, *CH_2*CH_3), 5.57 (d, *J* = 2.3 Hz, 2 H, N-CH_2), 7.01 (d, *J* = 2.5 Hz, 1 H, Ar), 7.06 (dd, *J* = 8.9, 2.4 Hz, 1 H, Ar), 7.14 (dd, *J* = 8.5, 1.5 Hz, 1 H, Ar), 7.16 – 7.26 (m, 2 H, 2xAr), 7.36 (br. s, 1 H, Ar), 7.55 (dd, *J* = 9.0, 1.8 Hz, 1 H, Ar), 7.61 (d, *J* = 8.5 Hz, 1 H, Ar), 8.26 – 8.30 (m, 1 H, Ar), 8.51 (s, 1 H, CH). **^{13}C-NMR (100 MHz, $CDCl_3$)** δ(ppm) = 14.4 (CH_3), 23.5 (CH_2), 29.1 (CH_2), 33.6 (CH_2), 42.2 (NH_2-*CH_2*), 60.9 (N-CH_2), 61.1 (*CH_2*CH_3), 67.9 (O-CH_2), 106.5 (Ar-H), 111.4 (*C*=CH), 119.82 (d, *J* = 22.7 Hz, Ar-H), 119.84 (Ar-H), 123.9 (d, *J* = 2.9 Hz, Ar-H), 124.3 (Ar-H), 125.0 (Ar-H), 125.5 (d, *J* = 8.1 Hz, Ar-H), 127.8 (Ar-H), 128.52 (d, *J* = 4.4 Hz, Ar-C_q), 128.56 (Ar-C_q), 129.3 (Ar-H), 130.4 (d, *J* = 1.5 Hz, Ar-C_q), 131.9 (Ar-C_q), 134.3 (Ar-C_q), 151.62 (CH), 151.88 (d, *J* = 250.9 Hz, Ar-CF), 157.6 (Ar-*C*O-), 165.4 (*C*OOEt), 173.2 (CO). **ESI-MS:** 476.55 *m/z* $[M+H]^+$, 239.05 *m/z* $[M+2H]^{2+}$

Ethyl 1-((6-((5-(((2-chloroethoxy)carbonyl)amino)pentyl)oxy)naphthalen-2-yl)methyl)-8-fluoro-4-oxo-1,4-dihydroquinoline-3-carboxylate 26b

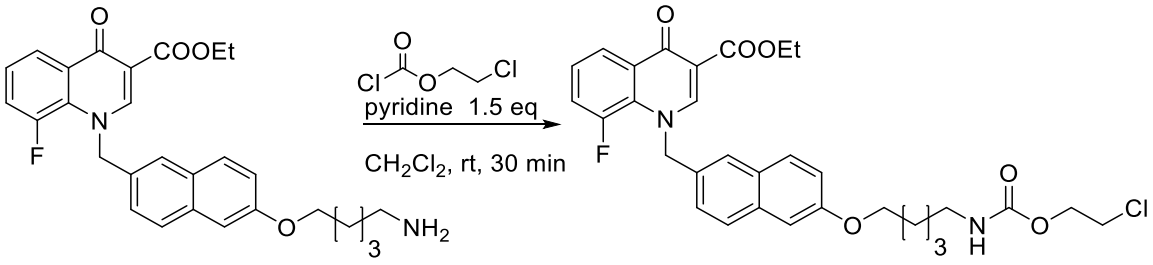

M = 583.05 g/mol

215 mg of the amine **25b** (0.45 mmol, 1 eq) were dissolved in 20 mL dichloromethane. 55 µL pyridine (0.68 mmol, 1.5 eq) and 56 µL 2-chloroethyl chloroformiate (0.54 mmol, 1.2 eq) were added. The mixture was stirred at room temperature for 30 min. Saturated ammonium chloride solution was added and the mixture extracted with dichloromethane. The organic phases were dried over sodium sulfate and the solvent was removed. Column chromatography (EtOAc 5:1 petroleum ether; on deactivated silica) gave 202 mg (0.35 mmol, 78 %) of the desired product as a colorless oil. **^{1}H-NMR (400 MHz, $CDCl_3$)** δ(ppm) = 1.32 (t, *J* = 7.2 Hz, 3 H, CH_3), 1.38 – 1.55 (m, 4 H, 2xCH_2), 1.75 (quin, *J* = 6.8 Hz, 2 H, CH_2), 3.13 (q, *J* = 6.5 Hz, 2 H, NH-*CH_2*), 3.56 (t, *J* = 5.6 Hz, 2 H, CH_2-Cl), 3.94 (t, *J* = 6.4 Hz, 2 H, O-CH_2), 4.20 (t, *J* = 5.6 Hz, 2 H, O-CH_2), 4.31 (q, *J* = 7.3 Hz, 2 H, *CH_2*-CH_3), 4.94 (br. s., 1 H, NH), 5.54 (d, *J* = 2.0 Hz, 2 H, N-CH_2), 6.98 (d, *J* = 2.3 Hz, 1 H, Ar), 7.03 (dd, *J* = 9.0, 2.5 Hz, 1 H, Ar), 7.10 – 7.24 (m, 3 H, 3xAr), 7.34 (br. s, 1 H, Ar), 7.53 (d, *J* = 9.0 Hz, 1 H, Ar), 7.59 (d, *J* = 8.5 Hz, 1 H, Ar), 8.23 – 8.28 (m, 1 H, Ar), 8.49 (s, 1 H, CH). **^{13}C-NMR (100 MHz, $CDCl_3$)** δ(ppm) = 14.4 (CH_3), 23.3 (CH_2), 28.8 (CH_2), 29.7 (CH_2), 40.9 (NH-CH_2), 42.3 (CH_2-Cl), 60.87/61.03 (N-CH_2), 61.07 (*CH_2*-CH_3), 64.4 (O-CH_2), 67.7 (O-CH_2), 106.5 (Ar-H), 111.3 (*C*=CH), 119.78 (Ar-H), 119.81 (d, *J* = 22.7 Hz, Ar-H), 123.79 (d, J = 2.9 Hz, Ar-H), 124.3 (Ar-H), 125.0 (Ar-H), 125.48 (d, *J* = 8.1 Hz, Ar-H), 127.8 (Ar-H), 128.52 (d, *J* = 8.8 Hz, Ar-C_q), 128.6 (Ar-C_q), 129.4 (Ar-H), 130.52 (d, *J* = 1.5 Hz, Ar-C_q), 131.9 (Ar-C_q), 134.3 (Ar-C_q), 151.62 (CH), 151.85 (d, *J* = 251.6 Hz, Ar-CF), 156.0 (NH*C*OO), 157.5 (Ar-*C*O-), 165.4 (*C*OOEt), 173.2 (CO). **ESI-MS:** 583.10 *m/z* $[M+H]^+$

2-(((5-((6-((3-Carboxy-8-fluoro-4-oxoquinolin-1(4*H*)-yl)methyl)naphthalen-2-yl)oxy)pentyl)carbamoyl)oxy)-*N*,*N*,*N*-trimethylethan-1-aminium formate 2b

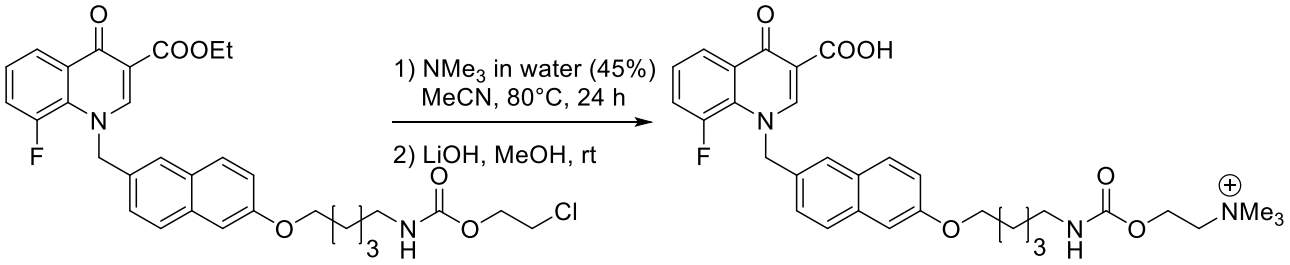

M = 578.66 g/mol

100 mg of the chloro-compound **26b** (0.17 mmol, 1 eq) were dissolved in 15 mL acetonitrile and 10 mL trimethylamine in water (45w%) were added. The mixture was heated to 80 °C for 1 d in a sealed vessel. Volatiles were removed. The residue was suspended in water and lithium hydroxide was added to adjust the pH ≥ 12. The mixture was stirred at room temperature until LCMS showed disappearance of the ester. 2M HCl was added to neutralize the mixture. Volatiles were removed, and the residue was purified by reversed phase column chromatography to give 15 mg (0.024 mmol, 14%) of the formiate salt of the product as a colorless oil. **^{1}H-NMR (400 MHz, $CDCl_3$)** δ(ppm) = 1.52 – 1.62 (m, 4 H, 2xCH_2), 1.82 (quin, *J* = 6.7 Hz, 2 H, CH_2), 3.15 (t, *J* = 6.8 Hz, 2 H, NH-*CH_2*), 3.20 (m, 9 H, NMe_3), 3.64 – 3.69 (m, 2 H, *CH_2*-NMe_3), 4.06 (t, *J* = 6.3 Hz, 2 H, O-CH_2), 4.46 – 4.53 (m, 2 H, O-CH_2), 5.92 (br. s., 2 H, N-CH_2), 7.09 (dd, *J* = 8.8, 2.0 Hz, 1 H, Ar), 7.15 – 7.20 (m, 1 H, Ar), 7.27 (br. d., 1 H, Ar), 7.50 – 7.63 (m, 3 H, 3xAr), 7.65 (d, *J* = 9.0 Hz, 1 H, Ar), 7.75 (d, *J* = 8.3 Hz, 1 H, Ar), 8.30 – 8.36 (m, 1 H, Ar), 9.05 (s, 1 H, CH). **^{13}C-NMR (100 MHz, $CDCl_3$)** δ(ppm) = 23.1 (CH_2), 28.6 (CH_2), 29.2 (CH_2), 40.4 (NH-CH_2), 53.08/53.12/53.16 (NMe_3), 57.7 (O-CH_2), 61.16/61.32 (N-CH_2), 65.15/65.18/65.21 (CH_2-NMe_3), 67.5 (O-CH_2), 106.1 (Ar-H), 107.9 (*C*=CH), 119.3 (Ar-H), 121.02 (d, *J* = 22.7 Hz, Ar-H), 122.45 (d, J = 3.7 Hz, Ar-H), 124.2 (Ar-H), 124.9 (Ar-H), 126.86 (d, *J* = 8.8 Hz, Ar-H), 127.5 (Ar-H), 128.7 (Ar-C_q), 128.95 (d, *J* = 8.8 Hz, Ar-C_q), 129.0 (Ar-H), 130.5 (Ar-C_q), 130.58 (d, *J* = 2.2 Hz, Ar-C_q), 134.5 (Ar-C_q), 151.8 (CH), 152.25 (d, *J* = 250.2 Hz, Ar-CF), 156.0 (NH*C*OO), 157.6 (Ar-*C*O-), 167.5 (*C*OOEt), 177.7 (CO). **ESI-MS:** 289.75 *m/z* $[M+H]^{2+}$, 578.20 *m/z* $[M]^{+}$

Synthesis of Target Compound **2c**:

Ethyl 1-((6-((8-((*tert*-butoxycarbonyl)amino)octyl)oxy)naphthalen-2-yl)methyl)-8-fluoro-4-oxo-1,4-dihydroquinoline-3-carboxylate 24c

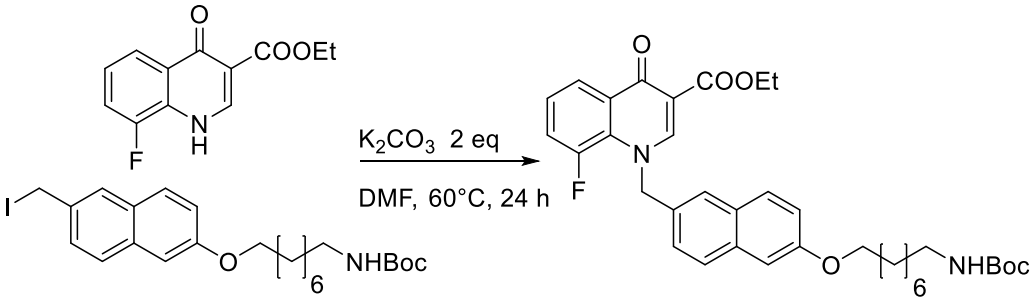

M = 618.75 g/mol

726 mg of the quinolone **15** (3.09 mmol, 1 eq) and 1.58 g of the iodo-compound **23c** (3.09 mmol, 1 eq) were dissolved in 30 mL dimethylformamide and 854 mg potassium carbonate (6.18 mmol, 2 eq) and a catalytic amount of potassium iodide were added. The mixture was heated to 60°C for 24 h. The mixture was concentrated, diluted with water and extracted with ethyl acetate. The organic phases were washed with water several times, washed with brine, dried over sodium sulfate and the solvent was removed. Column chromatography (petroleum ether : EtOAc 1:1 → 1:3) gave 803 mg (1.30 mmol, 42 %) of the desired product as an oily white solid. **^{1}H-NMR (400 MHz, $CDCl_3$)** δ(ppm) = 1.26 – 1.37 (m, 8 H, 4xCH_2), 1.38 – 1.51 (m, 4 H, 2xCH_2), 1.39 (t, *J* = 7.5 Hz, 3 H, CH_3), 1.43 (s, 9 H, Boc), 1.81 (quin, *J* = 7.0 Hz, 2 H, CH_2), 3.09 (q, *J* = 6.0 Hz, 2 H, BocNH-*CH_2*), 4.02 (t, *J* = 6.4 Hz, 2 H, -O-CH_2), 4.40 (q, *J* = 6.8 Hz, 2 H, *CH_2*-CH_3), 5.63 (br. s., 2 H, N-CH_2), 7.07 (br. s, 1 H, Ar), 7.12 (br. d, *J* = 8.8 Hz, 1 H, Ar), 7.18 – 7.33 (m, 3 H, 3xAr), 7.43 (br. s, 1 H, Ar), 7.61 (d, *J* = 8.8 Hz, 1 H, Ar), 7.68 (d, *J* = 8.3 Hz, 1 H, Ar), 8.34 (d, *J* = 7.5 Hz, 1 H, Ar), 8.57 (s, 1 H, CH). **^{13}C-NMR (100 MHz, $CDCl_3$)** δ(ppm) = 14.4 (CH_3), 26.0 (CH_2), 26.7 (CH_2), 28.4 (Boc-CH_3), 29.1 (CH_2), 29.2 (CH_2), 29.3 (CH_2), 30.1 (CH_2), 40.6 (BocNH-*CH_2*), 60.91/61.06 (N-CH_2), 61.09 (*CH_2*-CH_3), 68.0 (O-CH_2), 79.0 (Boc-C_q), 106.5 (Ar-H), 111.3 (*C*=CH), 119.80 (d, *J* = 22.7 Hz, Ar-H), 119.87 (Ar-H), 123.84 (d, *J* = 2.9 Hz, Ar-H), 124.2 (Ar-H), 125.00 (d, *J* = 1.5 Hz, Ar-H), 125.47 (d, *J* = 8.1 Hz, Ar-H), 127.8 (Ar-H), 128.53 (d, *J* = 7.3 Hz, Ar-C_q), 128.54 (Ar-C_q), 129.3 (Ar-H), 130.4 (Ar-C_q), 131.9 (Ar-C_q), 134.3 (Ar-C_q), 151.62 (CH), 151.88 (d, *J* = 249.4 Hz, Ar-CF), 156.0 (Boc-*C*OO), 157.7 (Ar-*C*O-), 165.4 (*C*OOEt), 173.2 (CO). **ESI-MS:** 534.10 *m/z* $[M+Na]^+$

Ethyl 1-((6-((8-aminooctyl)oxy)naphthalen-2-yl)methyl)-8-fluoro-4-oxo-1,4-dihydroquinoline-3-carboxylate 25c

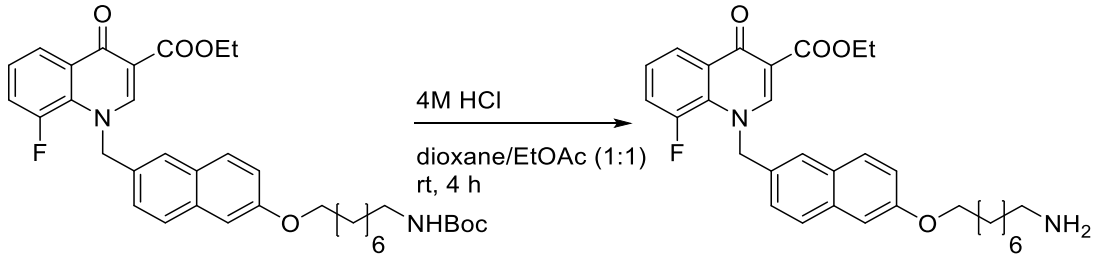

M = 518.63 g/mol

762 mg of the Boc-protected amine **24c** (1.23 mmol, 1 eq) were dissolved in 30 mL dioxane/ethyl acetate (1:1) and 43 mL 4M HCl (120 mmol, 100 eq) were added. The mixture was stirred at room temperature for 4 h. Volatiles were removed, and the residue dissolved in dichloromethane and water. The phases were separated. The inorganic phase was basified to pH ≥ 13 and extracted with dichloromethane several times. The combined organic phases were dried over sodium sulfate. Removal of the solvent gave 250 mg (0.44 mmol, 36 %) of the desired product as a brown oil. **^{1}H-NMR (400 MHz, $CDCl_3$)** δ(ppm) = 1.29 – 1.52 (m, 8 H, 4xCH_2), 1.41 (t, 3 H, CH_3), 1.77 – 1.87 (m, 4 H, 2xCH_2), 2.67 (t, *J* = 6.9 Hz, 2 H, NH_2-*CH_2*), 4.04 (t, *J* = 6.5 Hz, 2 H, O-CH_2), 4.41 (q, *J* = 7.2 Hz, 2 H, *CH_2*-CH_3), 5.64 (d, *J* = 2.0 Hz, 2 H, N-CH_2), 7.08 (d, *J* = 2.5 Hz, 1 H, Ar), 7.13 (dd, *J* = 8.8, 2.5 Hz, 1 H, Ar), 7.19 – 7.34 (m, 3 H, 3xAr), 7.44 (br. s, 1 H, Ar), 7.62 (d, *J* = 9.0 Hz, 1 H, Ar), 7.69 (d, *J* = 8.5 Hz, 2 H, 2xAr), 8.34 – 8.37 (m, 1 H, Ar), 8.58 (s, 1 H, CH). **^{13}C-NMR (100 MHz, $CDCl_3$)** δ(ppm) = 14.4 (CH_3), 26.0 (CH_2), 26.8 (CH_2), 29.1 (CH_2), 29.3 (CH_2), 33.4 (CH_2), 42.1 (CH_2), 51.5 (NH_2-CH_2), 60.84/61.00 (N-CH_2), 61.02 (*CH_2*-CH_3), 68.03 (O-CH_2), 105.4 (Ar-H), 110.2 (*C*=CH), 118.78 (d, *J* = 22.7 Hz, Ar-H), 118.81 (Ar-H), 122.74 (d, *J* = 2.9 Hz, Ar-H), 123.2 (Ar-H), 123.9 (Ar-H), 124.2 (d, *J* = 8.1 Hz, Ar-H), 126.8 (Ar-H), 127.48 (d, *J* = 6.6 Hz, Ar-C_q), 127.49 (Ar-C_q), 128.3 (Ar-H), 129.4 (Ar-C_q), 130.8 (Ar-C_q), 133.3 (Ar-C_q), 150.58 (CH), 150.74 (d, *J* = 251.6 Hz, Ar-CF), 156.6 (Ar-*C*O-), 164.3 (*C*OOEt), 172.1 (CO). **ESI-MS:** 519.15 *m/z* $[M+H]^+$, 260.15 *m/z* $[M+2H]^{2+}$

Ethyl 1-((6-((8-(((2-chloroethoxy)carbonyl)amino)octyl)oxy)naphthalen-2-yl)methyl)-8-fluoro-4-oxo-1,4-dihydroquinoline-3-carboxylate 26c

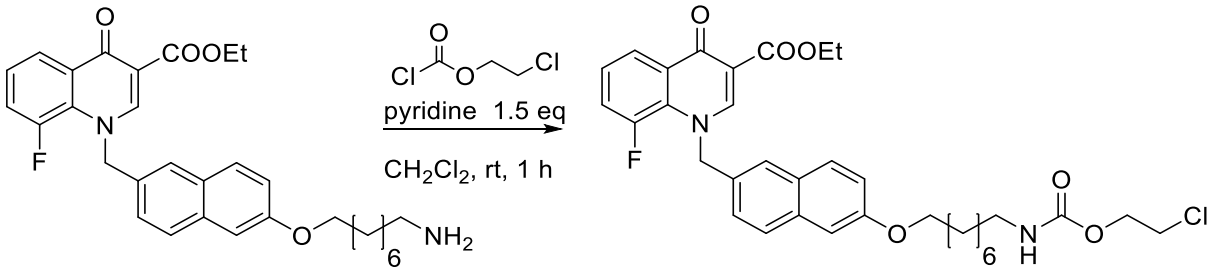

M = 625.13 g/mol

125 mg of the amine **25c** (0.22 mmol, 1 eq) were dissolved in 20 mL dichloromethane. 27 µL pyridine (0.33 mmol, 1.5 eq) and 27 µL 2-chloroethyl chloroformiate (0.26 mmol, 1.2 eq) were added. The mixture was stirred at room temperature for 1 h. Saturated ammonium chloride solution was added, and the mixture extracted with dichloromethane. The organic phases were dried over sodium sulfate and the solvent was removed. Column chromatography (EtOAc 5:1 petroleum ether) gave 40 mg (0.064 mmol, 29 %) of the desired product as a colorless oil. **^{1}H-NMR (400 MHz, $CDCl_3$)** δ(ppm) = 1.29 – 1.38 (m, 8 H, 4xCH_2), 1.41 (t, *J* = 7.2 Hz, 3 H, CH_3), 1.44 – 1.54 (m, 4 H, 2xCH_2), 1.77 – 1.86 (m, 2 H, CH_2), 3.17 (q, *J* = 6.6 Hz, 2 H, CH_2), 3.66 (t, *J* = 5.6 Hz, 2 H, CH_2-Cl), 4.03 (t, *J* = 6.5 Hz, 2 H, -O-CH_2), 4.29 (t, *J* = 5.6 Hz, 2 H, -O-CH_2), 4.41 (q, *J* = 7.0 Hz, 2 H, *CH_2*-CH_3), 5.65 (d, *J* = 2.0 Hz, 2 H, N-CH_2), 7.08 (d, *J* = 2.5 Hz, 1 H, Ar), 7.13 (dd, *J* = 8.8, 2.5 Hz, 1 H, Ar), 7.21 (dd, *J* = 8.5, 1.5 Hz, 1 H, Ar), 7.23 – 7.35 (m, 2 H, 2xAr), 7.44 (br. s, 1 H, Ar), 7.63 (d, *J* = 9.0 Hz, 1 H, Ar), 7.69 (d, *J* = 8.8 Hz, 1 H, Ar), 8.34 – 8.37 (m, 1 H, Ar), 8.58 (s, 1 H, CH). **^{13}C-NMR (100 MHz, $CDCl_3$)** δ(ppm) = 14.4 (CH_3), 26.0 (CH_2), 26.6 (CH_2), 29.1 (CH_2), 29.2 (CH_2), 29.3 (CH_2), 29.9 (CH_2), 41.1 (CH_2), 42.4 (CH_2-Cl), 60.94/61.10 (N-CH_2), 61.13 (*CH_2*-CH_3), 64.4 (-O-CH_2), 68.0 (-O-CH_2), 106.5 (Ar-H), 111.4 (*C*=CH), 119.84 (d, *J* = 23.5 Hz, Ar-H), 119.88 (Ar-H), 123.88 (d, J = 2.9 Hz, Ar-H), 124.3 (Ar-H), 125.01 (d, J = 1.5 Hz, Ar-H), 125.50 (d, J = 8.8 Hz, Ar-H), 127.8 (Ar-H), 128.55 (Ar-C_q), 128.57 (d, J = 2.2 Hz, Ar-C_q), 129.3 (Ar-H), 130.38 (d, J = 1.5 Hz, Ar-C_q), 132.0 (Ar-C_q), 134.4 (Ar-C_q), 151.64 (CH), 151.81 (d, J = 247.2 Hz, Ar-CF), 155.9 (NH*C*OO), 157.7 (Ar-*C*O-), 165.5 (*C*OOEt), 173.2 (CO). **ESI-MS:** 625.15 *m/z* $[M+H]^+$

3-Carboxy-8-fluoro-4-oxo-1-((6-((8-(((2-(trimethylammonio)ethoxy)carbonyl)amino)-octyl)oxy)naphthalen-2-yl)methyl)-1,4-dihydroquinolin-1-ium formate 2c

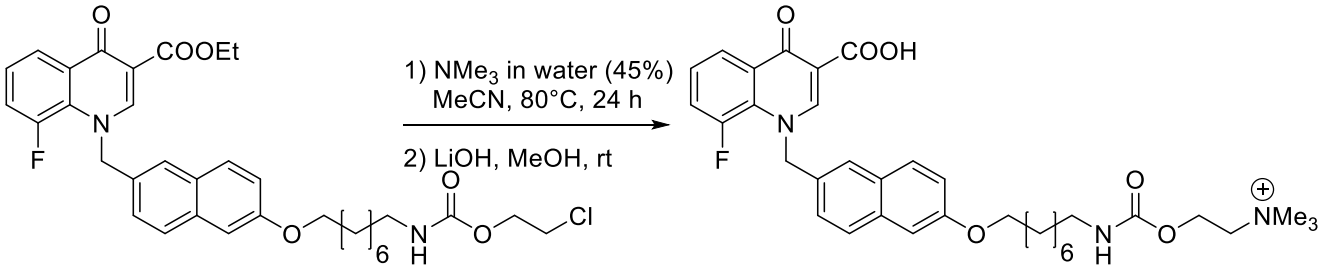

M = 620.74 g/mol

46 mg of the chloro-compound **26c** (0.074 mmol, 1 eq) were dissolved in 12 mL acetonitrile and 10 mL trimethylamine in water (45%) were added. The mixture was heated to 75 °C for 1 d in a sealed vessel. Volatiles were removed. The residue was dissolved in methanol and 10 mg lithium hydroxide (0.44 mmol, 6 eq) in water were added. The mixture was stirred at room temperature until LCMS showed disappearance of the ester. 2M HCl was added to neutralize the mixture. Volatiles were removed, and the residue was purified by preparative HPLC to give 10 mg (0.014 mmol, 19 %) of the formiate salt of the product as a colorless oil. **^{1}H-NMR (400 MHz, $CDCl_3$)** δ(ppm) = 1.33 – 1.41 (m, 6 H, 3xCH_2), 1.47 – 1.53 (m, 4 H, 2xCH_2), 1.77 – 1.85 (m, 2 H, CH_2), 3.10 (t, *J* = 7.0 Hz, 2 H, N-CH_2), 3.19 (s, 9 H, NMe_3), 3.63 – 3.68 (m, 2 H, *CH_2*-NMe_3), 4.05 (t, *J* = 6.3 Hz, 2 H, O-CH_2), 4.46 – 4.52 (m, 2 H, O-CH_2), 5.93 (br. s., 2 H, N-CH_2), 7.09 (dd, *J* = 9.0, 2.3 Hz, 1 H, Ar), 7.18 (d, *J* = 2.0 Hz, 1 H, Ar), 7.28 (d, *J* = 8.3 Hz, 1 H, Ar), 7.51 – 7.61 (m, 3 H, 3xAr), 7.66 (d, *J* = 9.0 Hz, 1 H, Ar), 7.75 (d, *J* = 8.3 Hz, 1 H, Ar), 8.34 (dd, *J* = 7.0, 2.3 Hz, 1 H, Ar), 8.38 (s, 1 H, $HCOO^-$), 9.06 (s, 1 H, CH). **^{13}C-NMR (100 MHz, $CDCl_3$)** δ(ppm) = 25.7 (CH_2), 26.4 (CH_2), 28.9 (2xCH_2), 29.0 (CH_2), 29.4 (CH_2), 40.5 (N-CH_2), 53.04/53.07/53.11 (NMe_3), 57.7 (O-CH_2), 61.15/61.30 (N-CH_2), 65.15/65.19/65.21 (*CH_2*-NMe_3), 67.6 (O-CH_2), 106.1 (Ar-H), 113.1 (*C*=CH), 119.3 (Ar-H), 121.00 (d, J = 23.5 Hz, Ar-H), 122.47 (d, J = 2.9 Hz, Ar-H), 124.2 (Ar-H), 124.9 (Ar-H), 126.82 (d, J = 8.8 Hz, Ar-H), 127.5 (Ar-H), 128.7 (Ar-C_q), 129.0 (Ar-H, Ar-C_q), 130.6 (Ar-C_q), 134.0 (Ar-C_q), 134.5 (Ar-C_q), 152.12 (d, J = 251.6 Hz, Ar-CF), 151.8 (CH), 156.0 (NH*C*OO), 157.7 (Ar-*C*O-), 166.7 ($HCOO^-$), 167.6 (COOH), 177.7 (CO). **ESI-MS:** 310.80 *m/z* $[M+H]^{2+}$, 620.30 *m/z* $[M]^+$

Synthesis of Compound **17**:

6-(3-Chloropropoxy)naphthalen-2-yl)methanol 20

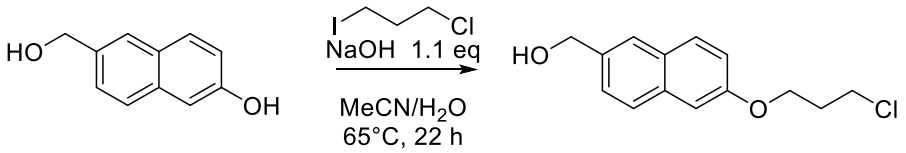

M = 250.72 g/mol

A solution of 750 mg 6-(hydroxymethyl)naphthalen-2-ol **19** (4.31 mmol, 1 eq), 0.51 mL 1-chloro-3-iodopropane (4.74 mmol, 1.1 eq), and 190 mg sodium hydroxide (4.74 mmol, 1.1 eq) in 30 mL acetonitrile/water (3:1) was stirred for 22 h at 65 °C. The reaction mixture was diluted with water (50 mL) and ethyl acetate (50 mL). The phases were separated, and the inorganic phase was extracted with ethyl acetate (2x50 mL). The combined organic phases were washed with brine, dried over sodium sulfate and the solvent was removed. The crude product was purified by column chromatography (petroleum ether: EtOAc 2:1 → 1:1), which gave 795 mg (3.17 mmol, 74 %) of the desired product as a white solid. **^{1}H-NMR (400 MHz, $CDCl_3$)** δ(ppm) = 2.27 – 2.34 (m, 2 H, CH_2), 3.80 (t, *J* = 6.4 Hz, 2 H, CH_2-Cl), 4.24 (t, *J* = 5.9 Hz, 2 H, CH_2-O-), 4.82 (s, 2 H, CH_2-OH), 7.12 – 7.17 (m, 2 H, Ar), 7.43 – 7.47 (m, 1 H, Ar), 7.70 – 7.76 (m, 3 H, Ar)

4-((6-(Hydroxymethyl)naphthalen-2-yl)oxy)butanenitrile 21

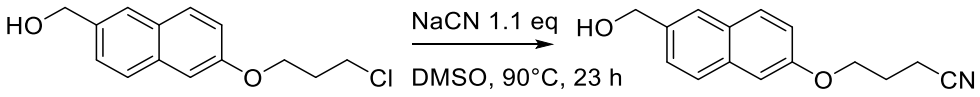

M = 241.29 g/mol

To a solution of 255 mg (6-(3-chloropropoxy)naphthalen-2-yl)methanol **20** (1.02 mmol, 1 eq) in 10 mL dimethyl sulfoxide, were added 55 mg sodium cyanide (1.122 mmol, 1.1 eq). The reaction mixture was stirred for 23 h at 90 °C. The mixture was diluted with water (25 mL) and extracted with diethyl ether (3x25 mL). The combined organic phases were washed with brine (2x25 mL), dried over sodium sulfate and the solvent was removed. The crude product was purified by column chromatography (petroleum ether 1:1 EtOAc), which gave 222 mg (0.92 mmol, 90 %) of the desired product as a white solid. **^{1}H-NMR (400 MHz, $CDCl_3$)** δ(ppm) = 2.16 – 2.24 (m, 2 H, CH_2), 2.63 (t, *J* = 7.2 Hz, 2 H, CH_2-CN), 4.19 (t, *J* = 5.6 Hz, 2 H, CH_2-O-),

4.82 (s, 2 H, CH_2-OH), 7.12 – 7.16 (m, 2 H, Ar), 7.46 (dd, *J* = 8.5, 1.8 Hz, 1 H, Ar), 7.71 – 7.76 (m, 3 H, Ar). **^{13}C-NMR (100 MHz, $CDCl_3$)** δ(ppm) = 14.3 (*CH_2*-CN), 25.5 (CH_2), 65.3 (CH_2-OH), 65.5 (CH_2-O-), 106.8 (Ar-H), 118.9 (Ar-H), 119.2 (CN), 125.5 (2x Ar-H), 126.0 (Ar-H), 127.2 (Ar-H), 129.6 (Ar-C_q), 134.0 (Ar-C_q), 136.4 (Ar-C_q), 156.4 (Ar-O-). **ESI-MS:** 264 *m/z* $[M+Na]^+$

4-((6-(Iodomethyl)naphthalen-2-yl)oxy)butanenitrile 16

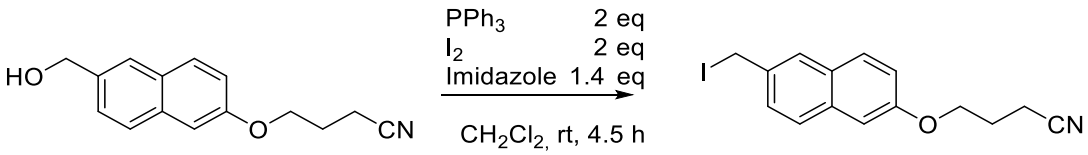

M = 351.19 g/mol

A mixture of 139 mg imidazole (2.04 mmol, 1.4 eq), 766 mg triphenylphosphine (2.92 mmol, 2 eq) and 741 mg iodine (2.92 mmol, 2 eq) in 30 mL dichloromethane was stirred at room temperature for 1 h. A solution of 352 mg of the alcohol **20** (1.46 mmol, 1 eq) in 10 mL dichloromethane was added slowly and the reaction mixture was stirred at room temperature for 4.5 h. The reaction mixture was poured into water (20 mL) and the phases were separated. The organic phase was washed with 10% aqueous HCl-solution (30 mL). The inorganic phases were extracted with dichloromethane (2x20 mL). The combined organic phases were dried over sodium sulfate and the solvent was removed. Column chromatography (petroleum ether: EtOAc 2:1 → 1:1, elute with CH_2Cl_2) gave 405 mg (1.15 mmol, 79 %) of the desired product as an orange solid. **^{1}H-NMR (400 MHz, $CDCl_3$)** δ(ppm) = 2.17 – 2.25 (m, 2 H, *CH_2*-CN), 2.64 (t, *J* = 7.2 Hz, 2 H, CH_2), 4.20 (t, *J* = 5.8 Hz, 2 H, *CH_2*-O), 4.63 (s, 2 H, CH_2-I), 7.09 – 7.15 (m, 2 H, Ar), 7.45 (dd, *J* = 8.5, 2.0 Hz, 1 H, Ar), 7.65 – 7.72 (m, 2 H, Ar), 7.76 (d, *J* = 1.5 Hz, 1 H, Ar). **^{13}C-NMR (100 MHz, $CDCl_3$)** δ(ppm) = 6.9 (CH_2-I), 14.3 (CH_2-CH_2-*CH_2*-CN), 25.5 (CH_2-*CH_2*-CH_2-CN), 65.4 (*CH_2*-CH_2-CH_2-CN), 106.9 (Ar-H), 119.1 (CN), 119.2 (Ar-H), 127.0 (Ar-H), 127.6 (2xAr-H), 129.5 (Ar-H), 133.9 (Ar-C_q), 134.6 (Ar-C_q), 135.3 (Ar-C_q), 156.8 (Ar-O-)

Ethyl 1-((6-(3-cyanopropoxy)naphthalen-2-yl) methyl)-8-fluoro-4-oxo-1,4-dihydro-quinoline-3-carboxylate 17

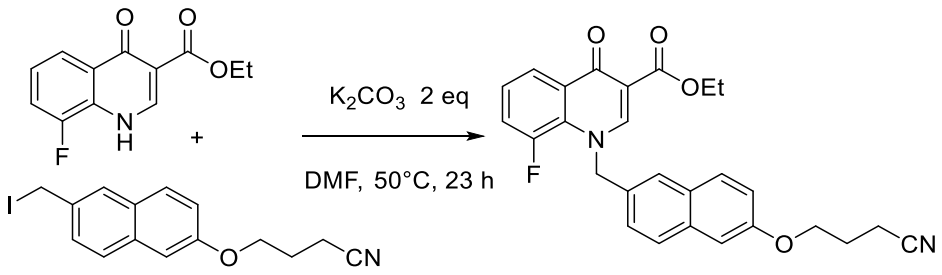

M = 458.49 g/mol

28 mg of the quinolone **15** (0.12 mmol, 1 eq), 50 mg of the iodo-compound **16** (0.14 mmol, 1.2 eq) were dissolved in 5 mL dimethylformamide and 32 mg potassium carbonate (0.23 mmol, 2 eq) and a catalytic amount of potassium iodide were added. The reaction mixture was heated at 50 °C for 23 h. The reaction mixture was diluted with water (20 mL) and ethyl acetate (20 mL) and the phases were separated. The inorganic phase was extracted with ethyl acetate (2x20 mL). The combined organic phases were dried over sodium sulfate and the solvent was removed. Column chromatography (petroleum ether : EtOAc 1:2 → 1:5) gave 39 mg (0.085 mmol, 71 %) of the desired product as a white solid. **^{1}H-NMR (400 MHz, $CDCl_3$)** δ(ppm) = 1.41 (t, *J* = 7.0 Hz, 3 H, CH_2-*CH_3*), 2.14 – 2.24 (m, 2 H, *CH_2*-CN), 2.62 (t, *J* = 7.2 Hz, 2 H, CH_2), 4.18 (t, *J* = 5.6 Hz, 2 H, *CH_2*-O), 4.41 (q, *J* = 7.3 Hz, 2 H, *CH_2*-CH_3), 5.66 (d, *J* = 2.0 Hz, 2 H, *CH_2*-N), 7.09 – 7.15 (m, 2 H, Ar), 7.22 – 7.35 (m, 3 H, Ar), 7.45 (s, 1 H, Ar), 7.63 – 7.73 (m, 2 H, Ar), 8.34 – 8.38 (m, 1 H, Ar), 8.59 (s, 1 H, Allyl-H). **ESI-MS:** 458 *m/z* $[M]^+$; 481 *m/z* $[M+Na]^+$

7.4. Synthesis of Reference Compounds **27** and **31**

Synthesis of Reference Compounds **27**:

General Procedure: 1 eq of the amine **3** and 1 eq of the alkyl halide were dissolved in dimethylformamide and 2 eq of potassium carbonate and a catalytic amount of potassium iodide were added. The reaction mixture was heated to 60 °C over night. The mixture was diluted with ethyl acetate and water. The phases were separated, and the inorganic phase was extracted with ethyl acetate. The combined organic phases were washed with water several times, dried over sodium sulfate and the solvent was removed. Column chromatography yielded the desired product.

1-(1-Propylpiperidin-4-yl)-1,3-dihydro-2*H*-benzo[*d*]imidazol-2-one 27a

0.69 mmol of the amine **3**, 0.69 mmol of 1-bromopropane, 1.38 mmol potassium carbonate and 10 ml dimethylformamide were used. Column chromatography (CH_2Cl_2 10:1 MeOH on deactivated silica) gave 130 mg (0.5 mmol, 73%) of the desired product as a colorless oil. **^{1}H-NMR (400 MHz, $CDCl_3$)** δ(ppm) = 0.92 (t, *J* = 7.3 Hz, 3 H, CH_3), 1.50 – 1.62 (m, 2 H, CH_2), 1.77 – 1.87 (m, 2 H, *CH_2*-CH), 2.10 – 2.19 (m, 2 H, *CH_2*-CH), 2.34 – 2.41 (m, 2 H, CH_2-N), 2.51 (qd, *J* = 12.5, 3.9 Hz, 2 H, CH_2-N), 3.12 (d, *J* = 11.8 Hz, 2 H, CH_2-N), 4.39 (tt, *J* = 12.5, 4.3 Hz, 1 H, CH), 6.99 (quind, *J* = 7.5, 1.5 Hz, 2 H, Ar), 7.09 – 7.14 (m, 1 H, Ar), 7.24 – 7.29 (m, 1 H, Ar), 10.98 (br. s., 1 H, NH). **^{13}C-NMR (100 MHz, $CDCl_3$)** δ(ppm) = 12.0 (CH_3), 20.2 (CH_2), 29.2 (2x CH-*CH_2*), 50.8 (CH), 53.3 (2xN-CH_2), 60.5 (N-CH_2), 109.8 (2xAr-H), 120.9 (Ar-H), 121.1 (Ar-H), 128.4 (Ar-C_q), 129.1 (Ar-C_q), 155.5 (CO). **ESI-MS:** 260.15 *m/z* $[M+H]^+$

1-(1-Pentylpiperidin-4-yl)-1,3-dihydro-2*H*-benzo[*d*]imidazol-2-one 27b

0.73 mmol of the amine **3**, 0.73 mmol of 1-bromopentane, 1.46 mmol potassium carbonate and 10 ml dimethylformamide were used. Column chromatography (CH_2Cl_2 15:1 MeOH on deactivated silica) gave 100 mg (0.35 mmol, 48%) of the desired product as a white solid. **^{1}H-NMR (400 MHz, $CDCl_3$)** δ(ppm) = 0.92 (t, *J* = 7.3 Hz, 3 H, CH_3), 1.27 – 1.40 (m, 4 H, 2xCH_2), 1.56

(dt, *J* = 15.1, 7.5 Hz, 2 H, CH_2), 1.80 – 1.89 (m, 2 H, *CH_2*-CH), 2.11 – 2.22 (m, 2 H, *CH_2*-CH), 2.38 – 2.46 (m, 2 H, CH_2-N), 2.53 (qd, *J* = 12.5, 3.8 Hz, 2 H, CH_2-N), 3.15 (br. d, *J* = 11.8 Hz, 2 H, CH_2-N), 4.42 (tt, *J* = 12.5, 4.2 Hz, 1 H, CH), 7.02 (quind, *J* = 7.3, 1.4 Hz, 2 H, 2xAr-H), 7.11 – 7.16 (m, 1 H, Ar-H), 7.26 – 7.31 (m, 1 H, Ar-H), 11.01 (br. s., 1 H, NH). **^{13}C-NMR (100 MHz, $CDCl_3$)** δ(ppm) = 14.7 (CH_3), 22.6 (CH_2), 26.8 (2x CH-*CH_2*), 29.2 (CH_2), 29.9 (CH_2), 50.8 (CH), 53.3 (2xN-CH_2), 58.7 (N-CH_2), 109.8 (2xAr-H), 120.9 (Ar-H), 121.1 (Ar-H), 128.4 (Ar-C_q), 129.1 (Ar-C_q), 155.5 (CO). **ESI-MS:** 288.15 *m/z* $[M+H]^+$

1-(1-Octylpiperidin-4-yl)-1,3-dihydro-2*H*-benzo[*d*]imidazol-2-one 27c

0.83 mmol of the amine **3**, 0.83 mmol of 1-bromooctane, 1.66 mmol potassium carbonate and 10 ml dimethylformamide were used. Column chromatography (CH_2Cl_2 15:1 MeOH on deactivated silica) gave 134 mg (0.41 mmol, 50%) of the desired product as a white solid. **^{1}H-NMR (400 MHz, $CDCl_3$)** δ(ppm) = 0.87 (t, *J* = 7.0 Hz, 3 H, CH_3), 1.20 – 1.36 (m, 10 H, 5xCH_2), 1.48 – 1.59 (m, 2 H. CH_2), 1.82 (dd, *J* = 11.9, 2.1 Hz, 2 H, *CH_2*-CH), 2.14 (t, *J* = 11.3 Hz, 2 H, *CH_2*-CH), 2.35 – 2.44 (m, 2 H, CH_2-N), 2.51 (qd, *J* = 12.4, 3.4 Hz, 2 H, CH_2-N), 3.12 (br. d, *J* = 11.5 Hz, 2 H, CH_2-N), 4.40 (tt, *J* = 12.5, 4.2 Hz, 1 H, CH), 6.99 (quind, *J* = 7.3, 1.4 Hz, 2 H, 2xAr-H), 7.09 – 7.14 (m, 1 H, Ar-H), 7.24 – 7.29 (m, 1 H, Ar-H), 11.01 (br. s., 1 H, NH). **^{13}C-NMR (100 MHz, $CDCl_3$)** δ(ppm) = 14.1 (CH_3), 22.7 (CH_2), 27.1 (CH-*CH_2*), 27.7 (CH-*CH_2*), 29.2 (2xCH_2), 29.9 (2xCH_2), 31.6 (CH_2), 50.8 (CH), 53.3 (2xN-CH_2), 58.7 (N-CH_2), 109.8 (2xAr-H), 120.8 (Ar-H), 121.1 (Ar-H), 128.4 (Ar-C_q), 129.1 (Ar-C_q), 155.5 (CO). **ESI-MS:** 330.30 *m/z* $[M+H]^+$

Synthesis of Reference Compounds **31**:

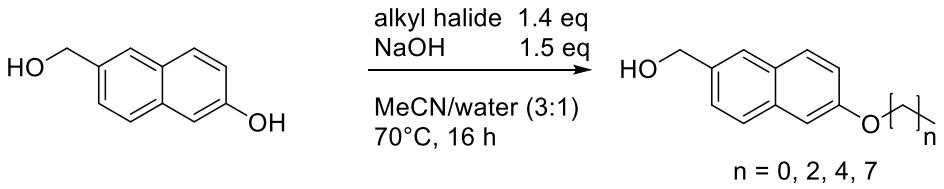

General Procedure: 1 eq of the alcohol **19**, 1.3-1.5 eq of the alkyl halide and 1.5 eq sodium hydroxide were dissolved in a mixture of acetonitrile and water (3:1). The mixture was heated to 70 °C over night. The mixture was diluted with water and extracted with ethyl acetate. The organic phases were washed with brine, dried over sodium sulfate and the solvent was removed. Column chromatography yielded the desired product.

(6-Propoxynaphthalen-2-yl)methanol 28a

2.9 mmol of the alcohol, 4.35 mmol of 1-bromopropane, 4.35 mmol sodium hydroxide and 20 mL of acetonitrile/water (3:1) were used. Column chromatography (petroleum ether 2:1 EtOAc) gave 550 mg (2.5 mmol, 87%) of the desired product as a white solid. **^{1}H-NMR (400 MHz, $CDCl_3$)** δ(ppm) = 1.10 (t, *J* = 7.4 Hz, 3 H, CH_3), 1.83 – 1.94 (m, 2 H, CH_2), 4.04 (t, *J* = 6.7 Hz, 2 H, CH_2), 4.78 (s, 2 H, CH_2-OH), 7.11 – 7.19 (m, 2 H, 2xAr), 7.42 (dd, *J* = 8.4, 1.9 Hz, 1 H, Ar), 7.67 – 7.72 (m, 3 H, 3xAr). **^{13}C-NMR (100 MHz, $CDCl_3$)** δ(ppm) = 10.6 (CH_3), 22.6 (CH_2), 65.5 (CH_2-OH), 69.6 (CH_2), 106.6 (Ar-H), 119.3 (Ar-H), 125.6 (Ar-H), 125.8 (Ar-H), 127.2 (Ar-H), 128.7 (Ar-C_q), 129.3 (Ar-H), 134.2 (Ar-C_q), 136.0 (Ar-C_q), 157.3 (Ar-*C*O-)

(6-(Pentyloxy)naphthalen-2-yl)methanol 28b

2.9 mmol of the alcohol, 4.35 mmol of 1-bromopropane, 4.35 mmol sodium hydroxide and 20 mL of acetonitrile/water (3:1) were used. Column chromatography (petroleum ether 2:1 EtOAc) gave 550 mg (2.25 mmol, 78%) of the desired product as a white solid. **^{1}H-NMR (400 MHz, $CDCl_3$)** δ(ppm) = 0.99 (t, *J* = 7.0 Hz, 3 H, CH_3), 1.38 – 1.56 (m, 4 H, 2xCH_2), 1.82 – 1.92 (m, 2 H, CH_2), 4.06 (t, *J* = 6.7 Hz, 2 H, CH_2), 4.75 (s, 2 H, CH_2-OH), 7.10 – 7.19 (m, 2 H, 2xAr), 7.41 (dd, *J* = 8.5, 1.8 Hz, 1 H, Ar), 7.64 – 7.72 (m, 3 H, 3xAr). **^{13}C-NMR (100 MHz, $CDCl_3$)** δ(ppm) = 14.1 (CH_3), 22.6 (CH_2), 28.3 (CH_2), 29.0 (CH_2), 65.4 (CH_2-OH), 68.1 (CH_2), 106.6 (Ar-H), 119.3 (Ar-H), 125.6 (Ar-H), 125.9 (Ar-H), 127.1 (Ar-H), 128.7 (Ar-C_q), 129.3 (Ar-H), 134.2 (Ar-C_q), 136.0 (Ar-C_q), 157.3 (Ar-*C*O-)

(6-(Octyloxy)naphthalen-2-yl)methanol 28c

2.9 mmol of the alcohol, 4.35 mmol of 1-bromopropane, 4.35 mmol sodium hydroxide and 20 mL of acetonitrile/water (3:1) were used. Column chromatography (petroleum ether 2:1 EtOAc) gave 550 mg (2.25 mmol, 78%) of the desired product as a white solid. **^{1}H-NMR (400 MHz, $CDCl_3$)** δ(ppm) = 0.93 (t, *J* = 7.0 Hz, 3 H, CH_3), 1.27 – 1.45 (m, 8 H, 4xCH_2), 1.47 – 1.57 (m, 2 H, CH_2), 1.81 – 1.91 (m, 2 H, CH_2), 4.06 (t, *J* = 6.7 Hz, 2 H, CH_2), 4.75 (s, 2 H, CH_2-OH), 7.10 – 7.19 (m, 2 H, 2xAr), 7.41 (dd, *J* = 8.4, 1.6 Hz, 1 H, Ar), 7.65 – 7.72 (m, 3 H, 3xAr). **^{13}C-NMR (100 MHz, $CDCl_3$)** δ(ppm) = 14.2 (CH_3), 22.7 (CH_2), 26.2 (CH_2), 29.3 (2xCH_2), 29.5 (CH_2), 31.9 (CH_2), 65.4 (CH_2-OH), 68.1 (CH_2), 106.6 (Ar-H), 119.3 (Ar-H), 125.6 (Ar-H), 125.8 (Ar-H), 127.1 (Ar-H), 128.7 (Ar-C_q), 129.3 (Ar-H), 134.2 (Ar-C_q), 136.0 (Ar-C_q), 157.3 (Ar-*C*O-)

(6-Methoxynaphthalen-2-yl)methanol 28d

2.9 mmol of the alcohol, 3.77 mmol of methyl iodide, 4.35 mmol sodium hydroxide and 20 mL of acetonitrile/water (3:1) were used. Column chromatography (petroleum ether 2:1 EtOAc) gave 309 mg (1.64 mmol, 57%) of the desired product as a white solid. **^{1}H-NMR (400 MHz, MeOD)** δ(ppm) = 3.86 (s, 3 H, CH_3), 4.70 (s, 2 H, CH_2-OH), 7.10 (dd, *J* = 8.9, 2.6 Hz, 1 H, Ar), 7.18 (d, *J* = 2.5 Hz, 1 H, Ar), 7.42 (dd, *J* = 8.3, 1.8 Hz, 1 H, Ar), 7.67 – 7.73 (m, 3 H, 3xAr). **^{13}C-NMR (100 MHz, MeOD)** δ(ppm) = 54.3 (CH_3), 64.0 (CH_2-OH), 105.4 (Ar-H), 118.4 (Ar-H), 125.0 (Ar-H), 125.6 (Ar-H), 126.7 (Ar-H), 128.9 (Ar-H, Ar-C_q), 134.2 (Ar-C_q), 136.4 (Ar-C_q), 157.7 (Ar-*C*O-)

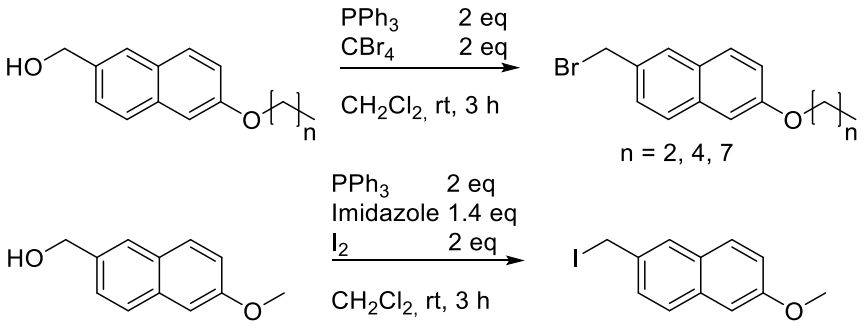

General Procedure: 2 eq of triphenylphosphine and 2 eq of tetrabromomethane were dissolved in dichloromethane. The mixture was cooled to 0 °C and a solution of 1 eq of the alcohol in dichloromethane was added. The mixture was stirred for 3 h at room temperature. Water was added and the mixture extracted with dichloromethane. The organic phases were dried over sodium sulfate and the solvent was removed. Column chromatography yielded the desired product.

2-(Bromomethyl)-6-propoxynaphthalene 29a

1.06 mmol of the alcohol **28a**, 2.12 mmol of triphenylphosphine, 2.12 mmol of tetrabromomethane and 20 mL of dichloromethane were used. Column chromatography (petroleum ether 20:1 EtOAc) gave 300 mg (1.07 mmol, quant.) of the desired product as a light yellow oil. **^{1}H-NMR (400 MHz, $CDCl_3$)** δ(ppm) = 1.11 (t, *J* = 7.4 Hz, 3 H, CH_3), 1.84 – 1.95 (m, 2 H, CH_2), 4.05 (t, *J* = 6.7 Hz, 2 H, CH_2), 4.67 (s, 2 H, CH_2-Br), 7.13 (d, *J* = 2.5 Hz, 1 H, Ar), 7.19 (dd, *J* = 8.8, 2.5 Hz, 1 H, Ar), 7.47 (dd, *J* = 8.4, 1.9 Hz, 1 H, Ar), 7.69 – 7.76 (m, 3 H, 3xAr)**. ^{13}C-NMR (100 MHz, $CDCl_3$)** δ(ppm) = 10.7 (CH_3), 22.6 (CH_2), 34.6 (CH_2-Br), 69.6 (CH_2), 106.6 (Ar-H), 119.6 (Ar-H), 127.3 (Ar-H), 127.6 (Ar-H), 127.8 (Ar- H), 128.6 (Ar-C_q), 129.4 (Ar-H), 132.7 (Ar-C_q), 134.5 (Ar-C_q), 157.8 (Ar-*C*O-)

2-(Bromomethyl)-6-(pentyloxy)naphthalene 29b

0.82 mmol of the alcohol **28b**, 1.64 mmol of triphenylphosphine, 1.64 mmol of tetrabromomethane and 20 mL of dichloromethane were used. Column chromatography (petroleum ether 15:1 EtOAc) gave 385 mg (0.93 mmol, quant.) of the desired product as a light brown oil. **^{1}H-NMR (400 MHz, $CDCl_3$)** δ(ppm) = 0.98 (t, *J* = 7.3 Hz, 3 H, CH_3), 1.39 - 1.55 (m, 4 H, 2xCH_2), 1.83 – 1.91 (m, 2 H, CH_2), 4.08 (t, *J* = 6.7 Hz, 2 H, CH_2), 4.74 (s, 2 H, CH_2-Br), 7.13 (d, *J* = 2.5 Hz, 1 H, Ar), 7.18 (dd, *J* = 8.8, 2.5 Hz, 1 H, Ar), 7.47 (dd, *J* = 8.5, 1.8 Hz, 1 H, Ar), 7.70 – 7.76 (m, 3 H, 3xAr)**. ^{13}C-NMR (100 MHz, $CDCl_3$)** δ(ppm) = 14.1 (CH_3), 22.5 (CH_2), 28.3

(CH_2), 29.0 (CH_2), 46.9 (CH_2-Br), 68.1 (CH_2), 106.6 (Ar-H), 119.6 (Ar-H), 126.8 (Ar-H), 127.5 (Ar-H), 128.5 (Ar- H), 128.6 (Ar-C_q), 129.4 (Ar-H), 132.4 (Ar-C_q), 134.5 (Ar-C_q), 157.8 (Ar-*C*O-)

2-(Bromomethyl)-6-(octyloxy)naphthalene 29c

1.0 mmol of the alcohol **28c**, 2.0 mmol of triphenylphosphine, 2.0 mmol of tetrabromomethane and 20 mL of dichloromethane were used. Column chromatography (petroleum ether 20:1 EtOAc) gave 286 mg (0.77 mmol, 77%) of the desired product as a light yellow oil. **^{1}H-NMR (400 MHz, $CDCl_3$)** δ(ppm) = 0.95 (t, *J* = 6.8 Hz, 3 H, CH_3), 1.28 – 1.45 (m, 8 H, 4xCH_2), 1.49 – 1.58 (m, 2 H, CH_2), 1.83 – 1.92 (m, 2 H, CH_2), 4.08 (t, *J* = 6.7 Hz, 2 H, CH_2), 4.66 (s, 2 H, CH_2-Br), 7.13 (d, *J* = 2.5 Hz, 1 H, Ar), 7.19 (dd, *J* = 9.0, 2.5 Hz, 1 H, Ar), 7.47 (dd, *J* = 8.4, 1.9 Hz, 1 H, Ar), 7.69 – 7.76 (m, 3 H, 3xAr)**. ^{13}C-NMR (100 MHz, $CDCl_3$)** δ(ppm) = 14.2 (CH_3), 22.7 (CH_2), 26.2 (CH_2), 29.3 (CH_2), 29.4 (CH_2), 29.5 (CH_2), 31.9 (CH_2), 46.8 (CH_2-Br), 68.0 (CH_2), 106.6 (Ar-H), 119.4 (Ar-H), 125.6 (Ar-H), 125.8 (Ar-H), 127.2 (Ar-H), 128.7 (Ar-C_q), 129.3 (Ar-H), 134.2 (Ar-C_q), 136.1 (Ar-C_q), 157.3 (Ar-*C*O-)

2-(Iodomethyl)-6-methoxynaphthalene 29d

860 mg Triphenylphosphine (3.28 mmol, 2 eq) and 157 mg imidazole (2.30 mmol, 1.4 eq) were dissolved in 30 mL dichloromethane and 833 mg iodine (3.28 mmol, 2 eq) were added slowly. The mixture was stirred for 1 h at room temperature and 309 mg of the alcohol **28d** (1.64 mmol, 1 eq) were added as a solution in 10 mL dichloromethane. The mixture was stirred at room temperature for 3 h and quenched with water. The phases were separated, and the organic phase was washed with HCl (10% *w/w*). The inorganic phases were extracted with dichloromethane. The organic phases were dried over sodium sulfate and the solvent was removed. Column chromatography (petroleum ether 15:1 EtOAc) gave 486 mg (1.63 mmol, 99 %) of the desired product as a brown solid. The product was used in the next reaction immediately. **^{1}H-NMR (400 MHz, $CDCl_3$)** δ(ppm) = 3.86 (s, 3 H, CH_3), 4.33 (s, 2 H, CH_2-I), 7.12 (d, *J* = 2.5 Hz, 1 H, Ar), 7.19 (dd, *J* = 8.8, 2.5 Hz, 1 H, Ar), 7.45 (dd, *J* = 8.4, 1.9 Hz, 1 H, Ar), 7.65 – 7.71 (m, 3 H, 3xAr). **^{13}C-NMR (100 MHz, $CDCl_3$)** δ(ppm) = 6.2 (CH_2-I), 54.3 (CH_3), 106.0 (Ar-H), 118.9 (Ar-H), 125.2 (Ar-H), 125.3 (Ar-H), 126.8 (Ar-H), 128.8 (Ar-H), 128.9 (Ar-C_q), 134.4 (Ar-C_q), 136.4 (Ar-C_q), 157.9 (Ar-*C*O-)

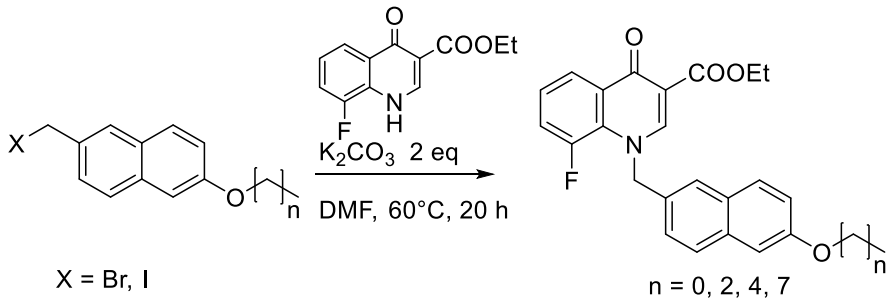

General Procedure: 1 eq of the alkyl halide **29** and 1 eq of the quinolone **15** were dissolved in dimethylformamide. 2 eq of potassium carbonate were added. The mixture was heated to 60 °C overnight. Water and ethyl acetate were added. The phases were separated, and the inorganic phase was extracted with ethyl acetate. The combined organic phases were washed with water several times, dried over sodium sulfate and the solvent was removed.

Ethyl 8-fluoro-4-oxo-1-((6-propoxynaphthalen-2-yl)methyl)-1,4-dihydroquinoline-3-carboxylate 30a

1.06 mmol of the bromo-compound **29a**, 1.06 mmol of the quinolone **15**, 2.12 mmol of potassium carbonate and 15 mL of dimethylformamide were used. Removal of the solvent after workup gave 286 mg (0.66 mmol, 62%) of the desired product as an orange solid. **^{1}H-NMR (400 MHz, $CDCl_3$)** δ(ppm) = 1.04 (t, *J* = 7.4 Hz, 3 H, CH_3), 1.39 (t, *J* = 7.2 Hz, 3 H, CH_3), 1.84 (sxt, *J* = 7.1 Hz, 2 H, CH_2), 3.99 (t, *J* = 6.7 Hz, 2 H, CH_2), 4.39 (q, *J* = 7.3 Hz, 2 H, CH_2), 5.63 (d, *J* = 2.3 Hz, 2 H, CH_2), 7.07 (d, *J* = 2.5 Hz, 1 H, Ar), 7.12 (dd, *J* = 9.0, 2.5 Hz, 1 H, Ar), 7.17 – 7.32 (m, 3 H, 3xAr), 7.42 (s, 1 H, Ar), 7.61 (d, *J* = 9.0 Hz, 1 H, Ar), 7.67 (d, *J* = 8.5 Hz, 1 H, Ar), 8.31 – 8.35 (m, 1 H, Ar), 8.57 (s, 1 H, CH). **^{13}C-NMR (100 MHz, $CDCl_3$)** δ(ppm) = 10.6 (CH_3), 14.4 (CH_3), 22.5 (CH_2), 60.9 (CH_2), 61.1 (CH_2), 69.6 (CH_2), 106.5 (Ar-H), 111.3 (*C*=CH), 119.84 (d, *J* = 22.7 Hz, Ar-H), 119.87 (Ar-H), 123.81 (d, *J* = 3.7 Hz, Ar-H), 124.3 (Ar-H), 125.0 (Ar-H), 125.51 (d, *J* = 8.1 Hz, Ar-H), 127.8 (Ar-H), 128.5 (Ar-C_q), 128.7 (Ar-C_q), 129.3 (Ar-H), 130.4 (Ar-C_q), 131.9 (Ar-C_q), 134.3 (Ar-C_q), 151.6 (CH), 151.79 (d, *J* = 250.9 Hz, Ar-CF), 157.7 (Ar-*C*O-), 165.4 (*C*OOEt), 173.3 (CO). **ESI-MS:** 434.25 *m/z* $[M+H]^+$

Ethyl 8-fluoro-4-oxo-1-((6-(pentyloxy)naphthalen-2-yl)methyl)-1,4-dihydroquinoline-3-carboxylate 30b

0.82 mmol of the bromo-compound **29b**, 0.82 mmol of the quinolone **15**, 1.64 mmol of potassium carbonate and 15 mL of dimethylformamide were used. Removal of the solvent after workup gave 265 mg (0.57 mmol, 70%) of the desired product as an orange solid. **^{1}H-NMR (400 MHz, $CDCl_3$)** δ(ppm) = 0.93 (t, *J* = 7.5 Hz, 3 H, CH_3), 1.33 – 1.51 (m, 4 H, CH_2), 1.40 (t, *J* = 7.2 Hz, 3 H, CH_3), 1.82 (quin, *J* = 7.5 Hz, 2 H, CH_2), 4.03 (t, *J* = 6.5 Hz, 2 H, CH_2), 4.40 (q, *J* = 7.1 Hz, 2 H, CH_2), 5.62 (s, 2 H, CH_2), 7.08 (d, *J* = 2.3 Hz, 1 H, Ar), 7.13 (dd, *J* = 8.9, 2.4 Hz, 1 H, Ar), 7.17 – 7.32 (m, 3 H, 3xAr), 7.42 (s, 1 H, Ar), 7.61 (d, *J* = 9.0 Hz, 1 H, Ar), 7.67 (d, *J* = 8.3 Hz, 1 H, Ar), 8.32 – 8.36 (m, 1 H, Ar), 8.57 (s, 1 H, CH). **^{13}C-NMR (100 MHz, $CDCl_3$)** δ(ppm) = 14.0 (CH_3), 14.4 (CH_3), 22.5 (CH_2), 28.3 (CH_2), 28.9 (CH_2), 60.9 (CH_2), 61.1 (CH_2), 68.1 (CH_2), 106.5 (Ar-H), 111.3 (*C*=CH), 119.82 (d, *J* = 22.7 Hz, Ar-H), 119.88 (Ar-H), 123.82 (d, *J* = 3.7 Hz, Ar-H), 124.3 (Ar-H), 124.99 (d, *J* = 1.5 Hz, Ar-H), 125.49 (d, *J* = 8.1 Hz, Ar-H), 127.8 (Ar-H), 128.5 (Ar-C_q), 128.7 (Ar-C_q), 129.3 (Ar-H), 130.39 (d, *J* = 1.5 Hz, Ar-C_q), 131.9 (Ar-C_q), 134.4 (Ar-C_q), 151.6 (CH), 151.79 (d, *J* = 250.9 Hz, Ar-CF), 157.7 (Ar-*C*O-), 165.4 (*C*OOEt), 173.3 (CO). **ESI-MS:** 462.25 *m/z* $[M+H]^+$

Ethyl 8-fluoro-1-((6-(octyloxy)naphthalen-2-yl)methyl)-4-oxo-1,4-dihydroquinoline-3-carboxylate 30c

0.77 mmol of the bromo-compound **29c**, 0.77 mmol of the quinolone **15**, 1.54 mmol of potassium carbonate and 15 mL of dimethylformamide were used. Removal of the solvent after workup gave 284 mg (0.56 mmol, 72%) of the desired product as an orange solid. **^{1}H-NMR (400 MHz, $CDCl_3$)** δ(ppm) = 0.87 (t, *J* = 7.3 Hz, 3 H, CH_3), 1.23 – 1.37 (m, 8 H, 4xCH_2), 1.39 (t, *J* = 7.0 Hz, 3 H, CH_3), 1.43 – 1.51 (m, 2 H, CH_2), 1.81 (quin, *J* = 6.5 Hz, 2 H, CH_2), 4.02 (t, *J* = 6.7 Hz, 2 H, CH_2), 4.35 – 4.42 (m, 2 H, CH_2), 5.63 (d, *J* = 2.0 Hz, 2 H, CH_2), 7.07 (d, *J* = 2.5 Hz, 1 H, Ar), 7.12 (dd, *J* = 9.0, 2.5 Hz, 1 H, Ar), 7.17 – 7.32 (m, 3 H, 3xAr), 7.42 (s, 1 H, Ar), 7.61 (d, *J* = 9.0 Hz, 1 H, Ar), 7.67 (d, *J* = 8.5 Hz, 1 H, Ar), 8.31 – 8.36 (m, 1 H, Ar), 8.57 (s, 1 H, CH). **^{13}C-NMR (100 MHz, $CDCl_3$)** δ(ppm) = 14.1 (CH_3), 14.4 (CH_3), 22.7 (CH_2), 26.1 (CH_2), 29.2 (2xCH_2), 29.4 (CH_2), 31.8 (CH_2), 60.9 (CH_2), 61.1 (CH_2), 68.1 (CH_2), 106.5 (Ar-H), 111.3 (*C*=CH), 119.83 (d, *J* = 23.5 Hz, Ar-H), 119.88 (Ar-H), 123.81 (d, *J* = 3.7 Hz, Ar-H), 124.2 (Ar-H), 124.99 (d, *J* = 1.5 Hz, Ar-H), 125.49 (d, *J* = 8.1 Hz, Ar-H), 127.8 (Ar-H), 128.53 (d, *J* = 6.6 Hz, Ar-C_q), 128.53 (Ar-C_q),

129.3 (Ar-H), 130.4 (Ar-C_q), 131.9 (Ar-C_q), 134.4 (Ar-C_q), 151.6 (CH), 151.79 (d, *J* = 250.2 Hz, Ar-CF), 157.7 (Ar-*C*O-), 165.3 (*C*OOEt), 173.2 (CO). **ESI-MS:** 504.25 *m/z* $[M+H]^+$

Ethyl 8-fluoro-1-((6-methoxynaphthalen-2-yl)methyl)-4-oxo-1,4-dihydroquinoline-3-carboxylate 30d

1.6 mmol of the iodo-compound **29d**, 1.6 mmol of the quinolone **15**, 3.2 mmol of potassium carbonate and 20 mL of dimethylformamide were used. Column chromatography (petroleum ether 1:3 EtOAc) gave 260 mg (0.64 mmol, 40%) of the desired product as a white solid. **^{1}H-NMR (400 MHz, $CDCl_3$)** δ(ppm) = 1.41 (t, *J* = 7.2 Hz, 3 H, CH_3), 3.89 (s, 3 H, OCH_3), 4.41 (q, *J* = 7.1 Hz, 2 H, CH_2), 5.65 (d, *J* = 2.0 Hz, 2 H, CH_2), 7.09 (d, *J* = 2.3 Hz, 1 H, Ar), 7.13 (dd, *J* = 8.9, 2.4 Hz, 1 H, Ar), 7.19 – 7.35 (m, 3 H, 3xAr), 7.45 (s, 1 H, Ar), 7.63 (d, *J* = 8.8 Hz, 1 H, Ar), 7.71 (d, *J* = 8.5 Hz, 1 H, Ar), 8.36 (dd, *J* = 7.9, 1.4 Hz, 1 H, Ar), 8.58 (s, 1 H, CH). **^{13}C-NMR (100 MHz, $CDCl_3$)** δ(ppm) = 14.4 (CH_3), 53.4 (CH_2), 55.4 (CH_3), 61.1 (CH_2), 105.7 (Ar-H), 111.4 (*C*=CH), 119.6 (Ar-H), 119.82 (d, *J* = 22.7 Hz, Ar-H), 123.87 (d, *J* = 3.7 Hz, Ar-H), 124.3 (Ar-H), 125.0 (Ar-H), 125.50 (d, *J* = 8.1 Hz, Ar-H), 127.9 (Ar-H), 128.5 (Ar-C_q), 128.7 (Ar-C_q), 129.4 (Ar-H), 130.54 (d, *J* = 1.5 Hz, Ar-C_q), 131.9 (Ar-C_q), 134.3 (Ar-C_q), 151.6 (CH), 151.75 (d, *J* = 251.0 Hz, Ar-CF), 158.2 (Ar-*C*O-), 165.4 (*C*OOEt), 173.2 (CO). **ESI-MS:** 406.10 *m/z* $[M+H]^+$

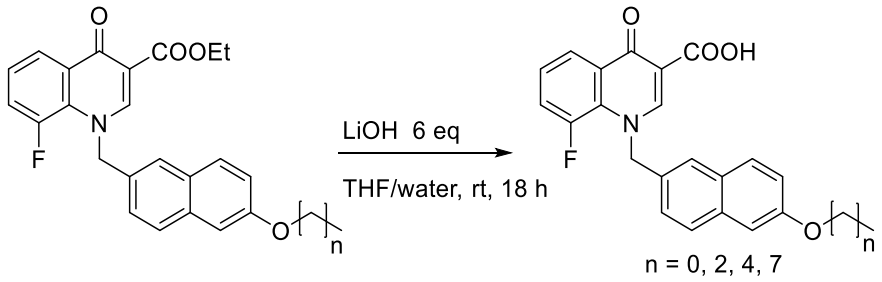

General Procedure: 1 eq of the ester **30** and 6 eq of LiOH were dissolved in a mixture of tetrahydrofuran and water. The clear solution was stirred at room temperature until LCMS showed full conversion. The mixture was acidified to pH=1-2 with 2M HCl and extracted with EtOAc. The combined organic phases were washed with water several times, dried over sodium sulfate and the solvent was removed to give the crude product.

8-Fluoro-4-oxo-1-((6-propoxynaphthalen-2-yl)methyl)-1,4-dihydroquinoline-3-carboxylic acid 31a

0.66 mmol of the ester **30a** and 4.0 mmol of LiOH were used. The dry crude product was taken up in MeOH and filtered. The solid was washed with petroleum ether and diethyl ether to give 142 mg (0.35 mmol, 53%) of the desired product as an off-white solid. **^{1}H-NMR (400 MHz, $CDCl_3$)** δ(ppm) = 1.06 (t, *J* = 7.4 Hz, 3 H, CH_3), 1.81 – 1.91 (m, 2 H), 4.01 (t, *J* = 6.5 Hz, 2 H, CH_2), 5.77 (d, *J* = 2.3 Hz, 2 H, CH_2), 7.09 (d, *J* = 2.5 Hz, 1 H, Ar), 7.15 (dd, *J* = 8.8, 2.5 Hz, 1 H, Ar), 7.20 (dd, *J* = 8.5, 1.5 Hz, 1 H, Ar), 7.40 – 7.50 (m, 3 H, 3xAr), 7.64 (d, *J* = 9.0 Hz, 1 H, Ar), 7.69 (d, *J* = 8.8 Hz, 1 H, Ar), 8.35 – 8.39 (m, 1 H, Ar), 8.89 (s, 1 H, CH), 14.61 (br. s., 1 H, COOH). **^{13}C-NMR (100 MHz, $CDCl_3$)** δ(ppm) = 10.6 (CH_3), 22.5 (CH_2), 62.0 (CH_2), 69.6 (CH_2), 106.5 (Ar-H), 109.1 (*C*=CH), 120.1 (Ar-H), 121.21 (d, *J* = 22.7 Hz, Ar-H), 123.29 (d, *J* = 3.7 Hz, Ar-H), 124.2 (Ar-H), 125.4 (Ar-H), 126.77 (d, *J* = 8.1 Hz, Ar-H), 128.0 (Ar-H), 128.5 (Ar-C_q), 129.3 (2xAr-C_q), 129.4 (Ar-H, Ar-C_q), 134.6 (Ar-C_q), 151.2 (CH), 152.40 (d, *J* = 251.8 Hz, Ar-CF), 157.9 (Ar-*C*O-), 166.4 (*C*OOH), 177.7 (CO). **ESI-MS:** 406.15 *m/z* $[M+H]^+$

8-Fluoro-4-oxo-1-((6-(pentyloxy)naphthalen-2-yl)methyl)-1,4-dihydroquinoline-3-carboxylic acid 31b

0.57 mmol of the ester **30b** and 1.3 mmol of LiOH were used. The dry crude product was taken up in MeOH and filtered. The solid was washed with petroleum ether and diethyl ether to give 113 mg (0.26 mmol, 46%) of the desired product as a light pink solid. **^{1}H-NMR (400 MHz, $CDCl_3$)** δ(ppm) = 0.94 (t, *J* = 7.0 Hz, 3 H, CH_3), 1.35 – 1.51 (m, 4 H, 2x CH_2), 1.80 – 1.88 (m, 2 H,

CH_2), 4.05 (t, *J* = 6.5 Hz, 2 H, CH_2), 5.78 (d, *J* = 2.3 Hz, 2 H, CH_2), 7.09 (d, *J* =2.5 Hz, 1 H, Ar), 7.15 (dd, *J* = 8.8, 2.5 Hz, 1 H, Ar), 7.21 (dd, *J* = 8.5, 1.3 Hz, 1 H, Ar), 7.41 – 7.51 (m, 3 H, 3xAr), 7.64 (d, *J* = 9.0 Hz, 1 H, Ar), 7.70 (d, *J* = 8.5 Hz, 1 H, Ar), 8.36 – 8.39 (m, 1 H, Ar), 8.89 (s, 1 H, CH), 14.60 (br. s., 1 H, COOH). **^{13}C-NMR (100 MHz, $CDCl_3$)** δ(ppm) = 14.0 (CH_3), 22.5 (CH_2), 28.2 (CH_2), 28.9 (CH_2), 62.0 (CH_2), 68.1 (CH_2), 106.5 (Ar-H), 109.2 (*C*=CH), 120.1 (Ar-H), 121.21 (d, *J* = 22.7 Hz, Ar-H), 123.32 (d, *J* = 3.7 Hz, Ar-H), 124.2 (Ar-H), 125.4 (Ar-H), 126.77 (d, *J* = 8.1 Hz, Ar-H), 128.1 (Ar-H), 128.5 (Ar-C_q), 129.3 (2xAr-C_q), 129.4 (Ar-H, Ar-C_q), 134.6 (Ar-C_q), 151.2 (CH), 151.77 (d, *J* = 252.4 Hz, Ar-CF), 157.9 (Ar-*C*O-), 166.4 (*C*OOH), 177.8 (CO). **ESI-MS:** 434.25 *m/z* $[M+H]^+$

8-Fluoro-1-((6-(octyloxy)naphthalen-2-yl)methyl)-4-oxo-1,4-dihydroquinoline-3-carboxylic acid 31c

0.56 mmol of the ester **30c** and 3.3 mmol of LiOH were used. The dry crude product was taken up in MeOH and filtered. The solid was washed with petroleum ether and diethyl ether to give 130 mg (0.27 mmol, 49%) of the desired product as a white solid. **^{1}H-NMR (400 MHz, $CDCl_3$)** δ(ppm) = 0.88 (t, *J* = 6.8 Hz, 3 H, CH_3), 1.23 – 1.41 (m, 8 H, 4xCH_2), 1.43 – 1.53 (m, 2 H, CH_2), 1.78 – 1.87 (m, 2 H, CH_2), 4.04 (t, *J* = 6.7 Hz, 2 H, CH_2), 5.78 (d, *J* = 2.3 Hz, 2 H, CH_2), 7.09 (d, *J* = 2.5 Hz, 1 H, Ar), 7.15 (dd, *J* = 8.8, 2.5 Hz, 1 H, Ar), 7.21 (dd, *J* = 8.5, 1.5 Hz, 1 H, Ar), 7.41 – 7.51 (m, 3 H, 3xAr), 7.64 (d, *J* = 8.8 Hz, 1 H, Ar), 7.70 (d, *J* = 8.8 Hz, 1 H, Ar), 8.35 – 8.40 (m, 1 H, Ar), 8.89 (s, 1 H, CH), 14.61 (s, 1 H, COOH). **^{13}C-NMR (100 MHz, $CDCl_3$)** δ(ppm) = 14.1 (CH_3), 22.7 (CH_2), 26.1 (CH_2), 29.2 (2xCH_2), 29.4 (CH_2), 31.8 (CH_2), 61.9 (CH_2), 68.2 (CH_2), 106.5 (Ar-H), 109.2 (*C*=CH), 120.1 (Ar-H), 121.21 (d, *J* = 23.5 Hz, Ar-H), 123.31 (d, *J* = 3.7 Hz, Ar-H), 124.1 (Ar-H), 125.4 (Ar-H), 126.77 (d, *J* = 8.8 Hz, Ar-H), 128.1 (Ar-H), 128.5 (Ar-C_q), 129.3 (2xAr-C_q), 129.4 (Ar-H, Ar-C_q), 134.6 (Ar-C_q), 151.2 (CH), 151.56 (d, *J* = 250.8 Hz, Ar-CF), 157.9 (Ar-*C*O-), 166.4 (*C*OOH), 177.7 (CO). **ESI-MS:** 476.35 *m/z* $[M+H]^+$

8-Fluoro-1-((6-methoxynaphthalen-2-yl)methyl)-4-oxo-1,4-dihydroquinoline-3-carboxylic acid 31d

0.64 mmol of the ester **30d** and 1.41 mmol of LiOH were used. The dry crude product was taken up in EtOAc and filtered. The solid was washed with water and petroleum ether to give 161 mg (0.43 mmol, 67%) of the desired product as an off-white solid. **^{1}H-NMR (400 MHz, DMSO-d_6)** δ(ppm) = 3.84 (s, 3 H, CH_3), 6.01 (d, *J* = 3.3 Hz, 2 H, CH_2), 7.12 (dd, *J* = 9.0, 2.5 Hz, 1 H, Ar), 7.29 (d, *J* = 2.5 Hz, 1 H, Ar), 7.32 (dd, *J* = 8.7, 1.6 Hz, 1 H, Ar), 7.54 (s, 1 H, Ar), 7.61 (td, *J*

= 8.0, 4.3 Hz, 1 H, Ar), 7.67 – 7.77 (m, 2 H, 2x Ar), 7.81 (d, *J* = 8.8 Hz, 1 H, Ar), 8.26 (dd, *J* = 8.0, 1.3 Hz, 1 H, Ar), 9.24 (s, 1 H, CH), 14.85 (s, 1 H, COOH). **^{13}C-NMR (100 MHz, DMSO-d$_6$)** δ(ppm) = 55.7 (CH_3), 61.3 (CH_2), 106.3 (Ar-H), 108.8 (*C*=CH), 119.5 (Ar-H), 121.82 (d, *J* = 22.7 Hz, Ar-H), 122.83 (d, *J* = 3.7 Hz, Ar-H), 124.6 (Ar-H), 125.1 (Ar-H), 127.6 (Ar-H), 127.7 (Ar-H), 127.9 (Ar-H), 128.7 (Ar-C_q), 128.7 (Ar-C_q), 129.0 (Ar-C_q), 129.5 (d, *J* = 7.3 Hz, Ar-C_q), 129.8 (Ar-H), 132.1 (Ar-C_q), 134.2 (Ar-C_q), 152.8 (CH), 152.35 (d, *J* = 252.4 Hz, Ar-CF), 158.0 (Ar-*C*O-), 166.1 (*C*OOH), 177.6 (CO). **ESI-MS:** 378.15 *m/z* $[M+H]^+$

8. References

[1] World Health Organisation, The top 10 causes of death. http://www.who.int/en/news-room/fact-sheets/detail/the-top-10-causes-of-death (accessed on 28.07.2018).

[2] Prince, M.; Comas-Herrera, A.; Knapp, M.; Guerchet, M.; Karagiannidou, M. World Alzheimer Report 2016. *Alzheimer's Disease International, London*, September **2016**.

[3] Ferri, C. P.; Prince, M.; Brayne, C.; Brodaty, H.; Fratiglioni, L.; Ganguli, M.; Hall, K.; Hasegawa, K.; Hendrie, H.; Huang, Y.; Jorm, A.; Mathers, C.; Menezes, P. R.; Rimmer, E.; Scazufca, M. Alzheimer's Disease International Global prevalence of dementia: a Delphi consensus study. *Lancet* **2005**, *366*, 2112-2117.

[4] Prince, M. The need for research on dementia in developing countries. *Trop. Med. Int. Health* **1997**, *2*, 993-1000.

[5] World Health Organisation, Dementia. http://www.who.int/news-room/fact-sheets/detail/dementia (accessed on 28.07.2018).

[6] Hardy, J. A.; Higgins, G. A. Alzheimer's Disease: The Amyloid Cascade Hypothesis. *Science* **1992**, 256, 184-185.

[7] Selkoe, D. J. The Molecular Pathology of Alzheimer's Disease. *Neuron* **1991**, *6*, 487-489.

[8] Blennow, K.; de Leon, M. J.; Zetterberg, H. Alzheimer's disease. *Lancet* **2006**, *368*, 387-403.

[9] O'Brien, R. J.; Wong, P. C. Amyloid Precursor Protein Processing and Alzheimer's Disease. *Annu. Rev. Neurosci*. **2011**, *34*, 185-204.

[10] van der Kant, R.; Goldstein, L. S. B. Cellular Functions of the Amyloid Precursor Protein from Development to Dementia. *Dev. Cell* **2015**, *32*, 502-515.

[11] Vingtdeux, V.; Marambaud, P. Identification and biology of α-secretase. *J. Neurochem.* **2012**, *120*, 34-45.

[12] Zhang, Y.; Thompson, R.; Zhang, H.; Xu, H. APP processing in Alzheimer's disease. *Mol. Brain* **2011**, *4*:3.

[13] Kummer, M. P.; Heneka, M. T. Truncated and modified amyloid-beta species. *Alzheimers Res. Ther.* **2014**, *6*:28.

[14] Sisodia, S.; St George-Hyslop, P. H. γ-secretase, notch, Aβ and Alzheimer's disease: Where do the presenilins fit in? *Neurosci.* **2002**, *3*, 281-290.

[15] De Strooper, B.; Vassar, R.; Golde, T. The secretases: enzymes with therapeutic potential in Alzheimer disease. *Nat. Rev. Neurol.* **2010**, *6*, 99-107.

[16] Karran, E.; De Strooper, B. The amyloid cascade hypothesis: are we poised for success or failure? *J. Neurochem*. **2016**, *139*, 237-252.

[17] Medeiros, R.; Baglietto-Vargas, D.; LaFerla, F. M. The Role of Tau in Alzheimer's Disease and Related Disorders. *CNS Neurosci. Ther.* **2011**, *17*, 514-524.

[18] Goedert, M.; Spillantini, M. C.; Jakes, R.; Rutherford, D.; Crowther, R. A. Multiple lsoforms of Human Microtubule-Associated Protein Tau: Sequences and localization in Neurofibrillary Tangles of Alzheimer's Disease. *Neuron* **1989**, *3*, 519-526.

[19] Himmler, A.; Drechsel, D.; Kirschner, M. W.; Martin Jr., D. W. Tau Consists of a Set of Proteins with Repeated C-Terminal Microtubule-Binding Domains and Variable N-Terminal Domains. *Mol. Cell. Biol.* **1989**, *9*, 1381-1388.

[20] Iqbal, K.; Grundke-Iqbal, I.; Zaidi, T.; Merz, P. A.; Wen, G. Y.; Shaikh, S. S.; Wisniewski, H. M. Defective Brain Microtubule assembly in Alzheimer's disease. *Lancet*, **1986**, *2*, 421-426.

[21] Köpke, E.; Tung, Y.-C.; Shaikh, S.; Alonso, A. C.; Iqbal, K.; Grundke-Iqbal, I. Microtubule-associated Protein Tau. *J. Biol. Chem.* **1993**, *32*, 24374-24384.

[22] Iqbal, K.; Liu, F.; Gong, C.-X.; Alonso, A. C.; Grundke-Iqbal, I. Mechanisms of tau-induced neurodegeneration. *Acta Neuropathol.* **2009**, *118*, 53-69.

[23] Iqbal, K.; Alonso, A. C.; Chen, S.; Chohan, M. O.; El-Akkad, E.; Gong, C.-X.; Khatoon, S.; Li, B.; Liu, F.; Rahman, A.; Tanimukai, H.; Grundke-Iqbal, I. Tau pathology in Alzheimer disease and other tauopathies. *Biochim. Biophys. Acta, Mol. Basis Dis.* **2005**, *1739*, 198-210.

[24] Brunden, K. R.; Trojanowski, J. Q.; Lee, V. M.-Y. Advances in Tau-focused drug discovery for Alzheimer's disease and related tauopathies. *Nat. Rev. Drug Discov*. **2009**, *8*, 783-793.

[25] Ferreira-Vieira, T. H.; Guimaraes, I. M.; Silva, F. R.; Ribeiro, F. M. Alzheimer's Disease: Targeting the Cholinergic System. *Curr. Neuropharmacol.* **2016**, *14*, 101-115.

[26] Potter, L. T. Synthesis, Storage and release of [^{14}C] acetylcholine in isolated rat diaphragm muscles. *J. Physiol.* **1970**, *206*, 145-166.

[27] Augustinsson, K.-B.; Nachmansohn, D. Distinction between Acetylcholine-Esterase and Other Choline Ester-splitting Enzymes. *Science* **1949**, *110*, 98-99.

[28] Tuček, S. Regulation of Acetylcholine Synthesis in the Brain. *J. Neurochem*. **1985**, *44*, 11-24.

[29] Ferguson, S. M.; Bazalakova, M.; Savchenko, V.; Tapia, J. C.; Wright, J.; Blakely, R. D. Lethal impairment of cholinergic neurotransmission in hemicholinium-3-sensitive choline transporter knockout mice. *Proc. Natl. Acad. Sci. U. S. A.* **2004**, *101*, 8762-8767.

[30] Bartus, R. T.; Dean III, R. L.; Beer, B.; Lippa, A. S. The Cholinergic Hypothesis of Geriatric Memory Dysfunction. *Science* **1982**, *217*, 408-414.

[31] Bartus, R. T. On Neurodegenerative Diseases, Models, and Treatment Strategies: Lessons Learned and Lessons Forgotten a Generation Following the Cholinergic Hypothesis. *Exp. Neurol.* **2000**, *163*, 495-529.

[32] Čolović, M. B.; Krstić, D. Z.; Lazarević-Pašti, D. T.; Bondžić, A. M.; Vasić, V. M. Acetylcholinesterase Inhibitors: Pharmacology and Toxicology. *Curr. Neuropharmacol.* **2013**, *11*, 315-335.

[33] Tiwari, P.; Dwivedi, S.; Singh, M. P.; Mishra, R.; Chandy, A. Basic and modern concepts on cholinergic receptor: A review. *Asian Pac. J. Trop. Dis.* **2013**, *3*, 413-420.

[34] Dani, J. A. Neuronal Nicotinic Acetylcholine Receptor Structure and Function and Response to Nicotine. *Int. Rev. Neurobiol.* **2015**, *124*, 3-19.

[35] Kruse, A. C.; Kobilka, B. K.; Gautam, D.; Sexton, P. M.; Christopoulos, A.; Wess, J. Muscarinic acetylcholine receptors: novel opportunities for drug development. *Nat. Rev. Drug Discovery* **2014**, *13*, 549-560.

[36] Eglen, R. M.; Choppin, A.; Watson, N. Therapeutic opportunities from muscarinic receptor research. *Trends Pharmacol. Sci.* **2001**, *22*, 409-414.

[37] Wess, J.; Eglen, R. M.; Gautam, D. Muscarinic acetylcholine receptors: mutant mice provide new insights for drug development. *Nat. Rev. Drug Discovery* **2007**, *6*, 721-733.

[38] Lanzafame, A. A.; Christopoulos, A.; Mitchelson, F. Cellular Signaling Mechanisms for Muscarinic Acetylcholine Receptors. *Recept. Channels* **2003**, *9*, 241-260.

[39] Ishii, M.; Kurachi, Y. Muscarinic Acetylcholine Receptors. *Curr. Pharm. Des.* **2006**, *12*, 3573-3581.

[40] Wess, J. Muscarinic Acetylcholine Receptor Knockout Mice: Novel Phenotypes and Clinical Implications. *Annu. Rev. Pharmacol. Toxicol.* **2004**, *44*, 423-450.

[41] Gomeza, J.; Shannon, H.; Kostenis, E.; Felder, C.; Zhang, L.; Brodkin, J.; Grinberg, A.; Sheng, H.; Wess, J. Pronounced pharmacologic deficits in M2 muscarinic acetylcholine receptor knockout mice. *Proc. Natl. Acad. Sci. U.S.A.* **1999**, *96*, 1692-1697.

[42] Chapiro, M. S.; Loose, M. D.; Hamilton, S. E.; Nathanson, N. M.; Gomeza, J.; Wess, J.; Hille, B. Assignment of muscarinic receptor subtypes mediating G-protein modulation of Ca^{2+} channels by using knockout mice. *Proc. Natl. Acad. Sci. U.S.A.* **1999**, *96*, 10899-10904.

[43] Stengel, P. W.; Gomeza, J.; Wess, J.; Cohen, M. L. M_2 and M_4 Receptor Knockout Mice: Muscarinic Receptor Function in Cardiac and Smooth Muscle In Vitro. *J. Pharmacol. Exp. Ther*. **2000**, *292*, 877-885.

[44] Matsui, M.; Motomura, D.; Karasawa, H.; Fujikawa, T.; Jiang, J.; Komiya, Y.; Takahashi, S.; Taketo, M. M. Multiple functional defects in peripheral autonomic organs in mice lacking muscarinic acetylcholine receptor gene for the M_3 subtype. *Proc. Natl. Acad. Sci. U.S.A.* **2000**, *97*, 9579-9584.

[45] Yamada, M.; Miyakawa, T.; Duttaroy, A.; Yamanakak, A.; Moriguchi, T.; Makita, R.; Ogawa, M.; Chou, C. J.; Xia, B.; Crawley, J. N.; FelderI, C. C.; Deng, C.-X.; Wess, J. Mice lacking the M3 muscarinic acetylcholine receptor are hypophagic and lean. *Nature* **2001**, *410*, 207-212.

[46] Gomeza, J.; Zhang, L.; Kostenis, E.; Felder, C.; Bymaster, F.; Brodkin, J.; Shannon, H.; Xia, B.; Deng, C.-X.; Wess, J. Enhancement of D1 dopamine receptor-mediated locomotor stimulation in M_4 muscarinic acetylcholine receptor knockout mice. *Proc. Natl. Acad. Sci. U.S.A.* **1999**, *96*, 10483-10488.

[47] Yamada, M.; Lamping, K. G.; Duttaroy, A.; Zhang, W.; Cui, Y.; Bymaster, F. P.; McKinzie, D. L.; Felder, C. C.; Deng, C.-X.; Faraci, F. M.; Wess, J. Cholinergic dilation of cerebral blood vessels is abolished in M_5 muscarinic acetylcholine receptor knockout mice. *Proc. Natl. Acad. Sci. U.S.A.* **2001**, *98*, 14096-14101.

[48] Fisher, A. Cholinergic Treatments with Emphasis on M1 Muscarinic Agonists as Potential Disease-Modifying Agents for Alzheimer's Disease. *Neurotherapeutics* **2008**, *5*, 433-442.

[49] Fisher, A. M1 Muscarinic Agonists Target Major Hallmarks of Alzheimer's Disease – The Pivotal Role of Brain M1 Receptors. *Neurodegenerative Dis*. **2008**, *5*, 237-240.

[50] Fisher, A. M1 Muscarinic Agonists Target Major Hallmarks of Alzheimer's Disease – an Update. *Curr. Alzheimer Res.* **2007**, *4*, 577-580.

[51] Fisher, A. Cholinergic modulation of amyloid precursor protein processing with emphasis on M1 muscarinic receptor: perspectives and challenges in treatment of Alzheimer's disease. *J. Neurochem*. **2012**, *120*, 22-33.

[52] De Sarno, P.; Shestopal, S. A.; King, T. D.; Zmijewska, A.; Song, L.; Jope, R. S. Muscarinic Receptor Activation Protects Cells from Apoptotic Effects of DNA Damage, Oxidative Stress, and Mitochondrial Inhibition. *J. Biol. Chem.* **2003**, *278*, 11086-11093.

[53] Overk, C. R.; Felder, C. C.; Tu, Y.; Schober, D. A.; Bales, K. R.; Wuu, J.; Mufson, E. J. Cortical M_1 Receptor Concentration Increases Without a Concomitant Change in Function in Alzheimer's Disease. *J. Chem. Neuroanat.* **2010**, *40*, 63-70.

[54] Lebois, E. P.; Schroeder, J. P.; Esparza, T. J.; Bridges, T. M.; Lindsley, C. W.; Conn, P. J.; Brody, D. L.; Daniels, J. S.; Levey, A. I. Disease-Modifying Effects of M_1 Muscarinic Acetylcholine Receptor Activation in an Alzheimer's Disease Mouse Model. *ACS Chem. Neurosci*. **2017**, *8*, 1177-1187.

[55] Christopoulos, A.; Changeux, J.-P.; Catterall, W. A.; Fabbro, D.; Burris, T. P.; Cidlowski, J. A.; Olsen, R. W.; Peters, J. A.; Neubig, R. R.; Pin, J.-P.; Sexton, P. M.; Kenakin, T. P.; Ehlert, F. J.; Spedding, M.; Langmead, C. J. International Union of Basic and Clinical Pharmacology. XC. Multisite Pharmacology: Recommendations for the Nomenclature of Receptor Allosterism and Allosteric Ligands. *Pharmacol. Rev*. **2014**, *66*, 918-947.

[56] Mohr, K.; Schmitz, J.; Schrage, R.; Tränkle, C.; Holzgrabe, U. Molecular Alliance—From Orthosteric and Allosteric Ligands to Dualsteric/Bitopic Agonists at G Protein Coupled Receptors. *Angew. Chem. Int. Ed*. **2013**, *52*, 508-516.

[57] Davie, B. J.; Christopoulos, A.; Scammells, P. J. Development of M_1 mAChR Allosteric and Bitopic Ligands: Prospective Therapeutics for the Treatment of Cognitive Deficits. *ACS Chem. Neurosci*. **2013**, *4*, 1026-1048.

[58] Thal, D. M.; Sun, B.; Feng, D.; Nawaratne, V.; Leach, K.; Felder, C. C.; Bures, M. G.; Evans, D. A.; Weis, W. I.; Bachhawat, P.; Kobilka, T. S.; Sexton, P. M.; Kobilka, B. K.; Christopoulos, A. Crystal Structures of the M_1 and M_4 Muscarinic Acetylcholine Receptors. *Nature* **2016**, *531*, 335-340.

[59] Shaarawy, T.; Sherwood, M.; Hitchings, R.; Crowston, J. Parasympathomimetics, in: *Glaucoma 2nd Edition*; Elsevier **2014**.

[60] Jones, C. K.; Brady, A. E.; Davis, A. A.; Xiang, Z.; Bubser, M.; Tantawy, M. N.; Kane, A. S.; Bridges, T. M.; Kennedy, J. P.; Bradley, S. R.; Peterson, T. E.; Ansari, M. S.; Baldwin, R. M.; Kessler, R. M.; Deutch, A. Y.; Lah, J. J.; Levey, A. I.; Lindsley, C. W.; Conn, P. J. Novel Selective Allosteric Activator of the M_1 Muscarinic Acetylcholine Receptor Regulates Amyloid Processing and Produces Antipsychotic-Like Activity in Rats. *J. Neurosci*. **2008**, *28*, 10422-10433.

[61] Markovic, D.; Holdich, J.; Al-Sabah, S.; Mistry, R.; Krasel, C.; Mahaut-Smith, M. P.; Challiss, R. A. J. FRET-Based Detection of M_1 Muscarinic Acetylcholine Receptor Activation by Orthosteric and Allosteric Agonists. *PLoS One* **2012**, *7*, e29946.

[62] Daval, S. B.; Valant, C.; Bonnet, D.; Kellenberger, E.; Hibert, M.; Galzi, J.-L.; Ilien, B. Fluorescent Derivatives of AC-42 To Probe Bitopic Orthosteric/Allosteric Binding Mechanisms on Muscarinic M1 Receptors. *J. Med. Chem*. **2012**, *55*, 2125-2143.

[63] Fisher, A.; Bar-Ner, N.; Karton, Y. Methods and Compositions for treatment of central and peripheral nervous system disorders and novel compounds useful therefore. US 7439,251 B2, Oct. 21, **2008**.

[64] Chen, X.; Klöckner, J.; Holze, J.; Zimmermann, C.; Seemann, W. K.; Schrage, R.; Bock, A.; Mohr, K.; Tränkle, C.; Holzgrabe, U.; Decker, M. Rational Design of Partial Agonists for the Muscarinic M_1 Acetylcholine Receptor. *J. Med. Chem*. **2015**, *58*, 560-576.

[65] Canals, M.; Lane, J. R.; Wen, A.; Scammells, P. J.; Sexton, P. M.; Christopoulos, A. A Monod-Wyman-Changeux Mechanism Can Explain G Protein-coupled Receptor (GPCR) Allosteric Modulation. *J. Biol. Chem*. **2012**, *287*, 650-659.

[66] Ma, L.; Seager, M. A.; Wittmann, M.; Jacobson, M.; Bickel, D.; Burno, M.; Jones, K.; Graufelds, V. K.; Xu, G.; Pearson, M.; McCampbell, A.; Gaspar, R.; Shughrue, P.; Danziger, A.; Regan, C.; Flick, R.; Pascarella, D.; Garson, S.; Doran, S.; Kreatsoulas, C.; Veng, L.; Lindsley, C. W.; Shipe, W.; Kuduk, S.; Sur, C.; Kinney, G.; Seabrook, G. R.; Ray, W. J. Selective activation of the M_1 muscarinic acetylcholine receptor achieved by allosteric potentiation. *Proc. Natl. Acad. Sci. U.S.A.* **2009**, *106*, 15950-15955.

[67] Shirey, J. K.; Brady, A. E.; Jones, P. J.; Davis, A. A.; Bridges, T. M.; Kennedy, J. P.; Jadhav, S. B.; Menon, U. N.; Xiang, Z.; Watson, M. L.; Christian, E. P.; Doherty, J. J.; Quirk, M. C.; Snyder, D. H.; Lah, J. J.; Levey, A. I.; Nicolle, M. M.; Lindsley, C. W.; Conn, P. J. Selective Allosteric Potentiator of the M_1 Muscarinic Acetylcholine Receptor Increases Activity of Medial Prefrontal Cortical Neurons and Restores Impairments in Reversal Learning. *J. Neurosci.* **2009**, *29*, 14271-14286.

[68] Decker, M.; Holzgrabe, U. M_1 muscarinic acetylcholine receptor allosteric modulators as potential therapeutic opportunities for treating Alzheimer's disease. *Med. Chem. Commun.* **2012**, *3*, 752-762.

[69] Kuduk, S. D.; Beshore, D. C. SAR Studies on Carboxylic Acid Series M_1 Selective Positive Allosteric Modulators (PAMs). *Curr. Top. Med. Chem.* **2014**, *14*, 1738-1754.

[70] Kuduk, S. D.; Di Marco, C. N.; Cofre, V.; Ray, W. J.; Ma, L.; Wittmann, M.; Seager, M. A.; Koeplinger, K. A.; Thompson, C. D.; Hartman, G. D.; Bilodeau, M. T. Fused heterocyclic M_1 positive allosteric modulators. *Bioorg. Med. Chem. Lett.* **2011**, *21*, 2769-2772.

[71] Budzik, B.; Garzya, V.; Shi, D.; Walker, G.; Woolley-Roberts, M.; Pardoe, J.; Lucas, A.; Tehan, B.; Rivero, R. A.; Langmead, C. J.; Watson, J.; Wu, Z.; Forbes, I. T.; Jin, J. Novel *N*-Substituted Benzimidazolones as Potent, Selective, CNS-Penetrant, and Orally Active M_1 mAChR Agonists. *ACS Med. Chem. Lett*. **2010**, *1*, 244-248.

[72] Henning, R.; Lattrell, R.; Gerhards, H. J.; Leven, M. Synthesis and Neuroleptic Activity of a Series of 1-[1-(Benzo-1,4-dioxan-2-ylmethyl)-4-piperidinyl]benzimidazolone Derivatives. *J. Med. Chem*. **1987**, *30*, 814-819.

[73] Xu, N.; Yang, C.; Gan, X.; Wie, S.; Ji, Z. Synthesis of 1-isopropyl-3-acyl-5-methyl-benzimidazolone Derivatives and Their Antimicrobial Activity. *Int. J. Mol. Sci*. **2013**, *14*, 6790-6804.

[74] Yang, F. V.; Shipe, W. D.; Bunda, J. L.; Nolt, M. B.; Wisnoski, D. D.; Zhao, Z.; Barrow, J. C.; Ray, W. J.; Ma, L.; Wittmann, M.; Seager, M. A.; Koeplinger, K. A.; Hartman, G. D.; Lindsley, C. W. Parallel synthesis of *N*-biaryl quinolone carboxylic acids as selective M_1 positive allosteric modulators. *Bioorg. Med. Chem Lett.* **2010**, *20*, 531-536.

[75] Gould Jr., G.; Jacobs, W. A. The Synthesis of Certain Substituted Quinolines and 5,6-Benzoquinolines. *J. Am. Chem. Soc*., **1939**, *61*, 2890-2895.

[76] McLean, T. H.; Parrish, J. C.; Braden, M. R.; Marona-Lewicka, D.; Gallardo-Godoy, A.; Nichols, D. E. 1-Aminomethylbenzocycloalkanes: Conformationally Restricted Hallucinogenic Phenethylamine Analogues as Functionally Selective 5-HT_{2A} Receptor Agonists. *J. Med. Chem*. **2006**, *49*, 5794-5803.

[77] Mazzei, M.; Sottofattori, E.; Ibrahim, M.; Balbi, A. Properties of Naphtho[2,1-B]pyrans Covalently Linked to Oligonucleotides. *Nucleosides Nucleotides Nucleic Acids* **1998**, *17*, 1885-1894.

[78] Andrew, R. G.; Raphael, R. A. A new total synthesis of Aaptamine. *Tetrahedron*, **1987**, *43*, 4803-4816.

[79] Trinquet, E.; Fink, M.; Bazin, H.; Grillet, F.; Maurin, F.; Bourrier, E.; Ansanay, H.; Leroy, C.; Michaud, A.; Durroux, T.; Maurel, D.; Malhaire, F.; Goudet, C.; Pin, J.-P.; Naval, M.; Hernout, O.; Chrétien, F.; Chapleur, Y.; Mathis, G. D-*myo*-Inositol 1-phosphate as a surrogate of D-*myo*-inositol 1,4,5-tris phosphate to monitor G protein-coupled receptor activation. *Anal. Biochem.* **2006**, *358*, 126-135.

[80] Zhang, J. Y.; Kowal, D. M.; Nawoschik, S. P.; Dunlop, J.; Pausch, M. H.; Peri, R. Development of an Improved IP_1 Assay for the Characterization of 5-HT_{2C} Receptor Ligands. *Assay Drug Dev. Technol.* **2010**, *8*, 106-113.

[81] Palmer, A. M. Neuroprotective therapeutics for Alzheimer's disease: progress and prospects. *Trends Pharmacol. Sci*. **2011**, *32*, 141-147.

[82] Praticò, D. Oxidative stress hypothesis in Alzheimer's disease: a reappraisal. *Trends Pharmacol. Sci*. **2008**, *29*, 609-615.

[83] Thanan, R.; Oikawa, S.; Hiraku, Y.; Ohnishi, S.; Ma, N.; Pinlaor, S.; Yongvanit, P.; Kawanishi, S.; Murata, M. Oxidative Stress and Its Significant Roles in Neurodegenerative Diseases and Cancer. *Int. J. Mol. Sci*. **2015**, *16*, 193-217.

[84] Aliev, G.; Obrenovich, M. E.; Reddy, V. P.; Shenk, J. C.; Moreira, P. I.; Nunomura, A.; Zhu, X.; Smith, M. A.; Perry, G. Antioxidant Therapy in Alzheimer's Disease: Theory and Practice. *Mini-Rev. Med. Chem*. **2008**, *8*, 1395-1406.

[85] Ismaili, L.; Romero, A.; do Carmo Carreiras, M.; Marco-Contelles, J. Multitarget-directed antioxidants as therapeutic agents: putting the focus on the oxidative stress, in: M. Decker (Ed.), *Design of hybrid molecules for drug development*, Elsevier, Oxford, UK **2017**, 5-46.

[86] Solanki, I.; Parihar, P.; Mansuri, M. L.; Parihar, M. S. Flavonoid-Based Therapies in the Early Management of Neurodegenerative Diseases. *Adv. Nutr*. **2015**, *6*, 64-72.

[87] Pérez-Hernández, J.; Zaldívar-Machorro, V. J.; Villanueva-Porras, D.; Vega-Ávila, E.; Chavarría, A. A Potential Alternative against Neurodegenerative Diseases: Phytodrugs. *Oxid. Med. Cell Longev.* **2016**, *2016*, 8378613.

[88] López-Alarcón, C.; Denicola, A. Evaluating the antioxidant capacity of natural products: A review on chemical and cellular-based assays. *Anal. Chim. Acta* **2013**, *763*, 1-10.

[89] Nelson, K. M.; Dahlin, J. L.; Bisson, J.; Graham, J.; Pauli, G. F.; Walters, M. A. The Essential Medicinal Chemistry of Curcumin. *J. Med. Chem*. **2017**, *60*, 1620-1637.

[90] Biedermann, D.; Vavříková, E.; Cvak, L.; Křen, V. Chemistry of silybin. *Nat. Prod. Rep*. **2014**, *31*, 1138-1157.

[91] Gažák, R.; Walterová, D.; Křen, V. Silybin and Silymarin – New and Emerging Applications in Medicine. *Curr. Med. Chem*. **2007**, *14*, 315-338.

[92] Agarwal, C.; Wadhwa, R.; Deep, G.; Biedermann, D.; Gažák, R.; Křen, V.; Agarwal, R. Anti-Cancer Efficacy of Silybin Derivatives - A Structure-Activity Relationship. *PLoS One* **2013**, *8*, e60074.

[93] Yang, L. X.; Huang, K. X.; Li, H. B.; Gong, J. X.; Wang, F.; Feng, Y. B.; Tao, Q. B.; Wu, Y. H.; Li, X. K.; Wu, X. M.; Zeng, S.; Spencer, S.; Zhao, Y.; Qu, J. Design, Synthesis, and Examination of Neuron Protective Properties of Alkenylated and Amidated Dehydro-Silybin Derivatives. *J. Med. Chem*. **2009**, *52*, 7732-7752.

[94] Zarrelli, A.; Sgambato, A.; Petito, V.; De Napoli, L.; Previtera, L.; Di Fabio, G. New C-23 modified of silybin and 2,3-dehydrosilybin: Synthesis and preliminary evaluation of antioxidant properties. *Bioorg. Med. Chem. Lett.* **2011**, *21*, 4389-4392.

[95] Wang, F.; Huang, K.; Yang, L.; Gong, J.; Tao, Q.; Li, H.; Zhao, Y.; Zeng, S.; Wua, X.; Stöckigt, J.; Li, X.; Qu, J. Preparation of C-23 esterified silybin derivatives and evaluation of their lipid peroxidation inhibitory and DNA protective properties. *Bioorg. Med. Chem.* **2009**, *17*, 6380-6389.

[96] Pascual, C.; Gonzalez, R.; Armesto, J.; Muriel, P. Effect of Silymarin and Silybinin on Oxygen Radicals. *Drug Dev. Res*. **1993**, *29*, 73-77.

[97] a) Nyiredy, S.; Samu, Z.; Szücs, Z.; Gulácsi, K.; Kurtán, T.; Antus, S. New Insight into the Biosynthesis of Flavanolignans in the White-Flowered Variant of *Silybum marianum*. *J. Chromatogr. Sci.* **2008**, *46*, 93-96. b) AbouZid, S. Silymarin, Natural Flavonolignans from Milk Thistle, in: V. Rao (Ed.), *Phytochemicals - A Global Perspective of Their Role in Nutrition and Health*, InTech **2012**, 255-277.

[98] Marhol, P.; Bednár, P.; Kolárová, P.; Vecera, R.; Ulrichová, J.; Tesarová, E.; Vavríková, E.; Kuzma, M.; Křen, V. Pharmacokinetics of pure silybin diastereoisomers and identification of their metabolites in rat plasma. *J. Funct. Foods* **2015**, *14*, 570-580.

[99] Sciacca, M. F. M.; Romanucci, V.; Zarrelli, A.; Monaco, I.; Lolicato, F.; Spinella, N.; Galati, C.; Grasso, G.; D'Urso, L.; Romeo, M.; Diomede, L.; Salmona, M.; Bongiorno, C.; Di Fabio, G.; La Rosa, C.; Milardi, D. Inhibition of Aβ Amyloid Growth and Toxicity by Silybins: The Crucial Role of Stereochemistry. *ACS Chem. Neurosci*. **2017**, *8*, 1767-1778.

[100] a) Davis-Searles, P. R.; Nakanishi, Y.; Kim, N.-C.; Graf, T. N.; Oberlies, N. H.; Wani, M. C.; Wall, M. E.; Agarwal, R.; Kroll, D. J. Milk Thistle and Prostate Cancer: Differential Effects of Pure Flavonolignans from Silybum marianum on Antiproliferative End Points in Human Prostate Carcinoma Cells. *Cancer Res*. **2005**, *65*, 4448-4457. b) Deep, G.; Oberlies, N. H.; Kroll, D. J.; Agarwal, R. Identifying the differential effects of silymarin constituents on cell growth and cell cycle regulatory molecules in human prostate cancer cells. *Int. J. Cancer* **2008**, *123*, 41-50.

[101] Gažák, R.; Valentová, K.; Fuksová, K.; Marhol, P.; Kuzma, M.; Ángel Medina, M.; Oborná, I.; Ulrichová, J.; Křen, V. Synthesis and Antiangiogenic Activity of New Silybin Galloyl Esters. *J. Med. Chem*. **2011**, *54*, 7397-7407.

[102] Filippopoulou, K.; Papaevgeniou, N.; Lefaki, M.; Paraskevopoulou, A.; Biedermann, D.; Křen, V.; Chondrogianni, N. 2,3-Dehydrosilybin A/B as a pro-longevity and anti-aggregation compound. *Free Radical Biol. Med*. **2017**, *103*, 256-267.

[103] Plíšková, M.; Vondráček, J.; Křen, V.; Gažák, R.; Sedmera, P.; Walterová, D.; Psotová, J.; Šimánek, V.; Machala, M. Effects of silymarin flavonolignans and synthetic silybin derivatives on estrogen and aryl hydrocarbon receptor activation. *Toxicology* **2005**, *215*, 80-89.

[104] a) Gažák, R.; Sedmera, P.; Marzorati, M.; Riva, S.; Křen, V. Laccase-mediated dimerization of the flavonolignan silybin. *J. Mol. Catal. B: Enzym*. **2008**, *50,* 87-92. b) Trouillas, P.;

Marsal, P.; Svobodová, A.; Vostálová, J.; Gažák, R.; Hrbáč, J.; Sedmera, P.; Křen, V.; Lazzaroni, R.; Duroux, J.-L.; Walterová, D. Mechanism of the Antioxidant Action of Silybin and 2,3-Dehydrosilybin Flavonolignans: A Joint Experimental and Theoretical Study. *J. Phys. Chem*. *A* **2008**, *112*, 1054-1063.

[105] Gažák, R.; Sedmera, P.; Vrbacký, M.; Vostálová, J.; Drahota, Z.; Marhol, P.; Walterová, D.; Křen, V. Molecular mechanisms of silybin and 2,3-dehydrosilybin antiradical activity—role of individual hydroxyl groups. *Free Radical Biol. Med*. **2009**, *46*, 745-758.

[106] György, I.; Antus, S.; Földiák, G. Pulse radiolysis of silybin: One-electron oxidation of the flavonoid at neutral pH. *Radiat. Phys. Chem*. **1992**, *39*, 81-84.

[107] Heilmann, J.; Calis, I.; Kirmizibekmez, H.; Schühly, W.; Harput, S.; Sticher, O. Radical scavenger activity of phenylethanoid glycosides in FMLP stimulated human polymorphonuclear leukocytes: structure-activity relationships. *Planta Med*. **2000**, *66*, 746-748.

[108] Ono, K.; Hirohata, M.; Yamada, M. Ferulic acid destabilizes preformed β-amyloid fibrils in vitro. *Biochem. Biophys. Res. Commun*. **2005**, *336*, 444-449.

[109] Yan, J.-J.; Cho, J.-Y.; Kim, H.-S.; Kim, K.-L.; Jung, J.-S.; Huh, S.-O.; Suh, H.-W.; Kim, Y.-H.; Song, D-K. Protection against β-amyloid peptide toxicity in vivo with long-term administration of ferulic acid. *Br. J. Pharmacol*. **2001**, *133*, 89-96.

[110] Murphy, T. H.; Miyamoto, M.; Sastre, A.; Schnaar, R. L.; Coyle, J. T. Glutamate Toxicity in a Neuronal Cell line Involves Inhibition of Cystine Transport Leading to Oxidative Stress. *Neuron* **1989**, *2*, 1547-1558.

[111] Monti, D.; Gažák, R.; Marhol, P.; Biedermann, D.; Purchartová, K.; Fedrigo, M.; Riva, S.; Křen, V. Enzymatic Kinetic Resolution of Silybin Diastereoisomers. *J. Nat. Prod*. **2010**, *73*, 613-619.

[112] Li, P.; Callery, P. S.; Gan, L.-S.; Balani, S. K. Esterase Inhibition by Grapefruit Juice Flavonoids Leading to a New Drug Interaction. *Drug Metab. Dispos*. **2007**, *35*, 1203-1208.

[113] Sharp, H.; Hollinshead, J.; Bartholomew, B. B.; Oben, J.; Watson, A.; Nash, R. J. Inhibitory Effects of *Cissus quadrangularis* L. Derived components on Lipase, Amylase and α-Glucosidase Activity *in vitro*. *Nat. Prod. Commun*. **2007**, 2, 817-822.

[114] a) Chen, X.; Zenger, K.; Lupp, A.; Kling, B.; Heilmann, J.; Fleck, C.; Kraus, B.; Decker, M. Tacrine-Silibinin Codrug Shows Neuro- and Hepatoprotective Effects *in Vitro* and Pro-Cognitive and Hepatoprotective Effects *in Vivo*. *J. Med. Chem.* **2012**, *55,* 5231-5242. b) Zenger, K.; Chen, X.; Decker, M.; Kraus, B. In-vitro stability and metabolism of a tacrine–silibinin codrug. *J. Pharm. Pharmacol*. **2013**, *65*, 1765-1772.

[115] Gažák, R.; Purchartová, K.; Marhol, P.; Živná, L.; Sedmera, P.; Valentová, K.; Kato, N.; Matsumura, N.; Kaihatsu, K.; Křen, V. Antioxidant and antiviral activities of silybin fatty acid conjugates. *Eur. J. Med. Chem*. **2010**, *45*, 1059-1067.

[116] Huang, G. Synthesis and *in Vitro* Evaluation of Experimental Anti-Alzheimer Therapeutics: Bivalent Ligands for Cannabinoid Receptors, Natural Product-based Cholinesterase Inhibitors and Neuroprotectants. Dissertation, Julius-Maximilians-Universität Würzburg, **2014**.

[117] a) Adjimani, J. P.; Asare, P. Antioxidant and free radical scavenging activity of iron chelators. *Toxicol. Rep*. **2015**, *2*, 721-728. b) I. Gülçin Antioxidant activity of caffeic acid (3,4-dihydroxycinnamic acid). *Toxicology* **2006**, *217*, 213-220.

[118] Takahashi, T.; Miyazawa, M. Tyrosinase inhibitory activities of cinnamic acid analogues. *Pharmazie* **2010**, *65*, 913-918.

[119] Gažák, R.; Svobodová, A.; Psotová, J.; Sedmera, P.; Prikrylová, V.; Walterová, D.; Křen, V. Oxidised derivatives of silybin and their antiradical and antioxidant activity. *Bioorg. Med. Chem*. **2004**, *12*, 5677-5687.

[120] Pyszková, M.; Biler, M.; Biedermann, D.; Valentová, K.; Kuzma, M.; Vrba, J.; Ulrichová, J.; Sokolová, R.; Mojović, M.; Popović-Bijelić, A.; Kubala, M.; Trouillas, P.; Křen, V.; Vacek, J. Flavonolignan2,3-dehydroderivatives: Preparation, antiradical and cytoprotective activity. *Free Radical Biol. Med*. **2016**, *90*, 114-125.

[121] Gažák, R.; Trouillas, P.; Biedermann, D.; Fuksová, K.; Marhol, P.; Kuzma, M.; Křen, V. Base-catalyzed oxidation of silybin and isosilybin into 2,3-dehydro derivatives. *Tetrahedron Lett*. **2013**, *54*, 315-317.

[122] Benzie, I. F. F.; Strain, J. J. The Ferric Reducing Ability of Plasma (FRAP) as a Measure of ‘‘Antioxidant Power’’: The FRAP Assay. *Anal. Biochem*. **1996**, *239*, 70-76.

[123] Pulido, R.; Bravo, L.; Saura-Calixto, F. Antioxidant Activity of Dietary Polyphenols As Determined by a Modified Ferric Reducing/Antioxidant Power Assay. *J. Agric. Food Chem*. **2000**, *48*, 3396-3402.

[124] Fang, L.; Kraus, B.; Lehmann, J.; Heilmann, J.; Zhang, Y.; Decker, M. Design and synthesis of tacrine–ferulic acid hybrids as multi-potent anti-Alzheimer drug candidates. *Bioorg. Med. Chem. Lett*. **2008**, *18*, 2905-2909.

[125] Huang, G.; Kling, B.; Darras, F. H.; Heilmann, J.; Decker, M. Identification of a neuroprotective and selective butyrylcholinesterase inhibitor derived from the natural alkaloid evodiamine. *Eur. J. Med. Chem*. **2014**, *81*, 15-21.

[126] Darras, F. H.; Kling, B.; Heilmann, J.; Decker, M. Neuroprotective Tri- and Tetracyclic BChE Inhibitors Releasing Reversible Inhibitors upon Carbamate Transfer. *ACS Med. Chem. Lett*. **2012**, *3*, 914-919.

[127] Kling, B.; Bücherl, D.; Palatzky, P.; Matysik, F.-M.; Decker, M.; Wegener, J.; Heilmann, J. Flavonoids, Flavonoid Metabolites, and Phenolic Acids Inhibit Oxidative Stress in the Neuronal Cell Line HT-22 Monitored by ECIS and MTT Assay: A Comparative Study. *J. Nat. Prod*. **2014**, *77*, 446-454.

[128] Ishige, K.; Schubert, D.; Sagara, Y. Flavonoids Protect Neuronal Cells From Oxidative Stress By Three Distinct Mechanisms. *Free Radical Biol. Med*. **2001**, *30*, 433-446.

[129] Davis, J. B.; Maher, P. Protein kinase C activation inhibits glutamate-induced cytotoxicity in a neuronal cell line. *Brain Res*. **1994**, *652*, 169-173.

[130] Maher, P.; Kontoghiorghes, G. J. Characterization of the Neuroprotective Potential of Derivatives of the Iron Chelating Drug Deferiprone. *Neurochem. Res*. **2015**, *40*, 609-620.

[131] Tan, S.; Wood, M.; Maher, P. Oxidative Stress Induces a Form of Programmed Cell Death with Characteristics of Both Apoptosis and Necrosis in Neuronal Cells. *J. Neurochem*. **1998**, *71*, 95-105.

[132] Tan, S.; Schubert, D.; Maher, P. Oxytosis: A Novel Form of Programmed Cell Death. *Curr. Top. Med. Chem*. **2001**, *1*, 497-506.

[133] Currais, A.; Chiruta, C.; Goujon-Svrzic, M.; Costa, G.; Santos, T.; Batista, M. T.; Paiva, J.; do Céu Madureira, M.; Maher, P. Screening and identification of neuroprotective compounds relevant to Alzheimer's disease from medicinal plants of S. Tomé e Príncipe. *J. Ethnopharmacol*. **2014**, *155*, 830-840.

[134] Saxena, U. Bioenergetics failure in neurodegenerative diseases: back to the future. *Expert Opin. Ther. Pat*. **2012**, *16*, 351-354.

[135] Wyss-Coray, T.; Rogers, J. Inflammation in Alzheimer Disease—A Brief Review of the Basic Science and Clinical Literature. *Cold Spring Harb. Perspect. Med*. **2012**, *2*, a006346.

[136] Sagara, Y.; Vanhnasy, J.; Maher, P. Induction of PC12 cell differentiation by flavonoids is dependent upon extracellular signal-regulated kinase activation. *J. Neurochem*. **2004**, *90*, 1144-1155.

[137] Espargaró, A.; Medina, A.; Di Pietro, O.; Muñoz-Torrero, D.; Sabate, R. Ultra rapid *in vivo* screening for anti-Alzheimer anti-amyloid drugs. *Sci. Rep*. **2016**, *6*, 23349.

[138] Espargaró, A.; Ginex, T.; del Mar Vadell, M.; Busquets, M. A.; Estelrich, J.; Muñoz-Torrero, D.; Luque, F. J.; Sabate, R. Combined in Vitro Cell-Based/in Silico Screening of Naturally Occurring Flavonoids and Phenolic Compounds as Potential Anti-Alzheimer Drugs. *J. Nat. Prod*. **2017**, *80*, 278-289.

[139] Zarrelli, A.; Romanucci, V.; De Napoli, L.; Previtera, L.; Di Fabio, G. Synthesis of New Silybin Derivatives and Evaluation of Their Antioxidant Properties. *Helv. Chim. Acta* **2015**, *98*, 399-408.

[140] Ahmad, U.; Akhtar, J.; Singh, S. P., Ahmad, F. J.; Siddiqui, S. Silymarin nanoemulsion against human hepatocellular carcinoma: development and optimization. *Artif. Cells Nanomed. Biotechnol.* **2018**, *46*, 231-241.

[141] Kosina, P.; Křen, V.; Gebhardt, R.; Grambal, F.; Ulrichová, J.; Walterová, D. Antioxidant Properties of Silybin Glycosides. *Phytother. Res*. **2002**, *16*, 33-39.

[142] Křen, V.; Kubisch, J.; Sedmera, P.; Halada, P.; Přikrylová, V.; Jegorov, A.; Cvak, L.; Gebhardt, R.; Ulrichová, J.; Šimánek, V. Glycosylation of silybin. *J. Chem. Soc., Perkin Trans. 1*, **1997**, *0*, 2467-2474.

[143] Vavříková, E.; Křen, V.; Jezova-Kalachova, L.; Biler, M.; Chantemargue, B.; Pyszková, M.; Riva, S.; Kuzma, M.; Valentová, K.; Ulrichová, J.; Vrba, J.; Trouillas, P.; Vacek, J. Novel flavonolignan hybrid antioxidants: From enzymatic preparation to molecular rationalization. *Eur. J. Med. Chem*. **2017**, *127*, 263-274.

[144] Zarrelli, A.; Romanucci, V.; Tuccillo, C.; Federico, A.; Loguercio, C.; Gravante, R.; Di Fabio, G. New silibinin glyco-conjugates: Synthesis and evaluation of antioxidant properties. *Bioorg. Med. Chem. Lett*. **2014**, *24*, 5147-5149.

[145] Zhang, P.; Ye, H.; Min, T.; Zhang, C. Water Soluble Poly(ethylene glycol) Prodrug of Silybin: Design, Synthesis, and Characterization. *J. Appl. Polym. Sci*. **2008**, *107*, 3230-3235.

[146] a) Koch, H. P.; Ritschel, W. A. Bioverfügbarkeit von Silymarin, 1. Mitt. Verteilungsvolumina von Silybin, Silydianin und Silychristin aus In-vitro-Daten. *Arch. Pharm. Pharm. Med. Chem.* **1981**, *314*, 515-517. b) Koch, H.; Demeter, T.; Zinsberger, G. Physikochemische Eigenschaften von Silymarin, 1. Mitt. pKa und Ionisationsprofil von Silybin, Silydianin und Silychristin. *Arch. Pharm. Pharm. Med. Chem.* **1980**, *313*, 565-571. c) Koch, H.; Zinsberger, G. Physikochemische Eigenschaften von Silymarin, 2. Mitt. Löslichkeitsparameter von Silybin, Silydianin und Silychristin. *Arch. Pharm. Pharm. Med. Chem.* **1980**, *313*, 526-533. d) Koch, H. P.; Tscherny, J.; Zinsberger, G. Bioverfügbarkeit von Silymarin, 2. Mitt. Stabilitätsuntersuchungen an Silybin-dihemisuccinat. *Arch. Pharm. Pharm. Med. Chem.* **1983**, *316*, 385-394. e) Koch, H.; Hecht, K. Physikochemische Eigenschaften von Silymarin, 3. Mitt. Verteilungskoeffizienten von Silybin, Silydianin und Silychristin. *Arch. Pharm. Pharm. Med. Chem.* **1980**, *313*, 533-537. f) Koch, H.; Tscherny, J. Bioverfügbarkeit von Silymarin, 3. Mitt. Spaltung von Silybin-dihemisuccinat dutch Plasma- und Leberesterasen. *Arch. Pharm. Pharm. Med. Chem.* **1983**, *316*, 426-430.

[147] Lu, P.; Mamiya, T.; Lu, L. L.; Mouri, A.; Zou, L. B.; Nagai, T.; Hiramatsu, M.; Ikejima, T.; Nabeshima, T. Silibinin prevents amyloid β peptide-induced memory impairment and oxidative stress in mice. *Br. J. Pharmacol.* **2009**, *157*, 1270-1277.

[148] Tota, S.; Kamat, P. K.; Shukla, R.; Nath, C. Improvement of brain energy metabolism and cholinergic functions contributes to the beneficial effects of silibinin against streptozotocin induced memory impairment. *Behav. Brain Res*. **2011**, *221*, 207-215.

[149] Joshi, R.; Garabadu, D.; Teja, G. R.; Krishnamurthy, S. Silibinin ameliorates LPS-induced memory deficits in experimental animals. *Neurobiol. Learn. Mem.* **2014**, *116*, 117-131.

[150] Lee, Y.; Park, H. R.; Chun, H. J.; Lee, J. Silibinin Prevents Dopaminergic Neuronal Loss in a Mouse Model of Parkinson's Disease Via Mitochondrial Stabilization. *J. Neurosci. Res*. **2015**, *93*, 755-765.

[151] Jin, G.; Bai, D.; Yin, S.; Yang, Z.; Zou, D.; Zhang, Z.; Li, X.; Sun, Y.; Zhu, Q. Silibinin rescues learning and memory deficits by attenuating microglia activation and preventing neuroinflammatory reactions in SAMP8 mice. *Neurosci. Lett*. **2016**, *629*, 256-261.

[152] Bai, D.; Jin, G.; Yin, S.; Zou, D.; Zhu, Q.; Yang, Z.; Liu, X.; Ren, L.; Sun, Y.; Gan, S. Antioxidative and Anti-Apoptotic Roles of Silibinin in Reversing Learning and Memory Deficits in APP/PS1 Mice. *Neurochem. Res*. **2017**, *42*, 3439-3445.

[153] Song, X.; Liu, B.; Cui, L.; Zhou, B.; Liu, W.; Xu, F.; Hayashi, T.; Hattori, S.; Ushiki-Kaku, Y.; Tashiro, S.; Ikejima, T. Silibinin ameliorates anxiety/depression-like behaviors in amyloid ß-treated rats by upregulating BDNF/TrkB pathway and attenuating autophagy in hippocampus. *Physiol. Behav.* **2017**, *149*, 487-493.

[154] Maurice, T.; Lockhart, B. P.; Privat, A. Amnesia induced in mice by centrally administered β-amyloid peptides involves cholinergic dysfunction. *Brain Res.* **1996**, *706*, 181-193.

Danksagung

Bedanken möchte ich mich bei meinen Eltern Anne und Ralph, auch für die finanzielle Unterstützung während des gesamten Studiums. Selbes gilt für den Rest meiner Familie und meiner Freunde!

Weiterhin möchte ich mich bei Professor Michael Decker für die Möglichkeit der Promotion in seinem Arbeitskreis, wie auch für die interessanten und herausfordernden Themen bedanken. Besonderer Dank gilt außerdem Dr. Xinyu Chen und Dr. Guozheng Huang für die Vorarbeiten und Starthilfen in die Projekte.

Bedanken muss ich mich bei allen Kooperationspartnern, die die biologischen Testungen durchgeführt oder diese möglich gemacht haben: Florian Lang, Marco Saedtler, Professor Petra Högger, Professor Lorenz Meinel, Judith Roa, Professor Raimon Sabaté, Dr. Pamela Maher und Dr. Tangui Maurice.

Ein großes Dankeschön an Luca Agnetta für die Testung der M_1 Verbindungen, Matthias Scheiner und Matthias Hoffmann für die Durchführung der *in vivo* Versuche und vor allem Sandra Gunesch für die Durchführung der Neuroprotektions-Assays!

Danke auch an alle weiteren Mitarbeiter aus dem Institut für die gute Arbeitsatmosphäre und eure Hilfsbereitschaft. Besonders bei: Patrick Nagl, Antonio Ferraro, Marco Saedtler, Florian Lang, Joachim Wahl, Ines Schmidt, Jens Schmitz, Daniela Volpato, Kathrin Schreiber und den Mitarbeitern aus der Werkstatt und dem Sekretariat.

Außerdem möchte ich mich vor allem bei meinen Kollegen und Studenten aus unserer Arbeitsgruppe für die schöne Zeit, hilfreichen Diskussionen und für die entstandenen Freundschaften bedanken: Edgar Sawatzky, Sarah Wehle, Martin Nimczick, Patricia Stadtmüller, Xinyu Chen, Guozheng Huang, Dominik Dolles, Matthias Scheiner, Jacqueline Ramler, Regina Drescher, Carina Stiller, Peter Varga, Luca Agnetta, Matthias Hoffmann, Sandra Gunesch, Christian Gentzsch, Philipp Grad, Florian Behrendt, Manuel Horn, Julian Hofmann, Diego Alejandro Rodríguez-Soacha, Hubert Gerwe, Thorge Reiber und Carolina Kiermeier!

Danke euch allen!

Appendix [I]

Huang, G.; **Schramm**, **S**.; Heilmann, J.; Biedermann, D.; Křen, V.; Decker, M.

Unconventional application of the Mitsunobu reaction: Selective flavonolignan dehydration yielding hydnocarpins.

Beilstein J. Org. Chem. **2016**, *12*, 662-669.

Appendix [II]

Gunesch, S.; **Schramm**, **S**.; Decker, M.

Natural antioxidants in hybrids for the treatment of neurodegenerative diseases: a successful strategy?

Future Med. Chem. **2017**, *9*, 711-713.

Appendix [III]

Schramm, **S**.; Huang, G.; Gunesch, S.; Lang, F.; Roa, J.; Högger, P.; Sabaté, R.; Maher, P.; Decker, M.

Regioselective synthesis of 7-*O*-esters of the flavonolignan silibinin and SARs lead to compounds with overadditive neuroprotective effects.

Eur. J. Med. Chem. **2018**, *146*, 93-107.

Appendix [IV]

Schramm, **S**.; Gunesch, S.; Lang, F.; Saedtler, M.; Meinel, L.; Högger, P.; Decker, M.

Investigations into Neuroprotectivity, Stability and Water Solubility of 7-*O*-Cinnamoylsilibinin, its Hemisuccinate and Dehydro Derivatives.

Arch. Pharm. Chem. Life Sci., accepted.